UNIVERSITA' DEGLI STUDI DI VERONA

SCHOOL OF LIFE AND HEALTH SCIENCES

DEPARTMENT OF SURGERY, DENTISTRY, PAEDIATRICS, AND GYNAECOLOGY

DOCTORAL PROGRAM IN CARDIOVASCULAR SCIENCES

Cycle XXIX January 2014 – December 2016

Characterization of opioid receptors in post-heart transplantation, diabetic heart, great vessels, and cardioprotective role in myocardial ischemia-reperfusion injury

---

Mebratu Alebachew Gebrie

Ph.D. Coordinator: **Prof. Giovanni Battista Luciani**

Ph.D. Tutors: **Prof. Giuseppe Faggian**

Ass. Prof. Alessio Rungatscher

05/22/2017

UNIVERSITA' DEGLI STUDI DI VERONA

SCHOOL OF LIFE AND HEALTH SCIENCES

DEPARTMENT OF SURGERY, DENTISTRY, PAEDIATRICS, AND GYNAECOLOGY

DOCTORAL PROGRAM IN CARDIOVASCULAR SCIENCES

Cycle XXIX January 2014 – December 2016

Characterization of opioid receptors in post-heart transplantation, diabetic heart, great vessels, and cardioprotective role in myocardial ischemia-reperfusion injury

A Ph.D. thesis submitted to the University of Verona in partial fulfilment of the requirements for the Cardiovascular Sciences Ph.D. degree of the School of Life and Health Sciences, Department of Surgery, Dentistry, Paediatrics, and Gynaecology, University of Verona, Verona, Italy

Ph.D. Coordinator: Prof. Giovanni Battista Luciani

Signature: _____

Ph.D. Tutor: Prof. Giuseppe Faggian

Signature: _____

Ph.D. Co-Tutor: Ass. Prof. Alessio Rungatscher

Signature: _____

Doctoral candidate: Mebratu Alebachew Gebrie

Signature: _____

UNIVERSITA' DEGLI STUDI DI VERONA

SCHOOL OF LIFE AND HEALTH SCIENCES

DEPARTMENT OF SURGERY, DENTISTRY, PAEDIATRICS, AND GYNAECOLOGY

DOCTORAL PROGRAM IN CARDIOVASCULAR SCIENCES

External examiners

Prof. Bruno K. Podessor

Signature: _____

Prof. Mauro Rinaldi

Signature: _____

Prof. Gabor Szabo

Signature: _____

Doctoral candidate: Mebratu Alebachew Gebrie

Signature: _____

Abstract

Background: Despite several functions of opioid receptors/ORs in cardiovascular physiology and neurotransmission, expression in post-heart transplantation, diabetic heart, great vessels, and cardioprotective roles in neuropathic models of diabetic rat heart has not yet been addressed. The aims of this study were i) to investigate whether myocardial opioidergic system in transplanted and diabetic heart was altered, ii) to study the modulation of some pro-survival signaling proteins upon ORs blockade in diabetic rat model of post-myocardial ischemia-reperfusion injury (IRI), iii) to measure levels of apoptotic nuclei and infarct size in the presence of naloxone, iv) to evaluate and compare the expression of kappa (κ) and delta (δ) ORs in aorta and pulmonary arteries in rats.

Materials and methods: Endomyocardial biopsy from the orthotopically transplanted heart (OTH, human); tissues from heterotopic transplanted heart (HTH), diabetic rat heart in the presence and absence of naloxone after ischemia-reperfusion/IR following body weight and blood glucose measurement were collected and preserved in formalin and liquid nitrogen. The tissues were processed for total-RNA isolation, protein extraction, immunohistochemistry (IHC), immunofluorescence (IF), TUNEL, and Hematoxylin & eosin (H&E). The optical density (OD) of ORs immunoreactivity and a neuronal marker (CGRP-1) were measured. The pro-survival signaling pathways involved in alterations, phosphorylation levels of GSK-3α/β and p38, and TUNEL positive apoptotic nuclei were evaluated after IR-induction. 2, 3, 5-triphenyl tetrazolium chloride/TTC staining was also applied to measure levels of infarction of IR-induced rat heart with and without naloxone. H&E staining was performed to: grade the level of rejection; evaluate histopathology of sciatic nerve and pancreas in diabetic rats and any concurrent structural abnormalities of heart tissue. Immunohistochemically, κ- and δ-ORs were evaluated in endothelial and vascular smooth muscle cells in the aorta and pulmonary arteries of rats.

Results: IHC and IF observations showed the expression of δ- & κ-ORs in the heart with a significant reduction in the OD of DOR-1 & KOR-1 immunoreactivity in post-heart transplantation and in Streptozotocin-induced diabetic rat heart. However, MOR-1 was not detected in the rat heart. Dual labeling signals of KOR-1 with DOR-1 co-expression

were observed in both hearts of human and rats. The reduced OD of DOR-1 immuno-positive myocytes significantly correlated with the reduction of neuronal marker (CGRP-1) immunoreactivity.

Messenger RNA transcripts encoding the Oprd1 and Oprk1 were detected in human and rats, and downregulated in transplanted and diabetic hearts. Nevertheless, Oprm1 was not identified in rats` heart. Undetected Oprm1 RT-qPCR products also were shown by agarose gel electrophoresis. Densitometric quantification of immunoblots revealed that DOR-1 and KOR-1 proteins were also downregulated in transplanted and diabetic hearts of rats. Furthermore, an elevation of apoptotic nuclei of myocytes in transplanted and diabetic heart was observed. Histopathological examination of transplanted heart tissue demonstrated lymphocytes infiltrate in orthotopically and heterotpic transplanted heart in human and rats, respectively. Moreover, lower body weight and fasting blood glucose levels and abnormal distribution and shrinkages of βeta-cells of islet of pancreas, and connective tissue fibrosis around the epineurium and axonal swelling of the sciatic nerve were detected in diabetic rats. Mild morphological distortion of myocytes was observed in diabetic heart in the presence and absence of naloxone.

Process of cell-signaling showed that blockade of ORs by naloxone reduces the levels of phosphorylated pro-survival kinases (AKT, ERK1/2) in diabetic and IR-induced rat heart. On the contrary, the extent of phosphorylation of GSK-3β significantly elevated in the presence of naloxone. On the other hand, absence or poor phosphorylation of GSK-3α was observed in almost all groups tested. Moreover, elevation of p38 phosphorylation, TUNEL positive nuclei, and fibrosis was observed in the presence of naloxone after IR. TTC-stained ventricular slices showed a higher percentage of infarct size after ORs blockade. Comparative study of KOR-1 and DOR-1 on the aorta and pulmonary artery showed presence of κ- and δ-ORs in endothelial and vascular smooth muscle cells in the aorta and pulmonary arteries in rats dominantly KOR.

Conclusion: The δ- & κ-ORs possess a protective role in the heart against ischemia-reperfusion injury; however, the down-regulation of ORs may compromise the

effectiveness of pharmacological activities of opioids in transplanted and diabetic hearts that could reduce the potential role of ORs in the regulation of cardiac tissue. The ORs might promote cell survival by mediating the action of Akt and ERK1/2. The phosphorylation of GSK-3β and p38 might also be involved in ORs in regulation of myocardial tissue. The ORs dominantly KOR also play role in endothelial and smooth muscle cells in vascular system in rats.

Keywords: Opioid receptors, Cardiac transplantation, Cellular rejection, Ischemia-reperfusion injury, Diabetic neuropathy, Apoptosis, Myocardial infarction, Endomyocardial biopsy, Denervation, Vascular System

Acknowledgements

First of all, I would like to express my profound gratefulness to the almighty God for giving me endless hope.

I would like to extend my thankfulness to people who helped to bring this project to be fruitful. I would like to sincerely thank my supervisor Prof. Giuseppe Faggian for providing me the opportunity of taking part in Ph.D. program, and his valuable guidance, constructive comments, and excellent supervision throughout the entire program. Thank you once again, Prof. Faggian Giuseppe for adding colors and green light to my career and life.

I would like to gratefully thank my supervisor Prof. Alessio Rungatscher for proposing the project, collaborative work, and expertise involvement in heart transplant animal models and his close follow-up in each step of the experiment and evaluating reports and thesis with valuable and constructive comments. This work would not have been possible without his unreserved effort, and humble and positive attitude.

I would also like to thank Prof. Luciani Giovanni Battista for coordinating the program, giving valuable comments on each presentation, and creating opportunities to participate in seminars, International Conferences and advanced multidisciplinary Ph.D. courses.

I am grateful to examiners Prof. Bruno K. Podessor, Prof. Mauro Rinaldi, and Prof. Gabor Szabo for their time in reading the thesis, giving valuable comments and suggestions to improve the quality of the thesis.

I am grateful to Prof. Marina Bentivoglio for her kind permission to use her laboratory and providing some reagents for immunohistochemical study. I am also grateful to her collaborator Dr. Anna Andrioli for her excellent guidance and technical assistance during image acquisition, QImaging, and immunohistochemical experiments at the Department of Neuroscience, Biomedicine, and Movement.

I would like to thank Dr. Amenu Tolera for participating in the preliminary technical experiment and giving basic technical training. I would like to extend my appreciation to Dr. Laperchia Claudia and Dr. Azeez Idris for their technical assistance in the laboratory.

I would like to thank Dr. Linardi Daniele for his unreserved support in performing surgical procedures for animal models. Your solid technical ability and knowledge have really helped me to a great extent. I would like to thank also Dr. Livio San Biagio and Dr. Naseer Ahmed for their support in collection of samples and more.

I would also like to thank Department of Pathology and Diagnostics Research Team especially; Dr. Giulio Innamorati, Translational Surgery Laboratory for assisting laboratory works, ordering reagents, and giving valuable technical scientific support throughout the study. I would like to thank Dr. Erika Lorenzetto for her excellent assistance in fluorescence image acquisition. I am grateful to Dr. Borislav Rusev and Dr. Ivana Cataldo for their support in analysis of processed sections for histopathological analysis. I would like to thank Dr. Paul Takam for providing some reagents and giving technical advises during experiments.

I would like to thank Dr. Laura Marcazzan and Dr. Stefania Baschirotto for informing announcement of relevant meetings, lectures, seminars, symposium, conferences, and congresses timely, and for their best communication and advice in different administrative issues from the beginning to the end of my study.

My thankfulness also goes to the entire staff of Department of Surgery, Division of Cardiac Surgery especially, Dr. Maddalena Tessari, Prof. Alberto Forni, Dr. Ricardo Abbosciano, Dr. Mikhail Dodonov, Dr. Salvo Tozze, and Prof. Flavio Luciano Ribichini from Department of Cardiology (UOC, USF) Laboratory of Hemodynamics and Electrophysiology, AOUI for collecting biopsy samples.

I would like to thank also to my colleagues Dr. Dmitry Kosenkov, Dr. Mahmoud Ismail, Dr. Sajeela Ahmed, Dr. Laura Saracino, Dr. Federica Steccanella, Dr. Alessandro Soave,

Dr. Alice Giacomazzi, and Dr. Emanuela Fontana for their cooperation during the experimental work and for the time I spent in the laboratory. I would like to give special thankfulness to Dr. Nicola Sperandio for his kind direction and technical assistance. I would like to extend my appreciation to my friends Dr. Hayelom and Dr. Hailu for their encouragement during my study.

I would like to express my profound gratitude to my adored parents (Mr. Alebachew and Ms. Phelegush) for instilling in me the value of education, and many thanks go to my sisters (Ms. Abebech, Mss. Tiruwork, Ms. Tsege), brothers (Mr. Solomon, Mr. Getnet, Mr. Barnabas, Mr. Nega, Mr. Worku, Mr. Abrham) for supporting me during happiness, discomfort and my stay in Verona.

I would like to thank my beloved and beautiful wife Ms. Tigist for her wonderful visits and support in every problem I had during my study. I would like to thank Kidane`s family especially Mr. Dawit, Ms. Abeba, and Mss. Azenegash for their kindness.

Finally, I would also like to thank the University of Verona for giving me the chance and a grant/financial support to pursue my doctoral study. This study was supported by Department of Surgery, Division of Cardiac Surgery, University of Verona, School of Life and Health Sciences under the supervision of Prof. Giuseppe Faggian and co-supervisor Prof. Alessio Rungatscher. This accomplishment would not have been possible without the passionate encouragement of PVC throughout the study.

I thank God for the kind and special persons you`ve created!

May God bless Ethiopia, Italy, the World and their people!

Declaration

I declare that the work presented in this Ph.D. thesis was carried out in accordance with the regulations of the University of Verona. It hasn`t been submitted for any other academic award or is being published elsewhere. This work is original and every contribution and effort of others is acknowledged. Any views expressed in the thesis are those of the author, except where indicated by reference in the text.

Abbreviations, symbols, and acronyms used in the text

- **ABC**- Avidin-biotin complex
- **ACR** – Acute cellular rejection
- **BSA** - Bovine serum albumin
- **CTRL** - Control
- **DAB** - Diaminobenzidine
- **DAPI** - 4`, 6-Diamidino-2-Phenylindole
- **DM** - Diabetic Mellitus
- **DNP** - Diabetic neuropathy
- **DOR-1**- Delta opioid receptor
- **dUTP** – 2`-Deoxyuridine 5`- Triphosphate
- **EMB** - Endomyocardial biopsies
- **EMBOTH** - Endomyocardial biopsy of orthotopically transplanted heart
- **GAPDH** – Glyceraldehyde-3-phosphate dehydrogenase
- **GPCR** - G- protein- coupled receptors
- **H&E** – Hematoxylin and Eosin
- **Hr** – hour (s)
- **HTH**- Heterotopic transplanted heart
- **HTx** - Heart transplantation
- **IF** – Immunofluorescence
- **IHC** – Immunohistochemistry
- **IRI -** Ischemia-reperfusion injury
- **ISHLT** – International society for heart and lung transplantation
- **KOR-1**- Kappa opioid receptor
- **MI** – Myocardial infarction
- **Min** – minute (s)
- **mTOR** – mammalian target of rapamycin
- **NAL -** Naloxone
- **NC-IUPHAR** – International union of basic and clinical pharmacology
- **NH**- Naïve heart
- **NHS** - Normal horse serum
- **O.C.T** - Optimal cutting temperature
- **OD** - Optical density
- **OHT**-Orthotopic heart transplantation
- **ORs** - Opioid receptors
- **PBS** - Phosphate buffered saline
- **RIJV** – Right internal jugular vein
- **RT** – Room temperature
- **RT-qPCR** – Reverse Transcriptase quantitative real-time PCR.
- **Sec** – second (s)
- **SPSS** – Statistical package for the social science
- **STZ**-Streptozotocin
- **Tx** – Transplantation
- **TdT**- terminal deoxynucleotidyl transferase
- **TUNEL**- Terminal deoxynucleotidyl transferase, 2`-deoxyuridine 5`-Triphosphate Nick End Labeling
- **7TMR** - Seven transmembrane receptor
- **1^{o} and 2^{o} Abs** – Primary and secondary antibodies
- **μ** – mu, **δ** – delta, **κ** – kappa

Table of Contents

LIST OF TABLES

LIST OF FIGURES

CHAPTER ONE

1. General introduction

1.1. Background

Opioids are among the world's oldest known drugs (Manglik et al., 2012) that resemble morphine or other opiates in their pharmacological effects. They have long been known for their analgesic effects and work by binding to opioid receptors (ORs) which are found mainly in neural elements. In the last decade, pieces of evidence regarding local opioid regulation of heart physiology have been demonstrated (Mousa et al., 2011). The local opioids effects could be affected by innervations. Despite several functions of ORs in cardiovascular physiology and neurotransmission, their expression in post-heart transplantion, diabetic hearts, great vessels, and their cardioprotective roles in diabetes with neuropathy and ischemia-reperfusion/IR-induced models of rat heart have not been addressed yet.

Opioidergic effects on cardiovascular function are known by reducing arterial hypotension and bradycardia which is transmitted through a dorsal vagal complex in central nervous system (Treskatsch et al., 2015). The opioid is commonly administered to alleviate pain and unload the heart in patients with advanced heart failure (Bolte et al., 2009). The opioid effects are mediated by opioid receptors (MOR, DOR, and KOR) (López-Bellido et al., 2012; Matthes et al., 1996). Opioid receptors are activated by both endogenously produced opioid peptides and exogenously administered opiate compounds (Waldhoer et al., 2004). They include, mu, delta, and kappa ORs (μ-, δ-, and κ-OR, respectively), are G protein-coupled receptors (GPCRs) that regulate neurotransmission. Different documented evidence show that in many organ-systems, they mediate the beneficial as well as detrimental opioids effects in the body (Treskatsch et al., 2015).

Past and recent studies indicate the presence of ORs throughout the peripheral tissues of the body (Wittert et al., 1996), such as, heart (Theisen et al., 2014; Sobanski et al., 2014; Cao et al., 2003; Patel et al., 2006; Weil et al., 1998; Howells et al., 1986), intestines, adrenal medulla, kidney, lung, spleen, testis, ovary and uterus (Wittert et al., 1996), skin

(Salemi et al., 2005), MOR in vascular epithelium, cardiac epithelium, keratinocytes, vas deferens, and Sertoli cells (Lesniak and Lipkowski, 2011), autonomic ganglia (Janecka et al., 2004), vascular tissue (Feuerstein and Siren, 1987; Schultz et al., 1997), olfactory epithelium, limb bud and tooth (Zhu et al., 1998), both DOR and KOR in fibroblast-like synoviocytes (Shen et al., 2005), and both the μ- and δ- ORs in the boar sperm plasma membrane (are sperm kinematics regulators) (Vicente-Carrillo et al., 2016). The heart expresses high levels of endogenous opioids across species (Headrick et al., 2015; Howells et al., 1986). These receptors located in neural structures such as pontine angles, tonsils, olfactory bulb, deep cerebral cortex and peripheral sensory neurons (Martins et al., 2012).

Major families of the opioid system are endorphins, enkephalins and dynorphins, which in order are derivatives of the endogenous peptides pre-proopiomelanocortin, pre-proenkephalin A and pre-proenkephalin B (Koneru et al., 2009). Furthermore, opioids, sometimes considered as neurotransmitters, also possess autocrine, paracrine, or endocrine functions in the peripheral tissues (Barron, 2000).

The opioid receptors play great roles in cardiovascular function (Pugsley, 2002; Sobanski et al., 2014; Barry and Zuo, 2005). They also have been shown to regulate cardiovascular function in the healthy and diseased heart (Peart and Gross, 2006; Gross, 2003). They are known to modulate cardiac function, for instance, they exert strong cytoprotective activities (Williams-Pritchard et al., 2011). Furthermore, they play a significant role in cardiogenesis such as in regulation of vascular tone (Sobanski et al., 2014, Cao et al., 2003). Activation of DOR suppresses calcineurin and activates extracellular signal-related kinase (ERK) 1/2 which are thought to interact with the mechanism involved in cardioprotection (Rungatscher et al., 2013).

Since the description of ORs in 1973 by Pert and Snyder and endogenous opioids in 1975 by Hughes and colleagues, a large number of articles were published concerning the presence of a number of ORs and their roles in cardioprotection. After a study that supports the hypothesis of ORs roles in ischemic preconditioning in the rat myocardium

done in 1995 by Schultz and colleagues, many data also show the involvement of ORs in cardioprotection in different animal models (Schultz et al., 1997; Mayfield and D`Alecy, 1994; Benedict et al., 1999; Valtchanova-Matchouganska and Ojewole, 2003; Li et al., 2009; Peart and Gross, 2004; Zhang et al., 2006; Wu and Wong, 2003; Peart et al., 2005; Wu et al., 2004; Park et al., 2014; Karlsson et al., 2012; Zatta et al., 2008; Maslov et al., 2013; Wong et al., 2010; Guo et al., 2011; Kim et al., 2011; Al-Hasani and Bruchas, 2011) (Table. 2).

According to Marvin et al., (1980) in rat heart parasympathetic innervations develop before birth; while sympathetic innervations develop during 7 to 10 postnatal days (Mousa et al., 2011; Robinson et al., 1996). DOR and KOR are increased in number in the adult rat heart (Zimilichman et al., 1996) and within central nervous system (Spain et al., 1987) except a gradual disappearance of MOR (Zimilichman et al., 1996).

It is reported that DOR mRNA, protein, and binding sites that gradually increased from postnatal day 1 towards adulthood. The DOR-1 co-localization with VAChT principal neurons from the first day of birth and with small intensely fluorescent catecholaminergic cells and CGRP within intracardiac ganglia and atrial myocardium are reported. Moreover, the co-expression DOR with neuronal markers increasing with age (neonatal to adulthood) (Mousa et al., 2011) and these developmental expressions of ORs and sympathetic, parasympathetic and sensory innervations of the heart imply the regulation of ORs by cardiac autonomic innervations.

In another immunohistochemical localization qualitative study, it is demonstrated that delta and kappa ORs and CGRP sensory nerve fibers are expressed in heart tissue using only two individuals of sudden death (Sobanski et al., 2014); however, in transplanted and Streptozotocin (STZ) induced diabetic rats has not been addressed and/or characterized. The study of Sobanski et al., (2014) employed lacking quantitative approaches, transplanted and STZ-induced diabetic and neuropathic models for ORs characterization and IR-induced models to evaluate their cardioprotective roles in neuropathic IR-induced models.

Base on the suggested clue on the role of ORs in neural transmission and regulation of cardiomyocytes physiology (Sobanski et al., 2014) in the heart and modulation of these receptors by autonomic innervations which are lost due to transplantation, we hypothesized that they could be down-regulated after heart transplantation and neuropathic conditions. To test this hypothesis, this study was designed to investigate levels of opioid receptors and their mRNA, fragmented DNA (apoptotic level) after cardiac transplantation (orthotopic and heterotopic in human and rat, respectively) and STZ-induced diabetic rats using both qualitative and quantitative approaches.

Moreover, this study has dealt with the cardioprotective role of ORs after blockade in IR-induced model of diabetic rats. Moreover, concurrently any histopathological abnormalities of heart tissue in transplanted heart and diabetic rat heart. In addition, body weight, fasting blood glucose levels and histopathology of the pancreas to assess diabetic condition, and histopathology of the sciatic nerve to evaluate neuropathic changes are done.

This doctoral project entitled "Characterization of opioid receptors in post-heart transplantation, diabetic heart, great vessels, and cardioprotective role in myocardial ischemia-reperfusion injury". It consisted of seven major parts. The first four chapters deal with a general introduction and characterization of opioid receptors in orthotopically and heterotopic transplanted (human, rat, respectively), and STZ-induced diabetic (rat) heart. The fifth chapter deals with ORs signaling mechanisms after ischemia-reperfusion in the STZ-induced neuropathic model of diabetic rats in the presence of naloxone. The sixth one presents comparative study of kappa and delta opioid receptors in aorta and pulmonary artery in normal rats.

The thesis project contributes insight and a better understanding of the expression of ORs specifically in denervated/transplanted heart, diabetic heart, and great vessels using advanced approaches. It also evaluates role of opioid receptors in myocardial ischemia-reperfusion injury and levels of apoptotic nuclei in cardiomyocytes in post-

transplantation and diabetic hearts. Besides, expression of delta and kappa-ORs in pulmonary arteries and aorta are included in the study.

The novel findings of this study show denervated and diabetic heart might have implications as a possible mechanism for defective cardioprotection in patients with cardiac transplants and diabetes.

1.1.1. Opioidergic system: the opioids and opioid receptors

The existing anesthesia, the species being studied, the dose, the site of action in the brain, any concurrent respiratory system effects, receptor specificity, and the existing status of the cardiovascular system, particularly the degree of hypotension or hypertension contribute to the cardiovascular effects produced by the opioids (Gross, 1994). Another issue is the plasticity of the opioid receptor system that is capable of changing its level and distribution pattern in response to physiological or pathological changes (Feuerstein, 1985). The opioids decrease preload, afterload, contractility, and heart rate with a resulting decrease in cardiac output. In contrast, opioids also cause central respiratory depression (Gross, 1994).

In 1973, a pioneer study done by Pert and Snyder, has shown the existence of ORs in mammalian brain and guinea pig intestine through a powerful opiate antagonist (naloxone) (Snyder and Pasternak, 2003) and then in 1976 Martin and colleagues also demonstrated heterogeneity of ORs, and proposed names of μ and κ after they used morphine for μ receptor and ketocyclazocine for κ receptor. Another study in 1977 done by Lord and colleagues on effects of opioid peptides in mouse vas/ductus deferens tissue in which the receptor (δ) was first characterized. Consequently, the receptors were named using the first letter of the first ligand that was found to bind to the receptors.

Since the description of ORs in 1973 by Pert and Snyder and endogenous opioids in 1975 by Hughes and colleagues, a large number of articles were published concerning the presence of a number of ORs. Opioid receptors are a group of inhibitory GPCRs with

opioids as ligands, like other GPCRs in the cell membrane, are characterized by seven transmembrane domains (Fig. 1) (Koneru et al., 2009; Freye, 2008). They are activated by opioid peptides derived from endogenous ligands the endorphins, enkephalins, and dynorphin families (Williams-Pritchard et al., 2011).

Opioid receptors are classified as a classic (mu, delta, and kappa), and non-classic (ORL-1) and identified by molecular cloning. Each of the cloned ORs is derived from a single gene; however, a number of alternatively spliced variants/isoforms from their own genes have been isolated (Pan, 2003). The three classic closely related subtypes, mu, delta and kappa, share ~70% sequence identity in their seven transmembrane helices (Wu et al., 2012; Kobilka, 2007) (Fig.1, 2 and Table. 1), with more variations in extracellular loops and very little similarity in their amino and carboxyl terminal (Wu et al., 2012; Waldhoer et al., 2004; Janecka et al., 2004).

Based on pharmacological evidences, distinct subtypes of ORs were suggested with different nomenclatures (Table 1) that μ (mu, MOP), δ (delta, DOP) and κ (kappa, KOP) ORs with different variants such as μ_1 μ_2 μ_3, δ_1 δ_2, and κ_1 κ_2 subtypes, respectively (Williams-Pritchard et al., 2011; Cox et al., 2015). Although scientists have intensely studied and characterized these receptors in neural elements (Mansour and Watson, 1993), a lot of further studies are still needed especially in peripheral tissues, such as the heart.

Table: 1. NC- IUPHAR-approved nomenclatures for opioid peptide receptors and some agonists and antagonists

SN	Current NC-IUPHAR-approved nomenclature	Other (non-approved) nomenclature	Presumed endogenous ligand (s)
1	μ, mu or MOP	MOR, OP3	β-endorphins (not selective) Enkephalins (not selective) Endomorphin-1[b] Endomorphin-2[b]
2	δ, delta or DOP	DOR, OP1	Enkephalins (not selective) β-endorphin (not selective)
3	κ, kappa or KOP	KOR, OP2	Dynorphin A Dynorphin B α-neoendorphin
4	NOP, Nociceptin or FQ, Orphanin	ORL1, OP4	Nociceptin/Orphanin FQ (N/OFQ)
			IUPHAR Review 9 Cox et al., 2015.
	- Universal antagonist	Naloxone	
	- NOP/FQ antagonist	Antagonist JTC-801	Scoto et al., 2007 ; Redrobe et al., 2002
	- Agonists	Fentanyl for μ; DPDPE for δ; U50488H for κ.	Bolte et al., 2009 ; J Mol Cell Cardiol.
	- NOP/FQ agonist	Full agonist MCOPPB for FQ,	Hirao et al., 2008
		Partial agonist BU08028 for FQ,	Ding et al., 2016

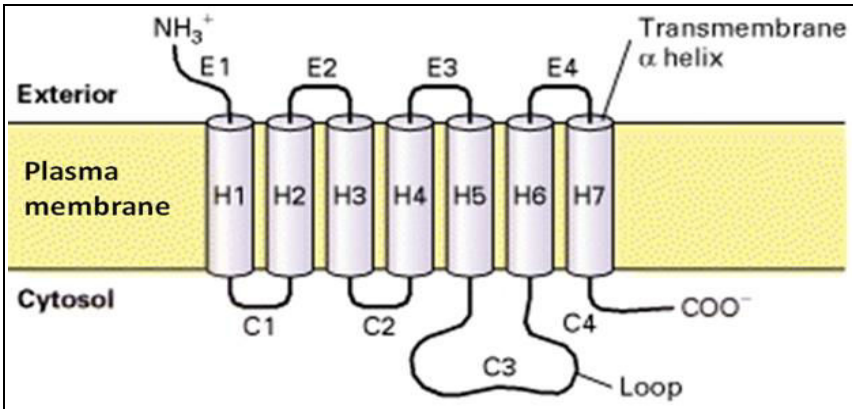

Figure: 1. Schematic representation of opioid receptor: The figure illustrates the sequence of the seven transmembrane domains, the extracellular and intracellular loops. All GPCRs contain 7TM α-helical regions. The loop between α-helices 5 and 6, and in cases between helices 3 and 4, which face the cytosol, are important for interactions with the coupled G-protein. E1-E4 implies extracellular loops; C1-C4 implies intracellular loops; H1-H7 implies 7TM domains. Reproduced from Lodish et al., (2000); Freye, (2008).

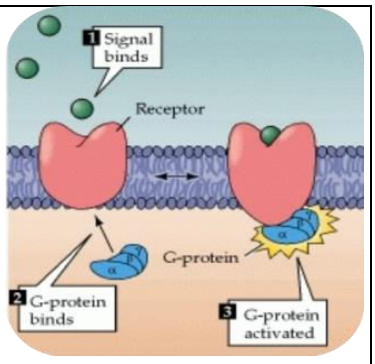

Figure: 2. How does signal bind to the receptors? When signal binds (1) to the receptor, GPCR regulates intracellular reaction by involving G-protein (2) that binds the receptor and then activated (3). Reproduced from Purves et al., (2001).

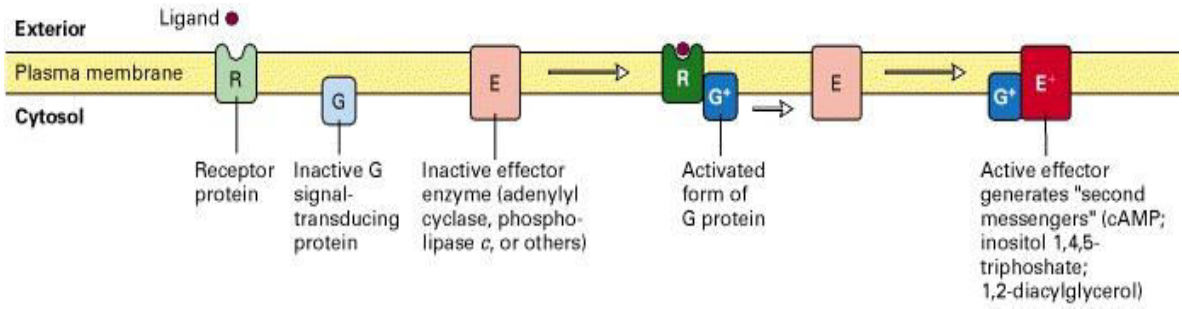

Figure: 3. Binding of ligands and activation of G-proteins: Binding of ligand to a receptor triggers activation of G-protein, which then binds to and activates an enzyme that catalyzes the synthesis of a specific second messenger. Reproduced from Lodish et al., (2000).

1.1.2. Myocardial opioid expression

There are pieces of evidence to indicate the presence of multiple opioid receptors in different organs of the body (Khachaturian et al., 1987). The heart expresses high levels of endogenous opioids across species (Headrick et al., 2015). Cardiomyocytes are major sites of opioid peptide synthesis, storage, release, and possess large stores of genes encoding the endogenous opioid precursors pre-proenkephalin, prodynorphin and pro-opiomelanocortin (Barron, 2000; Koneru et al., 2009). Ventricular myocardium may

contain the highest levels of pre-proenkephalin mRNA in the body (Howells et al., 1986) that assures the heart as an important neuroendocrine organ. Myocardial synthesis and release of opioid peptides are variable, increasing with ischemia, and cardioprotective intervention (Zatta et al., 2008). They are also influenced by aging (Caffrey et al., 1994), and disease state (Lendeckel et al., 2005). Relative quantities of myocardial transcripts imply a tendency to greater generation of endogenous DOR selective ligands (Headrick et al., 2015).

1.1.3. Intracellular signals following opioid binding

When opioids those bind to their receptors on a cell surface, a signal is transmitted or "transduced" to the cells interior to exert events like a series of chemical and physical reactions that produce biological responses. The biological responses include proliferation, cell differentiation, altered metabolism, migration, survival, apoptosis, and cell growth and division (Freye, 2008). Each receptor has extracellular, transmembrane, and intracellular components (Fig. 1, 2 and 3).

The binding of a ligand to the receptor is known as the first message. First messengers are extracellular substances such as opioid peptide ligands that bind to receptors. The second messengers are intracellular signaling molecules or mediators that relay information/signals from the receptor-ligand complex and diffuse from one part of the intracellular space to their spatial target molecules in the cytosol and/or nucleus (Berg et al., 2002). They have three major classes such as cyclic nucleotides (e.g. cAMP & cDMP), Inositol triphosphate (IP3), Diacylglycerol (DAG), and calcium ions (Berg et al., 2002).

In general, ligand binding to a receptor on the surface of the cell thus initiates a chain of intracellular reaction, ultimately reaching the target cell nucleus and resulting in programmed changes in gene expression (Cooper, 2000).

1.1.4. Opioids and opioid receptors cardioprotective action signal mechanism

Mechanisms of ORs which are involved in cardioprotection are not clearly understood. However, many studies documented different views. The study of Maslov and colleagues 2013 supports the occurrence of convergent pathways in which multiple GPCRs interact independently and transactivate epidermal growth factor (EGF) receptor-dependent kinase signaling to provide cytoprotection. Intracellular interaction of delta-1 ORs and adenosine A1 receptors is indicated as an example of transactivation of GPCRs (Maslov et al., 2013). It is also thought that both delta and kappa ORs which act via cellular mechanisms involving activation of ATP-sensitive (sarcolemmal) k+ channel via G(1/o) proteins, phosphatidylinositol pathway via activation of kinase C, and most likely cross talk between adrenergic and ORs in cardiomyocytes (Valtchanova-Matchouganska and Ojewole, 2003).

It is known that $G_{i/o}$ proteins are intermediary linkages that provide cellular signaling between ORs and protein kinase C (PKC) (Maslov et al., 2013). Nowadays, a number of studies have shown that the involvement of protein kinase C (PKC) in mediating anti-necrotic and anti-apoptotic actions of ORs agonists (Maslov et al., 2016; Maslov et al., 2013). Studies of Maslov and colleagues (2013) have demonstrated that PI3 and Akt kinases are involved in the cardioprotective effect of opioids. Besides, important roles of MEK1/2, ERK1/2, Src and JAK2 kinases and transactivation of ORs in the cardioprotective effect of opioids in the development tolerance of the heart to ischemia and reperfusion are indicated (Maslov et al., 2013). Opioid transactivation of epidermal growth factor receptor (EGFR) is a connecting link between ORs and ERK1/2 and PI3 kinase cascades (Maslov et al., 2013). The activation of the EGFR increases the Akt (protein kinase B) and Pl3 (phosphatidylinositol-3-kinase) in their activities (Krieg et al., 2002).

In the past decades, various investigators have shown their efforts to find out possible mediating effects of ORs against IR injury using different: pharmacological, ischemic and exercise preconditioning. DOR and KOR are strongly implicated in cardioprotection

including anti-infarct and anti-arrhythmic actions across models and species indicated as seen in the table below:

Table: 2. Cardioprotective effect of opioid receptors

SN	Preconditioning	Receptors	Cardioprotective effects	Models	Authors
1	Intermittent hypoxia conditioning (protects >90%) after 60min occlusion and 5hr reperfusion	DOR specific antagonist (naltrindole)	completely repels the reductions of IS and arrhythmia	Canine	Estrada et al., 2016
2	Remote electro-stimulation (RES)	specific antagonist targeting KOR and DOR	↑GSK3 and PKC expression levels in (RES) but ↓ δ and κ	Rats	Tsai et al., 2015
3	Remote electro-stimulation (RES)	specific antagonist targeting KOR	↓ IS in KOR antagonist than left	Rats	Tsai et al., 2015
4	Preconditioned EA	Sham RES = 50% (n=24) RES = 20% (n=20) RES+KOR left = 33% (n=9) RES+KOR blocked = 67% (n=18)	attenuated cardiomyocyte cell death and decrease mortality	Rats	Tsai et al., 2015 ; PLOS ONE
5	Restraint stress preconditioning	κ-selective antagonist	reduced the increases in MAP and HR ↓ the restraint stress-related pressor and tachycardic responses, IL KOR plays a facilitator role in the control of cardiovascular responses induced by RS.	Rats	Fassini et al., 2015
6	Exercise preconditioning	A specific DOR antagonist (naltrindole)	Abolished the protection against tissue necrosis - significantly elevated tissue necrosis /IS levels in comparison to sham.	Sprague–Dawley rats	Miller et al., 2015
7	Ischemic preconditioning (intrathecal morphine preconditioning)	IV naloxone methiodide; intrathecal naloxone methiodide	↓ IS/AAR	Sprague-Dawley rats	Wong et al., 2010
		μ-selective antagonist or naltrindole and δ-selective	No effects on the restraint-evoked increases in MAP and HR	Rats	Tsai et al., 2015

		antagonist			
8	Exercise preconditioning	naltrindole – DOR b-funaltrexamine - MOR nor-binalthorphimine – KOR	DOR blockade completely prevented the cardioprotection seen in the Exe group but not MOR and KOR	Wistar rats	Borges et al., 2014
9	Activation of delta opioid receptors	Delta-2 specific opioids deltorphin-II (Delt-II) Delt dvariat (Delt-Dvar) Deltorphin-E (Delt-E)	Cardiac tolerance to arrhythmogenic effect of ischemia	Rats	Maslov et al., 2013
10	MI/R + U50488H in the absence or presence of KOR selective antagonist (Nor-BNI)	KOR agonist (U-50488H)	KOR attenuated the expressions of TLR4 and NF-jB. - sig. inhibits TLR4/NF-kappa B signaling in rat heart subjected to I/R	Rats	Lin et al., 2013
11	Antagonists of ERK1/2 and PI3K perfused rat	KOR agonist (U50488H)	effective reduction of MI: Inhibition of ERK1/2 (26.8±2.9%) repels anti-infarct effect of KOR agonist (U50488H). Anti-infarct effect of KOR agonist is mediated by ERK1/2.	Rats	Kim et al., 2011
12	Stress with cold exposure and restraint for 3 h- attenuated IS induced by M/IR (from 36.64±1.8 to 22.85±2.6%) Morphine at 8 mg/kg attenuated the IS from 36.26 ± 1.6 to 20.30 ± 2.1%)	-naloxone, norbinaltorphimine, a selective KOR antagonist; -naltrindole, a selective DOR antagonist, or CTOP, a selective MOR antagonist.	↓effect of cold-restraint stress ↓effect of morphine All three types of ORs mediate the cardioprotective effect of morphine in the heart of the rat. The effects also attenuated by blockade of protein kinase C or the mitochondrial KATP channel	isolated perfused rat heart	Wu et al., 2004
13	After IR injury	DOR agonist (DADLE)	- Sig. decreased the infarct size (by 66%) compared to control	intact rat rats	Valtchanova-Matchouganska Ojewole, 2003
14	Hypoxic setting: drowning, head injury apnea, and complicated childbirths	mechanism of neuroprotection via decreasing body-T^{o} using delta agonist (BW373U86), DPDPE	- elevation of survival time during lethal hypoxia	mice	Bofetiado etal., 1996

1.1.5. Functions of opioid system in the body

The opioid system is one of the most multifaceted neurotransmitter systems in the body (Feng et al., 2012). Although opioids mainly are known in pain modulation and widely associated with analgesia for postoperative pain therapy (Hanlon et al., 2011), other important roles of the system in peripheral organs, especially in the heart has been the focus of many studies in the past decade. The release of endogenous opioids into the blood has a significant elevation of β-endorphin following muscle injury and hemorrhagic shock in naïve rats models (Molina, 2002) and works against pain by regulating nociceptive information.

The opioid system plays important roles in the regulation of cardiovascular system, especially in cardioprotection. The three subtypes (mu, delta, and kappa) opioid peptides have been found in cardiomyocytes, sympathetic nerve fibers and ganglion cells of the heart (Steele et al., 1996). The delta (Schultz et al., 1997) and kappa (Wu et al., 1999) opioid receptors have been shown to mediate cardioprotection by preconditioning with myocardial ischemia and metabolic inhibition.

Endogenous opioid systems are associated with the regulation of emotional responses (Saitoh et al., 2005). This system in the regulation of emotional response is not well studied; however, it has been reported that opioids are natural inhibitors of stress and anxiety (Saitoh et al., 2005), and produce antidepressant-like activity through DOR mechanism of action (Naidu et al., 2007).

Opioid receptors, especially, DOR, mediate neuroprotection against ischemic injury. Even though there have been major controversies in the past decade on the role of opioids in the neuronal responses to ischemic insults by activation and inhibition of opioid receptors, recent data Chao and Xia, (2010); Feng et al., (2009) have clarified their neuroprotective effects against ischemic neuronal injury. The up-regulation of DOR expression and activation increase the neuronal tolerance to ischemic stress through triggering different mechanisms (PKC-ERK-Bcl2), and stabilization of ionic homeostasis

(Chao et al., 2007) that reduce oxidative (Feng et al., 2012) and glutamate-induced (Zhang et al., 1999; Zhang et al., 2000) injury to reserve neuronal survival (Feng et al., 2012). DOR also play a crucial role in neurogenesis. It is indicated that DOR agonist (SNC80) promotes neural differentiation from multipotent neural stem cells (Narita et al., 2006).

Morphine and other opiates, act like cytokines to modulate the immune response (Eisenstein, 2011) in central and peripheral neurohumoral systems (Welters, 2003). According to Car and colleagues (1993), ORs stimulation exerts suppression in numerous parts of the immune defense responses. Opioid modulation of the immune response is mediated via the direct interaction with ORs expressed by immune cells (Finley et al., 2008). They are also involved in regulation of ionic homeostasis under normoxic and ischemic conditions by intracellular elevation of Ca^{2+} or inhibition of their entry.

Opioid receptors are also involved in regulation of feeding in animal (Marczak et al., 2009). Stimulation of ORs increases feeding, while inhibition of ORs reduces food intake in rodent models of obesity (Marczak et al., 2009).

It has been well established that opioids trigger respiratory depression in humans and animals (Pattinson, 2008) by a direct action on respiratory generating and high densities of ORs brain areas (Mutolo et al., 2007). The use of opioid drugs for pain relief results in a respiratory depression that creates a significant clinical problem for patients treated with the drugs in the postoperative period (Pattinson, 2008). The massive release of endogenous opioids or overdose of opioid drugs can cause a severe respiratory depression and may be lethal. On the other hand, excessive use and abuse of opioid compounds lead to opioid tolerance/addiction in the nervous system via desensitization and internalization (Koch and Höllt, 2008) which greatly affects body homeostasis and brain physiology.

In general, various well-established evidence has shown the role of the opioid system in cardioprotection, pain modulation, neuroprotection, modulating the immune response, feeding, respiration, reward and opioid addiction (Feng et al., 2012).

1.2. Brief notes on cardiac and vascular structure, function and its development

1.2.1. Development of the heart

The cardiovascular system is the first organ system to develop and function in the vertebrate embryo (Harris and Black, 2010). The heart develops from the precardiac lateral fold to form the primitive heart tube (Brutsaert et al., 1998). The mesodermal tissues that give rise to the heart first become evident when the embryo is undergoing the process known as gastrulation. In the human, this occurs during the third week of development, while for the mouse, at a comparable stage of development, around seven days will have elapsed from fertilization, and the embryo will be in the presomitic stage.

The embryonic plate in humans, initially possessing two layers, is ovoid, and is formed at the union between the yolk sac and the amniotic cavity. In the midline of the long axis of the oval disc is found the primitive streak, with the node at its cranial end. Through this streak, cells migrate from the upper layer by the process called gastrulation to form the three germ layers of the embryo proper: the ectoderm, the endoderm, and the mesoderm.

The cells that are destined to form the heart are also derived from this mesodermal layer (Moormon et al., 2003). The heart tube at the time of its formation is a two-layered structure, composed of an inner endothelial layer and an outer myocardial layer (Harris and Black, 2010). However, the caudal and cranial additions to the tube produce a pronounced elongation of the primary heart tube. The elongation, the dorsal mesocardium, originally connecting the left ventricle to the mediastinum, forms the larger part of the tube.

1.2.2. Layers, chambers, and valves of the heart

The heart is located in middle mediastinum, is surrounded by pericardium. The pericardium is a relatively avascular, double-walled fibrous sac that can normally contain 15 to 35 ml of serous fluid distributed mostly over atrial-ventricular and interventricular grooves (Little et al., 2006). The visceral layer is composed of a single layer of mesothelial cells that are adherent to the epicardium (Lewinter et al., 2005). The parietal

pericardium is a fibrous structure, is composed of mainly of collagen and a lesser amount of elastin (Lewinter et al., 2005). It protects the heart from friction, excessive dilatation, injury, shock. It provides a smooth lubricated sliding surface and attaches to the sternum, diaphragm, and anterior mediastinum (Little et al., 2006). It may also function as a barrier to infection because of its location (Little et al., 2006).

Layers/wall: The heart wall comprises of three layers: epicardium, myocardium, and endocardium. The epicardium outer layer is structurally characterized as a visceral layer of pericardium. A film of epicardial fat is found between epicardium and myocardium known as a true visceral fat depot of the heart, measures 1mm to 23mm thick using echocardiography (Iacobellis et al., 2009). It predominantly overlies the atrioventricular grooves and the right ventricle and houses coronary vessels, lymphatics, autonomic nerves, and a variable amount of fats (Herzog, 2014; Murphy and Lloyd et al., 2013). It plays a role in cardiovascular diseases because of its anatomical and functional proximity to the myocardium and its intense metabolic activity (Iacobellis et al., 2009). The epicardium gives rise to the precursors of the coronary vasculature and cardiac fibroblasts (Xin et al., 2013).

The myocardium is a complex three-dimensional network of myocytes in a fibrous tissue matrix (Ho and Nihoyannopoulos, 2006). It is the thickest and the middle layer of the heart; however, the levels of myocardial mass are varied within the heart. The myocardium is thinner in the left atrium and thickest in the left ventricle.

The endocardium is the inner layer in contact with blood. This large surface area is firmly attached to myocardium and lines the cavities and valves. The endocardium is further classified into smooth muscle cells, connective tissue, and subendocardial layers (Katz 2010). The endocardium is mainly composed of the endothelial cells. This endocardial endothelium modulates cardiac performance, rhythmicity, and growth (Brutsaert et al., 1998). It is also suggested that cardiac endothelium controls the development of the heart in both embryo and adult during hypertrophy. The endocardial endothelium may also act

as blood heart barrier and thus controls the ionic composition of the extracellular fluid (Milgrom-Hoffman et al., 2011).

Chambers of the heart: The heart is a muscular, four-chambered organ, situated in a thoracic region called middle mediastinum (Sundberg-Cohon et al., 2009). It contains an apex and base. The apex is pointed forward, downward, toward the left. The base is the broader end where cardiac plexus is located and great vessels emerge upward (Katz, 2010). The chambers are upper right and left atria, and lower right and left ventricles. The atria are relatively small and thin-walled located superior to ventricles, receive blood from large veins through Ostia unguarded by valves whereas, the ventricles are larger thick-walled designed to pump blood and perform most of the work (Sundberg-Cohon et al., 2009).

The right atrium is the upper right cardiac chamber that receives deoxygenated blood from the systemic venous and coronary sinus return (Malik et al., 2015). It is made of a smooth concavity and a rough muscular part, formed by pectinate muscles. These two regions are separated by an internal ridge known as crista terminalis and a vertical groove (sulcus terminalis) (Dingová et al., 2015). In the right atrium, there are a number of structures located, such as pacemakers of the heart (SA and AV nodes), venae cavae, and coronary sinus (Katz, 2010). It is slightly thicker than left atrium.

The left atrium is situated behind the right atrium and forms a greater part of the base. It receives oxygenated blood from pulmonary veins via its openings. Like right atrium, it comprises of a smooth concavity and a muscular left auricle. The atria are separated by an interatrial septum that prevents blood flow between the atria (Hara et al., 2005).

The right ventricle is the most anterior cardiac chamber located immediately behind the sternum (Ho and Nihoyannopoulos, 2006), is more triangular shaped when viewed from the front and its right edge is sharp, forming the acute margin of the heart. Fibers are oriented like left ventricle (Ho and Nihoyannopoulos, 2006). The ventricles are separated by an interventricular septum. The septum is curved and convexity into the right

ventricle. It comprises of muscles except for a thin fibrous structure beneath aortic valve (Ho, 2009). It is demonstrated that cardiac output of the right ventricle (RV) is five times lower than left ventricle (LV) (Katz, 2010).

The left ventricle is located at the left bottom portion of the left atrium. It has a conical shape and its concavity presents a circular outline (Ho, 2009). Its fibers direction is aligned mostly apex-base route and oriented longitudinally, obliquely, and circularly (Helm et al., 2006). The predominant longitudinal orientation of the myocytes forms the myofibers (Ho and Nihoyannopoulos, 2006). The LV is four times thicker than the RV. Its wall is thinner at the apex and it gradually becomes thicker towards the base (Ho, 2009).

Valves of the heart: The heart contains four valves and fibrous skeleton. The fibrous skeleton houses the annuli of the four valves, membranous septum, aortic intervalvular, right and left fibrous trigones (Movahed et al., 2009). The right trigone and the membranous septum together form a central fibrous body, which is penetrated by the bundle of His (Movahed et al., 2009). The fibrous skeleton, in addition to providing an electrophysiological dissociation of atria and ventricles, it gives structural support to the heart (Movahed et al., 2009).

1.2.3. Microscopic structures of the heart

The heart possesses well-orchestrated and highly heterogeneous cells (Burton et al., 2006). There are permanent and transient cells in the heart. The permanent cellular constitutes cardiomyocytes (Fig. 4), endothelial cells, cardiac fibroblasts, and vascular smooth muscle cells (Souders et al., 2009). Impermanent cells include lymphocytes, mast cells, and macrophages, which can interact with permanent cell types to affect the cardiac function (Souders et al., 2009). All these types contribute to structural, electrical, biochemical, and mechanical properties of functional heart (Xin et al., 2013).

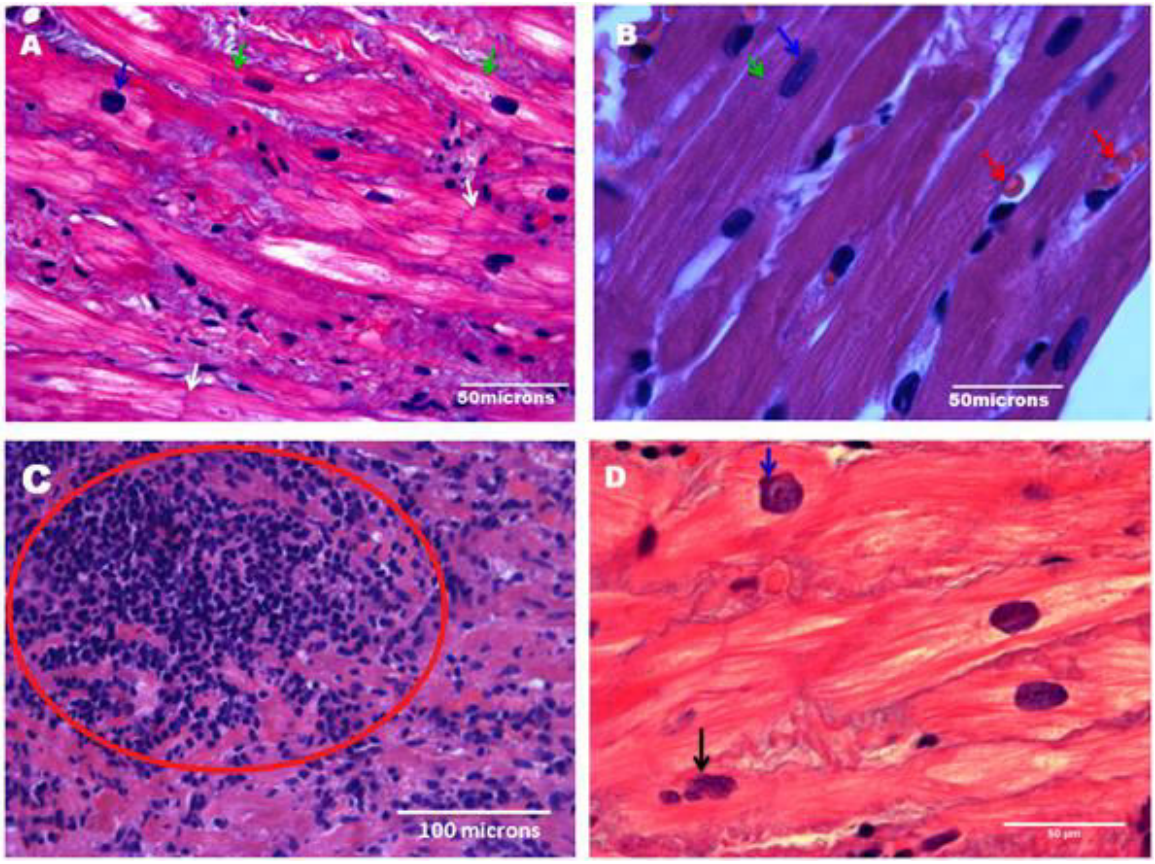

Figure: 4. Morphology of cardiomyocytes and nuclei in transplanted and normal heart: the above figure (Fig. 4A&B) illustrates the longitudinal structure of cardiomyocytes (in green and white), nuclei (in blue), striations, intercalated disc (ICD) and erythrocytes in human (Fig. 4. A) & rat (Fig. 4B). All sections are taken from the left ventricle. The figure 4C illustrates tissue a section is taken from heterotopic transplanted heart showing t-cell lymphocytes infiltrate (Fig.C encircled with red circular arrow) which are signs of acute cellular rejection in a red circle shaped arrow. Note: Green arrows in (Fig. 4A) and (Fig. 4B) illustrate the cardiomyocytes. Blue arrows indicate normal nuclei whereas; black arrow indicates shrinkages of nuclei in diabetic rat heart tissue sections. White arrows in figure 4A show ICD. Images are acquired using 400x magnification, scale bar = 50 microns (Fig. 4 A, B, D) and 200x magnification, scale bar = 100microns (Fig. 4C). ICD, Intercalated disc.

The cardiac muscle cells: The cardiac muscle cells include contractile cardiomyocytes and specialized conducting cardiomyocytes (pacemaker cells, Purkinje fibers) that make up the largest volume of the heart; however, non-cardiomyocytes cells dominate in terms of cell numbers especially cardiac fibroblasts (Souders et al., 2009). The contractile cells react to impulses of action potential from the pacemaker cells that generate and conduct

electrical impulses and then the contractile cells contract in response to the impulses to pump blood through the body (Katz, 2010).

Contractile cardiomyocytes: The human heart contains an estimated 2-3 billion rod-shaped cardiac muscle cells, but they account less than one-third of the total number of cells in the heart (Tirziu et al., 2010; Song et al., 2007; Nakano et al., 2012). In mouse, the number of the LV cardiomyocytes ranges 2-3.3 million. Each myocyte is long, thin and joined to its neighboring cells at the ends as well as at its side branches (Ho and Nihoyannopoulos, 2006). The ventricular myocytes are approximately 50% of the weight of the heart (Nakano et al., 2012).

Myofibrils (actin and myosin filaments) are rod-like shaped bundles that form the contractile elements within cardiomyocytes (Nakano et al., 2012). The myofibrils and mitochondria comprise 50% and 25% of the cell volume in an individual contracting cardiomyocyte, respectively (Nakano et al., 2012). The rest of the cell volume is occupied by the nucleus, sarcoplasmic reticulum, cytosol and other structures (Nakano et al., 2012).

The heart has two syncytia (branched network) in both atria and ventricles (Dingová, 2015). The transmission of contractile force between cardiomyocytes is arranged by intercalated discs (ICD) (Katz, 2010). Each cell in the heart is electrically coupled to the next one that enables the heart to work as a single functional organ or syncytium for rapid conduction of electrical impulses throughout the heart (Perriard et al., 2003).

In the mature heart, the ICD is situated at the bipolar ends of the rod-shaped cardiomyocytes and it is where myofibrils are anchored (Perriard et al., 2003). The myocytes are smaller and ellipsoidal shaped in atria (Nakano et al., 2012) that contain granules with a precursor of atrial natriuretic peptide (ANP) (Dingová, 2015). The ANP is a cardiac hormone involved in the physiological maintenance of blood volume and arterial blood pressure (Dietz, 2005). Secretion of ANP is most importantly governed by

mechanical stretching of the atria rather than several vasoconstrictors when extracellular fluid or blood volume is elevated (Dietz, 2005).

Conducting pacemaker cells: The pacemaker cells (Fig. 5) are specialized cardiomyocytes that generate and conduct electrical impulses. They comprise 1% of the cells of the heart. They are much smaller than the contractile cells, have fewer myofilaments running in all directions but they are not organized into myofibrils (Katz, 2010). A group of pacemaker cells at the junction of crista terminalis and veins forms cardiac pacemaker called SA node which has more rapid firing rate and directly in contact with atrial fibers.

The action potential propagates from SA node to atria and then to AV node located between atria and ventricles in the area of the tricuspid valve and to ventricles via a specialized conduction system that coordinates the rhythmic contraction of the heart (Sartiani et al., 2011). The electrical impulses spread from AV node to AV His bundle which can then be divided into right and left bundle branches to give terminal part of conducting system (Purkinje fibers). The Purkinje fibers are larger with few myofibrils and rich in glycogen.

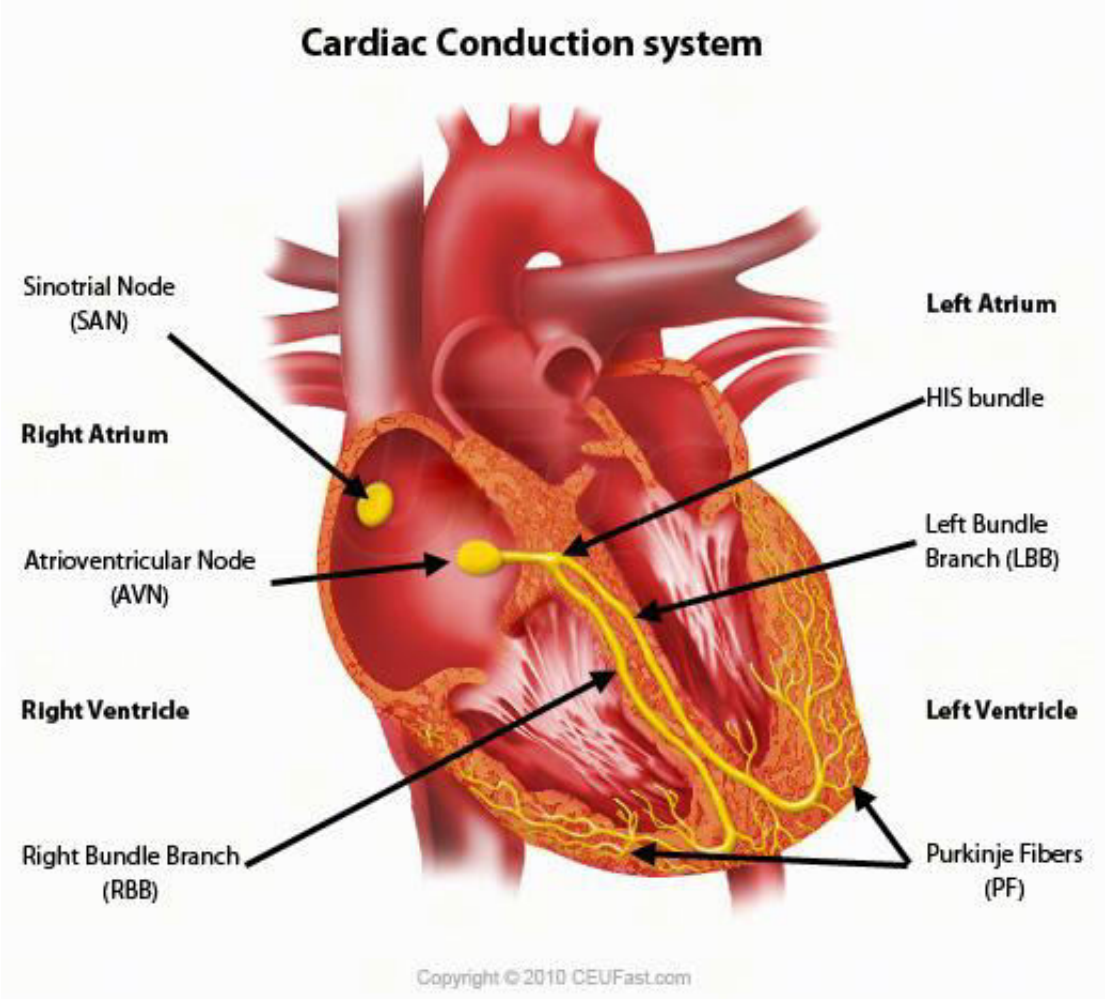

Figure: 5. Cardiac conduction system: This system is formed by specialized cardiac muscle cells (SA node, AV node, Bundle of His, Bundle branches, and Purkinje fibers) in the cardiac wall that send signals to cardiomyocytes result in contractility (Thomas, 2015).

The vascular smooth muscle cells (VSMC): Cardiac tissue is highly vascularized (Nam et al., 2013). The majority of blood vessels wall is comprised of VSMC. Myocardial infarction results from a blockage of a major coronary artery that closes the delivery of nutrients and oxygen to myocardium leading to cardiomyocytes necrosis (Montgomery et al., 2014). The vascular smooth muscle cells provide structural integrity of veins and regulate the caliber of the blood vessels in the body by contraction or relaxation in response to vasoactive stimuli (Metz et al., 2012).

The connective tissue cells: Heart myocytes are entangled in a complex array of connective tissue structures arranged in various levels of organizations, such as epimysium, perimysium, and endomysium (Robinson et al., 1988). They surround the

entire muscle, group of cells, and surround and interconnect individual cardiac myocytes, respectively. They also contribute to heart tensile strength and stiffness (Katz, 2010). The number of connective tissue cells increases with heart weight (Kohl, 2003). SA node contains many connective tissues, mainly collagen, and fibroblasts. More than 50% of the cells of the heart are cardiac fibroblast (Xin et al., 2013).

Many studies are showing the possibility of conversion of human fibroblast into functional cardiomyocytes. Programming somatic fibroblasts into alternating lineages provide a promising source of cells for regenerative therapy (Cao et al., 2016) through chemically induced cardiomyocyte-like cells that can uniformly contract and resemble human cardiomyocytes in their transcriptome, epigenesis, and electrophysiological properties (Cao et al., 2016). Cardiac fibroblasts play also a role in the regulation of myocardial proliferation through β1 integrin signaling (Ieda et al., 2009).

The endothelial cells: The heart contains not only cardiomyocytes but also other cell types such as endothelial cells (Zhang and Shah, 2014). The endothelial cells tightly attach squamous cells, construct the complex cavitary surface of the cardiac wall completely lined by endocardial endothelium (Brutsaert, 2003), and the interior lining of blood vessels and cardiac valves (Xin et al., 2013). The endocardial endothelium is recognized as a sheet of endothelial cells with a central nuclear bulge and extensive intracellular junctions (Brutsaert, 2003). The endocardial endothelial cells are larger than endothelial cells in most other portions of the circulatory system.

Cardiac endothelial cells are also distinguished from myocardium by the expression of endothelial markers. They create an adaptable life-support system because blood supply depends on the function of endothelial cells. The intracellular clefts between endocardial endothelial cells are 3 to 5 times deeper than endothelial-myocardial capillaries (Brutsaert, 2003). The functional cross-talk among the cardiac endothelial cells and other cardiac cells types is important for normal cardiac function and disease state (Zhang and Shah, 2014).

The cardiac nervous tissue cells: Fifteen years ago, Pauziene and colleagues (2000), in their morphological study of human intracardiac nerves under electron microscope have shown the normal structure of intracardiac nerves as baseline information for assessing the extent of nerve damage both in autonomic and sensory neuropathies in the human heart. Many intracardiac nerves are covered by epineurium. The nerve diameter determines the thickness of epineurium and perineurial sheath (Pauziene et al., 2000).

The perineurial sheath is varied from nerve to nerve and containing up to 12 layers of perineurial cells. The presence and complexity of the coats in the human intracardiac nerves and the blood supply of nerves depend directly on nerve diameter (Pauziene et al., 2000). However, an individual nerve fiber covering, endoneurium, is variable and independent of nerve diameter. Both myelinated and unmyelinated axons are found in the heart. They show normal ultrastructure. The number of unmyelinated axons within unmyelinated nerve fibers is related to nerve diameter. Thin cardiac nerves have fewer axons (Pauziene et al., 2000).

Cardiac tissue engineering: The mammalian adult heart has limited or no regenerative and repair capacity (Xin et al., 2013), and many forms of heart diseases result from a deficiency in a number of cardiomyocytes (Rubart and Field, 2006). Because of a limited regenerative capacity of the adult mammalian heart, any myocardial cell loss is mostly irreversible and may lead to progressive ventricular dysfunction and heart failure (Caspi et al., 2007). However, to treat these problems many experimental studies have done cell-based regenerative therapies (Feric and Radisic, 2016).

Tissue engineering plays very important role in creating functional tissue constructs that can re-establish the structure and function of the injured myocardium (Vunjak-Novakovici et al., 2010). Repopulation of the damaged heart with new myogenic cells can be a potential alternative method to reverse cardiac diseases (Rubart and Field, 2006) by increasing the function of the failing heart (Caspi et al., 2007). This can be done in two ways: by direct transplantation of isolated cells into the dysfunctional myocardial areas, and by combining of in-vitro cells with polymeric scaffolds generating a tissue-

engineered muscle construct, following in-vivo engraftment of the engineered tissue (Caspi et al., 2007). Now a day, cardiac regeneration is also getting favorable approaches through a direct conversion or transdifferentiation of non-cardiac cells into cardiomyocytes by forced expression of transcription factors and microRNA (Fu et al., 2015).

1.2.4. Innervations of the heart

The peripheral nervous system is the part of nervous system outside brain and spinal cord. Physiologically, peripheral nerves are categorized in motor, sensory, and automonmic nerves (Chung et al., 2014). The heart receives the innervations of autonomic nerves (Fig. 6) (Mauro et al., 2009; Olshansky et al., 2008). These sympathetic and parasympathetic nerves originate from thoracolumbar and craniosacral aspects of the spinal cord, respectively. They exchange information between CNS and the heart (Kukanova and Mravec, 2006).

The sympathetic nerves supply the heart by the sympathetic chain/gangliated cord, while the parasympathetic through the vagi (CNX) (Mauro et al., 2009). The cardiac sympathetic nerve fibers are located subepicardial and travel along the major coronary arteries. They represent the predominant autonomic component in ventricles. The sympathetic nervous system has a variety of cardiovascular actions; including acceleration of heart rate, increase the force of cardiac contractility, constriction of resistance vessels, and reduction of venous capacitance (Triposkiadis et al., 2009).

The parasympathetic nerve fibers are subendocardial and run with the vagus nerve, and present mainly in the atrial myocardium (Triposkiadis et al., 2009). The parasympathetic nervous system works by slowing heart rate through vagal impulses, decreasing the cardiac contractility, and dilating the coronary resistance vessels (Triposkiadis et al., 2009).

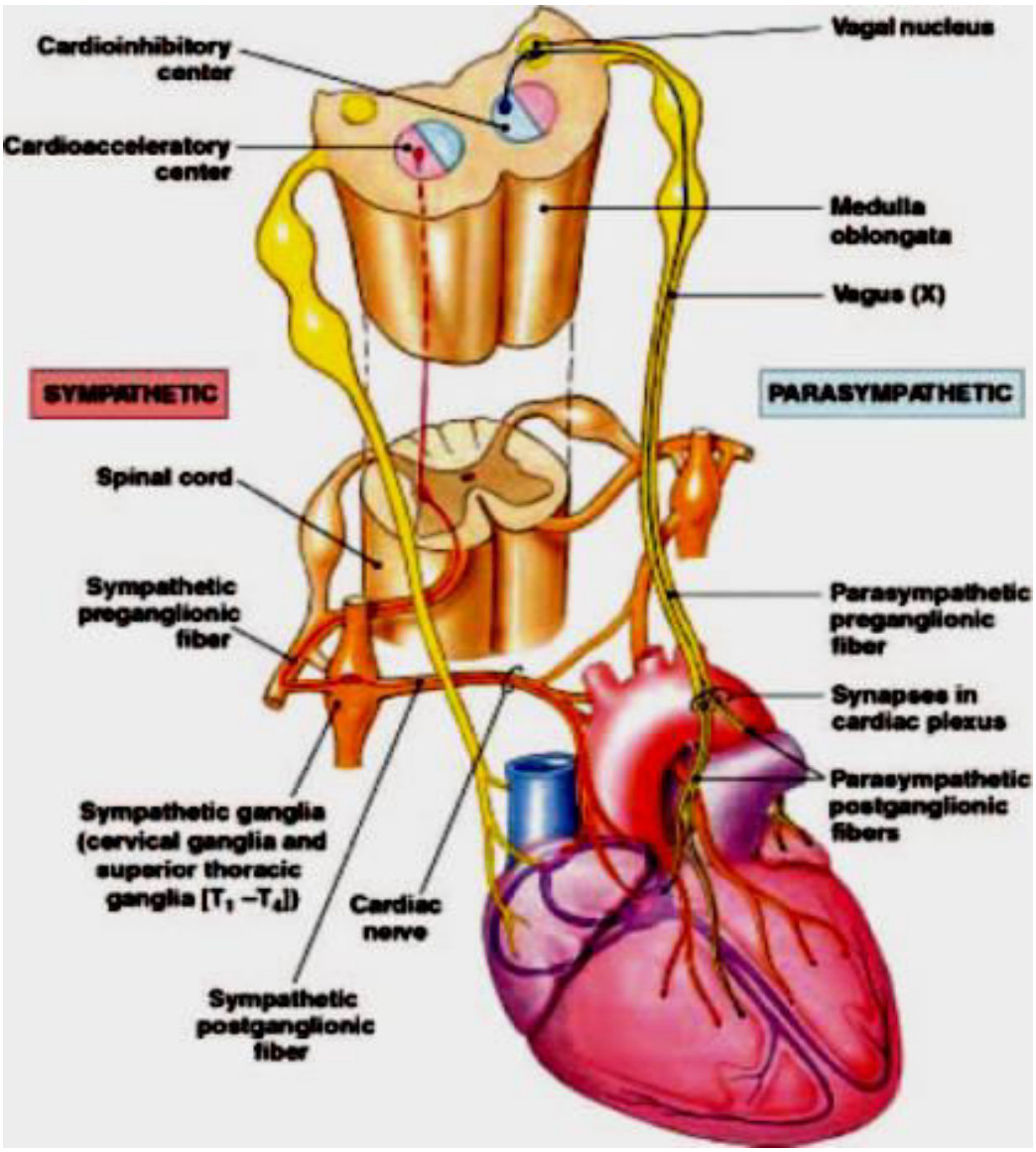

Figure: 6. Schematic illustration of cardiac autonomic innervations: The SA node is innervated by parasympathetic (vagal) and sympathetic fibers. Sympathetic efferents nerves are found throughout the atria (SA node), ventricles and in the cardiac conduction system. Reproduced from Olshansky et al., (2008).

Extracardiac innervations of the heart: The extra-cardiac nervous system includes pre- and post-ganglionic sympathetic and parasympathetic nerves (CNX). The preganglionic sympathetic nerves originate in the lateral gray columns of the spinal cord, while postganglionic sympathetic nerves originate in cervical and stellate sympathetic ganglia (Kawashima, 2005). The overall effect of sympathetic activation is to increase cardiac output, chronotropic (heart rate), dromotropic (conduction velocity), inotropy

(contractility), lusitropy (myocardial relaxation) and bathmotropic (excitability) of the heart (Klabunde, 2011; Triposkiadis et al., 2009).

The parasympathetic nervous system controls the heart through vagi nerves which originate from the brainstem. The parasympathetic ganglia are located proximal to or within the target organ (Mauro et al., 2009). Activation of the parasympathetic system affects heart performance via opposing fashion (Vaseghi and Shivkumar, 2008; Triposkiadis et al., 2009).

Intracardiac nervous network: Structural and functional complex nervous network of the heart is made by the interactions of neurons within intracardiac ganglia together with interconnections of individual ganglia (Kukanova and Mravec, 2006; Brack, 2015; Ardell, 2004). The intracardiac neurons are concentrated in multiple heart ganglia and play a significant role in the regulation of heart activity (Kukanova and Mravec, 2006; Brack, 2015).

The intracardiac nervous system amalgamates information from different neurons such as sympathetic and parasympathetic postganglionic, sensory afferent fibers, local interneurons, and paracrine signals that are mast cell signals (Hardwick et al., 2009). The communication of these intrinsic neurons works as a complex nervous network (plexuses and ganglia) in the heart (Kukanova and Mravec, 2006; Brack, 2015; Ardell, 2004). This intricate intrinsic network of neurons is called "little brain" in the chambers of the heart.

This "little brain" comprises spatially distributed sensory (afferent), interconnecting (local circuit) and motor (adrenergic and cholinergic efferent) neurons under the tonic influence of central neuronal command and circulating catecholamines (Armour, 2008). The complex intra-cardiac nervous network together with extracardiac neurons innervates and modulates the activity of the heart during both physiological and pathological conditions (Kukanova and Mravec, 2006).

1.2.5. Vascular structure

Vascular system is part of circulatory system and function to transport blood, lymph, nutrients, gases, hormones, and blood cells to and from cells to provide nourishement, facilitate fighting diseases, regulate temperature and pH, and maintain homeostasis. The cardiovascular system can be divided into four major components: the heart, the macrocirculation, the microcirculation, and the lymph vessels. The macrocirculation comprises all vessels (arteries and veins) (Young et al., 2006).

The inner lining is the endothelium surrounded by subendothelial connective tissue. A layer of vascular smooth muscle is well developed in arteries. The outer layer (Adventisia) contains nerves that supply muscular layer and nutrients capillaries in the larger blood vessels (Kupinski, 2017)

The blood vessels except capillaries comprise of these three main layers: Tunica intima, tunica media, and tunica adventisia. The tunica intima (interna) contains endothelial lining and its basal lamina, and a delicate layer of loose CT (loose CT, longitudinal oriented fibers). An internal elastic membrane delimits the outer margin of the tunica intima.

Tunica media (media), which is the thickest layer in arteries composed of circularly arranged layer of smooth muscle cells, and has variable amount of laminae/elastic and reticular fibers.

Tunica externa (adventisia) consists of fibroelastic connective tissue (collagen and elastic) its fibers occur in longitudinal array. The external elastic membrane separated the tunica adventisia from tunica media. It is the thickest layer in veins and contains vasa vasorum and nervi vasculares in large vessels (Fig. 7).

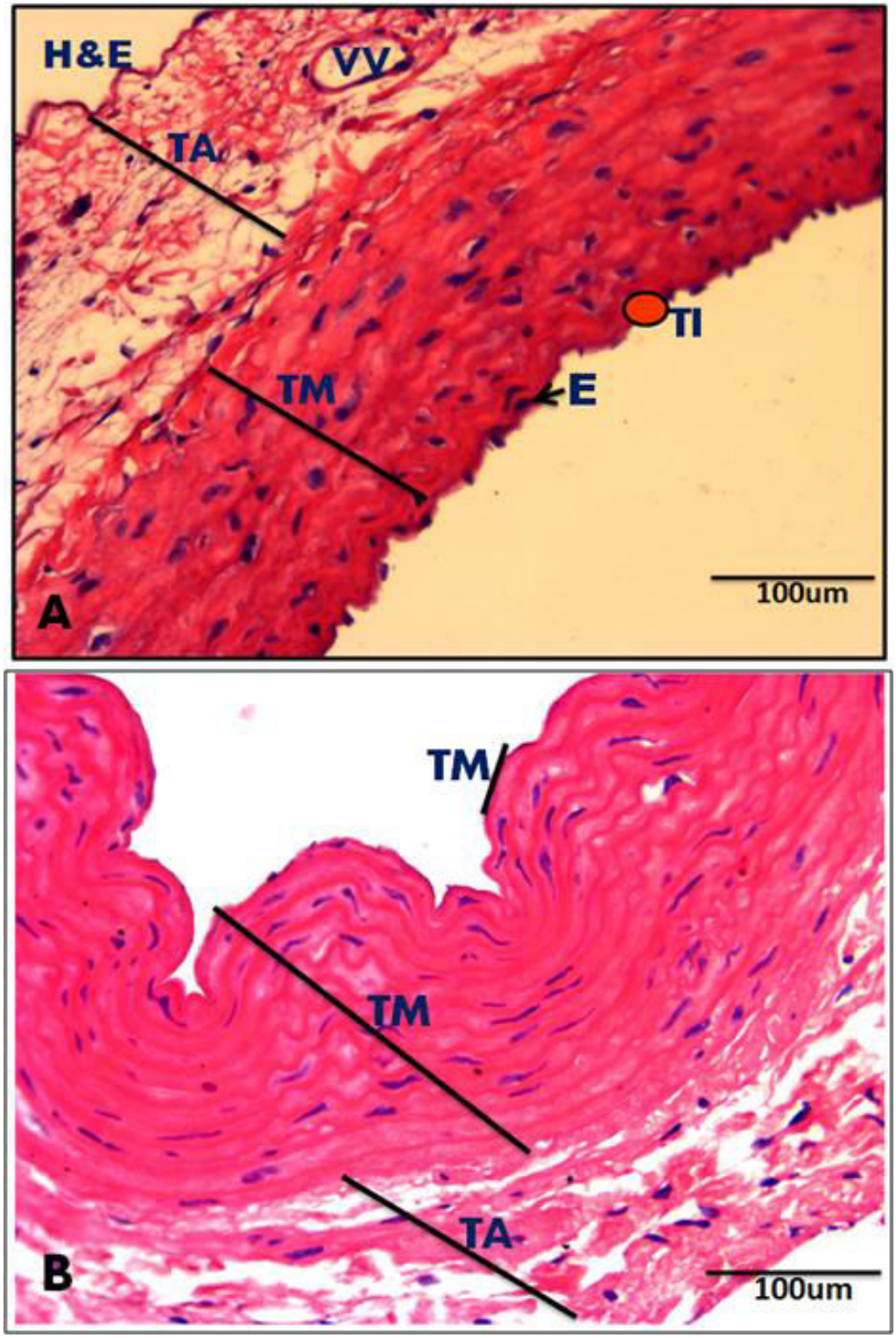

Figure: 7. Histological demonstration of layers of blood vessels: The section was taken from pulmonary artery (Fig 7. A) and aorta (Fig. 7. B) of rat. E, Endothelium, TI, Tunica intima; TM, Tunica media; TA, Tunica adventisia; VV, Vasa vasorum; H&E, Hematoxylin and Eosin. Scale bar = 100um.

CHAPTER TWO

2. Characterization of classical opioid receptors in orthotopically transplanted heart in human

2.1. Introduction

The opioid receptors are modulated by autonomic innervations, play roles in neural transmission and regulation of cardiomyocytes physiology (Sobanski et al., 2014) in the heart. However, transplanted heart is devoid of sensory, sympathetic and parasympathetic innervations (Valerio et al., 2014; Arrowood et al., 1997) and this might contribute for the down-regulation of these receptors in the denervated heart.

Therefore, this study aimed, to characterize opioidergic system specifically classical opioid receptors (μ, δ, and κ) at protein, mRNA, and level of fragmented DNA (apoptotic level) in orthotopically transplanted heart, to evaluate the impact of denervation using a sensory neuronal marker. Moreover, it identified the eventual occurrences of any associated cardio-pathological changes and possible signs of acute cellular rejections.

2.1.1. Heart transplantation and its brief history

Heart transplantation (HTx) is a life-saving surgical procedure in which a diseased heart or refractory end-stage heart failure is replaced with a donor`s healthier heart (Lee and Hong, 2014; Strecker et al., 2013; American Heart Association, 2009; Miniati and Robbins, 2002) to prolong survival (Lee and Hong, 2014; Strecker et al., 2013; American Heart Association, 2009) and to improve the quality of life for recipients (Miniati and Robbins, 2002; Hervàs et al., 2004). However, it is not a cure for heart disease (Burch and Aurora, 2004).

A cardiac allograft can be sewn in either a heterotopic or an orthotopic position. For this study, we used cardiac allograft sewn in orthotopic position (Fig.8A, 8B, 8C) for its easier approaches to obtain an endomyocardial biopsy, lesser pulmonary compression of the recipient and lesser need for anticoagulation. However, heterotopic transplantation is

an excellent technique for patients with severe pulmonary hypertension (Botta et al., 2016). Orthotopic heart transplantation is performed either with the classic/standard/traditional/ShumwayLower/biatrial technique or as a bicaval/total anastomosis (Botta et al., 2016; Davies et al., 2010).

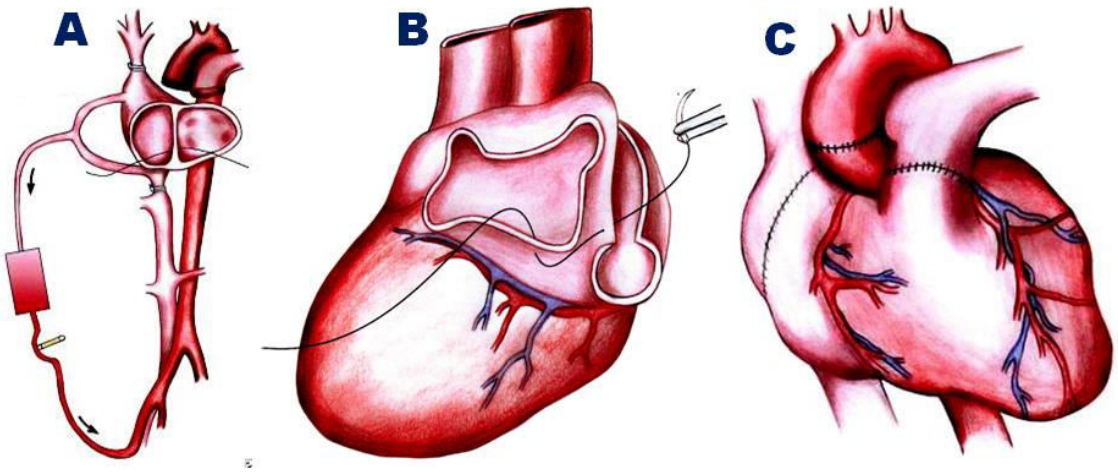

Figure: 8. Illustration of recipient's, donor`s, and complete heart transplantation: (Fig. 8A, B, and C) (Modified images from Botta et al., 2016; Heart transplantation technique, the heart.org. Medscape).

The history and development of cardiac surgery span 117 years to date (DiBardino, 1999). Even though the first heart cross-species transplantation (xenotransplantation) in human by using Chimpanzee heart performed by Hardy in 1964 (Cooper, 2012) which survived the patient for 2 hours, the advanced HTx we notice today started in an operation carried out by Barnard in 1967 at Groote Schuur Hospital that enables the recipient (53 yr old, Lewis Washkansky) to survive for only 18 days. It was recorded as World`s first human-to-human orthotopic HTx (Brink and Hassoulas, 2009).

Cardiac transplantation was full of challenges that have been overcome with many studies (DiBardino, 1999), advanced surgical procedures, such as the development of endomyocardial biopsy technique for diagnosis of acute rejection (Caves et al., 1974), understanding of immunology and rejection, pharmaceutical development with the discovery of anti-rejection medication (Cyclosporine and Tacrolimus); and clinical

management and better selection of donors and recipients (Lee and Hong, 2014) and myocardial protection. This overall advancement improves survival rates.

Studies on cardiac receptors which are known to be involved in cardioprotection are crucial for the understanding of the survival of denervated heart. However, the presence and the correlation between the opioid system and the defect of cardioprotection in transplanted heart are unclear. For this reason, we designed qualitative and quantitative methods to test the expressions of opioids receptors in heart of cardiac recipients, so as to investigate their pharmacological role and relationships in transplanted and innervated heart and to provide information about the levels of opioid receptors in the denervated heart.

In HTx, the two important common elements and objectives are avoiding potential risks such as rejection and infection brought by over-immunosuppression in recipients to help cardiac recipients (Budde et al., 2011, Valerio et al., 2014). Rejection is the major barrier to successful transplantation (Wood and Goto, 2012). As it is mentioned by Hammond and colleagues 1989, there are three patterns of allograft rejection which are designated as cellular, vascular/humoral, and mixed rejection.

Acute cellular rejection (ACR) is the most common in the first six months after HTx and is predominantly T-cell-mediated (Patel and Kobashigawa, 2006; Taylor et al., 2010). Just about 20 to 40% of recipients experience at least one episode of ACR in the first postoperative year (Patel and Kobashigawa, 2006). The number and severity of acute rejection episodes have been correlated with the development of cardiac allograft vasculopathy (CAV) and mortality.

The inflammation and cell death associated with acute rejection, first leads to myocardial edema that increase myocardial stiffness and diastolic dysfunction and if it is left untreated eventually leads to systolic dysfunction (Taylor et al., 2010). Standard cardiac biopsy rejection grading consensus first published in 1990 by ISHLT and eventually

updated in 2005 (Table. 3) used for scaling level of rejection in transplanted heart specimens in this study.

Table: 3. Standard cardiac biopsy grading

Grades	Features
Grade 0	No rejection
Grade 1 R, mild	Interstitial and/or perivascular infiltrate with up to 1 focus on myocyte damage
Grade 2 R, moderate	Two or more foci of infiltrating with associated myocyte damage
Grade 3 R, severe	Diffuse infiltrate with multifocal myocyte damage ± edema ± hemorrhage ± vasculitis

Note: "R" represents revised grade. Reproduced from Stewart et al., 2005; American Medical Association, 2014.

2.1.2. Epidemiology of heart transplantation

In the globe, approximately 3,500 heart transplants are performed every year (Cook et al., 2015). Data reported by Bouwman et al., 2013, a total of 31, 165 organs transplants were performed in the European Union countries in 2013. Organ transplantation consistently increased from 2004 to 2013 except a slight decline in 2008 and 2012 due to a shortage of donors (Matesanz, 2016). From 63,800 patients placed on organs` waiting lists about 3,400 patients have been heart waiting lists in 2012 (Matesanz, 2016).

In nineteen centers of transplant in Italy, 733 patients waiting for a heart transplant and out of 94 mortalities have been registered in 2011 (Bouwman et al., 2013). It is also reported that 4.6 and 3.8pmp rate of the heart transplant in 2011 and 2012, respectively, (Matesanz, 2011) in Italy. According to American Heart Association, Statistics reports, 2,192 and 2,125 the heart transplants performed in 2006 and 2005, respectively with 72.3% (male) and 67.6% (female) five years' survival rate as of 2007 in the United States (Tagerman et al., 2009).

2.1.3. Physiology of denervated heart

Heart activity is modulated by means of the autonomic nervous system, intrinsic regulatory mechanisms, and humoral factors (Kukanova and Mravec, 2006). Even though autonomic nervous system modulates the heart, transplanted heart is completely devoid of sensory, sympathetic and parasympathetic innervations (Valerio et al., 2014; Arrowood et al., 1997). However, few pieces of evidence indicate that with time some degree of sympathetic and parasympathetic re-innervations is progressively reestablished (Gómez-Ríos, 2012; Swami et al., 2011).

Cardiac physiology of transplanted heart is unique because the transplanted heart doesn`t provide the recipient with normal cardiac function (Cotts and Oren, 1997) due to alterations of afferent control mechanisms and efferent responses which lead to clinical abnormalities such as changes of cardiac electrophysiology, cardiovascular responses to exercise, and responses to cardiac pharmacologic agents (Cotts and Oren, 1997) Table: 4.

The most obvious alteration in hemodynamics of allograft recipients is the increase heart rate occurs due to the loss of resting vagal tone, which normally suppresses the intrinsic heart rate (Hosenpud et al., 1991) and as a result of afferent denervation of the myocardium ischemic myocardial pain is absent. Therefore, transplant recipients with severe vasculopathy and myocardial infarction are usually pain-free (Hosenpud et al., 1991). The difference in automatism, conduction and refractoriness between recipients and transplanted hearts are attributable to differences in the hemodynamic situation to denervation (Alvarez et al., 1990). It is also mentioned that the extensive cardiac sympathetic denervation that involves severe lateral ventricular wall in idiopathic Parkinson disease (Wong et al., 2012).

Table: 4. Physiological changes of denervated heart

SN	**Normal heart**	**Transplanted heart**
1	Innervated	Denervated/Loss of resting vagal tone
2	The nerves from the CNS supply connections to the heart	The nerves from the CNS don`t supply connections to the heart.
3	Responds to exertion by quickly increasing its rate after nerve supply	Doesn`t need connections to pump effectively
4	Presence of ischemic myocardial pain	Absence of ischemic myocardial pain
5	Increase it rate due to innervations from connections	Increases it rate only after catecholamines (e.g. adrenalin) are released and circulated through the blood to the heart
6	Increases its rate more faster with exertion and decreases its rate more faster with rest; faster recovery period	Increases its rate more gradually with exertion and decreases its rate more gradually with rest; slower recovery period.
7	Normal atrial contribution to SV	less atrial contribution to stroke volume/SV
8	Resting heart rate (60-100bpm)	Resting HR is faster (95 to 110 bpm)
9	Acceleration of HR is normal/faster during exercise depends on age and physical condition	Acceleration of HR is slower during exercise
10	Normal diastolic function with no rejection	The myocardium is stiff from some degree of rejection and possibly from denervation result in the moist common diastolic dysfunction
11		Autonomic cardiac denervation of the heart increase the incidence of ventricular arrhythmia (Mason et al., 1976) and play role in the genesis of malignant arrhythmic events (Rodrigues et al., 1996)
12		Cardiac response to psychological stress are altered by cardiac denervation (Shapiro et al., 1994)
13		Regional cardiac sympathetic denervation increases the risks to the antiarrhythmic drug (Yu et al., 2012)
14		Attributable to differences in the hemodynamic situation to denervation (Alvarez et al., 1990)

Alvarez et al., 1990; Mason et al., 1976; Yu et al., 2012; Shapiro et al., 1994; Rodrigues et al., 1996; Wong et al., 2012).

2. 2. Materials and methods

2.2.1. Human subjects and endomyocardial biopsy

In this study, three cardiac recipients from Department of Surgery, Cardiac Section and four cardiac recipients who have been following medical care at 30 days' post orthotopic heart transplantation were selected on their regular schedule from Department of Cardiology (UOC, USF) laboratory of Hemodynamics and Electrophysiology at University Hospital Integrated Verona - Ospedale Civile Maggiore (CMO) of Borgo Trento. All endomyocardial biopsies (EMBs, n = 9) were taken from septal part of right ventricle through the internal jugular vein approach. Control heart tissues (n = 10) were taken from the right atrium, septum, and left ventricle of patients who had been under surgical procedures for aortic valve surgery.

2.2.2. Surgical procedure of endomyocardial biopsy

Endomyocardial biopsy (EMB) is an invasive diagnostic procedure mainly used for rejection surveillance or immunosuppressive therapy survey after cardiac transplantation (Eisen 2008; Kilo et al., 2006), was used to take samples from cardiac recipients. The right internal jugular vein (RIJV) approach was used for the surgical procedure because it has a shorter operation and radiation exposure times than other approaches in cardiac recipients (Imamura et al., 2015; Fiorelli et al., 2011; Kilo et al., 2006). All recipients underwent EMBs by highly skilled and experienced cardiac biopsy experts.

Patients were placed in a supine position with extended neck and turned head to the left about 45% to facilitate venous puncture site. Conventional asepsis was applied to the skin of the surgical region of the neck and then surgical drapes were positioned at ease. The triangle vertex formed by sternal and clavicular heads of the sternocleidomastoid muscle and clavicle was served as a landmark to RIJV. Sonography of the neck was performed to evaluate diameter of the RIJV and demonstrate adjacent structures. The vein puncture was performed at the upper vertex of the triangle in ipsilateral nipple direction under local anesthesia (5 to 10ml of 2% Xylocaine/lidocaine) followed by insertion of a sheath/blunt cannula that passed over the guidewire in standard Seldinger technique.

The sheath was introduced with the help of guidewire. Under X-ray control, the appropriate position of guidewire was confirmed before the introduction of the sheath. After passing a sheath, the guidewire was withdrawn and the sampling device/bioptome was carefully threaded through the sheath into the internal jugular vein and advanced towards the right atrium, rotated to the left lateral side of the patient to direct through the right atrioventricular valve to ventricular septum. The bioptome's jaws were opened and touched the right ventricular wall and closed to take the specimen. Finally, the bioptome with the specimen was withdrawn slowly. After the procedure, the sheath was removed and external compression on the puncture site had been applied for a minimum of 30 min. All EMB specimens were obtained from the recipients` interventricular septum of the right ventricle through the internal jugular vein approach.

2.2.3. Tissue processing, embedding, and sectioning

After collection of EMBs and heart tissues were promptly and adequately fixed with 4% paraformaldehyde to produce superior morphology, washed three times for 10min each with phosphate buffer saline (PBS) (pH 7.35, 0.1M), and then dehydrated with increasing ethanol concentration (70% 1x, 90% 2x, 100 1x) for 1hr, $1^1/_2$ hrs, and 1hr each, respectively. Following dealcolization by two changes of xylene (100%) for 1hr, infiltrated with two changes of molten paraffin wax at 56^oc for 1hr to replace the xylene.

Next to infiltration, embedding was performed for better sectioning. In embedding step, the first small amount of paraffin was placed into the cassettes, and then specimens were transferred into the mold using warmed forceps and placed in the middle of the cassettes in preferred orientations, and then the cassettes were filled with molten paraffin wax with care to prevent under and over-filling. At the end, embedded specimens were put on ice, and stored in cold room at 4^oc overnight to form strong paraffin blocks. This paraffin embedded tissue processed for further IHC, IF, TUNEL, and H& E staining.

Once specimens embedded, they were cut into 3µm thickness sections using Leica RM 2255 CSA® US digital microtome. It is good to place blocks on ice prior to sectioning to

obtain unwrinkled sections. Sections were, floated on cold water bath and picked up by adhesion microscope slides (26x76MM, DIAMOND Blue, 33820B, Lot#300414, LABOINDUSTRIA S.P.A, IT) and FLEX IHC coated microscope slides with white-painted label area (Code: K8020, K802021-2, Wo503900201, 75mm, W x 25mm, D x 1mm, H), floated on a warm water bath to remove wrinkles of sections. Finally, the microtome cleaned with Vacuum Cleaner (Mode: AS10-A40, No. 0288112) and left in good condition.

2.2.4. Immunohistochemistry

Immunohistochemistry which is a key tool for the analysis of the localization of target molecules within tissues was used to evaluate DOR-1, KOR-1, MOR-1, and CGRP-1 immunoreactive cardiomyocytes and analyzed for relative distribution of ORs. In our immunohistochemical studies, immunoperoxidase and double immunofluorescence (IF) staining were done at a laboratory of Histology Section, Department of Neuroscience, Biomedicine, and Movement.

Markers used for detection of MOR-1, DOR-1, KOR-1, and CGRP-1, are the following: a rabbit polyclonal antibody (MOR-1, H-80: Cat. No. sc-15310), a rabbit polyclonal (DOR-1, H-60: sc-9111, Lot no. L2211), an affinity purified goat polyclonal (KOR-1, N-19: sc-7494, Lot: A2914) supplied from Santa Cruz Biotechnology, Inc, Europe, and a goat antibodies (CGRP-1, 1720-9007, Batch No. 051, BIO-RAD).

Immunoperoxidase staining: after mounted paraffin sections heated at 37^{o}C for 20min, immersed in 2 changes of xylene for 5min each and decreasing ethanol concentration. Sections on slides surrounded with a liquid blocker (PapPen) to prevent running away of the incubation solutions. Sections were washed in 1ml Triton X-10 in PBS and incubated for 20 min in H_2O_2 (30% J.T. Baker® lot no. 0625510001) in PBS to block endogenous peroxidase which is naturally found in the tissue that gives false positive background result when interacts with DAB staining to specific immunoperoxidase. Sections were pre-incubated for $1^1/_2$ hr in blocking solutions of 2% of Normal Horse Serum/NHS (S-

2000, Lot no. ZA0721), 0.25% Triton X-10 in PBS followed by incubated overnight in a rabbit polyclonal antibody (MOR-1, H-80: Cat. No. sc-15310), a rabbit polyclonal (DOR-1 (H-60): sc-9111, Lot no. L2211) and an affinity purified goat polyclonal (KOR-1 (N-19): sc-7494, Lot: A2914) primary antibodies (1^{o} Abs) at a 1:250 dilution rate in the following standard antibody diluents: 2% NHS, 0.25% Triton X-10 in PBS.

Following incubation in 1^{o} Abs, the sections were washed and incubated for 3hrs in secondary anti-rabbit IgG (H+L) biotinylated (BA- 1100, Lot no. ZA0319) made in horse for DOR-1 and MOR-1, and anti-goat IgG (H+L) biotinylated (BA- 9500, Lot no. Z0326) for KOR-1 and CGRP-1, diluted 1:1000 in PBS containing 2% NHS and 0.25% Triton X-10. Succeeding, 5min washes, avidin-biotin complex (The VECTASTAIN® Elite ABC Kit (Standard), Cat.No. PK-6100 Vector Laboratories, Inc. Burlingame, CA 94010 USA) in PBS was applied to the sections on slides for 1hr according to the manufacturer`s instruction. Finally, specific immunostaining was detected with DAB (Diaminobenzidine) in PBS containing 0.75% H_2O_2 and 3% nickel solution. Over-staining was controlled by applying PBS. The absence of the signal or specificity of staining was checked and confirmed by a negative control.

After sections dried overnight inside “CAPA” dehydrated with increasing ethanol concentration (50%, 70%, 80%, 96%, 100% and 100%). Ethanol was removed by two changes of Xylene (100%). Finally, drops of mountanat “Entellan" applied on tissue sections and covered with rectangular microscope cover glasses (ECN631-1574, Lot: 29339 017, 24x50mm), and prepared for analysis under a microscope.

Double immunofluorescence: this technique was also performed for the concurrent visualization of DOR-1 and KOR-1 immunoreactive signals on EMB of transplanted and control/innervated heart tissue sections. After removal of paraffin from sections using heat and xylene, rehydrated in decreasing alcohol concentration and distilled water. Following, a brief three times (5 min) wash in 1ml Triton X-10 in PBS, sections were pre-incubated for $1^{1}/_{2}$ hrs in 2% NHS and 0.25% Triton-X-10 in PBS and incubated

overnight in a solution of primary antibodies (DOR-1, Lot # L2211, H-60: sc-9111; KOR-1, Lot # A2914, N-19: sc 7494), 2% NHS and 0.25% Triton-X-10 in PBS.
Following overnight incubation, a brief 3 times 5 min wash (1ml Triton -X-10 in PBS) were performed, and then incubated for 3hrs in a mixture of Alexa Fluor 568 donkey anti-rabbit IgG (H+L) (1:1000, Ref. A10042, Lot no. 1668655, Eugene DR. USA) and Alexa Fluor 488 donkey anti-goat IgG (H+L) (1:1000, A11055, Lot no. 1627966, Eugene DR. USA) species-specific fluorescent secondary Abs raised in donkey supplied from Life Technologies, Italy, Europe with standard diluents 2% NHS and 0.25% Triton-X-10 in PBS. Thereafter, sections were washed with PBS and tap off excess rinsing solutions, and the nuclei stained bright blue with 4`, 6-Diamidino-2-Phenylindole (DAPI, 1: 100,000). Sections were washed three times for 5 min each and dried for 40 min in the dark at room temperature.

Finally, drops of mountant were added on sections and cover with rectangular microscope cover glasses (ECN631-1574, Lot: 29339 017, 24x50mm), Germany. The pressure was applied gently over glasses to remove bubbles before sealing of edges of cover glasses with nail polish and then stored at -20^{o}C until analysis was done by fluorescence and inverted confocal microscopes.

2.2.5. Hematoxylin and eosin staining for histopathological evaluation

The histological technique of routine H&E staining was performed to evaluate any eventual occurrence of structural abnormalities and level of acute cellular rejection in sections of EMBs. Levels of rejection of transplanted heart analyzed from sections stained with H&E with standard cardiac biopsy grading (Stewart et al., 2005) and the help of pathologists.

First, all staining solutions were prepared beforehand. The sections were immersed in a series of descending ethanol concentration (100%, 100%, 95%, 70%, and 50%) and dipped in 2 changes of distilled water for 2 min. The sections were immersed in hematoxylin solution for 1min. After washing with running tap water for 2 min, sections

were dipped in 2% eosin for 30 sec. Over-staining was controlled by washing with tap water. Sections were dehydrated with increasing alcohol concentration (95%, 100%, and 100%) for two min each and then ethanol was removed from the sections by two changes of xylene for 5 min because ethanol is not miscible with DePeX mountant ("Entellan"). Finally, sections were covered with cover glass and prepared for analysis.

2.2.6. Microscopy

Image acquisition of immunoperoxidase, TUNEL non-fluorescent, and H&E stained sections was done under Olympus System BX51 Universal research microscopy connected to both a computer and a camera (Camera-FAST 1394 QICAM) with different objectives (4X, 10X, 20X, and 40X) for immunoreactivity and pathological examination.

After sections processed for double immunofluorescence, laser scanning confocal microscopy (LSCM) technique was performed using laser scanning confocal microscope (Carl Zeiss LSM 510, Göttingen, Germany) at FIM 30% for obtaining multicolor optical images using drops of immersion fluid (Type F, Leica microsystems CMS GmbH, Ve = 46 cat. No. 115138559), Wetzlar, Germany at 40x obb. IMM magnification and 35.5um scale bar, and then images were extracted by Leica LAS AF Lite; Images were further synchronized by using ImageJ (Rasband, 1997-2015) and Leica software for better contrast.

2.2.7. Optical density measurement of immunoreactive myocytes

Prior to optical density (OD) measurement, slides were blindly assigned with code number and the thickness of the sections (3 to 3.5µm) was measured after processed by Stereoinvestigator. Thereafter, the mean of each sample of immunoreactive cells of the four sections was used for analysis.

Optical density measurement was done for DOR-1, KOR-1, MOR-1, and CGRP-1 strength of immunoreactivity using Figi version of ImageJ to quantify the strength of

immunoperoxidase staining in heart tissue sections of MOR, DOR, and CGRP-1 from images taken at 20X objective. Optical density/OD methods (Image-adjust, color-deconvolution/H DAB)-threshold with dark background) indicated by Jensen, 2013 was used with the following formula: OD = log (255 ÷ Mean Intensity).

2.2.8. Cryosectioning

Endomyocardial biopsy and heart tissue specimens were collected and placed in liquid nitrogen with drops of optimal cutting temperature (O.C.T.) medium in NALGENE® tube and stored at -80^{o}C until used. Tissues were pre-cooled at -21^{o}C and placed into cryostat (Leica CM 1900-V5.3 ENGLISH-10/2006) for 30 min prior to sectioning to attain thermal balance. The chamber of cryostat was set to -20^{o}C and 8µm thickness.

Freezing/cryostat embedding medium (Lot: 140410) was applied to cover the specimen plate/the round metallic mount of the cryostat. When the medium began to frost, tissues were placed in the center as straight as possible horizontally. Once the media was completely frozen, the specimen plate was placed into holder and knob was turned clockwise to tight it. The blade was pre-cooled to -20^{o}C and placed onto the stage with maintained O.C.T before cryosectioning. The tissues were cryosectioned at 8µm and 20 sections were collected with sterile Eppendorf tube and sections were kept inside the cryostat machine on ice to keep cold while continuing to cryosectioning, and then immediately stored at -80 ^{o}C until the commencement of the experiment (Rüegg and Meinen, 2014; Peters, 2010). Finally, the blade, all trimmings, and specimen wastes were removed, and the machine was left in a clean and safe condition.

2.2.9. RNA isolation

Frozen sections (10mg) were taken on the ice and homogenized by adding 200µl TRIzol to each tube and centrifuged at 4^{o}C for 6 min and lysis cells by vigorously pipetting few minutes with a syringe needle. The pipette samples were centrifuged at 12,000rpm for 10min and then the clear supernatant homogenate transferred to each new Eppendorf tube

(190µl), and the bottom insoluble materials (10µl) was discarded. Chloroform (40µl) was added to each Eppendorf tube and shook vigorously by hands and then pre-incubated for 2 to 3min at RT before centrifuged at 12, 000rpm for 15min at 4 ^{o}C. The upper aqueous supernatant was transferred to new Eppendorf tube without disturbing the lower organic part.

Isopropanol (100ul) was added to each tube and incubated at RT for 10min. Following 10min centrifugation at 12,000rpm, the supernatant was discarded except the small pellet at the bottom. Afterward, 200µl of 70% of ethanol was added and centrifuged at 12,000rpm for 10min and then RNA formed a gel-like pellet on the bottom side of the Eppendorf tube. The ethanol supernatant and any residual ethanol were removed by pipetting. The RNA-pellet remained at the bottom and further air dried for 10min. 20µl RNase-free water was added to resuspend the RNA-pellet and incubated at 60^{o}C for 10min in a water bath. Finally, RNA concentration was measured by Nanodrop (2000/2000c) and stored at -80^{o}C until required. The total RNA preparations were used for RT-qPCR.

2.2.10. Synthesis of cDNA

cDNA synthesis was done using the protocol and cDNA synthesis kit obtained from SIGMA® Saint Louis Missouri 63103 USA. The following reagents were added to a thin-walled 200µl PCR microcentrifuge tube on ice in the first mix: RNA template (0.25µg/µl FC, SIGMA), deoxynucleotide mix (dNTPs), random nonamers and water for a total volume of 10µl. The mixes were centrifuged gently and briefly to collect all components to the bottom of the tubes, and tubes were placed in the thermal cycler at 70^{o}C for 10min.

After 10min, tubes were removed from thermal cycler and placed on ice, centrifuged and the following second mixes were added: a 10x buffer for eAMV-RT (2µl), enhanced avian RT (1µl), RNase inhibitor (1µl), water (6µl). Finally, 20µl of reaction tubes at 25^{o}C for 15min, and placed in a thermocycler at 50 ^{o}C for 10min. The cDNA concentration was measured by Nanodrop and stored at -80^{o}C until required. Afterward, cDNAs were

diluted in 50ul water. One ul of this reaction mix was used as a template for RT-qPCR using the SYBR Green protocol with the readymade SYBR®Green qPCR ReadyMix™, with ROX™ 2X (KCQS02).

2.2.11. Quantitative Real-Time PCR

The readymade SYBR®Green qPCR ReadyMix™, with ROX™ 2X (KCQS02) that contains all components except primers and cDNA template was used. Following primer mix for DOR, KOR (Sigma), and GAPDH (Invitrogen, 059901, M5583 (A02, A01), mixed with ROX, and then appropriately added to each well with sample mix in four duplicate. Amplification didn`t exceed 200bp. SYBR®Green dye that binds to the minor groove of dsDNA and detects any dsDNA generated during amplification was done using Applied Biosystems 7300 Real Time System instrument. Finally, the green fluorescence light emitted when bound to dsDNA was measured for proper PCR amplification, and then the data calculated by the delta-delta method indicated by Livak and Schmittgen, 2001).

Table: 5. Primer sequence used for real-time PCR SYBR Green amplification

Gene	Forward human (5`-3`)	Reverse human (5`-3`)	Product size (bp)
OPRD1	AACTGAGTCCTTAAACAGGG	CTCCAAGTTAGAAACCGAAG	76
OPRK1	CGATACACAAAGATGAAGACAG	AAGTAGACCGTACTCTGAAAG	165
GAPDH	ATCAGCAATGCCTCCTGCAC	TGGTCATGAGTCCTTCCACG	

2.2.12. Terminal deoxynucleotidyl transferase, 2`-deoxyuridine 5`- Triphosphate Nick End Labeling (TUNEL) Assay

TUNEL assay is the most widely used method to detect apoptotic nuclei of a cell within tissue samples. Apoptosis is a part of normal development and carefully regulated process but ultimately result in cell death. The study of apoptosis is very important because modifications of these processes have been implicated in cancer, autoimmune diseases, and degenerative conditions. The whole mark of late apoptosis is the fragmentation of DNA. To detect DNA fragmentation, a specialized DNA polymerase (terminal deoxynucleotidyl transferase/TdT) slots-in unlabeled and fluorescently labeled nucleotide 2`-deoxyuridine 5`- triphosphate (adds dUTP) at the end of the fragmented DNA. The TdT is, template independent nucleotide addition enzyme, recruited a lot when

there is a breakdown of double stranded DNA. If there is a breakdown of DNA, i.e. cells are undergoing apoptosis. The apoptosis can be, correlated with the amount of TdT active inside the cell, measured by the fluorescein-dUTP from double-stranded breaks.

In this study, all TUNEL staining solutions were prepared ahead. The sections were dewaxed and rehydrated in a series of two changes of xylene (5min), descending ethanol concentration (100%, 100%, 95%, 80%, 70%, and 30%, 5min), and two changes of distilled water (2min). Slides were heated for 10min at 60^{o}C. Following brief 3 cycles washing in PBS, sections were incubated with Proteinase K/0.1% triton (100X) and then slides were rinsed twice in PBS. After PBS was wiped, sections were circled around by ImmEdgesTM Pen (Cat. No. H-4000, Vector Laboratories, Inc, Burlingame, CA 94010). During treatment, TUNEL solutions were prepared and equilibrated using In Situ Cell Death Detection kit, AP (ref. 11684809910, Version 11, Roche Diagnostics Indianapolis IN, USA) containing vial 1, 2 & 3 as follows: 100ul of labeling solution (vial 2) was taken to two negative controls to assess reagent performance and 50ul of enzyme (vial 1) enzyme was added to the remaining labeling solution.

Tissue sections were incubated for 1hr in a mixture of vial 1 and vial 2 at 37^{o}C. DNase I recombinant (1500U/ml, from Bovine pancreas, REF. 04536282001, Lot# 18831000, Roche, Germany) was diluted with 50mM Tris, 10mM mgcl2, and 1mg/ml Albumin, from bovine serum/BSA, Lot#119K1526, A3912-50G, Prod. 1000784619, Sigma, Life Science, the USA for positive control and incubated for 10min at RT. Hoechst (33342 nucleic acid stain, trihydrochloride trihydrate) for a cell-permeant nuclear counterstain that emits blue fluorescence when bound to dsDNA was used.

At this stage following a brief washing in PBS, analysis was done in a drop of at excitation wavelength (500nM) and detection in the range of 515-565nM (Green) under fluorescent microscope (EVOS® imaging system, Thermo Scientific Brand, ZP-PKGA-0665, Pub. No. MAN0007716, Rev.1.0, 2013, Life Technologies) with drops of PBS on sections using slide holder (AMEP-VH001). Converter (vial 3) was added to each section and incubated for 30min at 37^{o}C, and then washed with PBS. The substrate (BCIP/NBT-

Liquid substrate system, Cat. No. B1911, Sigma-Aldrich)/Novex®AP Chromogenic substrate (BCIP/NBT, Lot#02054161, Invitrogen by Life Technologies, Part no. 100002902, USA) was added to sections and incubated for 10min, and then counterstained with hematoxylin, mounted and covered with coverslip prior to analysis by light microscopy.

2.2.13. Study setting and ethical issue

This qualitative immunohistochemical experiment and cell counting were conducted at the Department of Neuroscience, Biomedicine, and Movement. RT-q PCR was performed at LURM and Laboratory of Cardiovascular Sciences. All experiments were carried out with the authorization of ethical Research Committee at University of Verona and MOH.

2.2.14. Statistical analysis

Mean value of positive cells ± SD in each group and independent samples t-test for the significance of means of independent groups of a number of KOR-1 and DOR-1 immunopositive cells of transplanted and control heart were used for statistical analysis using IBM Corp. Released 2011 IBM SPSS® Statistics for Windows, Version 20.0. Armonk, NY: IBM Corp software. Microsoft office Excel 2007 was also used to extract line graphs. P value < 0.05 was regarded as statistically significant. For relative quantification of real-time PCR data, the $2^{-\Delta\Delta Ct}$ method mentioned by Livak and Schmittgen 2001 was used.

2.3. Results

2.3.1. Histopathological observation of H&E stained endomyocardial biopsy of orthotopically transplanted and control heart tissue sections

Histopathological data of control heart tissue sections (CHT) (Fig. 9. A, C, E, G, I) demonstrated normal morphology except wavy shaped fibers histopathological changes (Fig. 9. C). However, Septal part of right ventricle endomyocardial biopsy sections (Fig. 9. B, D, F, H and J) of transplanted heart showed mild cellular rejection (Grade 1 R) based on ISHLT, 2005 updates as compared to CHT sections. The mild cellular rejection was demonstrated by interstitial, scattered and perivascular lymphocytes infiltrate without distorting the normal morphology of myocytes (Fig. 9. B, F, H and J). In addition to scattered, perivascular and interstitial lymphocytes infiltrate focal cardiomyocytes necrosis was shown (Fig. 9.D).

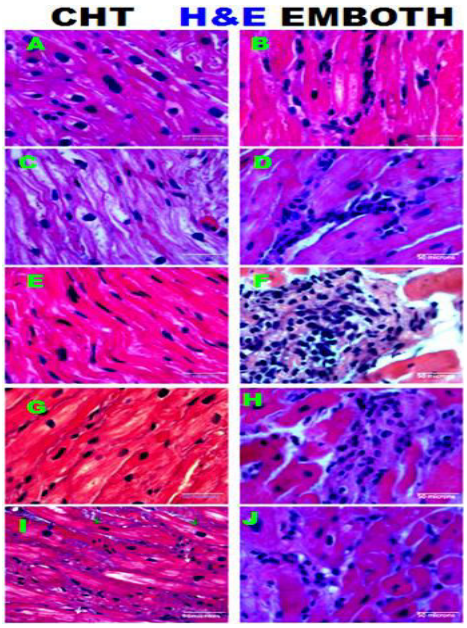

Figure: 9. T-cell-mediated rejection of and lymphocytes infiltrate in endomyocardial biopsy sections in orthotopically transplanted heart: the above figure hematoxylin and eosin stain tissue sections (Fig. 9. B, F, H, J) illustrated myocardial biopsy from septal part of right ventricles of human transplanted heart showing mild cellular rejection represented by interstitial, scattered, perivascular lymphocytes infiltrate, and (Fig. 9. D) focal necrosis. Control heart tissue sections (Fig. 9. A, C, E, G, and I) showing the normal morphology of cardiomyocytes except wavy shaped fibers and hyperplasia (Fig. 9. C), mild degenerative aspects (Fig. 9. A, E). H&E, Hematoxylin and Eosin; EMBOTH, Endomyocardial biopsy of orthotopically transplanted heart; CHT, Control heart tissue. Images acquired at 200x magnification. Scale bar 100 µm

2.3.2. Immunoperoxidase stained MOR-1 immunoreactive myocytes and its optical density in endomyocardial biopsy after 30 days of orthotopically transplanted heart

MOR-1 is a GPCR for β-endorphin, morphine and other opiates. It inhibits neurotransmitter release. In our qualitative data, immunoperoxidase stained MOR-1 immunopositive myocytes were observed both in orthotopic transplanted and control human heart (Fig. 10). Even though MOR-1 immunoreactivity was observed in both groups (EMBOTH and CHT) and didn`t reach a significant threshold P>0.05 in its OD immunoreactivity, analysis of MOR-1 immunoreactivity OD reduced in EMBOTH (0.18±0.02) compared to CHT sections (0.244±0.15).

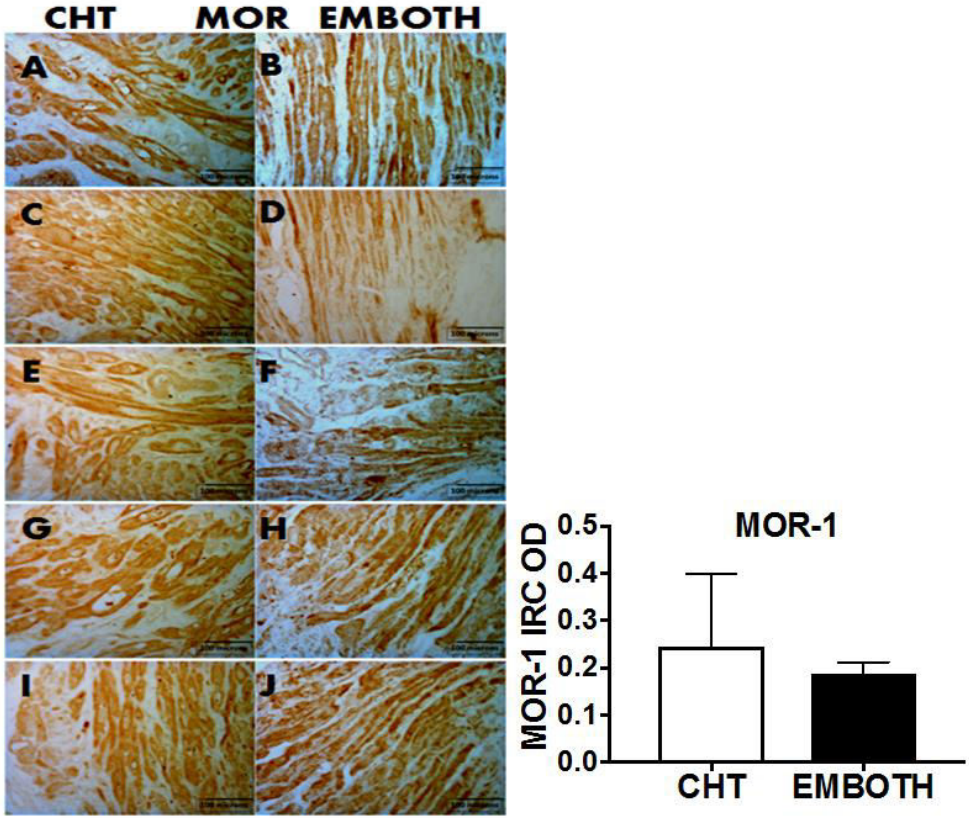

Figure: 10. Representative images of MOR-1 immunoreactive myocytes in endomyocardial biopsy of orthotopically transplanted and control heart tissue sections and MOR-1 immunoreactive optical density: There was a slight difference in microscopic observation of MOR-1 immunoreactivity between endomyocardial biopsy of orthotopically transplanted (Fig. 10. B, D, F, H and J) and control heart tissue (Fig. 10. A, C, E, G, I) sections. The graph showed OD of MOR-1 immunoreactivity in EMBOTH and CHT. Mean ± STD, P<0.05 was considered as significant. MOR-1, mu opioid receptor; EMBOTH, Endomyocardial biopsy of orthotopically transplanted heart; CHT, Control heart tissue; IRC, Immunoreactive cell; OD, Optical density; GPCR, Gi protein-coupled receptor. Images acquired at 200x magnification. Scale bar 100microns.

2.3.3. Immunoperoxidase stained DOR-1 immunoreactive myocytes and its optical density in endomyocardial biopsy sections after 30 days of orthotopically transplanted heart

Immuno-peroxidase stained DOR-1 immunopositive myocytes were observed both in transplanted (Fig. 11 B, D, F, H, and J) and control heart (Fig. 11 A, C, E, G, and I). Similarly, the qualitative data of inverted confocal microscopy also reflected DOR-1 immunoreactive signals. The optical density of DOR-1 immunoreactivity of myocytes was significantly declined in endomyocardial biopsy of orthotopically transplanted heart (0.134±0.18) compared to control heart tissue (0.37±0.08), P = 0.018.

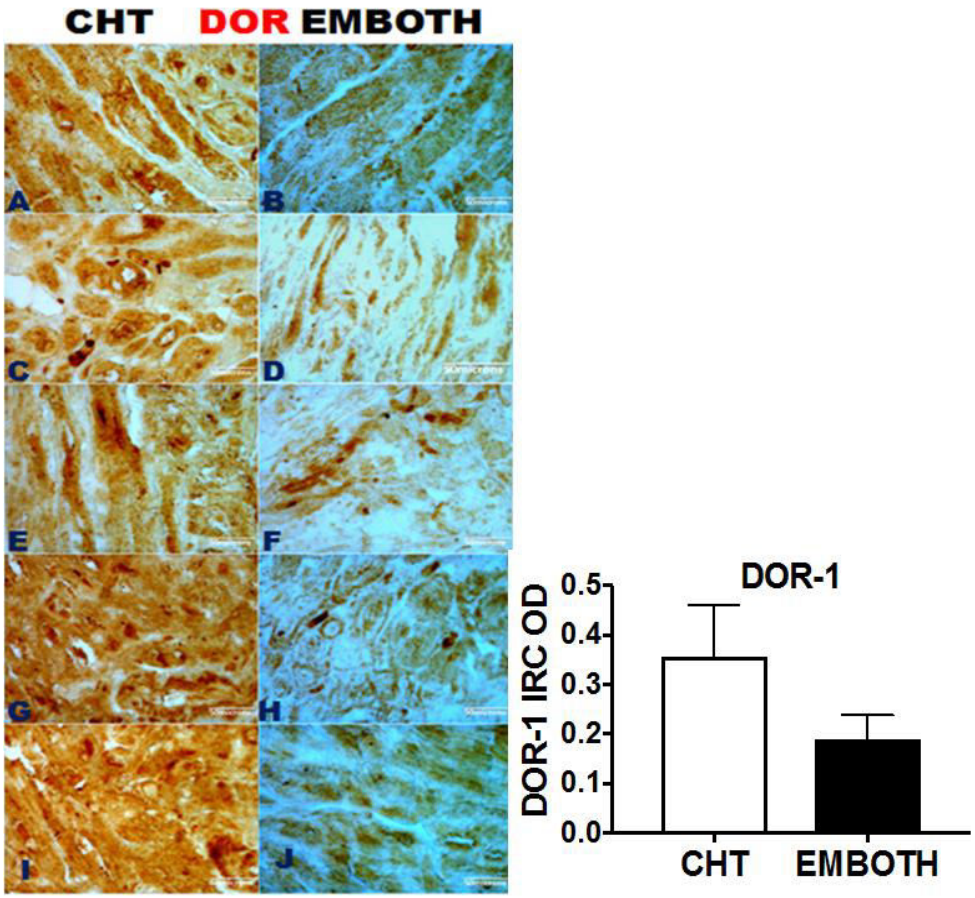

Figure: 11. A: Representative images of DOR-1 immunoreactive myocytes in endomyocardial biopsy of orthotopically transplanted (EMBOTH) and control heart tissue (CHT) sections and DOR-1 immunoreactive optical density: Immunoperoxidase DOR-1 labeled EMBOTH (Fig. 11. B, D, F, H and J) showed poor immunoreactivity myocytes of septa of right ventricle compared to control heart tissue (Fig.11. A, C, E, G, and I) sections. **B:** Graph showing the results obtained using Image-Pro Plus. Counts of DOR-1 immunoreactive cardiomyocytes in EMB of transplanted and control heart tissue sections DOR, Delta opioid receptor; EMBOTH, Endomyocardial biopsy of orthotopically transplanted heart. IRC – Immunoreactive cells. Images acquired at 400x magnification, Scale bar 50µm

2.3.4. Immunoperoxidase stained KOR-1 immunoreactive myocytes and its optical density in endomyocardial biopsy sections after 30 days of orthotopically transplanted heart

In our qualitative data, immunoperoxidase stained KOR-1 immunopositive myocytes were observed both in orthotopically transplanted and control heart (Fig. 12). However, analysis of the optical density of KOR-1 immunopositive cardiomyocytes showed an apparent reduction on orthotopically transplanted heart compared to control (Fig. 12). The optical density of KOR-1 immunoreactivity of EMBOTH (0.19±0.05) was significantly reduced compared to control heart (0.35±0.1) p = 0.004. Furthermore, the qualitative data showed less frequent appearance number of KOR-1 immunoreactive myocytes in transplanted heart tissue sections (Fig. 12).

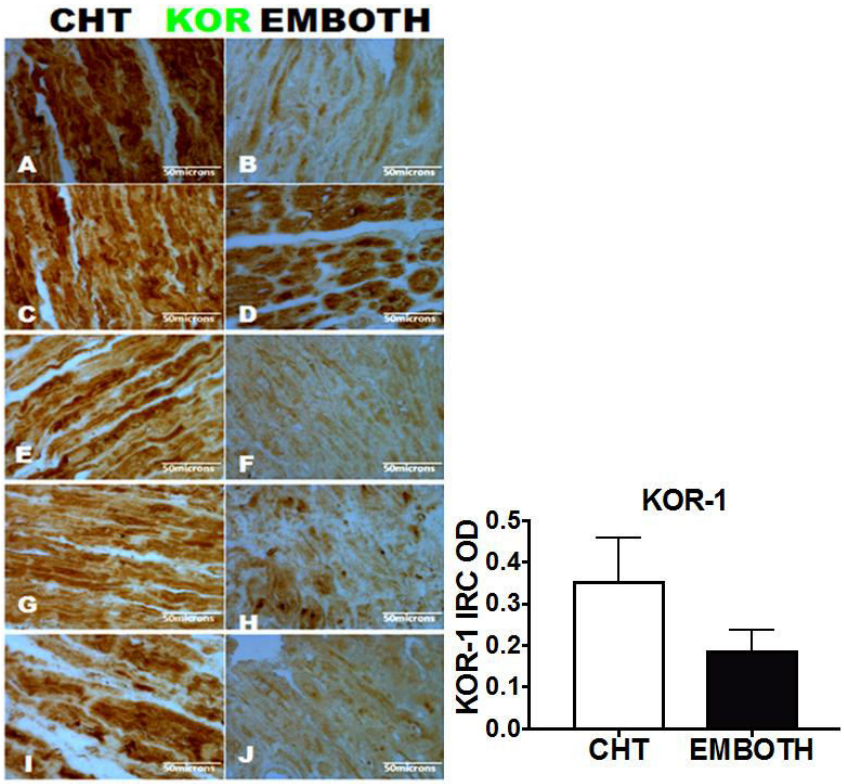

Figure: 12. Representative images of KOR-1 immunoreactive myocytes in endomyocardial biopsy of orthotopically transplanted (EMBOTH) and control heart tissue (CHT) sections and KOR-1 immunoreactive optical density: Immunoperoxidase DOR-1 labeled EMBOTH (Fig. 12. B, D, F, H and J) showed lightly stained immunoreactivity in septa of right ventricle compared to control heart tissue (Fig.12. A, C, E, G, and I) sections of right atria, septum and left ventricles. The graph showing the results obtained using Image-Pro Plus. Counts of KOR-1 immunoreactive cardiomyocytes in EMB of transplanted and control heart tissue sections KOR, Kappa opioid receptor; EMBOTH, Endomyocardial biopsy of orthotopically transplanted heart. IRC – Immunoreactive cells. Images acquired at 200x magnification, Scale bar = 50 microns.

2.3.5. Immunoperoxidase stained CGRP-1 immunoreactive cells and its optical density in endomyocardial biopsy sections after 30 days of orthotopically transplanted heart

In this study, a neuropeptide (CGRP-1) of sensory and motor neurons was evaluated in EMBOTH. Immunoperoxidase stained immunoreactivity of CGRP-1 was detected as a sparse individual fiber of myocytes in both EMBOTH and CHT. Nevertheless, its immunoreactivity to sensory nerves was limited to nerve bundles of control heart (Fig. 13 A, C, E, G, and I). Even though CGRP-1 immunoreactivity was detected in both EMBOTH and CHT groups, an optical density of CGRP immunopositive fibers of EMBOTH (0.37±0.53) was significantly reduced compared to control heart (0.44±0.26) p = 0.035.

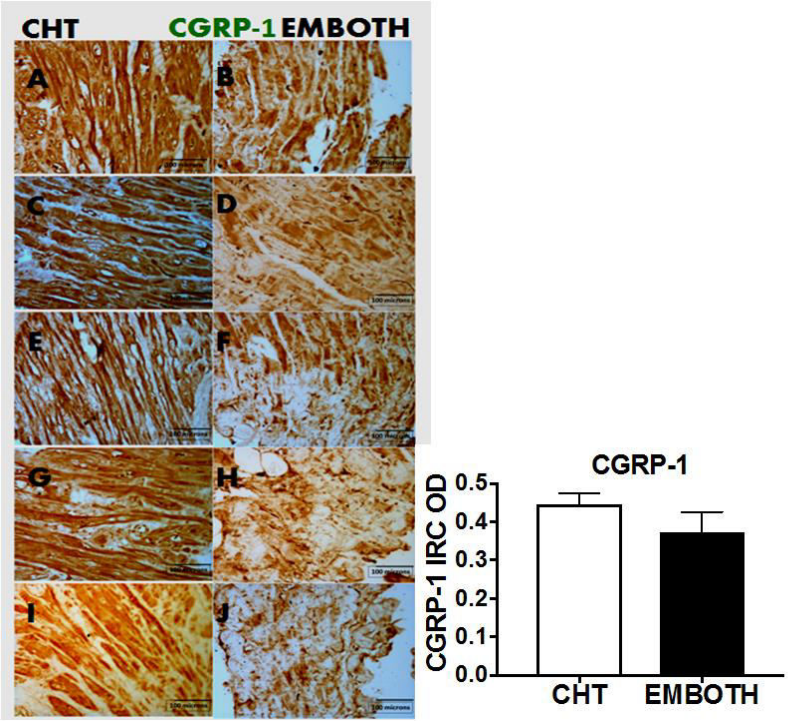

Figure: 13. Representative images of CGRP-1 immunoreactive myocytes in endomyocardial biopsy of orthotopically transplanted (EMBOTH) and control heart tissue (CHT) sections and CGRP-1 immunoreactive optical density: Immunoperoxidase CGRP-1 labeled EMBOTH (Fig. 13. B, D, F, H and J) showed sparely stained immunoreactivity in septa of right ventricle compared to control heart tissue (Fig.13. A, C, E, G, and I) sections of right atria, septum and left ventricles. The above graph is showing OD of CGRP-1 immunoreactivity in EMBOTH and CHT. Mean±STD, P<0.05 was considered as significant. CGRP, Calcitonin gene-related peptide; EMBOTH, Endomyocardial biopsy of orthotopically transplanted heart; CHT, Control heart tissue; IR, Immunoreactivity; OD, Optical density. Images acquired at 200x magnification. Scale bar 100microns.

2.3.6. Confocal microscopic observation of immunofluorescence labeled DOR-1 immunoreactive signals on endomyocardial biopsy of orthotopically transplanted and control heart tissue

Immunofluorescence qualitative observational data demonstrated that DOR-1 immunopositive cardiomyocytes signals were detected in both endomyocardial biopsy of orthotopically transplated (EMBOTH) (Fig. 14. B, D, F, H, J) and control heart tissue (Fig. 14. A, C, E, G, I) sections. However, except C and D, there was no clear immunoreactive signal difference between transplanted (Fig. 14. B, D, F, H, J) and control heart (Fig. 14. A, C, E, G, I) tissue sections.

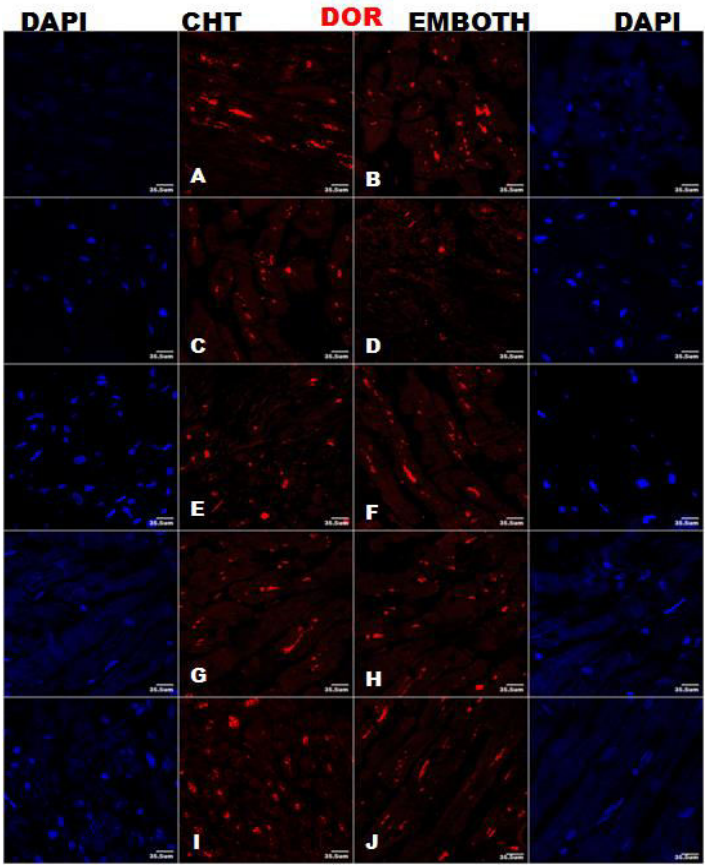

Figure: 14. Representative images of fluorescence labeled DOR-1 immunoreactive cardiomyocytes of the human heart: Immunofluorescence microscopy of EMBOTH and control heart tissue. Immunofluorescence staining of DOR-1 immunoreactive signals was shown in myocytes of EMBOTH (Fig. 14. B, D, F, H and J) and control heart tissue (Fig. 14. A, C, E, G and I). The left column of the images indicated control heart tissue sections of Fig.14. A, C, RA, E, Septum, G & I, LV, and the right one indicated the endomyocardial biopsy sections of the orthotopically transplanted heart of interventricular septum. DOR, Delta opioid receptor; EMBOTH, Endomyocardial biopsy of orthotopically transplanted heart; CHT, Control heart tissue; RA, Right atrium; LV, Left ventricle, Scale bar = 35.5µm.

2.3.7. Confocal microscopic observation of immunofluorescence labeled KOR-1 immunoreactive signals on endomyocardial biopsy and control heart tissue

Qualitative observational data demonstrated DOR-1 immunopositive cardiomyocytes signals in both endomyocardial biopsy orthotopically transplanted (EMBOTH) (Fig. 15. B, D, F, H, J) and control heart tissue (Fig. 15. A, C, E, G, I) sections. However, the expression was weak as compared to DOR-1 immunoreactivity in both EMBOTH (Fig. 14. B, D, F, H, J) and CHT (Fig. 15. A, C, E, G, I) tissue sections.

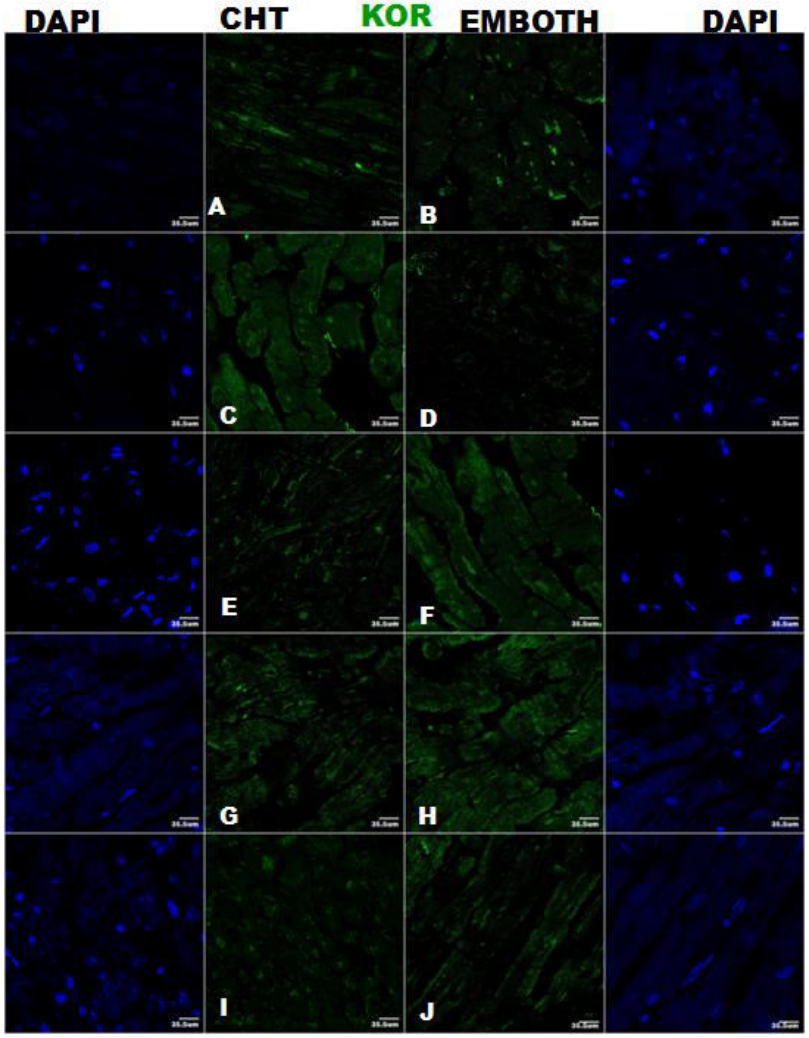

Figure: 15. Representative images of immunofluorescence labeled KOR-1 immunoreactive cardiomyocytes of the human heart: Immunofluorescence microscopy of EMBOTH and control heart tissue. Immunofluorescence staining of DOR-1 immunoreactive signals was shown in myocytes of EMBOTH (Fig. 15. B, D, F, H and J) and control heart tissue (CHT) (Fig. 15. A, C, E, G and I). The left column of the images indicates control heart tissue sections of Fig.15. A, C = RA, E= Septum, G & I = LV, and the right one indicates EMB sections of transplanted heart. KOR, Kappa opioid receptor; EMBOTH, Endomyocardial biopsy of orthotopically transplanted heart; RA, Right atrium; LV, Left ventricle. Scale bar = 35.5µm.

2.3.8. Co-localization of confocal microscopic double immunofluorescence labeled DOR-1 and KOR-1 immunoreactive signals in septal part of right ventricular of orthotopically transplanted and control heart tissue sections

Co-localization of DOR-1 and KOR-1 immunopositive myocyte signals was also evaluated in endomyocardial biopsy of orthotopically transplanted and control heart tissue sections under confocal technique. Delta- and kappa-OR-1 immunoreactive signals co-localization was observed in EMBOTH (Fig. 16 B4) and control heart tissue (Fig.16. A4 merged) myocytes. Throughout our evaluation of the delta and kappa opioid receptors, we observed very rearly expression of delta opioid receptors in intracellular structure as it is evident from the figure 16 (Fig. 16. CHT) that co-localized with DAPI stained nuclei of cardiomyocytes. In previous studies, it was also suggested its expression not only limited to plasma membrane receptor but also in intracellular structure.

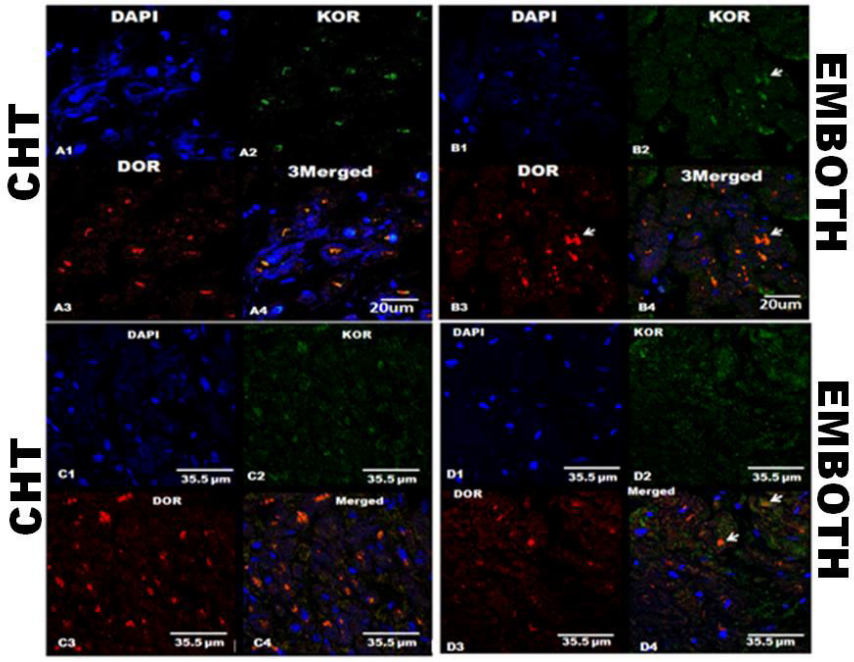

Figure: 16. Confocal microscopy of double immunofluorescence images showing the overlap of DOR-1 and KOR-1 immunofluorescence reactive signals in the cardiomyocytes in orthotopically transplanted and control heart in human: Confocal microscopy images of DAPI (blue A1, B1, C1, D1) showing bright blue stained nuclei, DOR (red A3, B3, C2, D3), KOR (green A2, B2, C2, D2). Representative images of double immunofluorescence for DOR-1, KOR-1, and DAPI nuclei staining (Fig. 16 A1 C1, DAPI; A2 C2, KOR; A3 C3, DOR; A4 C4, Merged A1 C1, A2 C2, A3 C3 & A4 C4) in orthotopically transplanted heart endomyocardial biopsy and control heart tissue section (Fig. 16. B1, B2, B3, & B4) in confocal microscopy which shows cardiomyocytes containing DOR-1 and KOR-1 immunoreactive cells on EMB of transplanted heart. The arrows point to the same landmark for spatial reference. Note: DAPI, A1, B1, C1, & D1; KOR, A2, B2, C2, & D2; DOR, A3, B3, C3 & D3; Merged, A4&B4, C4&D4. DAPI, 4`, 6-Diamidino-2-Phenylindole, DOR-Delta opioid receptor; KOR, Kappa opioid receptor; EMBOTH, Endomyocardial biopsy of orthotopically transplanted heart. Images were acquired at 400x magnification, Scale bar = 35.5µm.

2.3.9. Confocal microscopic observation of CGRP-1 and MOR-1immunofluorescence labeled fibers on endomyocardial biopsy of orthotopically transplanted and control heart tissue sections

Confocal microscopic observation demonstrated poorly detected CGRP-1 immunopositive sensory neuronal signals in EMBOTH (Fig. 17 B and D) compared to CHT (Fig. 17. A and C) sections. Moreover, immuno-positive MOR-1 signals were also detected in EMBOTH and CHT (Fig 17).

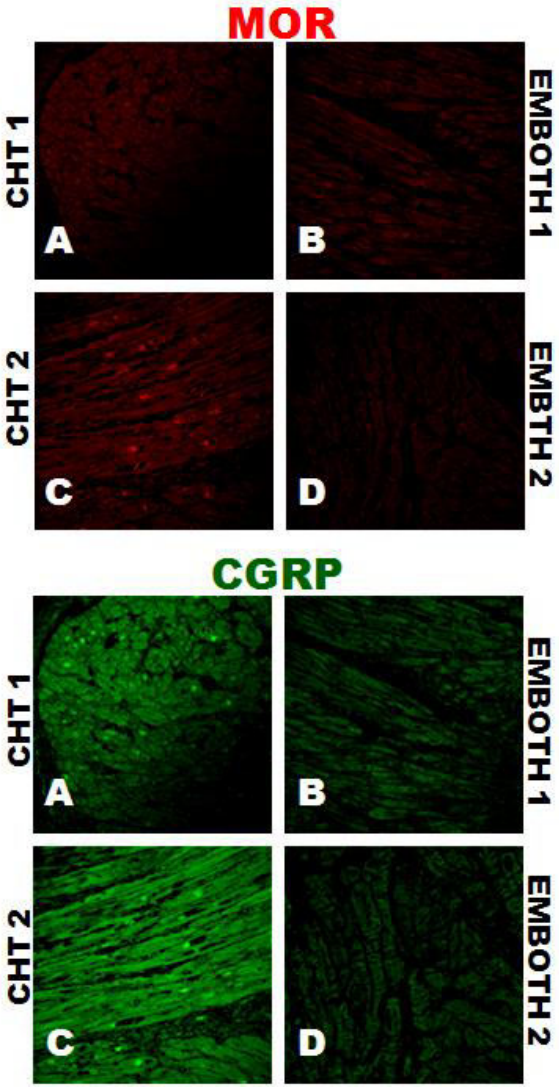

Figure: 17. Representative images of double immunofluorescence labeled MOR-1 and CGRP-1 immunoreactive cardiomyocytes of the human heart: Immunofluorescence staining of MOR-1 immunoreactive signals was shown in myocytes of EMBOTH (Fig. 17. B and D) and control heart tissue (CHT) (Fig. 17. A and C); however, poor CGRP-1immunofluorescence signals was observed inEMBOTH compared to CHT. MOR, mu opioid receptor; CGRP-1, Calcitonin gene-related peptide; EMBOTH, Endomyocardial biopsy of orthotopically transplanted heart; RA, Right atrium; LV, Left ventricle. Scale bar = 35.5µm.

2.3.10. RT-qPCR analysis for expression of DOR and KOR mRNA in human

In this study, a relative quantitative real-time RT-PCR assay was applied to detect mRNA transcripts encoding DOR and KOR in the orthotopically transplanted heart. The mRNA transcript encoding the DOR and KOR was identified in endomyocardial biopsy of the orthotopically transplanted heart taken from septal part of the right ventricle in human. Similar results were shown in different studies (Lendeckel et al., 2005).

In this study, δ and κ-opioid receptors are detected in human heart (Fig. 18). However, mRNA encoding KOR and DOR was down-regulated in EMBOTH, and KOR was found lower than DOR in EMBOTH. Weak signal of KOR in rat heart was also reported by Wittert et al., (1996).

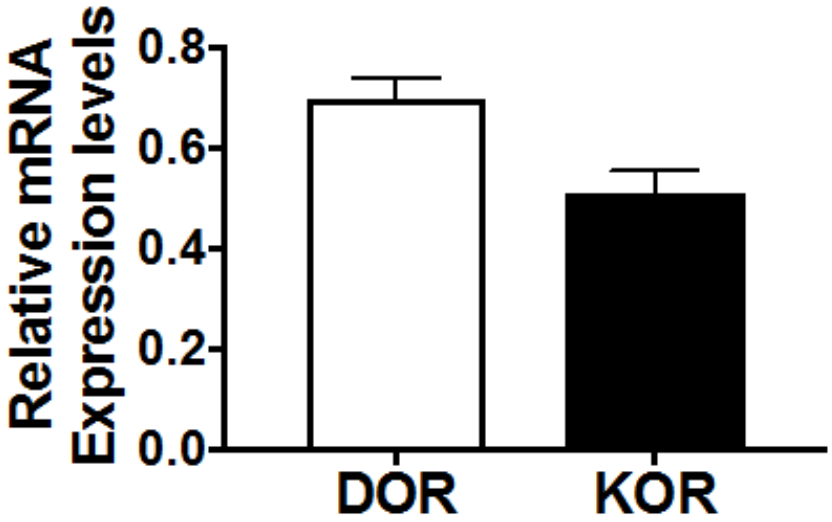

Figure: 18. The graph showing relative KOR & DOR mRNA gene expression: quantitative real-time RT-PCR assay was developed to quantify DOR and KOR mRNA in transplanted heart. GAPDH gene was used as a reference gene to normalize sample variations. DOR, Delta opioid receptor; KOR, Kappa opioid receptor, GAPDH, Glyceraldehyde-3-phosphate dehydrogenase; RT-qPCR; Reverse transcriptase quantitative real-time polymerase chain reaction; RNA, Ribonucleic acid; EMBOTH, Endomyocardial biopsy of orthotopically transplanted heart.

2.3.11. TUNEL positive apoptotic nuclei in endomyocardial biopsy of orthotopically transplanted and control heart tissue sections in human and TUNEL positive nuclei counts

Apoptosis/programmed cell death is a highly regulated and energy requiring process characterized by shrinkage of cell and nucleus (Krijnen et al., 2002). Cardiomyocyte death result from myocardial infarction (MI) is not only due to necrosis but also result in apoptosis in the process of tissue injury from MI. In our TUNEL analysis of endomyocardial biopsy of orthotopic transplanted human heart, DNA fragmentation in the nuclei of myocytes through labeling of the terminal end of nucleic acid was assessed. The observed apoptotic nuclei of myocardium results from apoptotic signaling cascades in orthotopically transplanted heart were found significantly elevated (7.82±0.59) compared to control (9.45±0.925), P=0.013 (Fig 19). The occurrence apoptotic markers in the myocardium are related to heart failure and only observed in patients with end-stage heart failure undergoing heart transplantation (Bott-Flügel et al., 2008). Saraste and colleagues, 1999 have reported a significant increase in a number of apoptotic cardiomyocytes in dilated cardiomyopathy and the increase apoptotic cells also correlate with clinical complications.

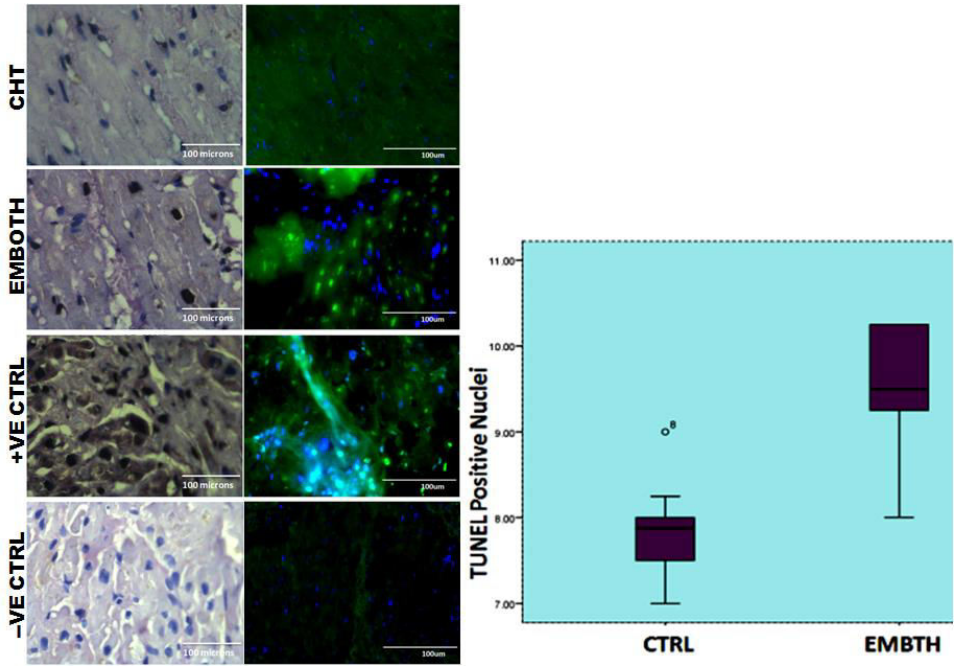

Figure: 19. Representative photomicrographs of endomyocardial biopsy of orthotopically transplanted and control heart tissue sections showing TUNEL stained apoptotic cells: Number of TUNEL positive nuclei was significantly elevated in EMBOTH. TUNEL+ Hematoxylin (H); OTH, Orthotopic transplanted heart; CTRL, Control; TUNEL, Terminal deoxynucleotidyl transferase; dUTP, 2'-deoxyuridine 5'-triphosphate; Nick End Labeling. Mean±STD, P<0.05 was considered as significant.

2.4. Discussion

Our data indicates the presence of classical opioid receptors in the human heart with a down-regulation in the orthotopically transplanted heart. There are many shreds of evidence indicating the presence of opioid receptors in multiple organs of the body (Khachaturian et al., 1987). The heart expresses high levels of endogenous opioids across species (Headrick et al., 2015). In a study which detects delta and kappa opioid receptors, it is reported that δ & κ opioid receptors in human atria selectively down-regulates the k-OR during atrial fibrillation (Lendeckel et al., 2005). Moreover, Sobanski et al., 2014 proved detection of immunoreactivity of all the three classic opioid receptors, principally kappa-OR in myocardial cells of the human heart (Sobanski et al., 2014).

Although studies have shown the presence of ORs in myocardial tissue of different species, there is no data indicates the presence of classical opioid receptors in endomyocardial biopsy of orthotopically transplanted heart in the human. This study contributes in identifying the level of classical opioid receptors in transplanted heart that can contribute to understand the effectiveness of opioid and opiate-like drugs in transplant patients.

This study, therefore, confirms that mRNA encoding delta and kappa ORs, and MOR-1 immunoreactive myocytes at the protein level are present in orthotopically transplanted heart and normal heart in the human. The study was in agreement with previous studies showing the presence of mu, delta and kappa opioid receptors on cardiomyocytes of humans (Sobanski et al., 2014) and (delta and kappa) animals` heart (Theisen et al., 2014; Cao, 2003; Patel et al., 2006; Weil et al., 1998; Howells et al., 1986).

Besides, delta and kappa opioid receptors expression are observed not only on the immunoreactive plasma membrane receptors but also in few intracellular labeling of DOR-1 and KOR-1 in line with other studies which observed both in membranes bound and intracellular in the porcine myocardium (Theisen et al., 2014; Al-Hasani and Bruchas, 2011).

Interestingly, this study shows a down-regulation of Oprk1 and Oprd1 mRNA in orthotopically transplanted human heart tissues, and reduction of the number of KOR-1 immunoreactive cells at the protein level. Even though the strength (optical density) of immunostaining/immunoreactivity of MOR-1 didn`t reach a significant threshold, analysis of MOR-1 immunoreactivity reduces in the orthotopically transplanted heart. This implies a great contribution and influence of innervation to the functioning of opioid receptors in the heart.

In our TUNEL analysis of endomyocardial biopsy of orthotopically transplanted heart, it is shown a significant elevation of apoptotic nuclei in transplanted heart. Koch et al., 2008 has shown apoptotic cell death during acute rejection episodes in 27 human heart transplants in the interstitial cells. Cristóbal and colleagues (2010) have also strengthened detection of apoptotic myocytes in 81.5% of 130 endomyocardial biopsies during the first six months of post-heart transplantation.

On the otherhand, Bott-Flügel et al., (2008) have shown the occurrence of apoptotic markers in the myocardium that are related to heart failure and only observed in patients with end-stage heart failure undergoing heart transplantation. Saraste and colleagues, 1999 have added a report on a significant increase in a number of apoptotic cardiomyocytes in dilated cardiomyopathy and the correlation of increased apoptotic cells with clinical complications. The decreasing number of DOR-1 and KOR-1 immunoreactive cardiomyocytes might be due to the histopathological changes, elevated TUNEL positive nuclei of myocytes observed in the denervated heart tissue and lack of innervations. This down-regulation might also be due to the involvement of an autocrine process of ORs in which opioid peptides may be released from cardiomyocytes locally and interact with ORs of the heart that mediates cardioprotection.

This mechanism may be because of the increase in the synthesis and release of opioid peptides into the peripheral circulation due to histopathological changes (Paradis et al., 1992). On the contrary, increased the level of enkephalins in ventricles of rats following myocardial infarction is also reported (Paradis et al., 1992).

Furthermore, DOR-1 and KOR-1immunopositive signals co-localization with the same cell receptors are also observed in the orthotopically transplanted heart. The overlap of these receptors that are found in fluorescence DOR-1 and KOR-1 implies the strong functional association on cardiomyocytes and contributions in the regulation of cardiovascular function in transplanted heart.

Generally, in this study, expression of delta and kappa ORs are detected in orthotopically transplanted and normal human heart with a decline in Oprk1 and Oprd1 mRNA and proteins of cardiomyocytes in transplanted heart. Co-localization of DOR-1 and KOR-1 immunoreactive signals is observed in transplanted heart. Elevation of apoptotic nuclei in transplanted heart myocardium is also observed.

The findings suggest clues toward a tendency of reduction in the pharmacological activities of opioids in the regulation of cardiac tissue in transplanted heart and vulnerability of denervated heart to ischemia and reperfusion injury.

CHAPTER THREE

3. Expression of classical opioid receptors in heterotopic transplanted and naïve hearts in rat

3.1. Introduction

The distribution of endogenous peptides in rats` heart has been elaborated after findings from a study of peripheral distribution of preproenkephalin mRNA that show surprising large amounts (Howells et al., 1986) of endogenous peptides (Koneru et al., 2009) preproenkephalin mRNA in Sprague Dawley rats' cardiac ventricular tissue than any other tissue including brain (Howells et al., 1986), and species such as guinea pig, bovine, and mouse hearts. Preproenkephalin is an endogenous peptide where the two major families of the opioid system, enkephalins, and dynorphins are derived. This study has initiated other studies to emerge on expression, and protective effects of translational products derived from preproenkephalin on different peripheral tissues, and then rats' heart become a useful model for investigation of translational control of protein synthesis. The clue that we obtained from our previous study of orthotopically transplanted heart in human on the expression of opioid receptors. This study aimed to characterize the expression of mu-, delta- and kappa- opioid receptors in naïve and donor rat cardiac tissue.

The Sprague Dawley rat is an outbred multipurpose breed of albino rat used extensively in medical research. These animals are an important aspect of cardiac research where a variety of cardiac processes and therapeutic targets can be studied. They belong to the Rodentia and family Muridae. The rat has short hair, a long naked tail, rounded erect ears, protruding eyes, and five toes on each foot. Rats have a much longer tail; however, they have no gall bladder. They have the following normative values: lifespan (2.5-3.5 years), adult weight (males 300-500g, females 250-300g), birth weight(5-6g), heart rate (330-480 b/min), respiratory rate (85 breaths/min), body temperature (35.9-37.5ºC), blood volume (50-70 ml/kg), urine volume (3.3 ml/100g body weight/day), allergens (dander, urinary protein) (Koolhaas, 2010).

Heterotopic abdominal HTx in rats involves an aortic-aortic and a pulmonary artery-inferior vena cava anastomosis (Fig. 20). In this kind of transplantation rat model, the left ventricle is volume unloaded, receiving the smallest cardiac veins (Thebesian veins). However, it is not entirely pressure unloaded (Ibrahim et al., 2013). Based on recipient`s operative time and graft survival, abdominal was preferred to cervical heart transplant (Ma and Wang, 2011) for the procedure.

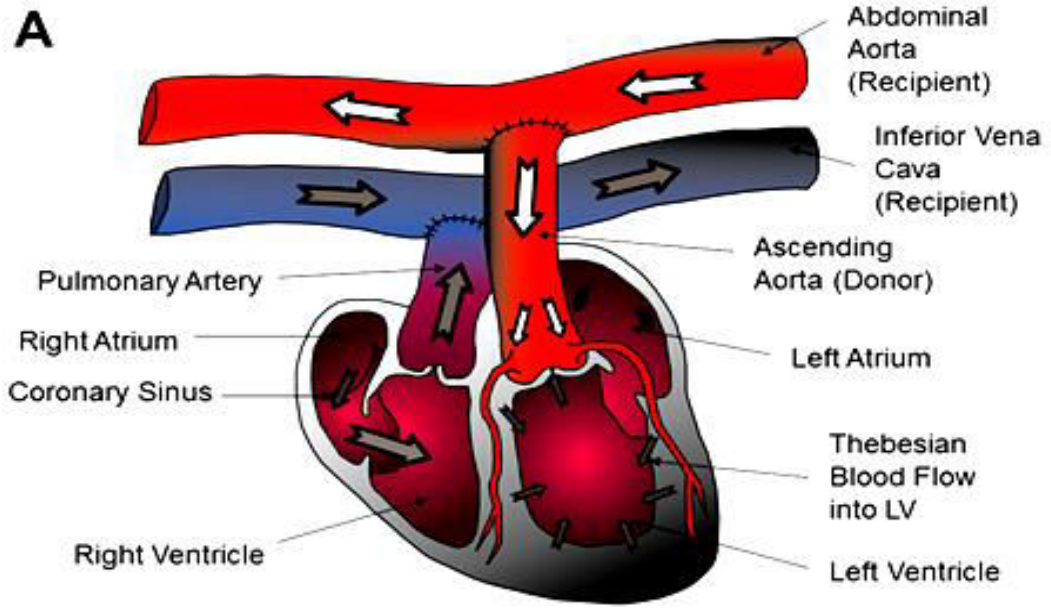

Figure: 20. Illustration of a heterotopic heart transplantation (mechanical unloading) model in rats: The coronary arteries are perfused via retrograde through the aortic anastomosis, thus allowing the circulation of the graft. The left ventricle - except for the flow in transit from the veins of Tebesio - is completely excluded from circulation: the blood is collected in fact - thanks to the coronary venous circulation - in the sections of the right heart, through the pulmonary vein and its anastomosis with the inferior vena cava, the pump in the systemic venous circulation of the recipient rat. Ibrahim et al., Journal of Surgical Reseach. 2013; I79: E3I-E29.

The first execution technique of heart transplantation in small experimental animals dates back in mid-sixties, then perfected further, in the following years; if it were not for these jobs, they would be few authors who have helped to shed light on techniques for the surgical and anesthetic management of heterotopic heart transplantation procedure in rodents. This procedure involves implanting in the abdomen of a recipient (abdominal heterotopic) a heart removed from a donor animal, to which is supplied the blood supply thanks to the execution of two anastomoses. The first is abdominal aorta of the recipient with the ascending aorta graft and inferior vena cava of the recipient with graft

pulmonary trunk is the second one. The blood of the recipient rat - pumped around from its native heart - perfusing retrograde coronary graft and (with them, the entire myocardium) due to the presence of aorta-aortic anastomosis; the effluent blood is then drained from the coronary venous circulation which, in turn, enters blood in the right heart sections: the blood is ejected from the pulmonary artery of the graft that, thanks to pulmonary-cava anastomosis, it drains into the inferior vena cava of the recipient rat.

In this way, the left sections of the graft are excluded from the bloodstream: in fact, the heterotopic transplant model is set up as a left unloaded (in reality left ventricular preload model is present and represented by the blood flow through the veins of Tebesio), in which the graft takes on more or less the same function as an LVAD (Fig. 21).

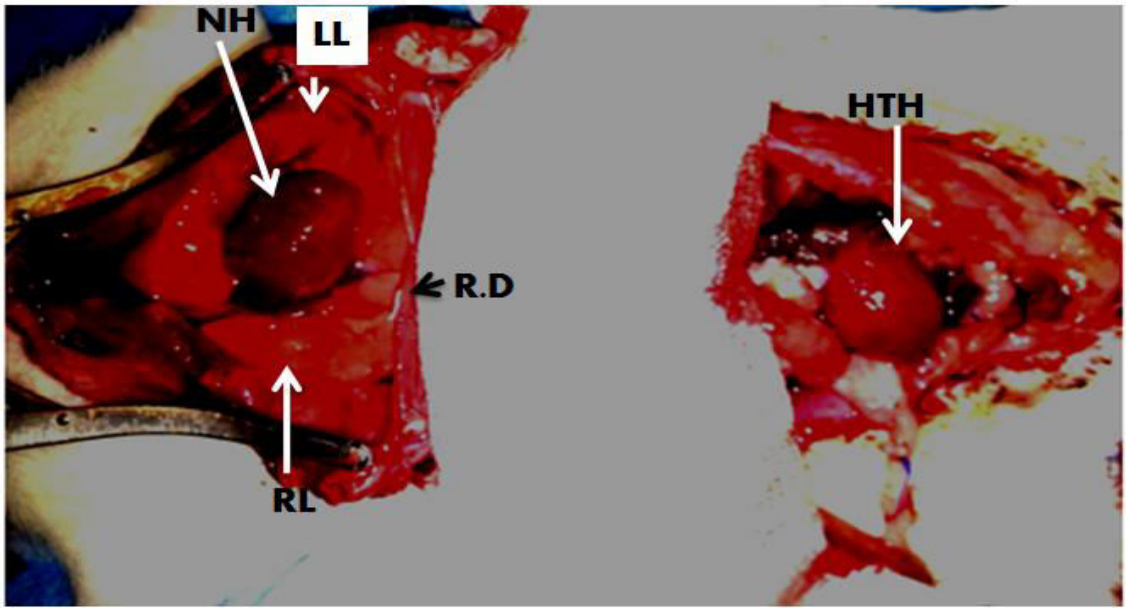

Figure: 21. Illustration of abdominal heterotopic transplanted and naïve heart model of a rat: The above figure illustrates naïve and heterotopic transplanted heart model of rat. Aortic-aortic and a pulmonary artery-inferior vena cava anastomosis were done with the help of Surgeons, University of Verona, Department of Surgery, and Cardiac Section. HTH, Heterotropic transplanted heart; NH, Naïve heart; LL, Left lung; RL, Right lung; R.D, respiratory diaphragm.

3.2. Materials and methods

3.2.1. Study design and experimental animals

The study designed comprising of adult male Sprague-Dawley rats, weighing about 350-400g. The out-bred multipurpose breed of Sprague-Dawley rats was used. These animals are an important aspect of cardiac research where a variety of cardiac processes and therapeutic targets can be studied. They were housed 1 per cage in a setup cage system at Interdepartmental Center of Experimental Research Service/CIRSAL, the University of Verona at a temperature controlled room (21±2^{o}C) with food (ad libitum) and water available under a 12 hours' light/dark cycle. They were acclimatized for 7 days before the beginning of the experiment in order to adapt them to the laboratory conditions. These rats grouped into recipients and donors. Four rats were assigned to recipients and donors to obtain rats with final dual hearts (Naïve and Heterotopic) in each rat. All tests were done during the light hours. The study was carried out in accordance with the ethical guidelines for investigations of experimental pain in conscious animals (Zimmermann, 1983; CIRSAL, University of Verona).

3.2.2. Transplants preparation and abdominal cava and aortic exposure, explantation and plantation

Two syringes (10ml) and container for a dipping heart with cardioplegia were prepared and syringe with 10ml saline left in the fridge. Rats were stun/unconscious with diethyl ether vapors Pentothal administered 40mg/kg anesthesia with isofluorane with a mask or through gold tracheal intubation (cannula 16G to 17G 3.0 prolene thread).

After preparation of cotton fioce, suture threads 6.0, cautery (destroying abdominal tissue), gauze saline, wire 3.0 to encircle and vena cava and aorta, explanations were done as follows: An overdose of Pentothal was administered to the donor rat. Heparin was administered in the 1 ml syringe and cold cardioplegia in 10ml syringe through the abdominal aorta. Afterword, clips and wire insula to 3.0 were prepared for vessels and administered a second 10ml syringe of cardioplegia in the coronary sinus and then explanted heart placed in a container with cardioplegia. Prior to the plantation, heparin in 1 ml syringe, suture thread 8.0, cotton fioce, physiological cold, positioning the syringe

of saline solution under a heating lamp, hot gauzes, fabotamp, and suture thread 4.0 for closing abdomen were prepared. Later, the donor`s thoracic aorta was anastomosed to the recipient's infrarenal abdominal aorta, and the donor`s pulmonary artery was anastomosed to the recipient`s inferior vena cava as described by Ma and Wang, (2011).

3.2.3. Duration of the post-transplantation and sample collection

The post-transplantation stay was six weeks. Later, rats were sacrificed to collect tissues from all chambers and septa of the hearts from both naïve and abdominal transplanted donor`s heart and processed with different techniques such as immunohistochemistry, immunofluorescence, western blot, hematoxylin and eosin, real-time polymerase chain reaction, and TUNEL.

3.2.4. Tissue processing, embedding, and sectioning

After collection of heart tissues, fixed promptly and adequately with 4% paraformaldehyde to produce superior morphology, washed three times for 10min each with PBS (pH 7.35, 0.1M), and then dehydrated with increasing ethanol concentration (70% 1x, 90% 2x, 100 1x) for 1hr, $1^1/_2$ hrs, and 1hr each, respectively. Following dealcolization by two changes of xylene (100%) for 1hr, infiltrated with two changes of molten paraffin wax at 56^oc for 1hr to replace the xylene.

Next, to infiltration, embedding was performed for better sectioning. In embedding step, a first small amount of paraffin was placed into the cassettes, and then specimens were transferred into the mold using warmed forceps and placed in the middle of the cassettes in preferred orientations, and then the cassettes were filled with molten paraffin wax with care to prevent under and over-filling. At the end, embedded specimens were put on ice, and stored in cold room at 4^oc overnight to form strong blocks. This paraffin embedded tissue process was used for further IHC, IF, TUNEL, and H& E staining.

Once specimens embedded, they were cut into 3µm thickness sections using Leica RM 2255 CSA® US digital microtome. It is good to place blocks on ice prior to sectioning to obtain unwrinkled sections. Sections were, floated on cold water bath and picked up by

adhesion microscope slides (26x76MM, DIAMOND Blue, 33820B, Lot#300414, LABOINDUSTRIA S.P.A, IT) and FLEX IHC coated microscope slides with white-painted label area (Code: K8020, K802021-2, Wo503900201, 75mm, W x 25mm, D x 1mm, H), floated on a warm water bath to remove wrinkles of sections. Finally, the microtome cleaned with Vacuum Cleaner (Mode: AS10-A40, No. 0288112) and left in good condition.

3.2.5. Hematoxylin and eosin staining for histopathological study

Hematoxylin and eosin staining were done as indicated previously to evaluate any histopathologicalchanges and level of rejection in HTH tissue sections. Any structural abnormalities of H&E stained tissue sections were analyzed with the help of pathologist.

3.2.6. Immunohistochemistry (immunoperoxidase and immunofluorescence)

Immunohistochemical studies, such as immunoperoxidase and double immunofluorescence (IF) were done as described in previous studies to evaluate MOR-1, DOR-1, KOR-1, and CGRP-1 immunoreactive cardiomyocytes, and analyzed for relative distribution of opioid receptors on heterotopic transplanted and control rat heart tissue sections. Markers used for detection of MOR-1 were used as indicated earlier. However, different primary antibodies for DOR-1(a rabbit polyclonal antibody (H-80): Cat. No. sc-15310, a goat polyclonal antibody (M-20): Cat. No. sc-7492) and KOR-1 (a mouse monoclonal antibody (D-8): Cat. No. sc-374479).

In immunoperoxidase staining, tissue sections were processed of dewaxation, rehydration, treatment with antigen retrieval solutions, and incubation for 20min in H_2O_2, pre-incubation in 2% of Normal Horse Serum, incubation with primary antibodies (MOR-1, DOR-1, and KOR-1). Following incubation in 1^o Abs, incubated 2^o anti-rabbit IgG (H+L) biotinylated (BA- 1100, Lot no. ZA0319) and anti-goat IgG (H+L) biotinylated (BA- 9500, Lot no. Z0326), and anti-mouse Abs made in horse for MOR-1, DOR-1, and KOR-1, respectively, and then incubated with ABC solution. Finally, specific immunostaining was detected with DAB (Diaminobenzidine) in PBS containing

0.75% H_2O_2. Finally, sections dried, dehydrated with ethanol and xylene, and prepared for analysis.

Double immunofluorescence technique was also performed for the concurrent visualization of MOR-1, DOR-1 and KOR-1 immunoreactive signals on cardiomyocytes. Following overnight incubation with primary antibodies (MOR-1, DOR-1, KOR-1), a brief wash was performed and incubated in a mixture of Alexa Fluor 568 donkey anti-rabbit IgG (H+L) (1:1000, Ref. A10042, Lot no. 1668655, Eugene DR. USA), Alexa Fluor 488 donkey anti-goat IgG (H+L) (1:1000, A11055, Lot no. 1627966, Eugene DR. USA), and anti-mouse species-specific fluorescent secondary antibodies raised in donkey supplied from Life Technologies, Italy, Europe were used, respectively. The cell nuclei stained blue using Hoechst 33342 at a dilution of 1:10,000 (Thermo Fisher Scientific). Finally, drops of mountant were added on sections and cover with rectangular microscope cover glasses (ECN631-1574, Lot: 29339 017, 24x50mm), Germany. The pressure was applied gently over cover glasses to remove bubbles before sealing of edges of cover glasses with nail polish and then stored at -20^{o}C until analysis was done by inverted confocal microscope. Note: We used the KOR-1 monoclonal primary antibody for post-heterotopic heart transplanted study.

3.2.7. Microscopy, optical density measurement, and analyses of MOR-1, DOR-1, KOR-1, and CGRP-1 immunoreactivity

Microscopy, counting and analyses of MOR-1, DOR-1, KOR-1, and CGRP-1 IRC were done as previously described in chapter two. Prior to counting, slides were blindly assigned with code number by another investigator and sections thickness was measured. Counts of DOR-1 and KOR-1 immunoreactive cardiomyocytes were performed using 20X objective at 3 to 3.5µm. The only observed longitudinal full length of KOR-1 immunoreactive cardiomyocyte in the focal field of the live preview was used as a counting unit. Four sections were selected randomly from each sample. The counting was done using Image-Pro Plus software in workspace preview. Fiji version of ImageJ was used to quantify the strength of immunoperoxidase staining in heart tissue of MOR,

DOR, KOR, and CGRP proteins using the instruction indicated by Jensen, 2013. Instructions (Open DAB image-color-color, Deconvolution-H DAH-choose the 2nd metrics, run measure). Immunofluorescence images were quantified using Figi`s image by running adjust with auto-threshold for only evaluation purpose. Laser scanning confocal microscope (Carl Zeiss LSM 510, Göttingen, Germany) was used for obtaining multicolor optical images from sections of specimens. Images were further harmonized by using Leica LAS AF lite software for better contrast.

3.2.8. Cryosectioning for RNA isolation and western blot

Tissues were taken from heterotopic transplanted rat heart. Naïve hearts in rats were used as controls. Preserved in formalin and snap frozen in liquid nitrogen, and then processed for RNA isolation (RT-qPCR), protein extraction (immuno-blotting), IHC, IF, TUNEL, and H&E. snap frost tissue was stored at -80^{o}C until used, and then pre-cooled at -21^{o}C and placed into cryostat (Leica CM 1900-V5.3 ENGLISH-10/2006) for 30 min prior to sectioning to attain thermal balance.

The chamber of cryostat was set to -20^{o}C and 5µm thickness. Freezing/cryostat embedding medium (Lot: 140410) was applied to cover the specimen plate/the round metallic mount of the cryostat. When the medium began to frost, tissues were placed in the center as straight as possible horizontally. Once the media was completely frozen, the specimen plate was placed into holder and knob was turned clockwise to tight it. The blade was pre-cooled to -20^{o}C and placed onto the stage with maintained O.C.T before cryosectioning. Thirty sections for RNA isolation and 45 sections for immunoblotting analysis at 5µm thickness were used. The blade, all trimmings, and specimen wastes were removed, and the machine was left in a clean and safe condition.

3.2.9. RNA extraction, cDNA synthesis, and qPCR

After RNA extraction done using MiniKit, RNA concentration was measured by Nanodrop (2000/2000c) and placed at -80^{o}C until required. The total RNA preparations were used for RT-qPCR. Following RNA isolation process, cDNA synthesis was done immediately using the protocol and cDNA synthesis kit obtained from SIGMA® Saint

Louis Missouri 63103 USA. cDNAs were diluted in 50ul water. One µl of this reaction mix was used as a template for RT-qPCR assembly using the SYBR Green protocol with the readymade SYBR®Green qPCR ReadyMix™, with ROX™ 2X (KCQS02).

Following primer mix for DOR, KOR (Sigma), and GAPDH (Invitrogen, 059901, M5583 (A02, A01), mixed with ROX and then appropriately added to each well with sample mix in triplicate and run in the following conditions (initial denaturation 95^{O}C, 3min, 40 cycles PCR cycling 95^{O}C, 15sec, and data were collected at the end of extension step 60^{O}C, 60sec).

The relative expression level of each gene was normalized to GAPDH in the same sample. Amplification didn`t exceed 200bp. SYBR®Green dye that binds to the minor groove of dsDNA and detects any dsDNA generated during amplification was done using Applied Biosystems 7300 Real Time System connected with the computer. The data calculated using the delta-delta method indicated by Livak and Schmittgen, (2001).

The readymade SYBR®Green qPCR ReadyMix™, with ROX™ 2X (KCQS02) that contains all components except primers and cDNA template was used. Following primer mix for DOR, KOR (Sigma), and GAPDH (Invitrogen, 059901, M5583 (A02, A01), mixed with ROX and then appropriately added to each well with sample mix in two duplicate. Amplification didn`t exceed 200bp. SYBR®Green dye that binds to the minor groove of dsDNA and detects any dsDNA generated during amplification was done using Applied Biosystems 7300 Real Time System instrument. Finally, the green fluorescence light emitted when bound to dsDNA was measured for proper PCR amplification and then the data calculated by the delta-delta method indicated by Livak and Schmittgen, 2001).

Table: 6. Primer sequence used for real-time PCR SYBR Green amplification

Gene	**Forward Rat (5`-3`)**	**Reverse Rat (5`-3`)**
Oprm1	CTAACCACCAGCTAGAAAATC	TTTGAATGCAGGATCAGATG
Oprd1	AATCGTCCGGTACACTAAG	AACATGTTGTAGTAGTCAATGG
Oprk1	GTCATCATCCGATACACAAAG	GGCCAAGAATTCATCAAGTAG

3.2.10. Western blot

Lysate preparation: whole tissue from chambers of the heart was used for lysate preparation. Cold lysis buffer (RIPA) was used for lysate preparation. The sample(s) was sonicated. The lysate (s) was supplemented with additional protease and phosphatase inhibitors to prevent degradation by proteases. Samples were centrifuged for 20min at 12,000rpm at 4^{o}C in a microcentrifuge. Tubes have gently removed the centrifuge and placed on ice and the supernatant aspirated and placed in a fresh tube and kept at -80 ^{o}C until used. Protein concentration was measured using BCA assay (Fig. 22).

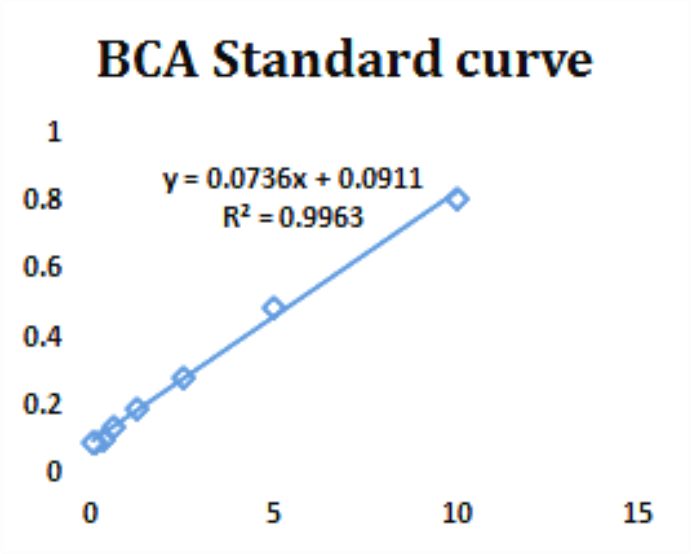

Figure: 22. BCA standard curvefor protein concentration measurement: BCA assay was done to measure unknown protein concentration after standard curve was plotted using known BSA protein concentrations. The unknown concentration of solutions of different groups of rats` heart tissue samples was calculated at 560nm.

The lysate was stored at -80^{o}C. In this protein quantification assay for loading and running the gel, small and equal amount of protein (35µg/25µl) was loaded from tissue homogenate in the wells of the SDS-PAGE gel, along with Mol. Wt. marker (SIGMA, Aldrich) in 1.5mm spaced glass slide. Lysate in sample buffer was boiled at 60^{o}C for 10min to reduce and denature. Loading and positive control were used. Gel acrylamide 10% was used in the gel based on the size of the protein. PVDF membrane (0.45µm pore size) was activated with methanol for 1min and rinse with transfer buffer. Stack was prepared as follows: (Fig. 23).

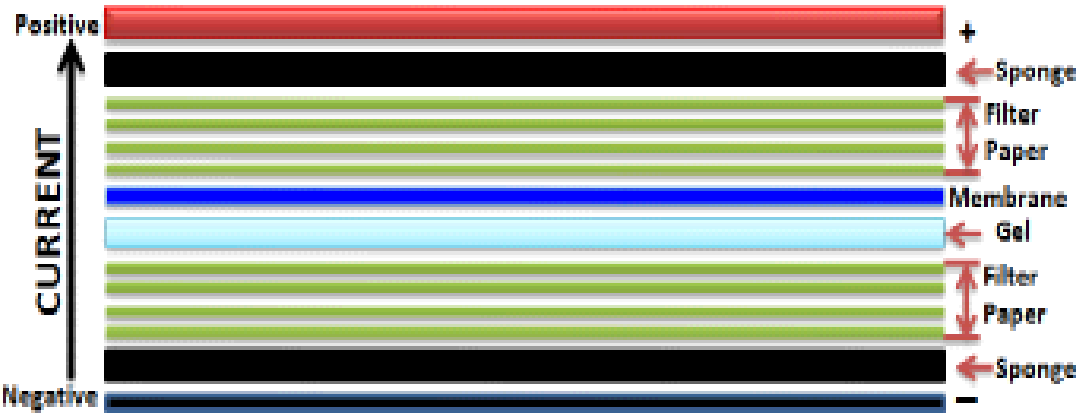

Figure: 23. Preparation of stack for the protein transfer from the gel to the membrane: Stack preparation can be done during a running of proteins.

The proteins were transferred in wet transfer with containing 25 mM Tris-base, 0.2 M Glycine, 20% Methanol, pH 8.5 for 2 hrs in 300 mAmps and 100V. In antibody staining, the membrane was blocked with 5% non-fat milk in TBS-T (0.1% Tween-20, Lot # 8T006910, A4974, 0250, CAS-No: 9005-64-5, AppliChem, Germany) for 1hr at RT.

The membrane incubated with specific primary antibodies DOR-1, and KOR-1 in blocking buffer overnight. The dilution rates of all primary antibodies were 1:1000. For signal development, following three cycles of 5min washes, drops of Luminata™ Forte Western HRP Substrate (Cat.No. WBLUF0500, Lot No. 140525, Millipore Corporation, Billerica, MA 01821) were added on membrane above 4 IN. X 125 FT. ROLL Lab-PARAFILM® (Pechiney Plastic Packaging, Menash, WI 54952, Chicago, IL, 60631), and then membrane developed for 3min exposure using G: Box Chem.XR5 Genesys version 1.0.7.0 with Synoptics 5.0MP Camera and 1.4 database version. By removing excess reagent and covering in a transparent plastic wrap, the membrane was developed for 30min exposure time.

The bands were visualized by enhanced chemiluminescence. Images were immediately saved in tift for densitometric quantification of the immunoreactive bands using the software ImageJ. GAPDH was used for standardization of the results.

3.2.11.TUNEL Assay

The TUNEL assay was performed as described in chapter two. All TUNEL staining solutions were prepared ahead using the protocol and AP cell death detection kit supplied from Roche for fluorescent and light microscopic analysis.

3.2.12. Statistical analysis

Mean value of immunoreactive cells ± SD in each group and independent samples t-test for the significance of means of independent groups of a number of KOR-1 and DOR-1 immunopositive cells of transplanted and control heart were used for statistical analysis using IBM Corp. Released 2011. IBM SPSS® Statistics for Windows, Version 20.0. Armonk, NY: IBM Corp software. Microsoft office Excel 2007 and Graph prism were also used to extract graphs. For relative quantification of real-time PCR data, the $2^{-\Delta\Delta Ct}$ method mentioned by Livak and Schmittgen 2001 was used. P value < 0.05 was regarded as statistically significant.

3.2.13. Study setting and ethical issue

This qualitative immunohistochemical experiment and IRC were conducted at the Department of Neurological, Biomedical and Movement Sciences. Quantitative experiments, immunoblotting, and RT-qPCR were performed at Laboratory of Cardiovascular Sciences and L.U.R.M. All experiments were carried out with the authorization of ethical Research Committee and Departmental Biobank at Department of Surgery, University of Verona and the Italian MOE.

3.3. Results

3.3.1. Histopathological observation of H&E stained tissue sections in heterotopic transplanted and naïve heart in rats

Histopathological observation of hematoxylin-eosin stained heterotopic transplanted and naïve heart tissue sections was done. As it is shown in figure 24, heterotopically transplanted heart tissue sections showed cellular rejection characterized by interstitial, scattered and perivascular lymphocytes infiltrate with a mild distorting morphology of myocytes compared to naïve heart. Ventricles and right atrium exhibited severe acute cellular rejection expressed by diffuse myocardial inflammation (Fig. 24).

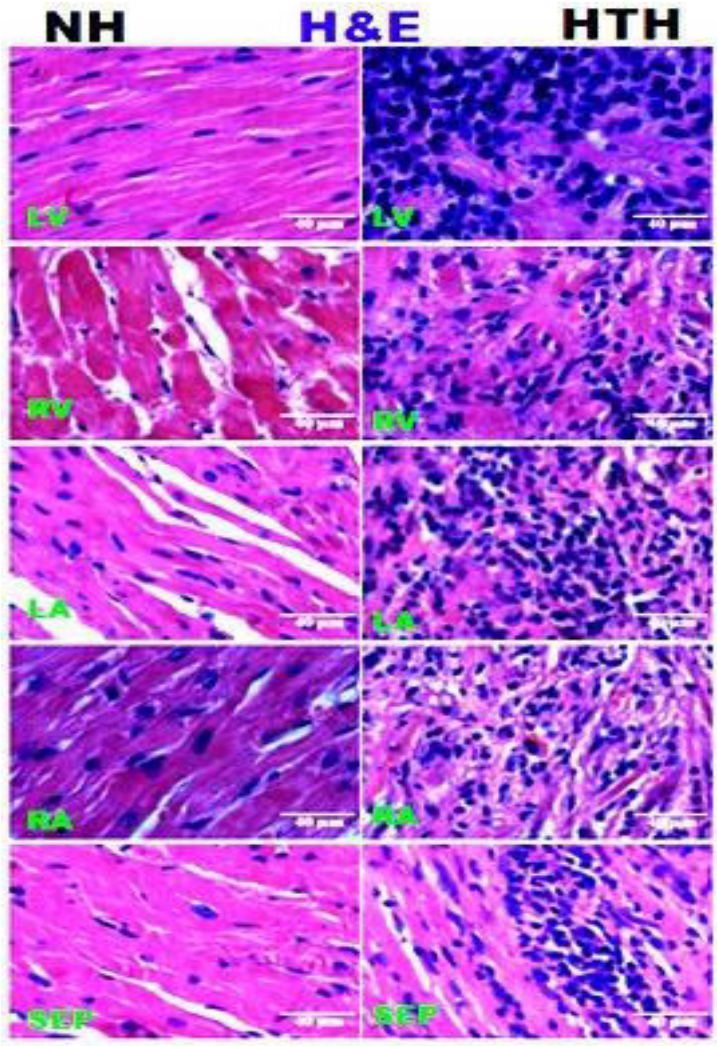

Figure: 24. Histopathological microscopic observation of H&E stained heterotopically transplanted and naïve heart tissue sections: Microscopic observation of Infiltrates of lymphocytes is showing in heterotopic transplanted heart. NH, Naïve heart; HTH, Heterotopic transplanted heart; LV, Left ventricle; RV, Right ventricle; LA, Left atrium; RA, Right atrium; SEP, Septum. Images were acquired at 400x magnification, Scale bar = 40µm.

3.3.2. Microscopic observation of immunoperoxidase stained DOR-1 immunoreactive myocytes and its optical density in heterotopic transplanted and naïve heart tissue sections in rats

Immunoperoxidase stained DOR-1 immunoreactivity was observed in both heterotopic transplanted and naïve heart tissue sections. In our study, it was found that DOR-1 immunoreactivity was reduced in optical density in heterotopic transplanted heart (0.097±0.02) compared to naïve heart (0.145± 0.04) tissue sections p = 0.035 (Fig. 25).

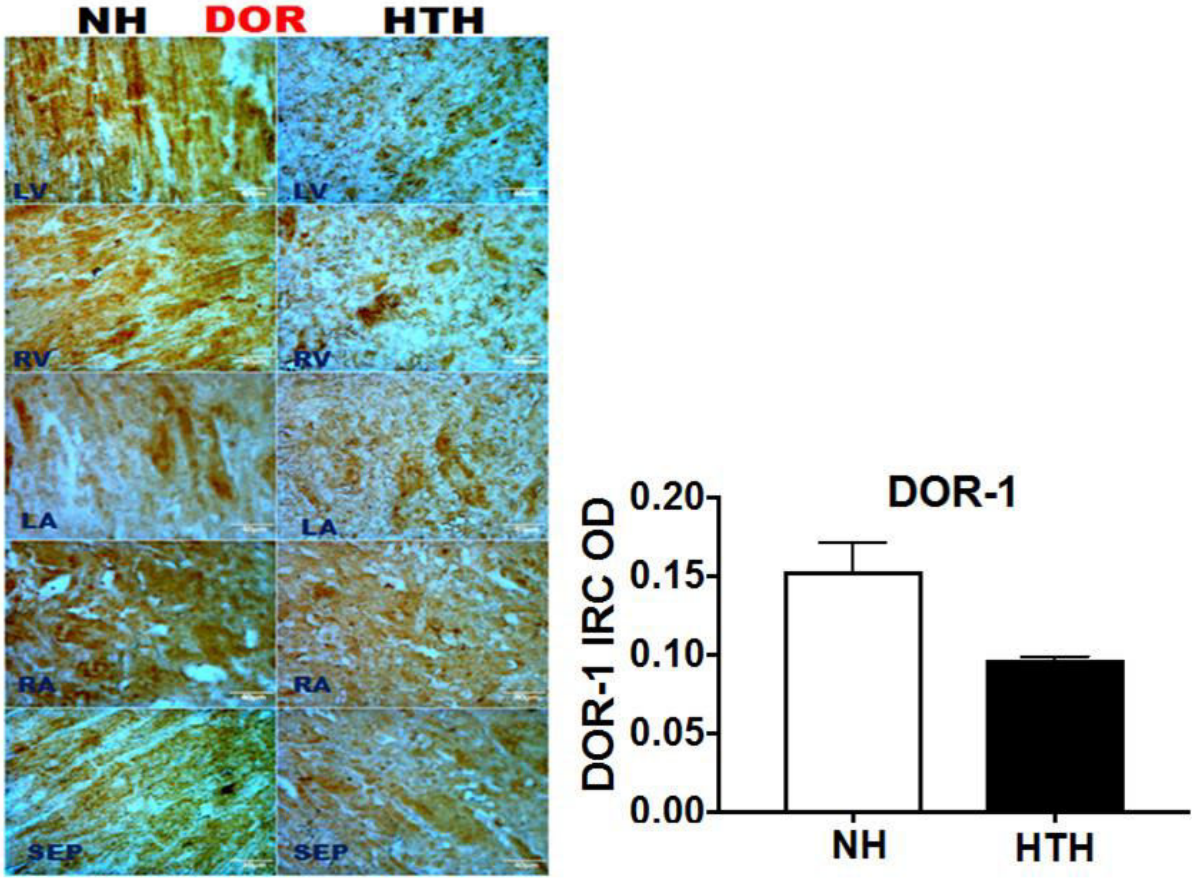

Figure: 25. Representative images of heterotopic transplanted and naïve heart tissue sections of LV, RV, LA, RA, and SEP with labeled DOR-1 immunoreactive cardiomyocytes and graph showing optical density for the strength of immunoreactivity of DOR-1 in cardiomyocytes of heterotopic transplanted and naïve heart tissue sections: heterotopic transplanted heart tissue sections showed lower strength of DOR-1immunoreactivity compared to naïve heart. Images were acquired at 400x magnification from each chamber and four representative images were taken from each chamber for optical density measurement, Scale bar 40µm. DOR, Delta opioid receptor; OD, Optical density NH, Naïve heart; HTH, Heterotopic transplanted heart; LV, Left ventricle; RV, Right ventricle; LA, Left atrium; RA, Right atrium; SEP, Septum.

3.3.3. KOR-1 immunoreactivity and its optical density in heterotopic transplanted and naïve heart tissue sections in rats

Immunoperoxidase stained KOR-1 immunoreactivity was observed both heterotopic transplanted and naïve heart. KOR-1 immunoreactivity (Fig. 26) was significantly reduced in heterotopic transplanted heart tissue sections (0.09±0.05) compared to naïve heart (0.19± 0.09) p = 0.036. Throughout our evaluation kappa opioid receptor was dominant in rats` heart compared to delta opioid receptor.

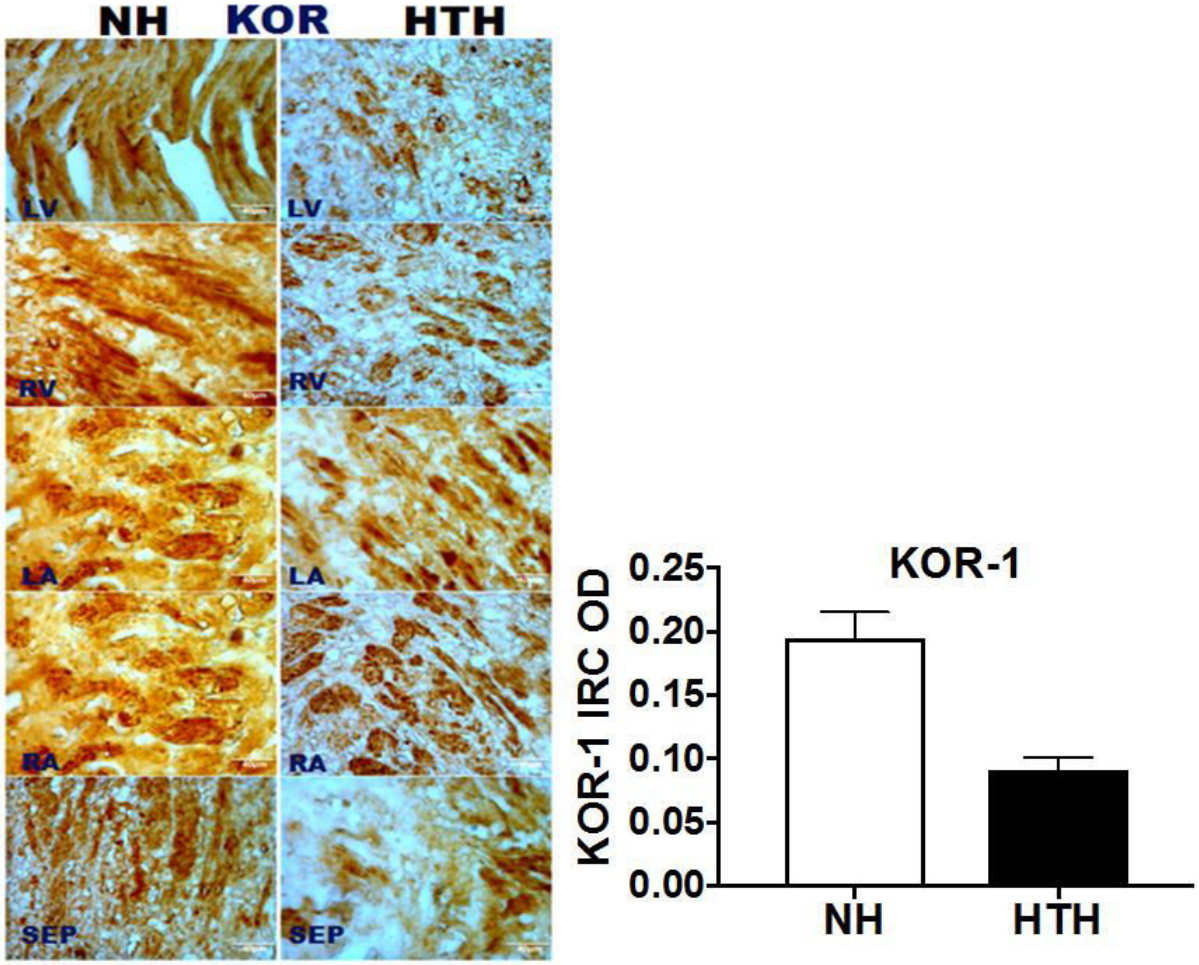

Figure: 26. Representative images of heterotopic transplanted and naïve heart tissue sections of KOR-1 labeled immunoreactive cardiomyocytes and OD of their immunoreactivity: Immunoperoxidase stained KOR-1 immunoreactive myocytes are apparently observed in NH compared to HTH. The graph illustrates the optical density measured for the strength of immunoreactivity of KOR-1 in heterotopic transplanted and naïve heart tissue sections: Images were acquired at 400x magnification from each chamber and 4 representative images were taken from each chamber for OD measurement, Scale bar 40µm. KOR, Kappa opioid receptor; OD, Optical density NH, Naïve heart; HTH, Heterotopic transplanted heart; LV, Left ventricle; RV, Right ventricle; LA, Left atrium; RA, Right atrium; SEP, Septum.

3.3.4. Microscopic observation of MOR-1 immunoreactivity in heterotopic transplanted and naïve heart tissue sections in rats

Expression of MOR-1 was examined in heterotopic transplanted and naïve heart tissue sections on the protein level by immunohistochemistry. In a number of repeated immunostaining experiments, MOR-1 immunoreactivity was not detected in both heterotopic transplanted and naïve heart tissue sections in the rat (Fig.27).

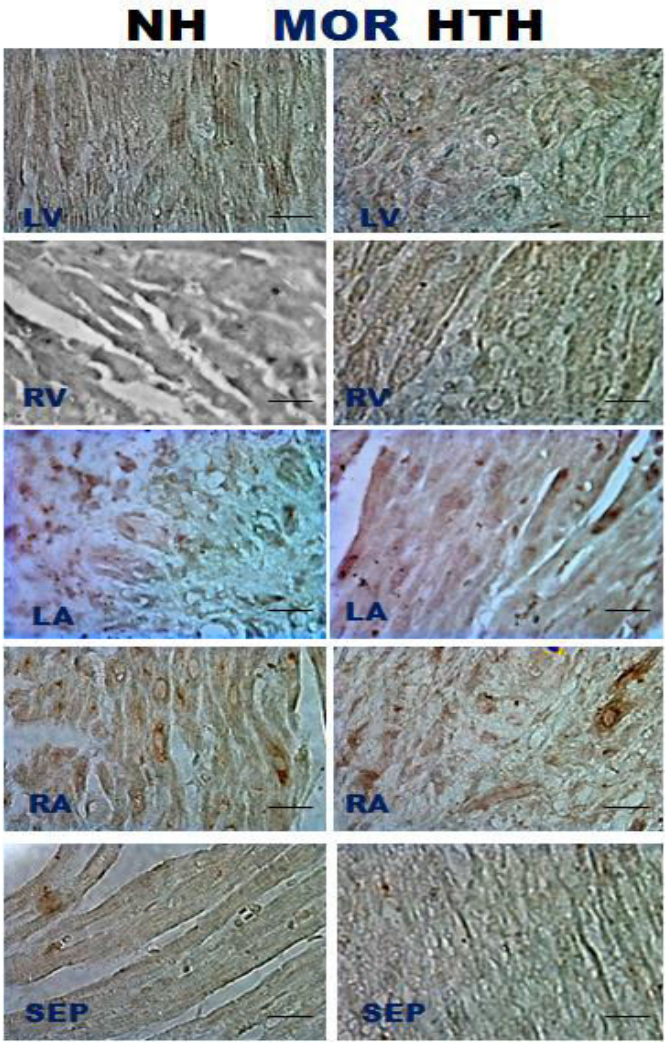

Figure: 27. Chamber-wise representative images of MOR-1 immunoreactivity in heterotopic transplanted and naïve heart tissue sections. In this immunohistochemical analyses MOR-1 immunoreactivity was not localized in hearts of rat. NH, naïve heart; HTH, Heterotopic transplanted heart; LV, Left ventricle; RV, Right ventricle; LA, Left atrium; RA, Right atrium; SEP, Septum. Images were acquired at 400x magnification, Scale bar, 40µm

3.3.5. Immunoperoxidase stained CGRP-1 immunoreactive cells and its optical density in heterotopic transplanted and naïve heart tissue sections

Microscopic observation of CGRP-1 immunoreactivity was evaluated in heterotopic transplanted and naïve heart. The immunoreactive CGRP-1 which is known to express in sensory and motor neurons was expressed both in heterotopic transplanted and naïve heart tissue sections. This neuronal marker was detected not only in nerve fibers but also in myocytes of both groups. However, it was weak in its expression in heterotopic transplanted heart tissue sections (Fig. 28) compared to naïve heart. The optical density of CGRP-1 IRC was significantly declined in heterotopic transplanted heart (0.298±0.054) compared to naïve heart tissue sections (0.368±0.05) p = 0.047. The prominent reduction of GCRP-1 immunoreactivity was observed in the heart tissue section where there was a reduction of kappa opioid receptors in transplanted heart.

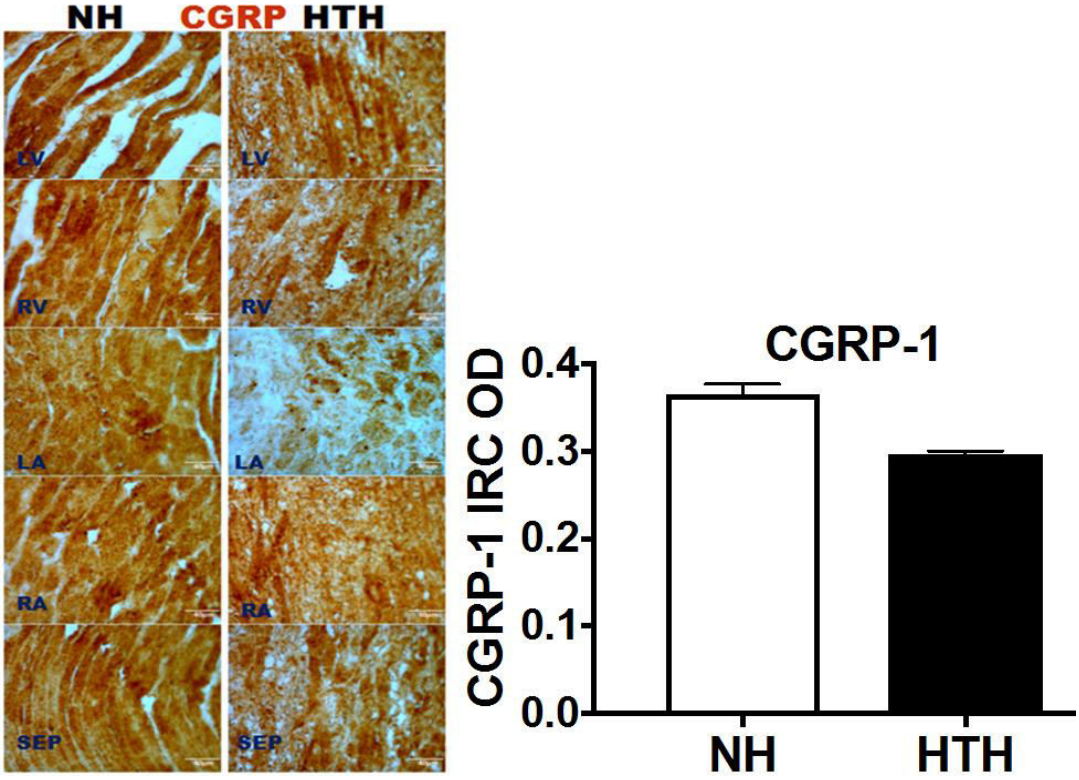

Figure: 28. Representative images showing CGRP-1 immunoreactive myocytes and graph showing the strength of CGRP-1 immunoreactivity of myocytes on heterotopic transplanted and naïve heart tissue sections: Images were acquired at 400x magnification from each chamber and 4 representative images were taken from each chamber for OD measurement, Scale bar 40µm. CGRP, Calcitonin gene-related peptide; OD, Optical density NH, Naïve heart; HTH, Heterotopic transplanted heart; LV, left ventricle; RV, Right ventricle; LA, Left atrium; RA, Right atrium; SEP, Septum; IRC, Immunoreactive cells.

3.3.6. Immunofluorescence stained KOR-1 and DOR-1 signals in heterotopic transplanted and naïve heart tissue sections in rats

Immunofluorescence labeled KOR-1 and DOR-1 immunoreactivity signals were detected under an inverted confocal microscope in naïve and heterotopic transplanted heart tissue (Fig. 29). This immunofluorescence technique, the prominent appearance of KOR-1 immunofluorescent signals in naïve heart was observed compared to heterotopic transplanted heart tissue sections. Moreover; poor DOR-1 immunofluorescence signals were identified in transplanted heart. DOR-1 was found weaker immunoreactive over KOR-1 in all sections of naïve and transplanted heart tissue.

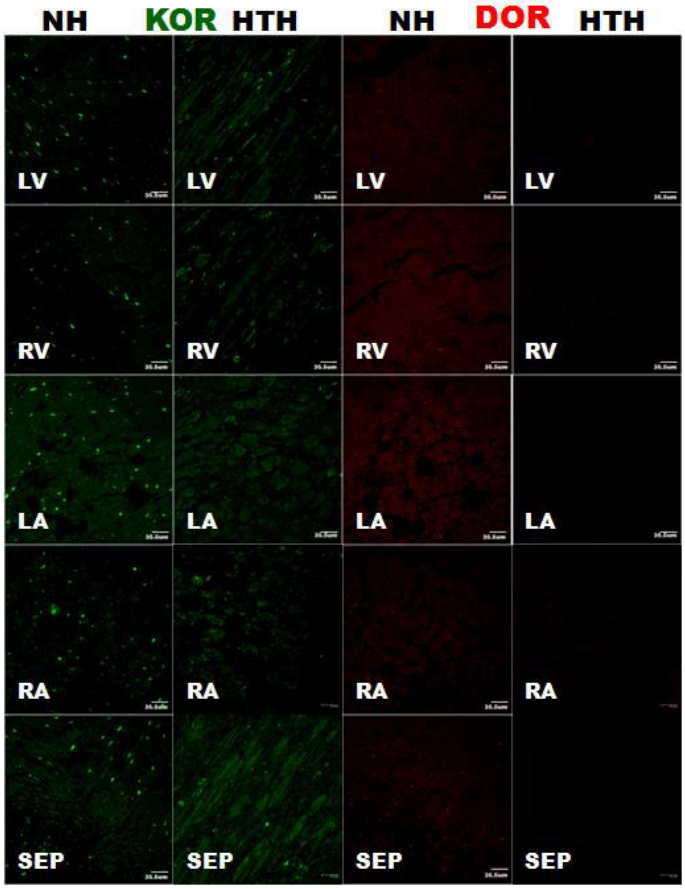

Figure: 29. Chamber wise confocal microscopy of KOR-1 and DOR-1 immunofluorescent reactive containing signals in naïve and heterotopic transplanted heart tissue sections in the rat: A: heterotopic transplanted heart tissue sections (Fig. 29. KOR, HTH) demonstrated KOR-1 immunofluorescent weak signals compared to naïve heart in each chamber (LV, RV, LA, RA, and SEP) of the heart. DOR-1 immunofluorescent signals were also observed more in naïve heart related to heterotopic transplanted heart in each chamber (LV, RV, LA, RA, and SEP). The performance of staining was confirmed by absence of signal in all negative control tissue sections. DOR, delta opioid receptor; KOR, kappa opioid receptor; HTH, heterotopic transplanted heart; NH, Naïve heart, KOR-1, Green; DOR-1 Red. LV, left ventricle; RV, Right ventricle; LA, Left atrium; RA, Right atrium; SEP, Septum. Scale bar, 35.5µm.

3.3.7. Co-expression KOR-1 and DOR-1 labeled double immunofluorescence immunoreactive signals in heterotopic transplanted heart tissue section

The double immunofluorescence KOR-1 and DOR-1 labeling immunoreactive signals showed co-localization of KOR-1 and DOR-1 in myocytes of heterotopic transplanted heart tissue sections (Fig. 30).

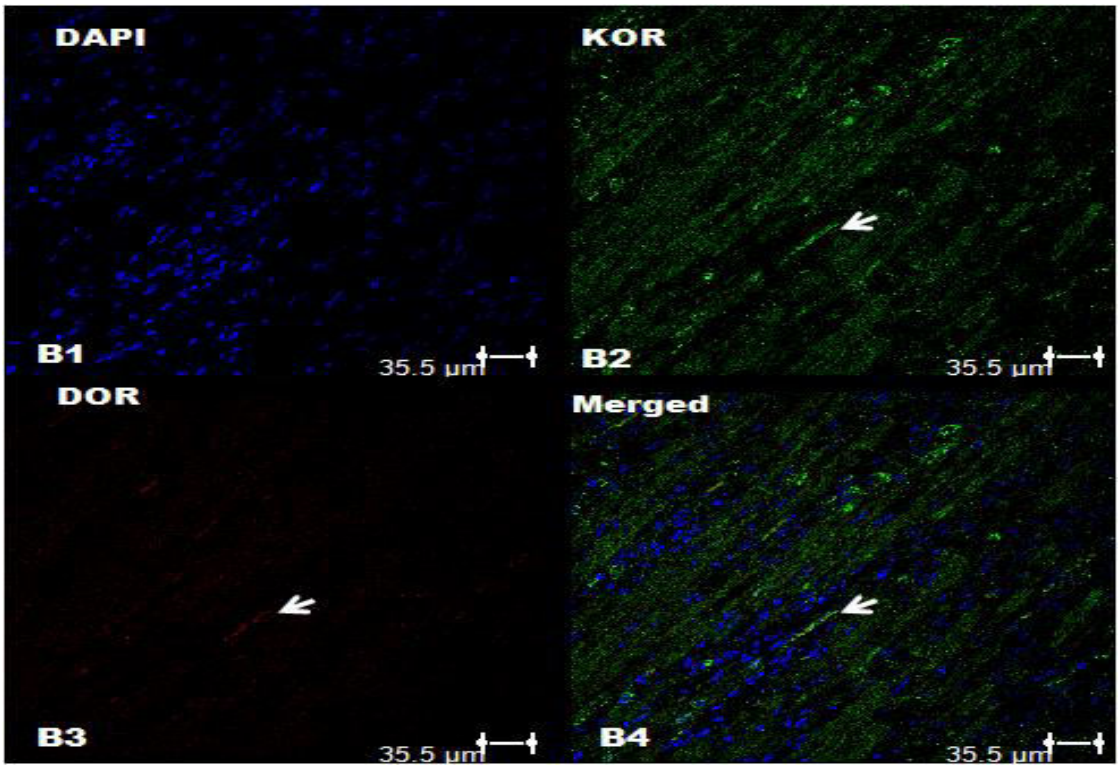

Figure: 30. Confocal microscopy of double immunofluorescence DOR-1 and KOR-1 labeled immunoreactive signals in heterotopic transplanted heart tissue sections: Co-localization of DOR-1 and KOR-1 was detected in heterotopic transplanted heart tissue sections. Note: absence of signal confirmed in negative control LV tissue section. KOR, kappa opioid receptor; HTH, heterotopic transplanted heart; NH, Naïve heart, KOR-1, Green; DOR-1 Red. Scale bar, 35.5µm.

3.3.8. RT-qPCR analysis for expression of Oprd1 and Oprk1 mRNA in rats

In this study, RT-qPCR technique was performed to detect the mRNA transcript encoding the three classical opioid receptors (μ, δ, κ) in heterotopic transplanted and naive heart in the rat. Data were generated by threshold cycle and Ct values were ranged from 24.05 to 28.8 (Oprk1 and Oprd1), 22.05 to 24.05 rGapdh, respectively. The mRNA transcript encoding the Oprd1 and Oprk1 was identified in heterotopic transplanted heart in atria and ventricles. The relative quantification of mRNA encoding Oprd1 and Oprk1 showed down-regulation of the mRNA transcript encoding the DOR and KOR in heterotopic transplanted rat heart. Moreover, our findings didn`t find the mRNA transcript encoding μ-opioid receptors in rat heart even up to 50$^{th}$ amplification cycle (Fig. 31). Thus, various previous and our current studies suggest that μ-opioid receptor is not expressed in rats` cardiac tissues. However, δ and κ-opioid receptors are detected in all chambers of the rat heart and down-regulated in heterotopic transplanted heart.

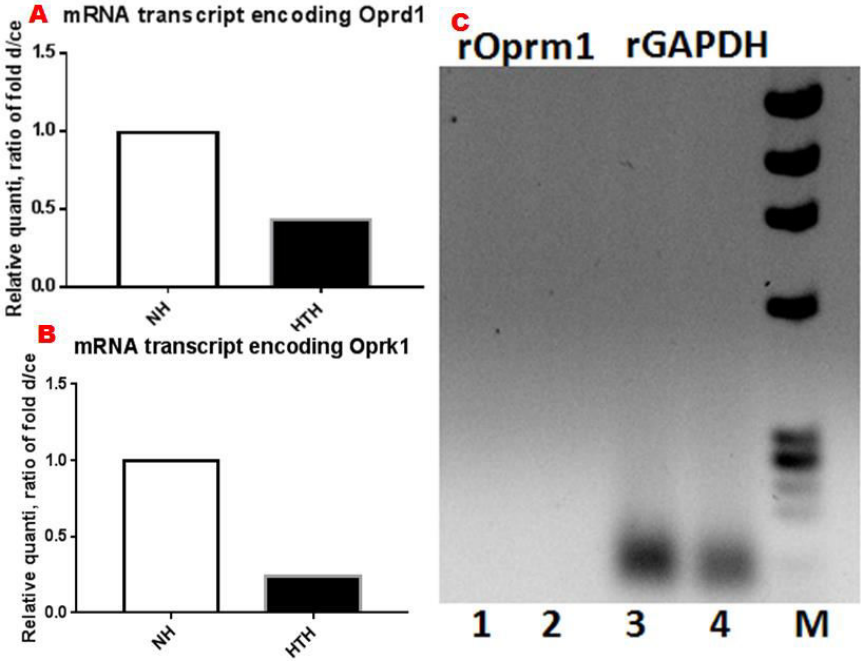

Figure: 31. Relative Oprd1 and Oprk1 mRNA expression: A&B: mRNA encoding DOR and KOR was detected and downregulated in HTH. rGAPDH gene was used as a reference gene to normalize sample variations; however, Gene encoding Oprm1 didn`t express in rat heart. C: Agarose gel electrophoresis of RT-qPCR product of Oprm1 (Fig. 31: 1 & 2) showing absence of rOprm1. Fig. C. 3&4 showing rGAPDH. Oprd1, Gene encodes Delta Opioid Receptor; Oprk1, Gene encodes kappa opioid receptor; Oprm1, Gene encodes Delta Opioid Receptor; rGAPDH, rat Glyceraldehyde-3-phosphate dehydrogenase

3.3.9. Western blot analysis of DOR-1 and KOR-1 immunoreactive proteins in heterotopic transplanted and naïve heart tissue in rats

Western blot analysis of KOR-1 and DOR-1 immunoreactive proteins in heterotopic transplanted and naïve heart was done and found at the estimated molecular weight. As shown in figure 32 the amount of KOR in HTH (30.13±2) compared to naïve heart (46.61±4.4), p=0.03. Similarly, δ- ORs proteins were lowered in HTH (Fig. 32). The reduction in the amount of κ- & δ- ORs proteins in HTH was also supported by their reduced mRNA levels.

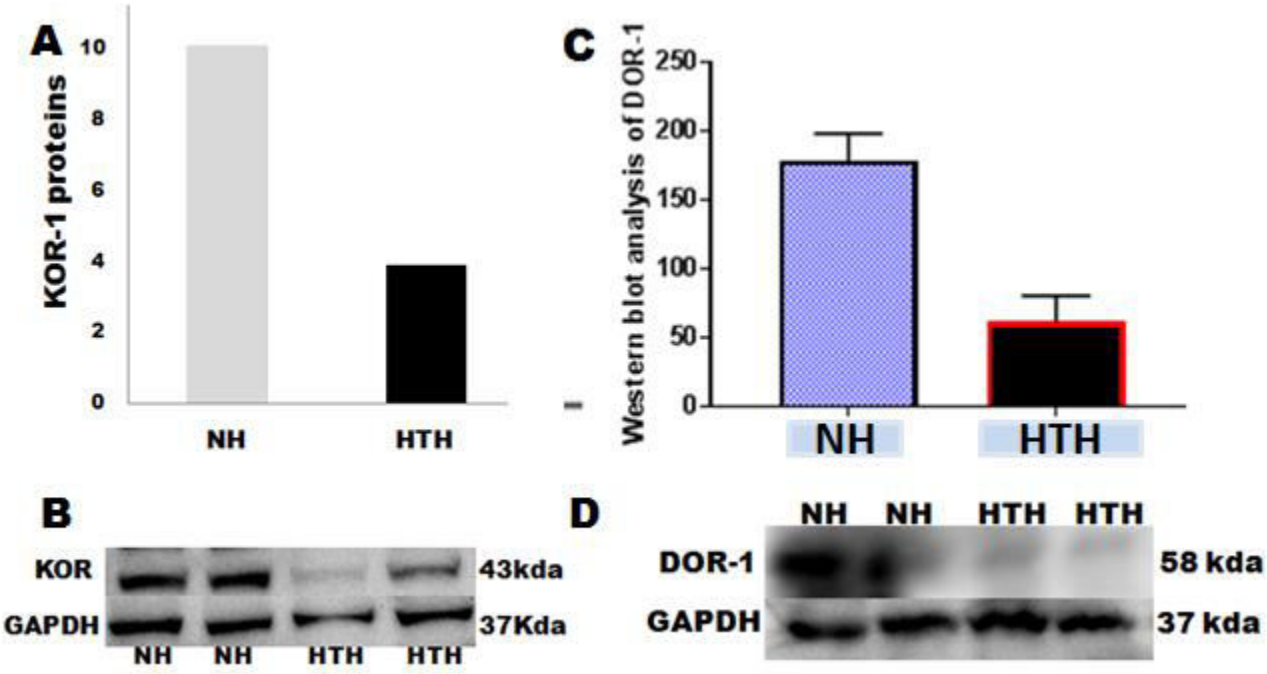

Figure: 32. **Immunoblot analysis of KOR-1 and DOR-1 proteins in heterotopic transplanted and naïve heart tissue in rat**: KOR-1 and DOR-1 proteins analysis was done using 25ug of protein per 25ul which was loaded to 10% acrylamide gel. NH, Naïve heart; HTH, transplanted heart. Quantification of KOR-1 and DOR-1 proteins optical density was done using ImageJ. Mean ± STD, $p<0.05$ was considered as statistically significant.

3.3.10. Apoptotic nuclei in heterotopic transplanted and naïve heart tissue sections in rat and TUNEL positive nuclei count

TUNEL positive nuclei were observed in heterotopic transplanted heart with a significant elevation (6.9±74) compared to naïve heart (3.33±0.68), $p<0.001$ (Fig. 33). Moreover, significant elevated apoptotic nuclei also observed in the interstitial cells. It is known that many regulatory proteins (Bcl2, Bax) play role in apoptosis. The abnormally elevated apoptosis that brings cell death later express Bax that elevates apoptosis and could decrease an apoptotic inhibitor (Bcl2) that could cause necrosis of myocytes.

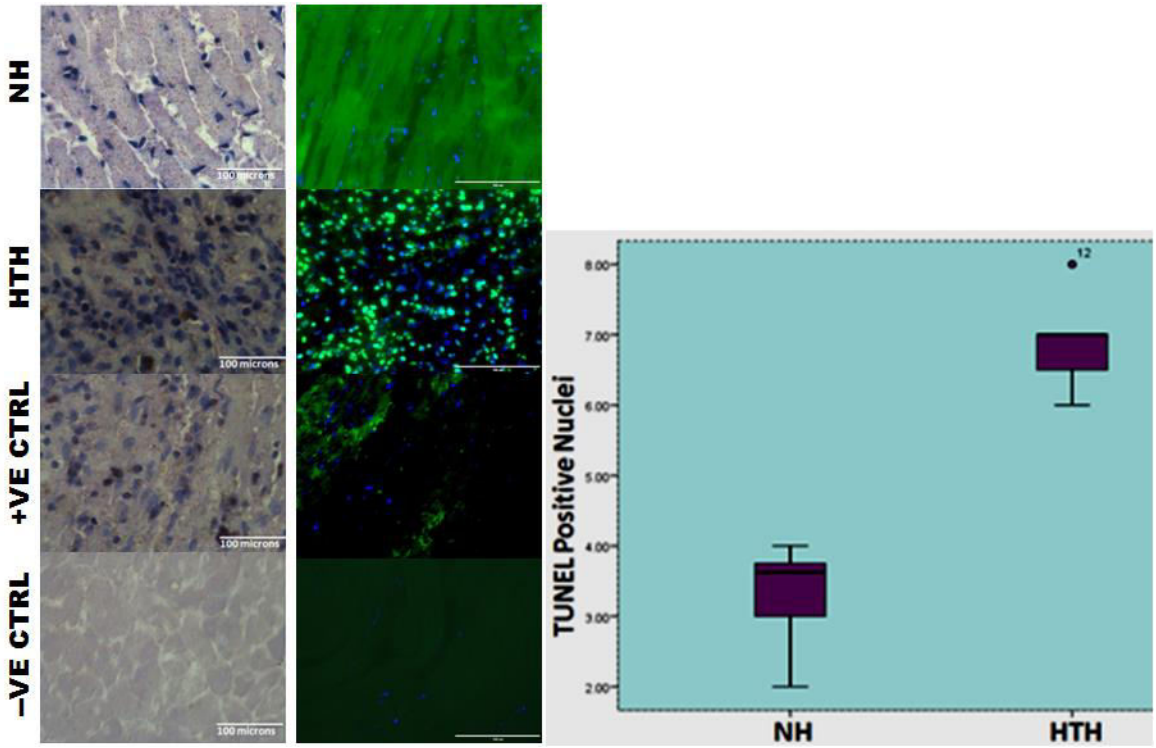

Figure: 33. Representative photomicrographs of TUNEL positive nuclei of myocytes in heterotopic transplanted and naïve heart tissue sections and apoptotic nuclei counts: TUNEL positive apoptotic nuclei found significantly elevated in heterotopic transplanted heart compared to naïve heart. Mean±STD, $P<0.05$ was considered as significant. TUNEL+ Hematoxylin (H); HTH, Heterotopic transplanted heart; NH, Naïve heart; OI, Oil immersion; TUNEL, Terminal deoxynucleotidyl transferase; dUTP, 2'-deoxyuridine 5'-triphosphate; Nick End Labeling; +VE CTRL, Positive control; -VE CTRL, Negative control.

3.4. Discussion

Before two decades a study of ORs expression during heart ontogeny has shown the existence of ORs in Wistar Kyoto rats' heart in the early developmental period. On the other hand, the same study has demonstrated a reduction and disappearance of mu-OR after 7days of the postnatal period (Zimilichman et al., 1996). Thus, Kappa OR is the first to be detected developmentally in mouse heart (Zhu et al., 1998). This study shows the expression of δ & κ-ORs in rat heart as shown in porcine (Karlsson et al., 2012), in all chambers of human but in another study, it is only seen in human atria (Lendeckel et al., 2005; Sobanski et al., 2014).

There is a great disparity and debates regarding the distribution of opioid receptors subtype in the heart chambers (Krumins et al., 1985) and between species (Karlsson et al., 2012). Many studies support the presence of kappa and delta ORs in rat heart (Ela et al., 1997; Ventura et al., 1989), whereas some studies show that mu-OR is decreased or not expressed in heart tissue (Theisen et al., 2014), or is disappeared after seventh day of postnatal age (Zimlichman et al., 1996). The findings of this study shown that mRNA encoding Oprk1 and Oprd1 delta and kappa opioid receptors are detected in rat heart of all chambers, and interestingly, the study has shown a reduction of DOR-1 and KOR-1 immunoreactivity at the protein levels in heterotopic transplanted rat heart tissues. However, mRNA encoding Oprm1 and proteins on cardiomyocytes of transplanted rats` heart are not detected. A similar immunohistochemical result has reported recently that MOR is absent in any of the cardiac tissue in porcine (Theisen et al., 2014).

In the developmental study, Mousa and colleagues (2011) have shown co-localization of DOR-1 with VAChT principal neurons from the first day of birth and with small intensely fluorescent catecholaminergic cells and CGRP within intracardiac ganglia and atrial myocardium. They also demonstrated the co-expression of DOR with neuronal markers increasing with age (neonatal to adulthood) (Mousa et al., 2011) and gradual increase of DOR mRNA, protein, and binding sites from postnatal day 1 towards adulthood. These developmental expressions of opioid receptors and sympathetic,

parasympathetic and sensory innervations of the heart imply the regulation of opioid receptors by cardiac autonomic innervations. Likewise, in our immunohistochemical study, co-localization of the neuronal marker (CGRP-1) and kappa opioid receptor signals are detected in both naive and heterotopic transplanted heart in the rats.

In another immunohistochemical localization report, delta and kappa ORs and CGRP sensory nerve fibers are expressed in heart tissue done by using only two individuals of sudden death (Sobanski et al., 2014); however, in transplanted and STZ-induced diabetic rats has not been addressed and/or characterized. Sobanski et al., 2014 employed lacking quantitative approaches, in transplanted heart model for opioid receptors characterization studies in the denervated heart. Thus, this study might show the correlation of denervation and opioid receptors regulation.

3.5. Conclusions

The findings of this study reveal down-regulation of delta and kappa ORs and elevated apoptotic nuclei in heterotopic transplanted heart. Therefore, heterotopic transplanted model in rats may expound the role of opioid receptors (δ & κ) in cardioprotection and pathophysiology in cardiac transplants.

CHAPTER FOUR

4. Characterization of opioid receptors in STZ-induced diabetic heart of rats

4.1. Introduction

The term "diabetes" was first coined by Apollonius of Memphis around 250 BC (Mandal, 2012). Later, in 1675, the word "Mellitus" was added after the sweetness of urine and blood had been noticed by the ancient Greeks, Chinese, Egyptians, Indians, and Persians (Mandal, 2012). In diabetic patients, ischemic heart disease is a major complication and remains the first cause of death worldwide (Wider and Przyklenk, 2014).

Globally, an estimated 108 million in 1980 (WHO, 2016), 171 million in 2000 (Wild et al., 2004), 422 million in 2014 adult people were living with diabetes (WHO, 2016). It is projected to rise to 366 million in 2030 (Wild et al., 2004). Over 4.3 million cases of diabetes in Italy were reported in 2000. The global prevalence of diabetes for all age-groups was estimated to be 2.8% in 2000 (Wild et al., 2004). Nowadays, it is alarmingly rising from 4.7% to 8.5% in the adult population (WHO, 2016). In diabetes, nerve damage is mentioned among the major complications such as heart attack, stroke, kidney failure, leg amputation and vision loss (WHO, 2016). Moreover, it could also result in fetal death during pregnancy due to poorly managed diabetes (WHO, 2016).

Diabetic neuropathy (DNP) is the most common microvascular complication of diabetes mellitus (DM) (Shaikh and Somani, 2010; Bansal et al., 2006), which occurs in more than 50% of patients and affects nerve fibers of peripheral nervous system (Erbas et al., 2016; Said, 2007). It leads to allodynia, nerve conduction slowing and progressive sensory loss (Parkar and Addeoalli, 2014). This may affect on the level of opioid receptors expression in the heart of neuropathic model of diabetic rats. Several investigators have studied about diabetes to battle its complications. Thus, this study may contribute to filling the gap through a study that aimed to characterize the expression of opioid receptors (mu, delta, and kappa) in the STZ-induced neuropathic model of diabetic rat heart.

4.2. Materials and methods

4.2.1. Experimental design

The experimental design consisted of two groups of Sprague-Dawley rats: control (n=11) and treated (n=10) groups. The control group was given 50mM citrate buffer. The treated group was injected with Streptozotocin (STZ) at a single dose of 65mg/kg/bw diluted with citrate buffer.

4.2.2. Experimental animals and housing

Adult male Sprague-Dawley rats (weighing 300-350g) were obtained from Charles River Laboratories, Italy. They were housed 2 per cage in a setup cage system at Interdepartmental Center of Experimental Research Service/CIRSAL, the University of Verona at a temperature controlled room (21±2^{o}C) with food (ad libitum) and water available under a 12 hours' light/dark cycle. They were acclimatized for a week before the beginning of the experiment in order to adapt them to the laboratory conditions. All tests were done during the light hours. The study was carried out in accordance with the ethical guidelines for investigations of experimental pain in conscious animals (Zimmermann, 1983; CIRSAL, University of Verona).

4.2.3. Drugs and citrate buffer (0.1M) preparation

Citrate buffer (100ml) was prepared by adding 100ml of ddH_2O to 294.12mg of trisodium citrate dehydrate and 210.14mg of citric acid monohydrate each separately. Thereafter, 55.5 ml and 45.5ml of each solution were mixed to obtain citrate buffer (pH 4.5). The buffer was filtered with a 20um filter using filtration vacuum before used. This buffer was prepared during rats` fasting time. Streptozotocin (STZ) mixed anomers (STZ, product ref. S0130-500MG, Lot. No. WXBC2044V, SIGMA-Aldrich Chemie GmbH Kappelweg Schnelldorf, Germany) was dilute in 1ml of citrate buffer (10mM, pH 4.5) to maintain the stability of STZ solution in 1.5ml microcentrifuge tube covered with aluminum foil for each rat. Streptozotocin solution was immediately administered within 5min of dissolving to prevent degradation of the drug.

4.2.4. Preparation of STZ-induced rat model and sample collection

In STZ-induced model of diabetic rats' preparation, pilot experiment for dosing of the drug (STZ) was optimized at different doses to assess survival of rats after STZ i.p. injection for the chronic diabetic condition. Among the 10^{th} rats used for the pilot experiment weighing ≥400g subjected to the procedure, the survival rate was 70%. Then, younger and weighing 300-320g rats freshly prepared 65mg/kg (32.5mg/ml) of STZ dissolved in 10mM citrate buffer (45.5ml 0.1M citrate acid and 55.5ml 0.1M Na2HPO4, pH 4.5) was injected i.p to overnight fasted Sprague-Dawley rats after measuring fasting blood glucose level.

Animals were placed on a regular diet after 4hrs of STZ i.p injection. STZ-injected animals exhibited hyperglycemia within 24hrs. The animals with fasting blood glucose levels ≥250 mg/dl were considered diabetic (Rao et al., 2010; Thakur et al., 2011).

The rats in all groups were sacrificed after six weeks. Heart tissue samples were collected from all chambers and septum of the heart both in paraformaldehyde for paraffin embedding and in liquid nitrogen for isolation total RNA (RT-qPCR) and proteins (western blot).

4.2.5. Body weight and fasting blood glucose level measurement

Body weights of all groups of the rat were taken at the beginning before STZ injection and after three and seven weeks of i.p. injection. Rats were pre-warmed with red lump to have more blood in the tail. The blood collection site of the tail was wiped with 70% ethanol (DIAPATH S.p.A, Lot: 2016X01177, Ref. A0123) prior to placed droplet of blood on a glucometer test strip. A blood sample obtained by pricking the lateral tail vein using a sterile needle and then the blood was gently milked from lateral tail vein and placed droplet of blood on a glucometer test strip and read using $^{\text{STAT STRIP}}$*Xpress-i* glucometer mg/dl (SN 138038215324, Nova Biomedical UK) and STAS-STRIP GLU SENSOR (Lot: 0315123309). Fasting blood glucose levels was measured after 24hrs, two and six weeks of STZ-induction.

4.2.6. Tissue processing, paraffin embedding, and sectioning

The tissue processing, paraffin embedding, and sectioning were performed as described in the second and third chapters.

4.2.7. Hematoxylin and Eosin staining for histopathological study

Routine H&E staining histo-technique was performed as indicated in the previously studies to evaluate any structural abnormalities and level of neuropathy in sections of sciatic nerves. Any structural abnormalities of the sciatic nerve in H&E stained tissue sections were analyzed with the help of pathologist.

4.2.8. Immunohistochemistry: Immunoperoxidase and Immunofluorescence

Immunohistochemical studies, such as immunoperoxidase and double immunofluorescence (IF) were used done as described in previous studies to evaluate MOR-1, DOR-1, KOR-1 and CGRP-1 immunoreactive cardiomyocytes, and analyzed for relative distribution of opioid receptors on STZ-induced diabetic and control rat tissue sections.

In immunoperoxidase staining was performed using markers for detection of MOR-1, DOR-1 and KOR-1 (a rabbit polyclonal antibody (H-80): Cat. No. sc-15310, a goat polyclonal antibody (M-20): Cat. No. sc-7492, and a mouse monoclonal antibody (D-8): Cat. No. sc-374479, respectively). Secondary Abs (anti-rabbit IgG (H+L) biotinylated (BA- 1100, Lot no. ZA0319) and anti-goat IgG (H+L) biotinylated (BA- 9500, Lot no. Z0326), and anti-mouse Abs made in a horse for MOR-1, DOR-1, and KOR-1, respectively). Primary Abs markers were diluted 1:250, while secondary at 1:1000 in PBS containing 2% NHS and 0.25% Triton X-10.

Double immunofluorescence was also performed for the concurrent visualization of MOR-1, DOR-1 and KOR-1 immunoreactive signals on cardiomyocytes in overnight incubation with mixture of primary antibodies (MOR-1, DOR-1, KOR-1) with three hrs different fluorescent secondary antibody Alexa Fluor 568 donkey anti-rabbit IgG (H+L) (1:1000, Ref. A10042, Lot no. 1668655, Eugene DR. USA), Alexa Fluor 488 donkey

anti-goat IgG (H+L) (1:1000, A11055, Lot no. 1627966, Eugene DR. USA), and anti-mouse species-specific fluorescent secondary antibodies raised in donkey supplied from Life Technologies, Italy, Europe. The cell nuclei stained blue using Hoechst 33342 at a dilution of 1:10,000 (Thermo Fisher Scientific). Finally, drops of mountant were added on sections and cover with rectangular microscope cover glasses (ECN631-1574, Lot: 29339 017, 24x50mm), Germany. The pressure was applied gently over cover glasses to remove bubbles before sealing of edges of cover glasses with nail polish and then stored at -20^{o}C until analysis was done by inverted confocal microscope.

4.2.9. Immunoblotting

Immunoblotting analysis with the method indicated earlier. Protein concentration was measured using BCA assay (Fig. 34). An equal amount of protein (35µg/25µl) was loaded from tissue homogenate in the wells of the SDS-PAGE gel, along with Mol. Wt. marker (SIGMA, Aldrich).

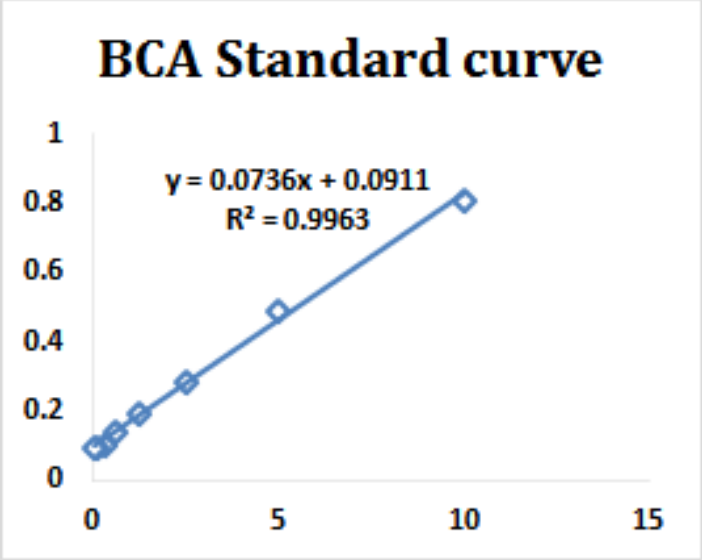

Figure: 34. BCA standard curve for protein concentration measurement: BCA assay was done to measure unknown protein concentration after standard curve was plotted using known BSA protein concentrations. The unknown concentration of solutions of different groups of rats` heart tissue samples was calculated at 560nm.

The membrane incubated with specific primary antibodies anti-DOR-1 (goat) and anti-KOR-1 (mouse) at a dilution rate of 1:1000 in blocking buffer overnight, and then

incubated with appropriate secondary antibodies. The bands were visualized by enhanced chemiluminescence.

4.2.10. Microscopy, optical density measurement and analyses of MOR-1, DOR-1, and KOR-1 immunoreactivity

Microscopy, counting, and analyses of DOR-1, KOR-1, and CGRP-1 IRC were done as indicated in previously studies. Prior to counting, slides were blindly assigned with code number and sections thickness was measured. Counts of KOR-1 immunoreactive cardiomyocytes were performed using 20X objective at 3 to 3.5µm.

The only observed longitudinal full length of KOR-1 immunoreactive cardiomyocyte in the focal field of the live preview was used as a counting unit. Four sections were selected randomly from each sample. The counting was done using Image-Pro Plus software (7.0, 2009, QImaging, Media Cybernetics, Silver Spring MD, USA) installed on a computer with workspace preview for KOR immunoreactive cells using circle classed symbol and tag points to count the number of immunopositive cells.

Optical density measurement was done for DOR-1 and CGRP-1 using Figi version of ImageJ to quantify the strength of immunoperoxidase staining in heart tissue sections of MOR, DOR, and CGRP-1 proteins in STZ-induced diabetic rats. Optical density/OD methods (Image-adjust, color-deconvolution/H DAB)-threshold with dark background) indicated by Jensen, 2013 was used with the following formula: OD = log (255 ÷ Mean Intensity).

Laser scanning confocal microscope (Carl Zeiss LSM 510, Göttingen, Germany) was used for obtaining multicolor optical images from sections of specimens of STZ-induced diabetic and control heart. Immunofluorescence images were further harmonized by using Leica LAS AF lite software for better contrast.

4.2.11. Cryosectioning, RNA isolation, and synthesis of cDNA

The same method was applied as indicated the earlier study of Heterotopic transplanted heart for cryo-sectioning, RNA isolation, cDNA synthesis, and quantitative Real-Time PCR.The primers sequence used for real-time PCR SYBR Green amplification were forward rat 5`-3` (Oprm1, CTAACCACCAGCTAGAAAATC; Oprd1, AATCGTCCGGTACACTAAG; Oprk1, GTCATCATCCGATACACAAAG) and reverse rat 5`-3` (Oprm1, TTTGAATGCAGGATCAGATG; Oprd1, AACATGTTGTAGTAGTCAATGG; Oprk1, GGCCAAGAATTCATCAAGTAG) supplied by SIGMA Aldrich.

4.2.12.TUNEL Assay

The TUNEL assay was performed as indicated earlier. All TUNEL staining solutions were prepared ahead using the protocol and AP cell death detection kit supplied from Roche for fluorescent and light microscopic analysis.

4.2.13. Statistical analysis

Repeated measures ANOVA with Bonferroni comparison test were used to evaluate body weights and fasting blood glucose levels before and after STZ-injection of rats.

4.3. Results

4.3.1. Observation, body weight, fasting blood glucose level measurement, and histopathology of pancreas

The pilot experiment evaluating survival rate of rats after i.p. STZ-injection revealed higher rate (90%) of death in older and >400g weighing rats within 1 week. Thereafter, younger rats weighing 320-380g were injected with STZ. Rats became diabetic within 24hrs following the injection, and they displayed common symptoms of diabetes such as weight loss, polyuria, glucosuria, drowsiness, polydipsia (Okon et al., 2015), and behavioral signs of toxicity (erection of hairs, slow locomotion) Fig. 35.

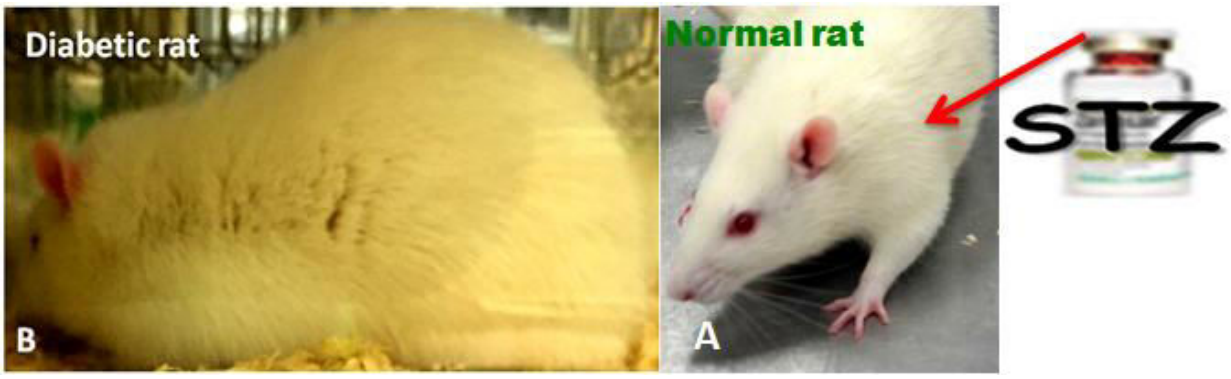

Figure: 35. Streptozotocin-induced diabetic and normal rats: Rats before and after (Fig.35 B) STZ-i.p. injection. STZ-induced diabetic rats showed (Fig.35 B) showed excessive thirst, drowsiness, erection of hairs, and production of large volume of urine.

Body weights were measured at the beginning, and 24hrs, 3 weeks and 7 weeks following STZ-injection. Average body weights of rats following three (337±12, $P<0.05$) & seven (319±15.57, $P<0.001$) weeks of the injection showed statistical significant reduction compared to initial body weight (350±6.124). However, 24hrs following the injection did not show any significant difference matched up to initial body weight (Fig. 36).

Fasting blood glucose levels were measured before, and after 24hrs and 7weeks of STZ-injection. Average fasting blood glucose levels (FBGL) following 24hrs (348.33±38) and seven weeks (497.44±26.5) of STZ injection were found statistically significant compared to initial fasting blood glucose levels (110.44 ±10.36) $P<0.001$. The proportion

of FBGL was 22.2%, 70%, and 7.78% after 24hrs, 7 weeks, and initial FBGL, respectively (Fig. 36).

Histopathological observation of H&E stained pancreatic tissue sections in diabetic rats showed abnormal distribution and damage of of langerhans islet cells such as shrinkage and necrotic of islet beta-cells due to the effect of Streptozotocin (Fig 36 B2). In the contrary, the control rats demonstrated normal islets distributions.

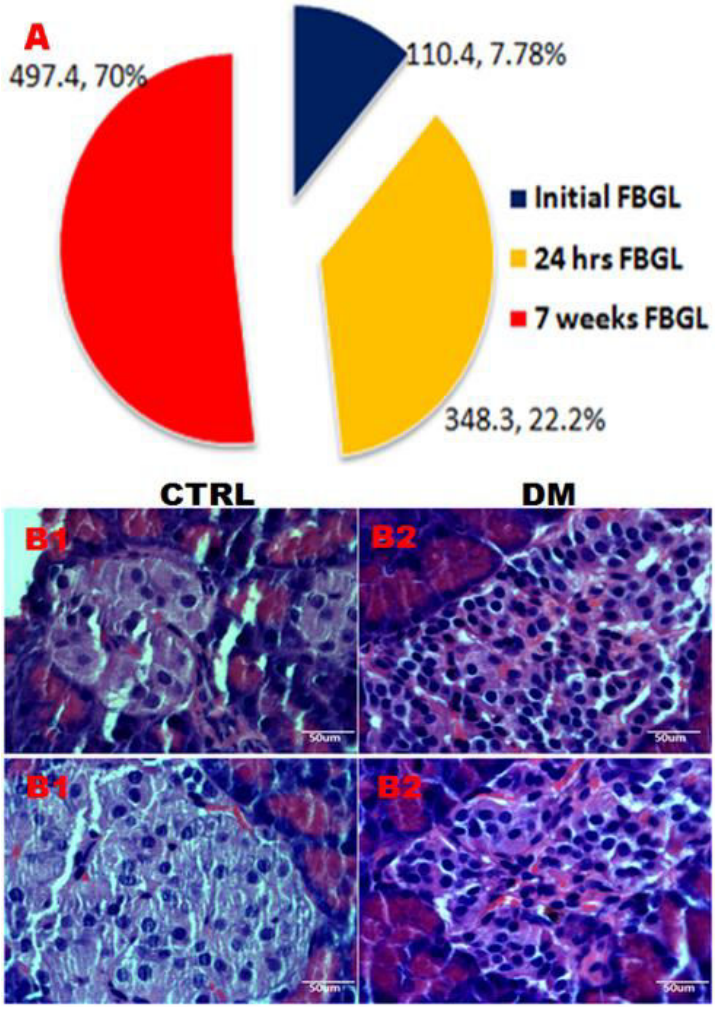

Figure: 36. Higher percentage of fasting blood glucose level and histopathology of pancreatic tissue sections of diabetic rats: A: The pie chart illustrating the percentage of FBGL which was measured at the beginning of the experiment, after 24hr and 7 weeks of STZ-injection. B1&B2: Pancreatic tissue of normal and diabetic rats. **B2:** Pancreatic tissue sections showed abnormal distribution and damage of of langerhans islet cells such as shrinkage and necrotic of islet beta-cells due to the effect of Streptozotocin, H&E stain 400x magnification) FBGL, Fasting blood glucose level; CTRL, Control; DM, Diabetic mellitus, STZ, Streptozotocin; i.p, Intraperitoneal.

4.3.2. Histopathological observation of H&E stained sciatic nerve and heart tissue sections in diabetic and control rats` heart

Histopathology of sciatic nerve and heart tissue sections was evaluated. Transverse (Fig 37. A1, B1) and longitudinal (Fig. 37 A2, B2) sections of sciatic nerve tissue of STZ-induced diabetic rats demonstrated an increase in connective tissue (CT) fibrosis around the epineurium and axonal swelling (Fig.37. B1, B2) which are common pathological features of neuropathic nerve; however, these changes were not observed in non-diabetic rats (Fig.37. A1, A2). Heart tissue sections of diabetic rats showed abnormally arranged and disorganized cardimyocytes with first stage of fibrosis. However, normal, single and oval centrally located nuclei of myocytes with regularly arranged cardiac fibers were observed in control rats (Fig.37. D).

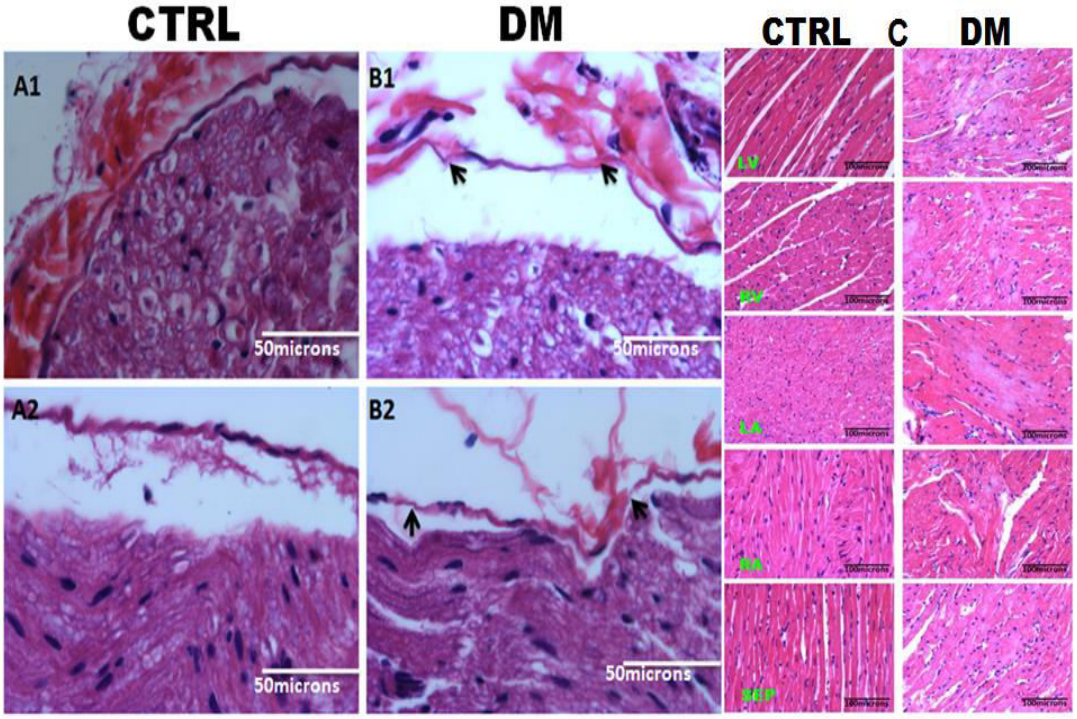

Figure: 37. FFPE tissue histopathological evaluation of diabetic rat heart and sciatic nerve tissue sections: A: The above figures illustrated the effect of STZ- induced diabetes on microscopic morphological changes in rats` sciatic and heart tissue. Cross-section (Fig.37. **A2)** transverse sections (Fig. 37. **B2)** of sciatic nerve showed CT with fibrosis around epineurium and axonal swelling in STZ-induced diabetic rats (400x magnifications) scale bar = 50microns. **C:** Heart tissue sections of diabetic rats (DM) showed abnormally arranged and disorganized cardimyocytes with first stage of fibrosis. However, normal, single and oval centrally located nuclei of myocytes with regularly arranged cardiac fibers were observed in control (200x magnifications) scale bar = 100microns. STZ, Streptozotocin; CTRL, control sciatic nerve tissue section; CT, Connective tissue; FFPE, Formalin fixed paraffin embedded; DM, Diabetic Mellitus; CTRL, Control. Scale bar, 50microns

4.3.3. Immunoperoxidase stained DOR-1, KOR-1, MOR-1, and CGRP-1 immunoreactive myocytes and their optical density in heart tissue of diabetic and control rats

Microscopic observation of DOR-1 and KOR-1immunoperoxidase-stained tissue sections of heart demonstrated poor expression in diabetic rats compared to control heart tissue sections (Fig.38). Moreover, CGRP-1 immunoreactivity expressed densely as a sparse individual fiber of myocytes (OD: 0.45±0.04, CTRL, 0.101 DM, p=0.01) and correlated with the expression of DOR-1 (CTRL, 0.45±0.05; DM, 0.094±0.04, p=0.01); however, MOR-1 was not expressed in both groups. As shown in the graph, KOR-1 IRC counts significantly declined (7.4±2.702) in STZ-induced diabetic rats compared to control (10.4±2.881) P=0.0036.

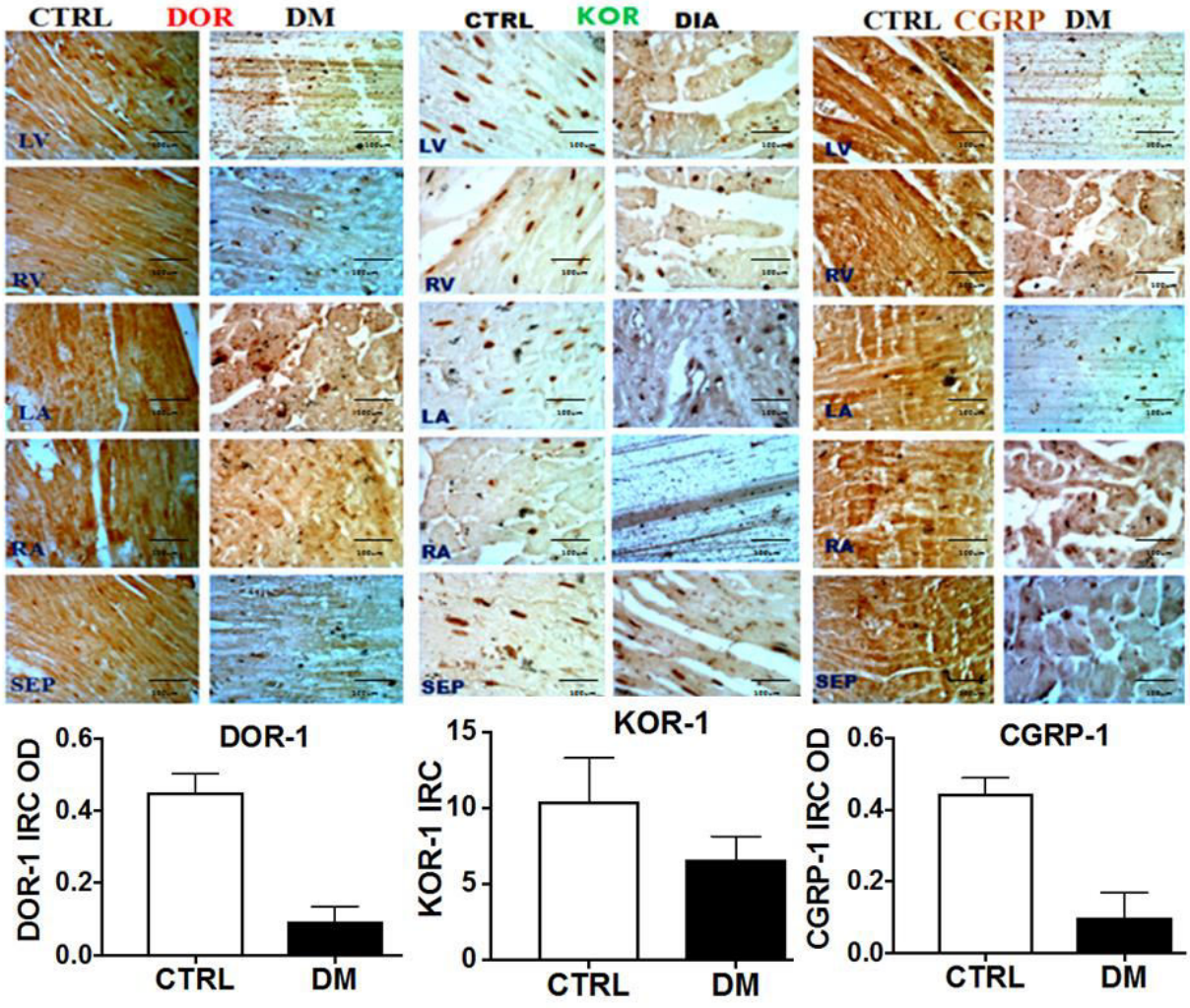

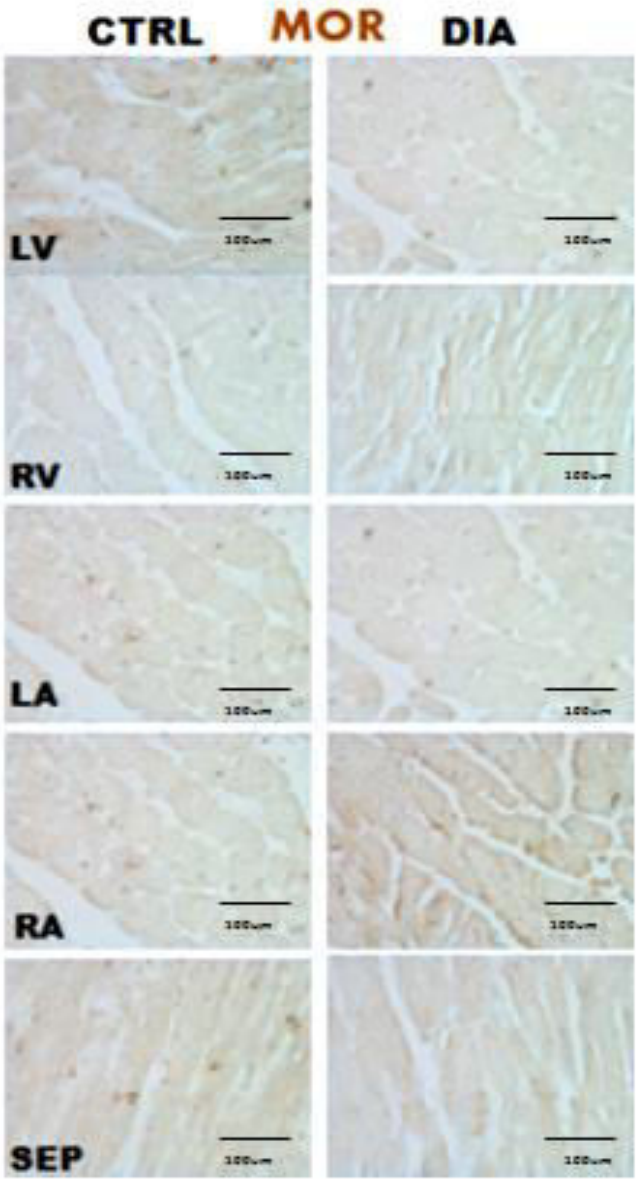

Figure: 38. Chamber wise representative images of immunoperoxidase stained DOR-1, KOR-1, CGRP-1, and MOR-1 immunoreactivity in diabetic and control rat heart tissue sections: The immunoperoxidase DOR-1 and KOR-1 reactivity showed poor and lightly stained immunoreactive fibers expression in diabetic rat heart tissue sections. On the contrary, control heart tissue showed marked expression of DOR-1, KOR-1, and CGRP-1, but, not MOR-1. The above graphs represent OD of DOR-1 and CGRP-1, and IRC count of KOR-1 quantified using Figi version of ImageJ from which OD calculated and Proplus live preview IRC count, respectively. The strength of immunoperoxidase DOR-1 and CGRP-1 proteins reactivity in heart tissue sections was significantly reduced in diabetic rats compared to control. Number of KOR-1 IRC in diabetic rat was reduced compared to control. STZ, Streptozotocin; IRC = Immunoreactive cells, DOR-1, Delta Opioid Receptor; MOR-1, mu Opioid Receptor; CGRP-1, Calcitonin Gene Related Peptide; LV, left ventricle; RV, right ventricle; LA, left atrium; RA, right atrium; SEP, septum; DM, Diabetic mellitus; DIA, Diabetes; IRC, Immunoreactive cells; OD, Optical density. Scale bar, 100µm.

4.3.4. Immunofluorescence stained DOR-1, KOR-1 and CGRP-1 containing signals in diabetic and normal heart tissue sections

Imunofluorescence labeled KOR-1, DOR-1, and CGRP-1 immunoreactivity was done in all chambers of the heart. KOR-1 and CGRP-1 immunofluoresce weak signals were detected in diabetic compared to control rats' heart tissue sections. However, there was no any observed change for immunoreactive DOR-1 in diabetic and normal heart except a slight increase in number of signals in control. CGRP-1 Immunofluoresce reactive myocytes were apparently expressed in normal heart tissue compared to diabetic rats`s heart tissue sections (Fig. 39).

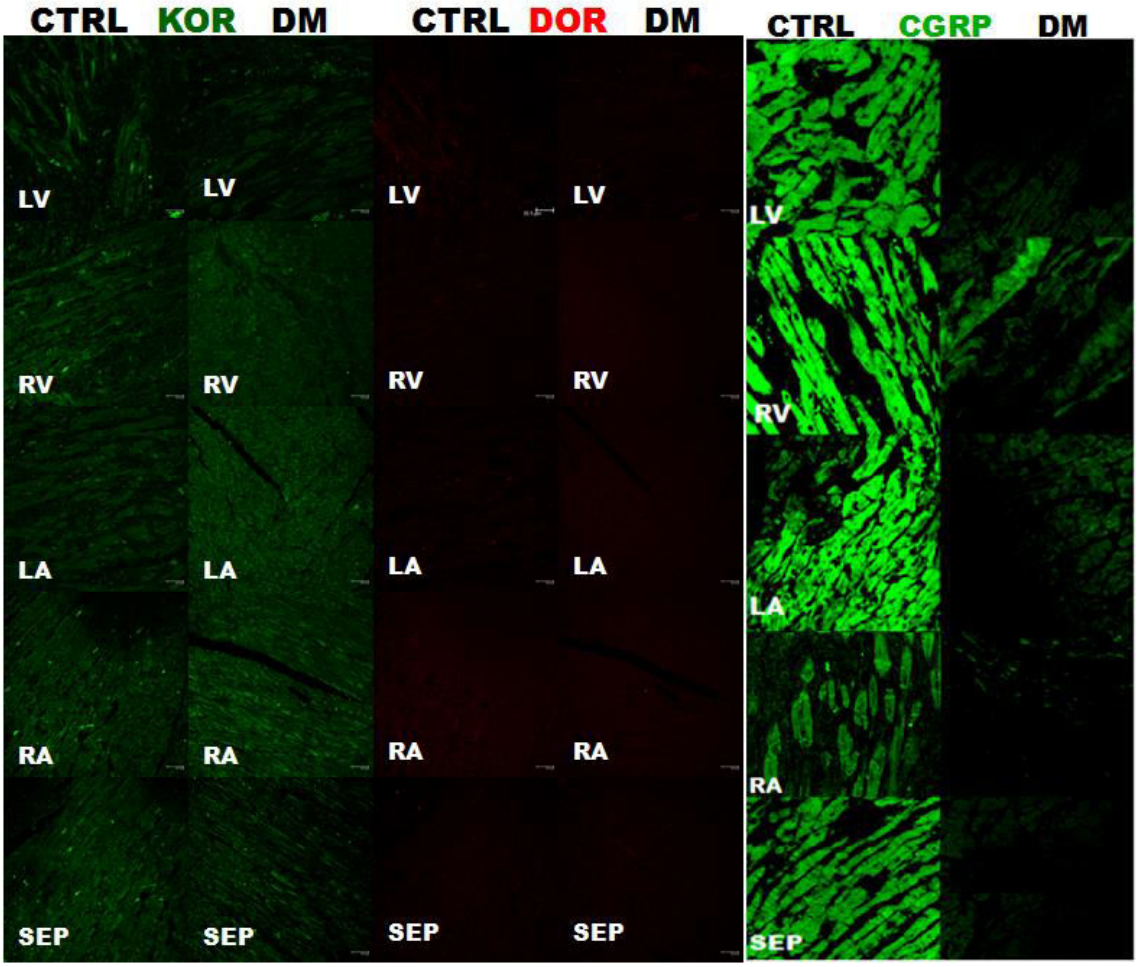

Figure: 39. The above figure illustrates chamber wise confocal microscopy of immunofluorescence DOR-1, KOR-1, and CGRP-1 containing immunoreactive signals in fibers of diabetic and control rats` heart tissue sections: STZ, Streptozotocin; DOR-1, Delta Opioid Receptor; KOR-1, Kappa Opioid Receptor; CGRP-1, Calcitonin Gene Related Peptide; LV, left ventricle; RV, right ventricle; LA, left atrium; RA, right atrium; SEP, septum. Scale bar = 35.3µm.

4.3.5. Delta and kappa opioid receptors mRNA expression in hearts of diabetic rats

Real-time RT-qPCR assay was used to evaluate the relative expression of Oprd1, Oprk1 and Oprm1 in diabetic heart tissue. This assay analysis showed Oprd1 and Oprk1 mRNA expression in the heart tissue of rat were significantly reduced (Fig. 40) in diabetic rats. However, Oprm1 was not amplified even at 50 cycles in both control and diabetic rat heart. The significant reduced expression of Oprd1 and Oprk1 mRNA were confirmed by immunoblot analysis and immunohistochemical localization. Therefore, this study found that mRNA encoding Oprd1 and Oprk1 transcripts were detected in hearts of rat with down-regulation in diabetic heart (Fig. 40).

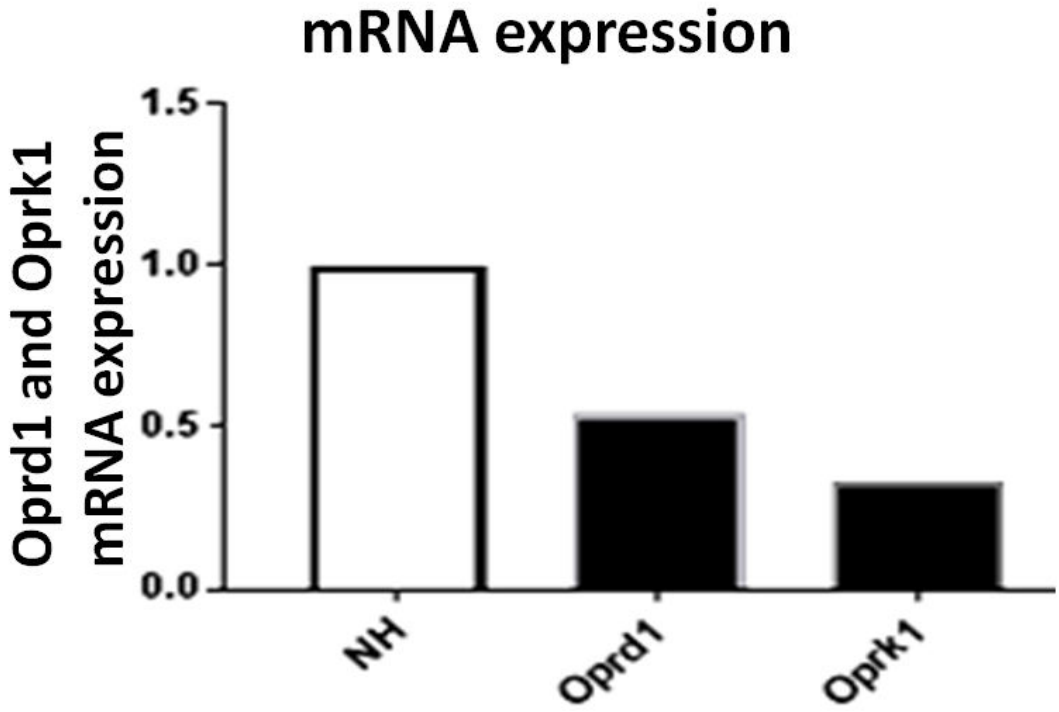

Figure: 40. Relative Oprd1 and Oprk1 mRNA expression: Real-time RT-qPCR was used to evaluate the expression of Oprd1 and Oprk1 mRNA in diabetic rats` heart. The expression of Oprd1 and Oprk1relative quantification normalized against reference gene (rGAPDH). The fold changes were calculated using $2^{-DeltaDeltaCt}$. Oprd1, Gene encodes Delta Opioid Receptor; Oprk1, Gene encodes kappa opioid receptor; GAPDH, Gene encodes Glyceraldehyde-3-phosphate dehydrogenase; NH, Normal heart.

4.3.6. Expression of κ- and δ- opioid receptors immunopositive proteins in hearts of diabetic and normal rats

In western blot analysis, KOR-1 and DOR-1 expression were evaluated in both diabetic and normal heart tissue. Expression of KOR-1 proteins was significantly reduced in diabetic heart (0.17±0.033) compared to control rats heart (0.73±0.09), p=0.0059 (Fig 41). Moreover, optical density of DOR-1 reactive proteins insignificantly declined in diabetic heart (0.32±0.1) compared to control heart (0.74±0.04), p=0.06.

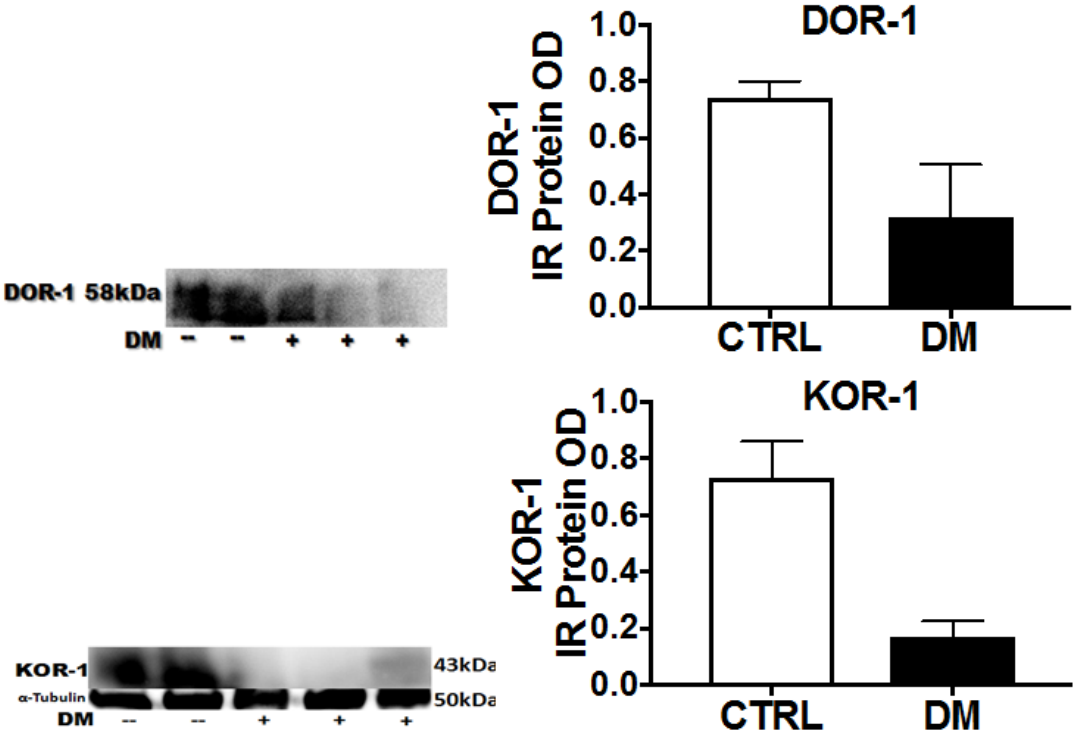

Figure: 41. Western blotting analysis of KOR-1 and DOR-1 immunoreactive proteins in diabetic and control heart tissue of rats. 30µg of protein was loaded to each well. Data expressed as mean±SD, P<0.05, standardized with α-tubulin. KOR-1, Kappa opioid receptor; DOR-1, Delta opioid receptor; DM, Diabetic Mellitus; IR, Immunoreactive; OD, Optical density.

4.3.7. Apoptotic nuceli in heart tissue sections of diabetic and normal rats and TUNEL positive nuclei counts

TUNEL assay was performed to evaluate number of apoptotic nuclei in diabetic and normal heart tissue sections. A significant elevation TUNEL positive myocytes in diabetic rats` heart (9±082) was found compared to control hearts of rats (2.25±0.95) P<0.001. Moreover, it was also observed more apoptotic nuclei in diabetic heart tissue sections compared to normal heart (Fig. 42).

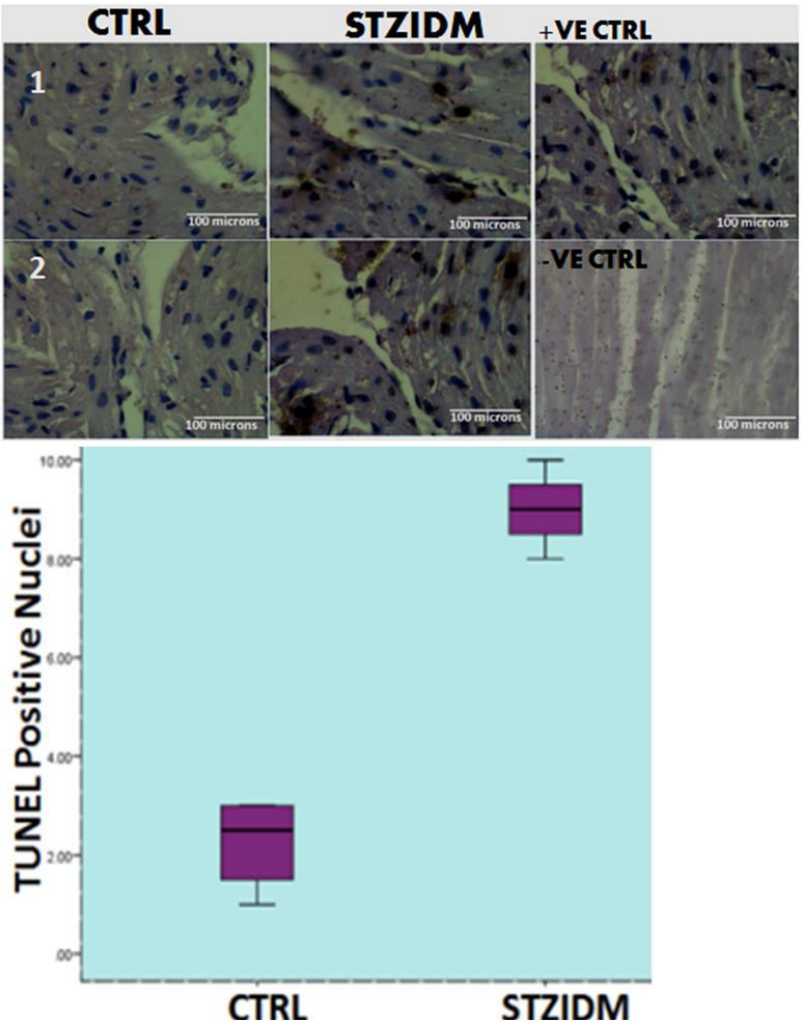

Figure: 42. Representative photomicrographs of TUNEL positive nuclei myocyte of STZ-induced diabetic and control rat heart tissue sections: There was frequent appreance of TUNEL stained apoptotic nuclei in diabetic rat heart tissue compared to control. TUNEL+ Hematoxylin (H). STZ; Streptozotocin. TUNEL positive nuclei in diabetic rats' heart tissue sections showed a significant elevation compared to CTRL. Mean±STD, P<0.05 was considered as significant. STZIDM, Streptozotocin induced diabetic mellitus. STZ; Streptozotocin; CTRL, Control; TUNEL, TdT, Terminal deoxynucleotidyl transferase; dUTP, 2'-deoxyuridine 5'-triphosphate; Nick End Labeling; +VE CRTL, Positive control; -VE CTRL, Negative control. 1, LV; 2, RV

4.4. Discussion

It has been established previously that opioid receptors are present in the heart (Theisen et al., 2014; Sobanski et al., 2014; Cao, 2003; Patel et al., 2006; Weil et al., 1998; Howells et al., 1986). The findings of this study confirm the presence of κ and δ opioid receptors in streptozotocin (STZ)-induced diabetic rats` heart tissue. However, MOR-1 is not expressed in STZ-induced diabetic rats myocardial tissue.

Apart from, the exhibits reduction of optical density of KOR-1 and DOR-1 immunoreactivity in STZ-induced diabetic rats` heart, this reduction is correlated with a sensory neuronal marker (CGRP-1). Co-localization of the neuronal marker (CGRP-1) and kappa opioid receptor signals are detected in hearts of diabetic rats. The selective expression of these distinct receptors (Gullberg, 1986) in diabetic heart might show neuro sensitivity of opioid receptors in the diabetic heart.

The findings of this study have shown that mRNA encoding Oprk1 and Oprd1 are expressed in rat heart of all chambers and with down-regulation in the diabetic heart. Furthermore, western blot analysis has shown lower KOR-1 proteins in diabetic heart. The neuropathic conditions observed in the histopathology of diabetic heart and lower neuronal marker (CGRP-1) might be one of the reasons for the reduction of δ & κ opioid receptors at the protein and mRNA levels. In our TUNEL analysis, it is also shown a significant elevation of apoptotic nuclei in the diabetic heart. These alterations suggest a tendency of reduction in the pharmacological activities of opioids in the regulation of cardiac tissue of neuropathic heart and susceptibility of diabetic rats to a possible mechanism that increases the susceptibility of neuropathic heart to ischemia and reperfusion injury.

Based on the findings obtained, we further proposed in ischemia-reperfusion model of the STZ-induced diabetic to figure out the effects of opioid receptors in ischemia-reperfusion injury and intracellular signaling proteins for down-regulation of the receptors in the

neuropathic model of STZ-induced diabetic rats using non-selective antagonist (naloxone) for the receptors.

CHAPTER FIVE

5. Effects of opioid receptors on signaling proteins in ischemia-reperfusion injury in STZ-induced diabetic and neuropathic model of rats

5.1. Introduction

Studies have shown possible mechanisms of cardioprotection gained through different models (pharmacological, ischemic, and exercise preconditioning) and mediating effects of opioid receptors against IRI by cytoprotection abolishing effects of selective and non-selective antagonist (Headrick et al., 2015; Castedo et al., 2005). The down-regulation of opioid receptors in heterotopic transplanted heart shown in our previous three characterization studies directs to do further convenient study in transplanted heart after ischemia and reperfusion (IR) to find out which signaling pathways involved in the alteration of on the expression of the delta and kappa opioid receptors in transplanted heart. However, due to the technical complexity to combine transplantation and IR models, we shifted the study to diabetic neuropathic and IR-induced rat models.

Therefore, this study was aimed to compare levels of pro-survival signaling proteins phosphorylation, the extent of fragmented DNA (apoptotic nuclei), and infarct size in IR-induced rats in the presence of naloxone. Moreover, concurrently any histopathological abnormalities of heart tissues in diabetic IR-induced rats were evaluated. This study contributes insight and better understanding on levels pro-survival signaling proteins due to inhibition of the receptors.

The diabetic condition of rats was confirmed through lower fasting blood glucose level, body weight, and abnormal distribution of islet cells (shrinkage, necrotic islet cells) of pancreas prior to IR-induced cell signaling studies after blockade of receptors. A histopathological observation was also confirmed neuropathy in sciatic nerve in diabetic rats.

Co-expression of delta and kappa ORs with neuronal markers (CGRP-1) in the heart tissue that is shown in our current, and (CGRP-1, $PGP_{9.5}$) in previous studies done by Sobanski et al., (2014) implicate their connection with the down-regulation of opioid receptors in neuropathic and diabetic rats. Activation of DOR suppresses calcineurin and activates extracellular signal-related kinases (ERK1/2) which are thought to interact with the mechanism involved in cardioprotection (Rungatscher et al., 2013).

5.1.1. Ischemia and reperfusion

Ischemia is a serious condition in which there is inadequate blood flow and oxygen to a specific part of the body and can occur in any muscle group, organ, or tissue in the body (VDF, 2012) from a major contributor (atherosclerosis) due to risk factors, such as smoking, advanced age, high cholesterol, high blood pressure, diabetes, a family history of cardiovascular disease, sedentary lifestyle, and obesity (VDF, 2012). It contributes to the pathophysiology of many conditions, including myocardial infarction, peripheral vascular insufficiency, stroke, and hypovolemic shock (Collard and Gelman, 2001).

Cellular processes are rapidly activated in response to ischemia reperfusion-induced stress. The ischemic part is a region of tissue that is immediately distal to an occluded artery, undergoes rapid, anoxic cell death within minutes of ischemia formation. Irreversible processes including mitochondrial collapse, rapid energy depletion, and ion pump failure result in large increases in intracellular calcium, extracellular potassium, and edematous cell swelling which are characteristics of necrotic cell death. Reperfusion, restoration of blood flow to an ischemic part is essential to prevent irreversible cellular injury. However, reperfusion may expand tissue injury in excess of that produced by ischemia alone (Collard and Gelman, 2001). Ischemia–reperfusion injury (IRI) is a cellular damage after reperfusion of previously viable ischemic tissues.

5.1.2. Roles of opioid receptors in ischemia-reperfusion injury

Evidence regarding the role of local opioids and opioid receptors in regulation of cardiovascular physiology and IRI has shown that activation of opioid receptors in the reduction of myocardial IRI through selective δ-opioid agonists when given acutely before ischemia and reperfusion (Tanaka et al., 2014). In a study, using administration of a potential and selective kappa opioid agonist, it has also shown antiarrhythmic effects depending on the activation of the k-opioid receptor (Tsibulnikov et al., 2015).

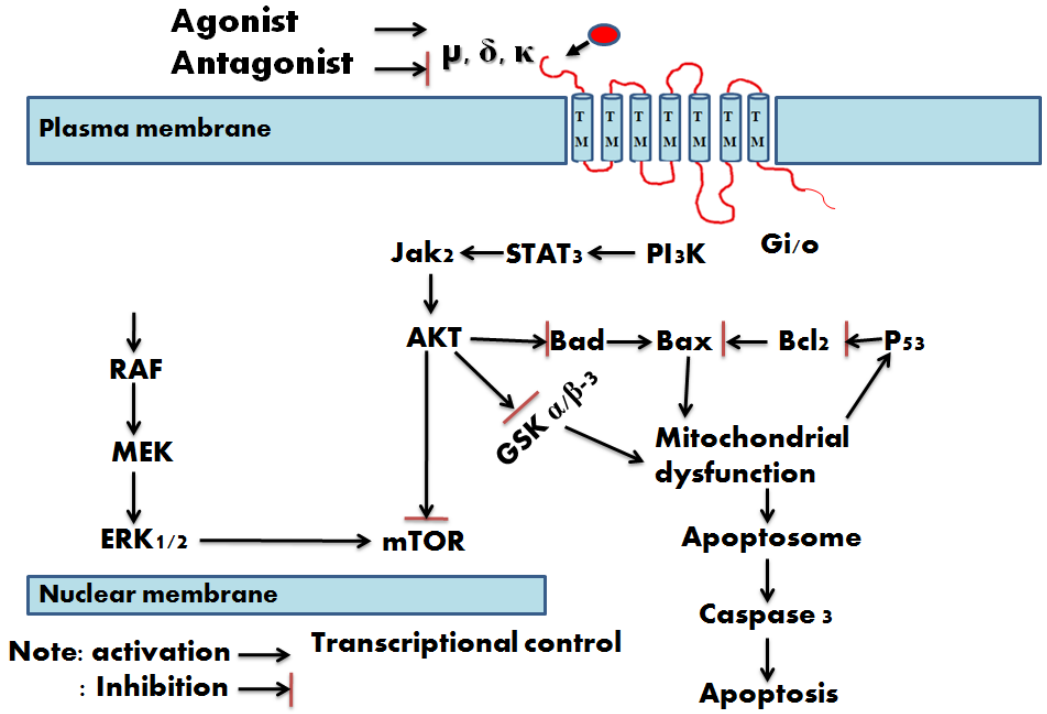

Figure: 43. Intracellular signal pathways coupled to the opioid receptors showed in ischemia-reperfusion injury of heart tissue and cardioprotection and apoptotic pathways: Opioid receptors antagonist leads to inactivation of P13K/Akt and risk pathways MAPKs (ERK) JAK-STAT signaling, phospho-regulation of effector molecules such as GSK3β and m-TOR. Naloxone (opioid receptor non-selective antagonist) may contribute to inactivation of the cardioprotective survivor activating factor enhancement (SAFE) pathways.

5.1.3. Pathophysiology of ischemia and reperfusion injury

Ischemia/reperfusion injury/IRI remains a serious problem affecting graft survival and outcome of transplantation. In its severest form, I-R injury results in multiple organ dysfunction syndromes (Verma et al., 2002). The myocardium can tolerate only up to 15min of severe and even total myocardial ischemia without resultant cardiomyocyte death (Verma et al., 2002). The restriction of blood supply to heart tissues that damage of cardiomyocytes can be reversible with prompt arterial reperfusion (Verma et al., 2002). The ischemic part undergoes rapid and anoxic cell death within minutes of ischemia formation. Irreversible processes including mitochondrial collapse, rapid energy depletion, and ion pump failure result in large increases in intracellular calcium, extracellular potassium, and edematous cell swelling which are characteristics of necrotic cell death.

In general, the ischemia, in cellular metabolic and ultrastructural levels, results in a variety of changes, including alteration of membrane potential, an increment of intracellular ions (Ca^{2+}/Na^{2+}) and hypoxanthine, reduction of ATP, phosphocreatine, and glutathione. It can also result in cellular acidosis. Ischemia-induced decreases in cellular oxidative phosphorylation results in a failure to resynthesize energy-rich phosphates, including ATP and phosphocreatine. Membrane ATP-dependent ionic pump function is thus altered, favoring the entry of calcium, sodium, and water into the cell. Furthermore, adenine nucleotide catabolism during ischemia results in the intracellular accumulation of hypoxanthine, which is subsequently converted into toxic reactive oxygen species (ROS) upon the reintroduction of molecular oxygen.

During ischemia, cellular ATP is degraded to form hypoxanthine. Normally, hypoxanthine is oxidized by xanthine dehydrogenase to xanthine. However, during ischemia, xanthine dehydrogenase is converted to xanthine oxidase. Unlike xanthine dehydrogenase, which uses nicotinamide adenine dinucleotide as its substrate, xanthine oxidase uses oxygen and therefore, during ischemia, is unable to catalyze the conversion of hypoxanthine to xanthine, resulting in a buildup of excess tissue levels of

hypoxanthine. When oxygen is reintroduced during reperfusion, conversion of the excess hypoxanthine by xanthine oxidase results in the formation of toxic ROS.

Reperfusion, restoration of blood flow to an ischemic part is essential to prevent irreversible cellular injury. However, reperfusion may expand tissue injury in excess of that produced by ischemia alone (Collard and Gelman, 2001). Ischemia–reperfusion injury (IRI) is a cellular damage after reperfusion of previously viable ischemic tissues. The principal mechanisms underlying IRI include oxidative stress during preservation and production of excess reactive oxygen species (ROS). Reperfusion of ischemic tissues results in the formation of toxic ROS which are potent oxidizing and reducing agents that directly damage cellular membranes by lipid peroxidation.

Ischemia, in cellular oxidative phosphorylation, results in a failure to re-synthesize energy-rich phosphates. Reperfusion of ischemic tissues results in the formation of toxic ROS (superoxide anions, O2 2; hydroxyl radicals, OH2; hypochlorous acid, HOCl; hydrogen peroxide, H2O2; nitric oxide–derived peroxynitrite), which are potent oxidizing and reducing agents that directly damage cellular membranes by lipid peroxidation.

In general, ischemia and reperfusion result in a local and systemic inflammatory response characterized by the production of oxidant, complement activation, leukocyte–endothelial cell adhesion, transendothelial leukocyte migration, platelet-leukocyte aggregation, increased microvascular permeability, and decreased endothelium-dependent relaxation (Carden and Granger, 2000; Collard and Gelman, 2001).

5.1.4. Epidemiology of ischemic heart disease

Cardiovascular disease represents the leading cause of death, morbidity and mortality and responsible for 17% of all health care related costs (Bokkelen and Werner, 2013). Ischemic heart disease (IHD), which comprises of primarily coronary heart disease (Fig. 44), is the prime manifestation of cardiovascular diseases (CVDs) and causes 46% of mortality in men and 38% in women (Wong, 2014). It is a leading cause of death

worldwide (WHO, 2014) and has become a true epidemic that respects no borders. In 2012, out of 17.5 million people died from CVDs, 7.4 million people died of IHD (Fig. 43) (WHO, 2014). Three-fourths of global deaths due to coronary heart disease occurred in the low and middle-income countries (Gaziano et al., 2010). The burden is expected to increase more in these countries in 2030 (Bovet and Paccaud, 2012). The need of method of cardioprotection from IR-injury is crucial because hospital mortality in patients with acute myocardial infarction is increasing (7.3% in Europe and 13.8% in Russia) (Tsibulnikov et al., 2015).

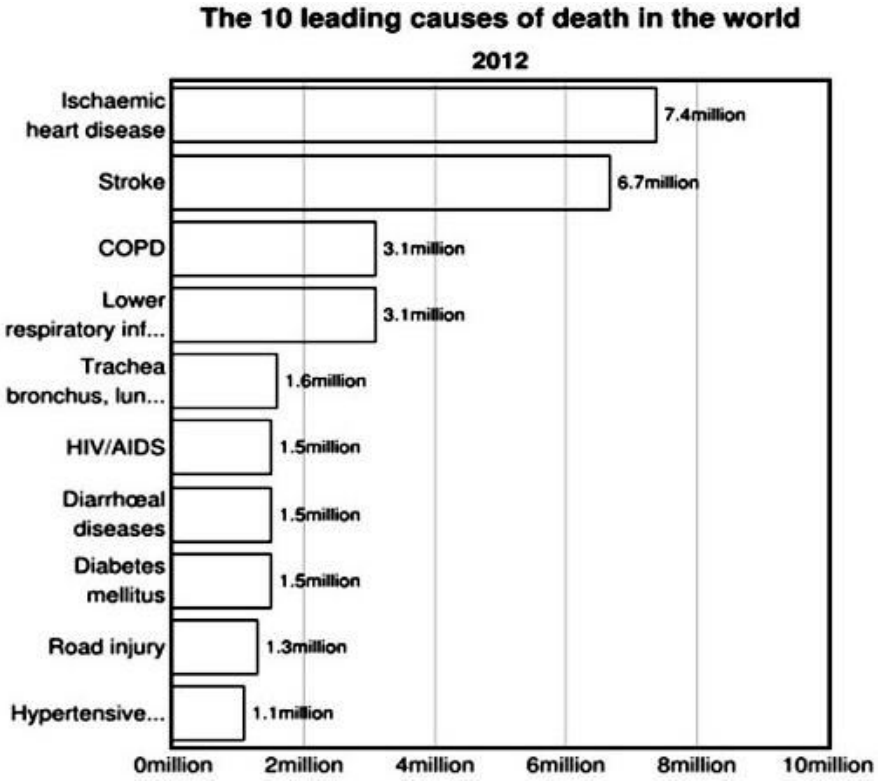

Figure: 44. The 10th leading cause of death in the world: Ischemic heart disease, a number one cause of deaths over the past decade, 2000-2012. Reproduced from World Health Organization, 2014.

5.1.5. Signaling pathways

Many signaling pathways are involved in cardioprotection. Although the role of opioid receptors on cardioprotection is well addressed, their protective effects are compromised in diabetic hearts as shown in the reported by Lei et al., (2015). It has been reported that PKC, PI3 kinase/Akt, ERK1/2, STAT3, and GSK-3β phosphorylation impairment in

diabetic hearts (Lei et al., 2015; Wider and Przyklenk, 2014) are the possible potential mechanisms that make the diabetic hearts more susceptible to IRI and less sensitive to opioid conditioning (Lei et al., 2015). Cross talk of the PI3K-AKT-mTOR pathway with Ras/Raf/MAPK pathways is common routes that control responses (Calvo et al., 2009). The findings of this study have shown diabetic heart in the presence of naloxone might be implicated in a possible mechanism for defective cardioprotection in the diabetic heart.

Akt is one of signaling protein is a serine/threonine kinase that belongs to family of protein kinases (protein kinase A/protein kinase G/protein kinase C-like) which possesses Threonine308 (Thr308) and Serine473 (Ser473) phosphorylation sites in in the kinase domain and in the regulatory domain (Vivanco and Sawyers, 2002). It affects activation and proliferation by regulating proteins of cell-cycle machinery, blocking transcription of the cell cycle inhibitor, inhibiting anti-proliferative effects of cyclic dependent kinase inhibitor (p21, p27) and glycogen synthase kinase-3 (GSK3), activating expression of pro-proliferative target genes by preventing β-catenin degradation (Osaki et al., 2004; Sarbassov et al., 2005).

The phosphatidylinoisitol 3-kinase (PI3K)- AKT pathway is situated in downstream tyrosine kinase receptors (TKRs) and regulates essential cellular functions such as proliferation, growth, and survival (Vivanco and Sawyers, 2002). The main downstream effectors of the PI3K-Akt pathway involvement is its proliferative and survival responses (Vivanco and Sawyers, 2002). The frequent alteration of PI3K-Akt signaling pathway in cancers is also mentioned (Calvo et al., 2009). Findings of DeBosch et al., 2006 has shown evidence that regulatory role of Akt1 in promoting physiological cardiac hypertrophy (growth) while another opposite signaling pathological hypertrophy in mice (DeBosch et al., 2006; Walsh, 2006).

Mitogen-activated protein kinase (MAPK/ERK) cascades are a chain of proteins that communicates a signal from receptor to DNA that expresses proteins that produce changes in the cell. This pathway comprises of many proteins which communicate by adding phosphate groups to a neighboring protein (Orton et al., 2005). They are key

signaling pathways involved in the regulation of normal cell proliferation, survival, and differentiation; and abnormal regulation of MAPK cascades contribute to human diseases (Roberts and Der, 2007). ERK is activated by the Raf serine/threonine kinases. Raf activates the MAPK/ERK kinase (MEK)1/2 dual-specificity protein kinases, which then activate ERK1/2 (Roberts and Der, 2007).

5.2. Materials and methods

5.2.1. Experiment design

The experimental design consisted of 25 Sprague-Dawley rats, weighing 340-380g. Ten rats were subjected to characterization study; ten of them were induced at a single dose (65mg/kg) injection of STZ diluted with citrate buffer. Rats were survived for seven weeks. The control rats were given 50mM citrate buffer. The animals for signaling study were designed with ten for STZ-induced diabetic and for 5 controls IR (Table. 7). These rats were classified into three groups. Each group consisted of 5 animals. The first group was assigned to 20 min of ischemia and 1hr reperfusion/IR-induction with administration of naloxone. The second group assigned to be diabetic-IR-induced control. The third one subjected to IR-induced control. The naloxone (1mg/kg) obtained from AOUI supplied from SIGMA Aldrich was administered via femoral vein. Following NAL administration, ligation of left anterior descending artery (LAD) for 20min to induce ischemia, and then 60 min reperfusion were performed (Table. 7).

In addition, three groups of Sprague-Dawley rats, weighing 350-360g were also used to measure the level of infarct size. First group was subjected with IR-induced in the presence of naloxone, second group was ischemia-reperfusion induced-control, and the third one was healthy controls. Rats weighing 360g were also used to measure the level of infarction in IR-induced rats following administration of naloxone, without naloxone after IR and in healthy control rats.

Table: 7. Group of rats, treatments, and duration of ischemia and reperfusion

SN	Pretreatment	Groups	Ligation of left anterior descending artery: Duration of Ischemia	Duration of Reperfusion
1	No STZ induction	Non-DIA-CTRL	20' Ischemia	60' Reperfusion
2	STZ induced DIA,	DIA +CTRL	20' Ischemia	60' Reperfusion
3	STZ induced DIA, 7 weeks	DIA+NAL 1mg/kg	20' Ischemia	60' Reperfusion

5.2.2. Experimental animals and housing

Male Sprague-Dawley rats (weighing 320-380g) were housed 2 per cage in a setup cage system at Interdepartmental Center of Experimental Research Service/CIRSAL, the University of Verona at a temperature controlled room (21±2^{o}C) with food (ad libitum) and water available under a 12 hours' light/dark cycle. They were acclimatized for 7 days before the beginning of the experiment in order to adapt them to the laboratory conditions. All tests were done during the light hours. The study was carried out in accordance with the ethical guidelines for investigations of experimental pain in conscious animals (Zimmermann, 1983; CIRSAL, University of Verona).

5.2.3. Drugs, and citrate buffer preparation,

The Streptozotocin mixed and citrate (0.1M) was prepared as indicated earlier in chapter four.

5.2.4. Body weight and fasting blood glucose level measurement

Body weights and FBGL of all groups of the rat were taken at the beginning, 24hr, and end diabetic conditions as the method indicated earlier.

5.2.5. Surgical procedure for ischemia and reperfusion and administration of naloxone

After stunned the rats with diethyl ether vapors, animals were laid in supine position on a flat board, and intubated for oro-tracheal away with a venous cannula 10G, and then rats were ventilated by a mechanical respirator to rodents (Rodent Servo Ventilator) with a mixture of oxygen and isoflurane 1.5% for the whole duration of the intervention, with a fraction of 90% inspired oxygen (FiO2), a tidal volume of 10ml / kg (350-400ml) and at respiratory rate of 70/min. The heart was exposed by opening the chest via median Sternotomy with Mayo scissors and after placing a retractor between pericardium. The left lung border was pushed to the side using a sponge guaze. After incised skin and pericardium edge was stitched using 60cm prolene suture needle (lot# JGR906). LAD

ligation (Fig. 45) was performed for 20min to induce ischemia at left ventricle (Fig. 45B) using prolene 3cm was used to ligate the left anterior descending coronary artery.

Myocardial ischemia was verified by blanching of the LV and by ECG changes, and then ligature and PE tubing were removed to perform reperfusion that restores blood flow for 1hr after 20min occlusion in rats with the help of surgeons at department of Surgery, University of Verona using the protocol indicated by Kolk et al., (2009) and Samsamshariat et al., (2005)

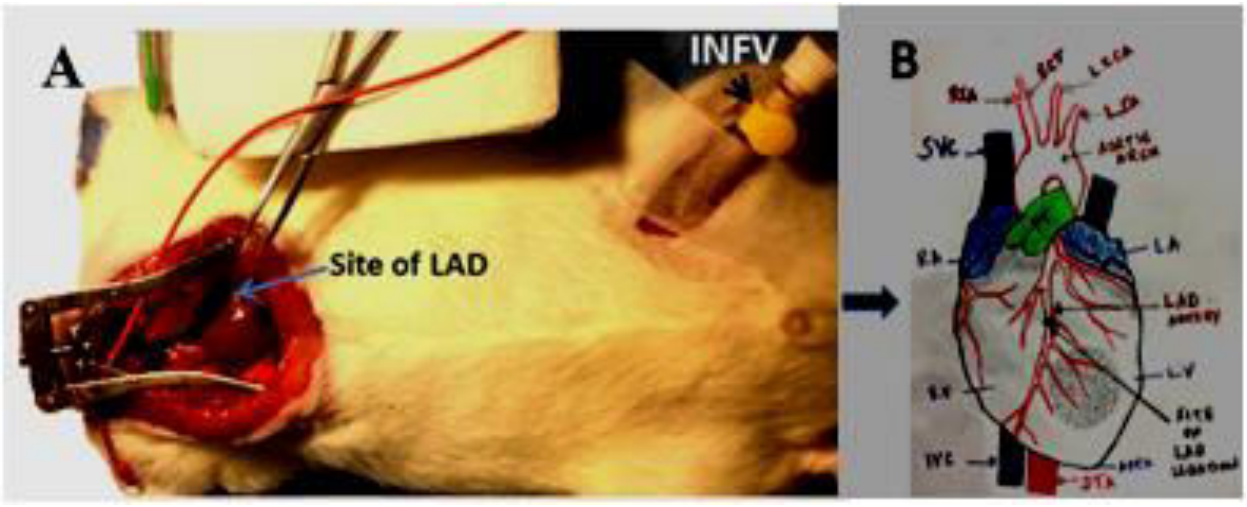

Figure: 45. Site of left anterior descending artery ligation and injection site for femoral vein in rat: The figures (A&B) showing the site of the left anterior descending (LAD) artery ligation and (A) injection of naloxone through femoral vein. SVC, superior vena cava; IVC, inferior vena cava; LV, left ventricle; RV, right ventricle; RA, right atrium; LA, left atrium; PT, Pulmonary trunk; RCCA, right common carotid artery; LCCA, left common carotid artery; BCT, Bracheocephalic trunk; RSA, right subclavian artery; LSA, left subclavian artery; INFV, Injection of Naloxone through Femoral Vein.

The opioid receptor antagonist naloxone (NAL) was obtained from AOUI supplied from SIGMA Aldrich. Naloxone (0.4mg/kg solution) was administered through femoral vein to each treated rat. Following NAL administration, 20 min ischemia and 60 min reperfusion were performed.

5.2.6. Tissue processing, embedding, and sectioning for TUNEL, IHC, H&E

The collected tissues were fixed with 4% paraformaldehyde and washed with PBS (pH 7.35, 0.1M). They were dehydrated with increasing ethanol concentration (70% 1x, 90% 2x, 100 1x). Following dealcolization by two changes of xylene (100%), specimens were infiltrated with two changes of molten paraffin wax at 56^{o}c to replace the xylene. Next to infiltration, embedding was performed stored at 4^{o}C overnight to form paraffin block. Once specimens embedded, they were cut into sections in 3µm thickness and immersed into warm (37^{o}C) water bath to remove wrinkles of sections.

5.2.7. Hematoxylin-Eosin staining for histopathological evaluation

Routine H&E staining histo-technique was performed to analyze any structural abnormalities of heart and sciatic nerves tissues section with the help of neuro-anatomist and pathology specialists. Following tissue processing, embedding and sectioning, the sections were immersed in a series of descending ethanol concentration and dipped in 2 changes of distilled water, and then stained with hematoxylin solution. After a brief washing with running tape water, sections were dipped in 2% eosin. Overstaining was controlled by washing with tap water. Sections were dehydrated with increasing alcohol concentration, and then ethanol was removed from the sections by two changes of xylene for its miscibility property with mountant. Finally, sections were covered with cover glass and prepared for analysis.

5.2.8. Immunohistochemistry: immunoperoxidase

Immunoperoxidase staining was done as earlier IHC method to evaluate p-p38 (Phospho-p38 MAPK (Thr180/Tyr182, D3F9, XP®Rabbit mAb) immunoreactive cardiomyocytes to analyze relative distribution of P-p38 reactive myocytes CIR, DIR, and DNIR groups. A marker used for detection of p-p38 was a rabbit mAb supplied from CSC.

5.2.9. Microscopy, p-38 immunoreactive phosphorylation and its IRC counts

Microscopy, immunoreactive/IRC counting, and analyses of p-p38 were done. Counts of p-p38 IRC were performed using 200X magnification using Image-Pro Plus software in workspace preview as mentioned in previous chapter for KOR-1.

5.2.10. Cryosectioning and western blot analysis

Heart tissue specimens were collected and placed snap frozen in liquid nitrogen with drop O.C.T. medium, and then 30 cryosectioned sections from each sample were used for lysate preparation using cold lysis buffer (RIPA). The sample were sonicated and supplemented with additional protease and phosphatase inhibitors cocktail (3DMSO solution 020M4009, P0044-1ml, SIGMA Aldrich) to prevent degradation by proteases. Samples were centrifuged at 12,000rpm at 4^{o}C. Tubes were gently removed the centrifuge and placed on ice and the supernatant (lysate) aspirated and placed in a fresh tube, and then protein concentration was measured using Pierce®BCA (Bicinchoninic Acid) protein assay kit, Lot # OH192608 containing detection Reagent A Lot # OG190483 Prod # 23228, Reagent B, Lot # OF189971 Prod # 1859078, and Albumin Standard, Lot # OG189315 Prod # 23209 supplied from Thermo Scientific. The assay solution run in PerkinElmer 2030 Multi-label Reader VICTOR™X4 connected with computer through INJECTOR from which standard curve was extracted (Fig. 46).

Equal amount of protein (20µg/20µl) was loaded in the wells of the SDS-PAGE gel, along with pre-stained Mol. Wt. marker (SDS7B2, SIGMA Aldrich) to evaluate the expression of p-Akt, t-Akt, p-ERK, t-ERK.

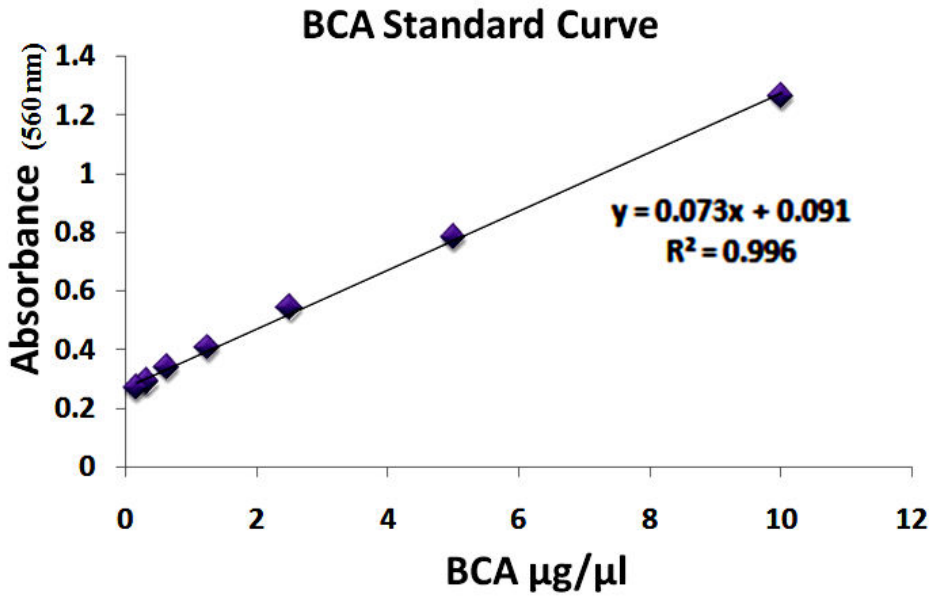

Figure: 46. BCA standard curve for protein concentration measurement: BCA assay was done to measure unknown protein concentration after standard curve was plotted using known BSA protein concentrations. Unknown concentration of solutions of different groups of rats` heart tissue samples was calculated at 560nm.

Lysate in sample buffer was boiled at 60^{o}C to reduce and denature. Gel acrylamide 10% was used in the gel based on the size of protein. Following preparation of stack, the separated proteins were transferred in wet with containing 25 mM Tris-base, 0.2 M Gycine, 20% methanol, pH 8.5 at 300 mAmps and 100V to PVDF, Lot # RH2217091, Prod # 88518, 0.45um, 26.5cm x 3.75m roll (Thermo Scientific).

In antibody staining, the membrane was blocked with 5% non-fat milk in TBS-T (0.1% Tween-20, Lot # 8T006910, A4974, 0250, CAS-No: 9005-64-5, AppliChem, Germany) at RT. The membrane incubated overnight at 4^{o}C with the following specific primary antibodies p-AKT (Ser473, 193H12, #4058) rabbit mAb, t-Akt (pan, C67E7, #4691) rabbit mAb supplied from CSC, p-ERK-1&2 (Monoclonal Anti-MAP Kinase Activated/monophosphorylated/ Phosphothreonine, #M7802 Ab produced in mouse), and t-ERK-1&2 (Anti-MAP kinase, #M5670) supplied from Sigma Aldrich.

After incubation with appropriate secondary antibodies at 1:10000 dilution rates for 2hrs at room temperature and three cycles of 5min washes, reactive protein signals/bands in

PVDF were developed and visualized in drops of Luminata™ Forte Western HRP Substrate (Cat.No. WBLUF0500, Lot No. 140525, Millipore Corporation, Billerica, MA 01821) solutions for 1min over a supporting membrane (4 IN. X 125 FT. ROLL Lab-PARAFILM® Pechiney Plastic Packaging, Menash, WI 54952, Chicago, IL, 60631) and immediately exposed to autoradiography films for 1 to 2 min using G: Box Chem.XR5 GeneSys version 1.0.7.0 with Synoptics 5.0MP Camera and 1.4 data base version. Finally, densitometric quantification of the immunoreactive bands was performed using the ImageJ software.

5.2.11. TUNEL Assay

The TUNEL assay was performed as indicated in earlier chapters. All TUNEL staining solutions were prepared ahead using the protocol and AP cell death detection kit supplied from Roche for fluorescent and light microscopic analysis.

5.2.12. 2,3,5-triphenyl tetrazolium chloride (TTC) staining

Prior to a well described, simple and accurate 2,3,5-Triphenyl tetrazolium chloride (T8877, Lot# BCBR5461V, P. code 101785783, Sigma, Life Science, Austria) staining, 1% of (1g/100ml) TTC solution was prepared in phosphate saline (PBS, 8.6pH) in dark. The solution was pre-warmed to 37^{o}C in water bath before used. Hearts dissected, cleaned and washed with phosphate buffered saline (PBS, 8.6) at 4^{o}C to remove excess blood. Hearts were chilled at -20^{o}C freezer for 4min to slightly harden the tissue for easy sectioning and facilitate tissue processing. Unfixed hearts were sectioned into total of 4 sections at 2mm transversely. The sections were placed in a Petri dish and stained in 25ml of 1% of TTC dissolved with PBS in dark. When TTC diffused into actively respiring tissues, electrons were accepted from mitochondrial electron transport chain and the stain reduced to yield a deep pink compound/Formosan (Wang-Fisher, 2008). The accumulation of the Formosan stained the tissues red, and the intensity of the red color was proportional to the rate of respiration in the tissues.

The infracted heart tissue sections didn`t convert TTC and remain negative/unstained/white. Following TTC staining, the stained slices were fixed in 10% formalin solution. The stained heart slices traced onto a clear acetate sheet over a glass plate under room light. The stained heart sections were photographed with Digital Camera. The infarct area of each heart section of both sides was measured blindly using ImageJ analysis software (ImageJ 1.50i Wayne Rasband NIH, USA; Java 1.6.0_24 (64-bit)) after validating the threshold. Finally, percentage of infarct size was calculated by total area of cardiac muscle slice.

5.2.13. Statistical analysis, study setting, and ethical issues

Repeated measures of One-way ANOVA with Bonferroni comparison test were used to evaluate body weights and fasting blood glucose levels before and after 24hrs, 3 weeks, and 7weeks of STZ-injection. Mean ± SD in each group and independent samples t-test for the significance of means of independent group was used for statistical analysis using IBM Corp. Released 2011. IBM SPSS® Statistics for Windows, Version 20.0. Armonk, NY: IBM Corp software. $P<0.05$ was regarded as statistically significant. Immunohistochemical experiments and IRC were conducted at Department of Neuroscience, Biomedicine, and Movement. Immuno-blotting and RT-qPCR, TUNEL, and TTC techniques were performed at Laboratory of Cardiovascular Sciences and L.U.R.M. All experiments were carried out with the authorization of ethical Research Committee and Departmental Bio-bank at Department of Surgery, University of Verona.

5.3. Results

5.3.1. TTC stained heart slice observation

Series of TTC cellular metabolic staining was applied to evaluate levels of infarct size in three groups of (NIR, CIR, CTRL) of rat after 30min ischemia and 1hr reperfusion. In IR-induced rats in the presence of naloxone, appearance of massive infarct in lower part of ventricle was observed compared to controls. Moderate infarct was also observed in IR-induced-control rats` heart around apex of ventricle; however, control rats didn`t show any lesions in any of the slices.

The infarct size percentage (47.42%) in NIR group was elevated compared to percentage (10.97%) of CIR. The changes in elevated phosphorylation in immunoreactivity p38 and TUNEL positive apoptotic nuclei (DNA fragmentation) of myocytes in diabetic rats treated with naloxone corresponds to the higher percentage of infarct size and morphological abnormalities of the heart tissue in diabetic rats after IR-induced in the presence of naloxone (Fig. 47).

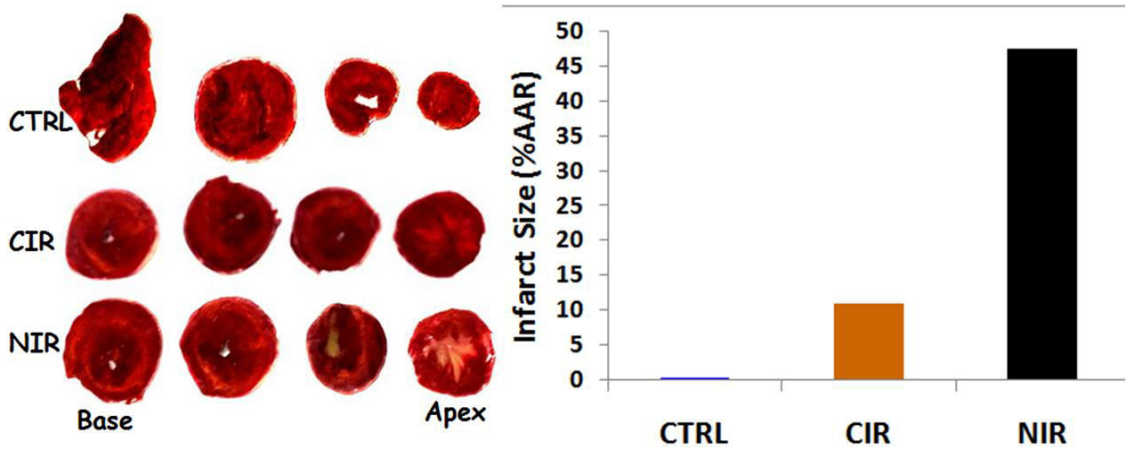

Figure: 47. Effect of naloxone on myocardial infarct size: The figure illustrates 2.3, 3-tetraphenyltetrazolim chloride (TTC) metabolic staining of the rats` heart slices of three groups (CTRL, CIR, NIR). NIR group of rats were subjected to injection of 1ml/kg naloxone through femoral vein prior to 30min LAD occlusion and 1hr reperfusion. CTRL group of rats were only induced with ischemia and reperfusion. The third group was with no treatment and ischemia and reperfusion. The infarct area of each heart section was measured blindly using ImageJ analysis software (ImageJ 1.50i Wayne Rasband NIH, USA; Java 1.6.0_24 (64-bit)) after validating the threshold. Infarct area (white) and the area at risk (red). Infarct size was measured based on the area-based method indicated by Takagawa et al., (2007). Mean ± STD, $P<0.05$ was considered as statistical significance. CTRL, Control; CIR, Control ischemia reperfusion; NIR, Naloxone-ischemia-reperfusion. Quantification of infarct size (IS) was expressed as percentage of area at risk (AAR).

5.3.2. Histopathological observation of H&E stained heart tissue sections in diabetic-ischemia-reperfusion-induced (DIR), diabetic-ischemia-reperfusion-induced with the presence of naloxone (DNIR), and control ischemia-reperfusion-induced (CIR)

Histopathology of left ventricle of tissue sections of DNIR, DIR, and CIR was analysed using H&E staining. Heart tissue sections of DNIR myocardial fibrosis compared to controls (DIR (D2) and CIR (D1). There was no marked structural alteration observed between DIR and CIR heart tissue sections. However, normal, single and oval centrally located nuclei of myocytes with regularly arranged cardiac fibers were observed in CIR rats (Fig.48. D).

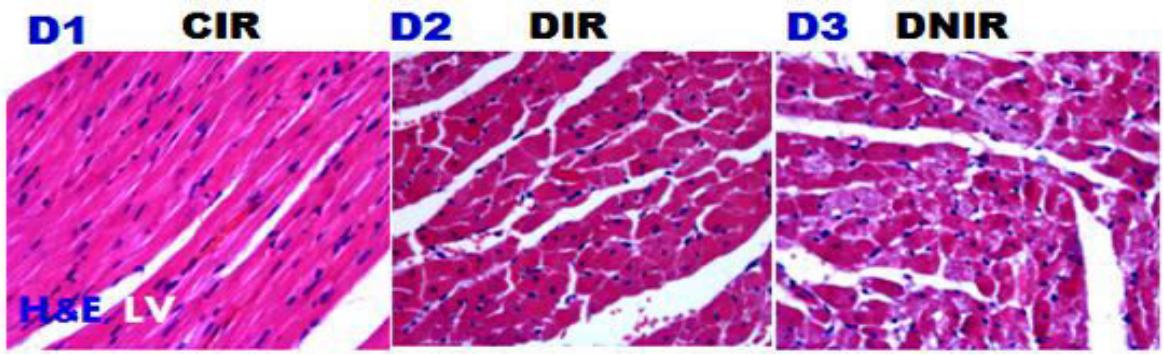

Figure: 48. FFPE tissue histopathological evaluation of diabetic rat heart with and without naloxone and control after IR-induction: Light microscopic analysis of H&E stained heart tissue sections taken from left ventricles after ischemia and reperfusion. The histopathology of DNIR (Fig. 48 D3) heart tissue sections showed myocardial fibrosis compared to controls (DIR (D2), and CIR (D1). There was no marked structural difference between DIR and CIR heart tissue sections observed. STZ, Streptozotocin; FFPE, Formalin fixed paraffin embedded; CTRL, Control; DNIR, diabetic naloxone-injected ischemia reperfusion-induced; DIR, diabetic ischemia reperfusion-induced; CIR, Control ischemia reperfusion-induced.

5.3.3. Effects of non-selective antagonist of opioid receptors on pro-survival signaling kinases and GSK-3α/β in ischemia-reperfusion-induced hearts of diabetic rats

Measurement of optical density from western blots analysis of well-established pro-survival signaling proteins (Akt and ERK1/2) were evaluated in three groups such as DNIR, CIR, and DIR rats` heart using equal amount of protein (20µg) to each well to 10% of acrylamide gel. The extent of phosphorylation of ERK42/44 of DNIR group was significantly reduced in the presence of naloxone (0.186±0.01) compared to IR-induced diabetic control (0.23±0.01). Similarly, it was significantly reduced in IR-induced control group (0.31±0.01) in the absence of naloxone. The extent of phosphorylation of ERK1/2 between three groups was significantly varied $p = 0.002$.

Moreover, the level of phosphorylation for Akt significantly lowered in DNIR group (1.51±0.22) in the presence of naloxone compared to IR-controls 2.76±0.65, ($p = 0.018$). However, even though it didn`t reach the significance threshold the extent of Akt phosphorylation (0.158±0.6) was declined in DNIR group compared to IR-induced diabetic heart (0.245±0.04) $p=0.055$ (Fig. 49).

On the contrary, the extent of phosphorylation of GSK-3β significantly ($p=0.047$) elevated (0.67±0.15) in DNIR group compared to DIR group (0.22±0.07) (Fig. 49) but, not significant compared to CIR (0.41±0.01) ($p=0.2$). On the other hand, absence or poor phosphorylation of GSK-3α was observed in almost all groups tested. These results might imply ERK1/2 and AKT pathways might be involved in regulation of these opioid receptors during blockade in neuropathic and diabetic rats` heart. The GSK-3β phosphorylation might also be modulated by Akt.

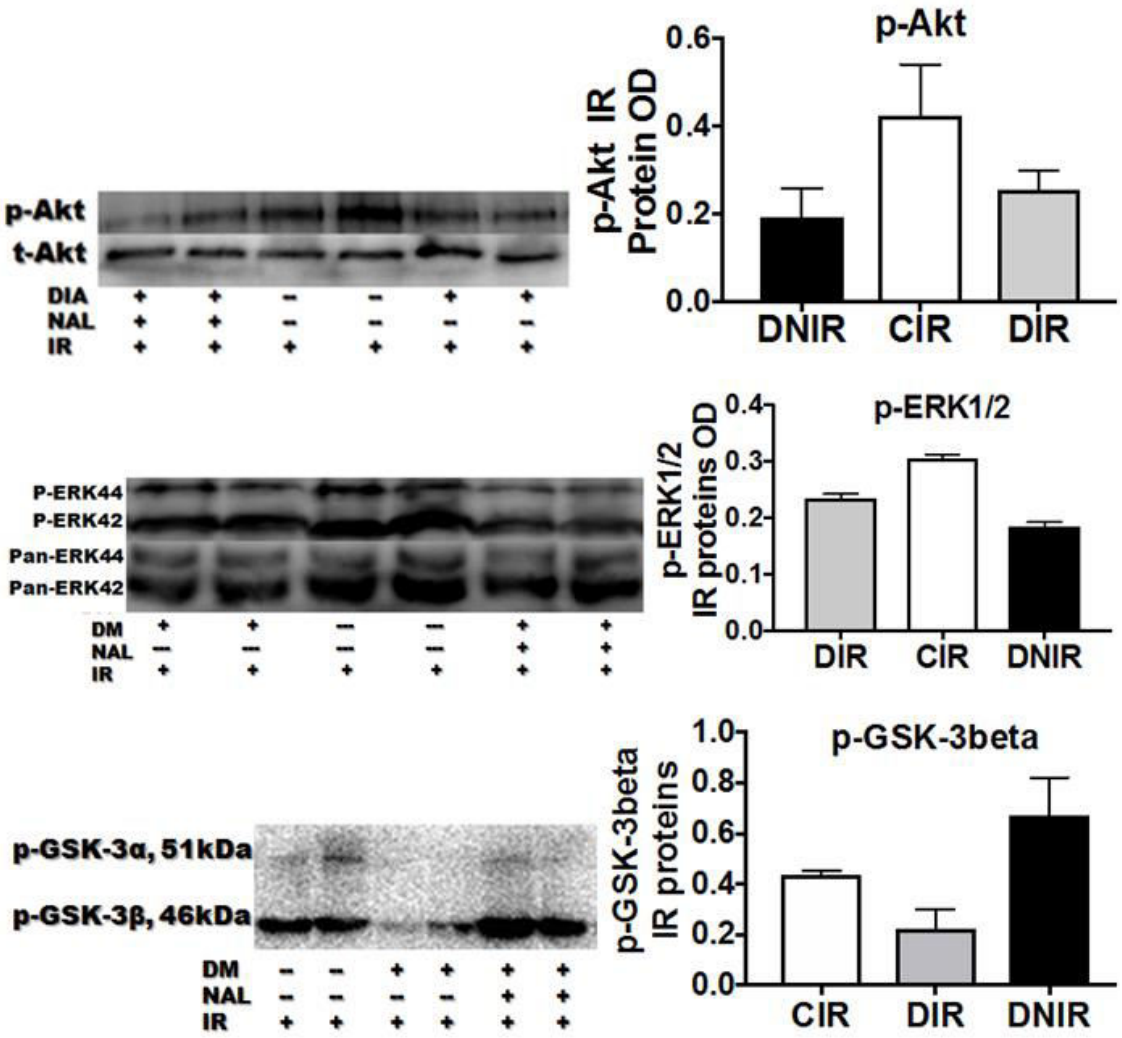

Figure: 49. Western blot analysis of phospho and total pro-survival proteins (ERK1/2 and AKT) and GSK-3α/β in DNIR, CIR, and DIR rats` heart: 20µg of proteins per 25µl of volume was loaded to 10% of acrylamide gel. Oneway ANOVA was used for between groups and independent T-test for DNIR group with DIR and CIR analysis. Mean ± STD, $P<0.05$ was considered as statistical significance. DNIR, diabetic naloxone-injected ischemia reperfusion-induced; DIR, diabetic ischemia reperfusion-induced; CIR, Control ischemia reperfusion-induced; NAL, Naloxone; DIA, Diabetic; IR, Ischemia/reperfusion; GSK, Glycogen synthase kinase.

5.3.4. Immunoreactive cells of phospho-p38 in diabetic with the presence (DNIR) and absence of naloxone (DIR) and normal (CIR) heart after ischemia and reperfusion in rats

P38 MAP kinases are stress-activated MAP kinases. It is activated in response to many cellular stresses and hematopoietic growth factors (Tamura et al., 2000). It regulates differentiation and/or survival of various cells types, including cardiomyocytes (Adams et al., 2000). Elevated p38 activity is associated to decreased myocardial contractility and onset of heart failure (Cross et al., 2009; Adams et al., 2000). Immunoperoxidase staining of p-p38 immunoreactive cells showed a significant elevation of p-p38 immunoreactive cells (29±0.2.74) in DNIR and (15.4±4.5) in DIR compared to CIR (3.4±1.14), P<0.001 (Fig. 50).

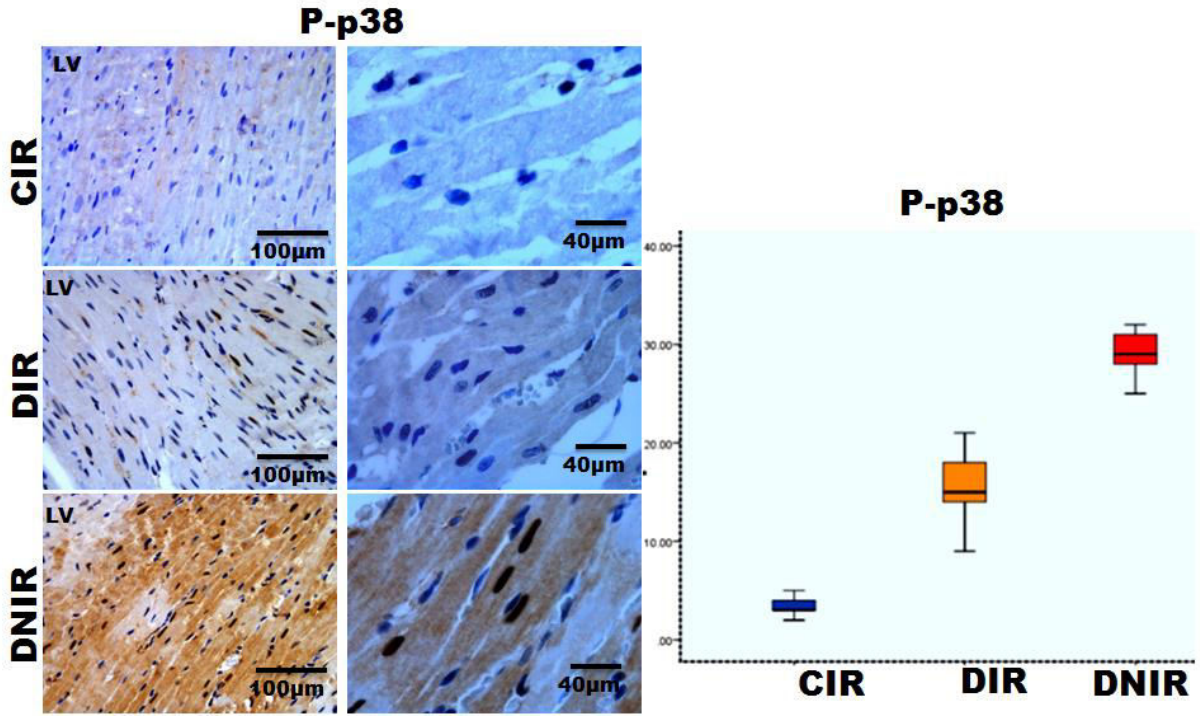

Figure: 50. P-p38 MAP kinase immunopositive myocyes in DNIR, DIR, and CIR-induced rats` heart tissue sections: A reduction in number of p-p38 MAP immunopositive cells of in DNIR, DIR, and CIR induced rats using Oneway ANOVA. DNIR, diabetic naloxone-injected ischemia reperfusion-induced; DIR, diabetic ischemia reperfusion-induced; CIR, Control ischemia reperfusion-induced

5.3.5. Apoptotic nuclei of TUNEL histochemical stained hearts tissue sections in the presence and absence of naloxone in diabetic and normal rats after ischemia and reperfusion, and TUNEL positive nuclei counts of each group

In our TUNEL analysis of formalin fixed tissue section STZ (diabetic) and IR-induced rat heart in the presence of naloxone, and diabetic control heart was found a significant elevated DNA fragmentation in the nuclei of myocytes in DNIR (17.75±2.14) compared to DIR (10.75±0.66) and CIR (4.9±0.67), P<0.001 (Fig. 51).

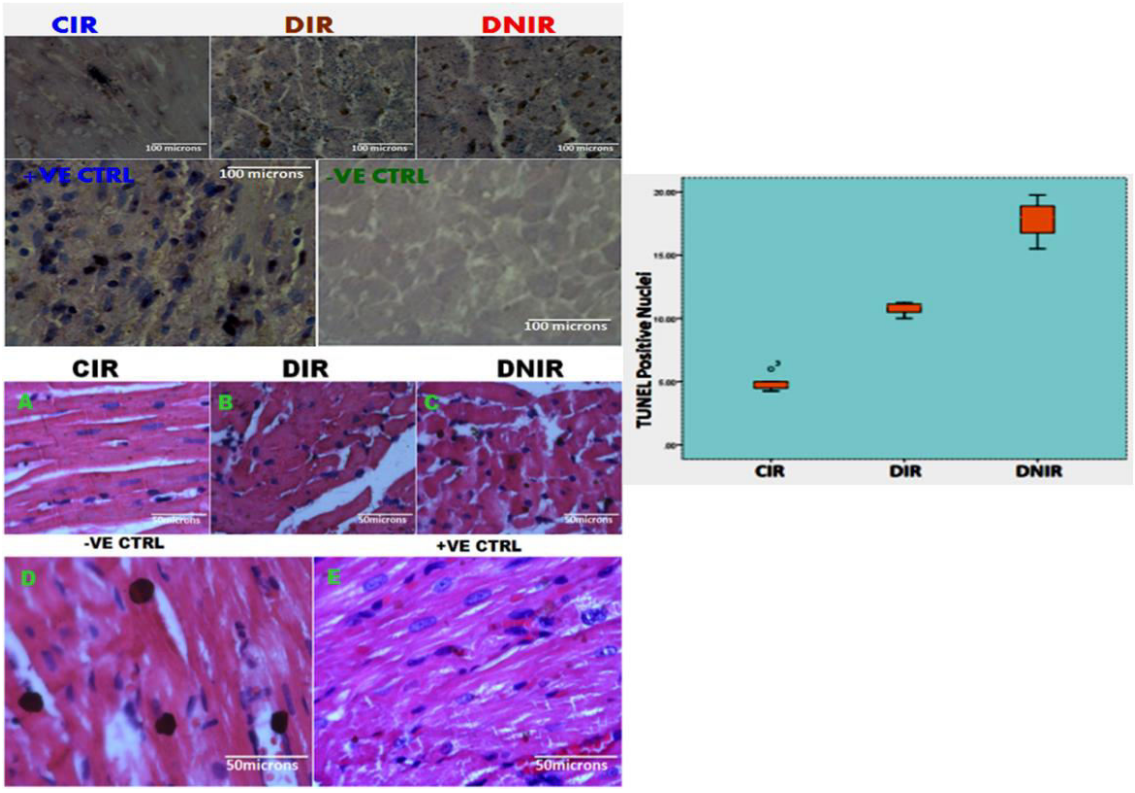

Figure: 51. Representative photomicrographs of TUNEL positive nuclei of myocytes of heart tissue sections in DNIR, DIR, and CIR induced rats after hematoxylin and HE counter staining: TUNEL positive apoptotic nuclei in cardiomyocytes was elevated in diabetic rat heart tissue sections in the presence of naloxone compared to diabetic control. Number of TUNEL positive nuclei in CIR, DIR, and DNIR induced heart tissue sections showing a significant elevation in number of apoptotic nuclei in DNIR induced rats compared to CIR-DIR. Mean ± STD, P<0.05 was considered as significant. One-way ANOVA was used for analysis. Mean ± STD, P<0.05 was considered as significant. One-way ANOVA was used for analysis. TUNEL+ Hematoxylin (H); DNIR, Diabetic, naloxone injected ischemia and reperfusion; DIR, Diabetic ischemia and reperfusion; CIR, Control ischemia and reperfusion; -VE CTRL, Negative control; LV, Left ventricle. Images TUNEL stained only acquired at 200x magnification, scale bar = 100microns; TUNEL and H&E stained, images acquired at 400x magnification scale bar 50microns.

5.3.6. Fluorescent labeled TUNEL stained apoptotic nuclei in the presence and absence of naloxone in heart tissue of diabetic and normal rats after ischemia-reperfusion, and TUNEL positive nuclei counts

In our fluorescence TUNEL analysis of formalin fixed tissue section of STZ-induced diabetic rat heart in the presence of naloxone, diabetic control and normal control heart after ischemia and reperfusion induction was done. A significant elevated DNA fragmentation in the nuclei of myocytes in DNIR was observed compared to DIR and CIR groups $p<0.001$ (Fig. 52).

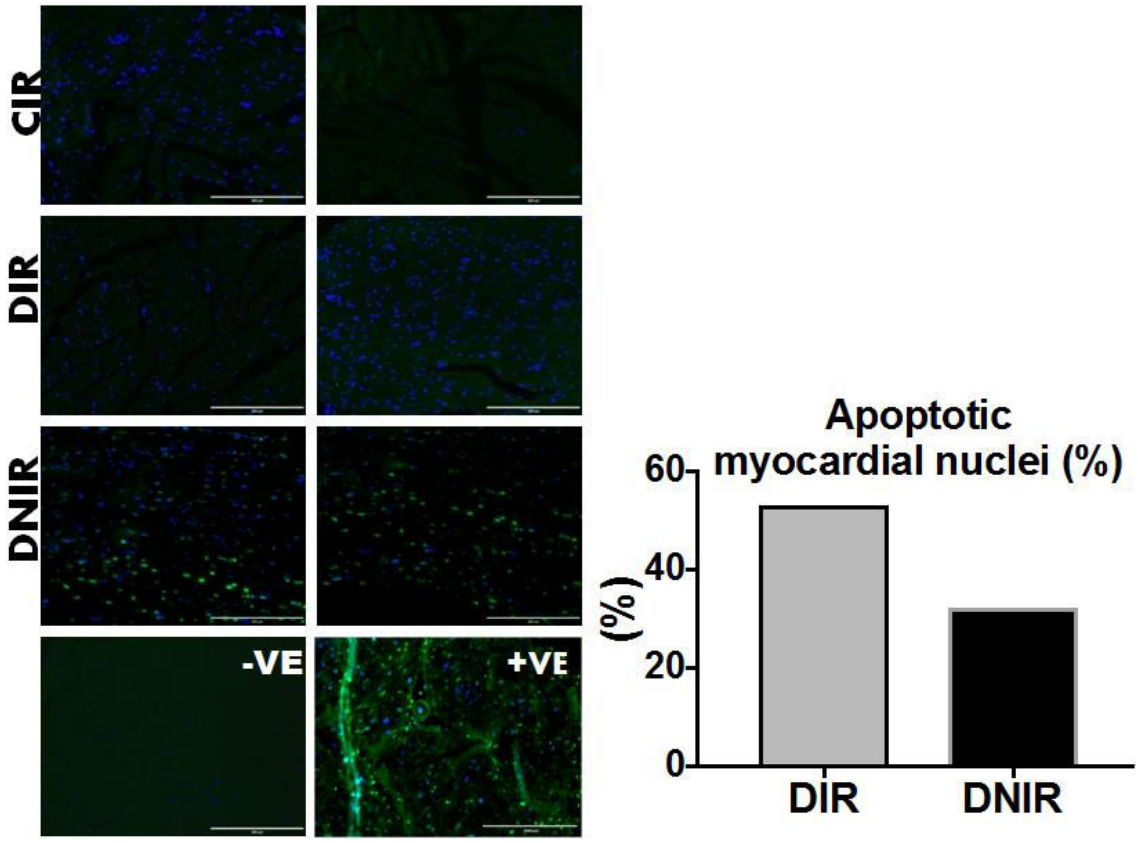

Figure: 52. Representative photomicrograph of heart tissue sections showing TUNEL positive fluorescence nuclei in DNIR, DIR, and CIR: All localization of myocardial nuclei is shown in blue (Hoechst) fluorescence and in green (TUNEL) fluorescence staining; apoptotic nuclei present in DNIR and DIR. Number of apoptotic cells significantly increased in DNIR-induced rats compared to DIR-induced rats. The graph shows percentage of apoptotic myocytes in DNIR and DIR-induced rats. Apoptotic index is expressed as the percentage of TUNEL positive nuclei relative to total Hoechst nuclei. TUNEL+ Hematoxylin (H); DNIR, Diabetic, naloxone injected ischemia and reperfusion; DIR, Diabetic ischemia and reperfusion; CIR, Control ischemia and reperfusion; -VE CTRL, Negative control; LV, Left ventricle. Fluorescent images acquired at 400x magnification at 100µm scale bar.

5.4. Discussion

The opioid receptors are, activated by endogenously opioid peptides and exogenously opiate compounds (Waldhoer et al., 2004), which expressed in multiple organs (Khachaturian et al., 1987) throughout the peripheral tissues of the body (Wittert et al., 1996; Zhu et al., 1998). The heart expresses high levels of endogenous opioids across species (Headrick et al., 2015; Howells et al., 1986; Theisen et al., 2014; Sobanski et al., 2014).

Although reports of Sobanski et al., (2014) proved the expression of the three (μ, δ, κ) classic subtypes of opioid receptors immunoreactivity in myocardial cells of human heart, there is a great disparities and debate regarding the distribution of opioid receptors subtypes in the heart chambers (Krumins et al., 1985) and between species (Karlsson et al., 2012). On the contrary, the increase in the level of enkephalins in ventricles of rats following myocardial infarction is reported (Paradis et al., 1992).

In an assortment of previous studies, kappa and delta ORs expression have been reported in the rat heart (Ela et al., 1997; Ventura et al., 1989), where as studies have also shown the absence of mu-OR at mRNA in all chambers of the porcine heart (Theisen et al., 2014) and including our studies in diabetic and heterotopic transplanted rats` heart. Before two decades, in earlier reports of Zimlichman et al (1996) the expression of mu-OR has only been detected in early developmental period; however, lately reduced during heart ontogeny after seventh day of postnatal age in rat heart. In 2012, Karlsson and colleagues have reported the expression of δ and κ ORs at both mRNA and proteins levels in myocardial biopsies of porcine. In agreement with Karlsson et al., (2012), Lendeckel et al., 2005 has detected δ and κ ORs in the human atria with a selective down-regulation of the k-OR during atrial fibrillation.

Correspondingly this study has mentioned earlier the presence of, mRNA encoding Oprd1 and Oprk1 and, proteins (DOR-1 and KOR-1) in rat heart with a down-regulated at mRNA and proteins levels in diabetic, and heterotopic transplanted hearts. Moreover,

decline CGRP-1 optical density immunoreactivity in diabetic rats has also shown in this study. The lower in the strength of DOR-1 immunoreactivity level was correlated with the reduced optical density immunoreactivity of CGRP-1. This result may, thefore, give a clue that downregulation of these receptors could be due to diabetic conditions or neuropathy that comes with diabetes. The double immunofluorescence data of this study also shows co-expressions KOR-1 and CGRP-1 in rats` heart. The observed fluorescent simultaneous overlap of signals on cells contained these receptors in tissue sections of diabetic and control rat heart implies the selective expression of these distinct receptors (Gullberg, 1986) and their strong functional association on cardiomyocytes and contributions in regulation of cardiovascular function in rat`s heart.

The decrease in strength of DOR-1 and KOR-1 immunoreactivity in cardiomyocytes might also be due to the involvement of an autocrine process of ORs in which opioid peptides are not released from cardiomyocytes locally and interact with ORs of the heart that mediate cardioprotection. The decrease in the synthesis and release of opioid peptides into the peripheral circulation could be due to stress (Paradis et al., 1992) and histopathological changes observed in the study.

Akt is a well established signaling pathway and mediator of cardioprotective against IRI (Sun et al., 2013). It is phosphorylated and activated by PI3K and blocks the expression of many pro-apoptotic proteins (Caspases, Bax, Bad, p53) to promote cell survival (Yu et al., 2010; Cantley, 2002). Tanaka et al., (2014) also stated the involvement of AKT and ERK activations in cardioprotection with similar results of Heiss et al., (2009) and Polakiewicz et al., (1998) that have shown association of cytoprotective and anti-apoptotic properties with activation of pro-survival kinase (AKT) due to opioid receptor agonists (DAMGO). Similarly, recent report has shown the compromised-protective effects of opioid conditioning against IRI like ischemic conditioning in diabetic condition (opioid-induced cardioprotection in diabetes) (Lei et al., 2015). It is also reported that the DOR mediated AKT signaling blockade as a result of naloxone involves Gi/o proteins in NG108-15 hybrid cells (Heiss et al., 2009).

In line with these reports, our signaling data provide evidence that inhibition of opioid receptors by non-selective antagonist (naloxone) lowers the extent of phosphorylation of pro-survival kinase (AKT) like wortmannin and LY294002 (Polakiewicz et al., 1998) at ser473 that implicate cell death in diabetic and IR-induced rat myocardium. Moreover, inhibition of the opioid receptors with naloxone reduces ERK1/2 phosphorylation in diabetic IR-induced rat heart. In other word, abnormal regulation of blood glucose and neuropathic conditions that could lead to downregulation of delta and kappa opioid receptors might imply a decrease AKT and ERK1/2 signaling in rats` heart. In this study, the demonstrated lower phosphorylation levels of pro-survival kinases (AKT, ERK) might compromise the well established protective effects of opioid conditioning against IRI. The lower levels of AKT phosphorylation might also possibly be regulated by a direct phosphorylation of mTOR (Polakiewicz et al., 1998) in naloxone injected IR-induced rats.

The lower phosphorylation of AKT and ERK1/2 phosphorylation may also infert the cross talk of PI3K-AKT pathway with Ras/Raf/MAPK pathways that control responses in regulation of opioid receptors. According to Heiss et al., (2009), naloxone induced AKT inactivity might also be via trans-inactivation of RTK because the inhibition of RTK that abolishes the effect of opioids stimulated AKT activity. The findings of our study indicate that opioid receptors have a potential role in reducing IRI. Hence, our study indicates that opioid receptors have a potential role in reducing IRI that might be affected by denervation, and neuropathic conditions diabetic in diabetic in rats reported in our unpublished data.

Another finding of our study has also shown higher extent of GSK-3β phosphorylation in diabetic rat heart in the presence of naloxone compared to controls. It is reported that GSK-3 can promote apoptosis through two ways either by activating p53 (Watcharasit et al., 2002) or by inactivating survival promoting factors (Grimes and Jope, 2001). According to a study done by Wang et al., (2009), inactivation of GSK-3β prevents diabetes-induced cardiac energy metabolism changes, fibrosis, and inflammation. The observed mild fibrosis and higher apoptotic number of nuclei of myocytes in heart tissue

with the presence of naloxone could be due to the higher extent of phosphorylation of GSK-3 in this group throught Akt dephosphorylation (Fig. 53).

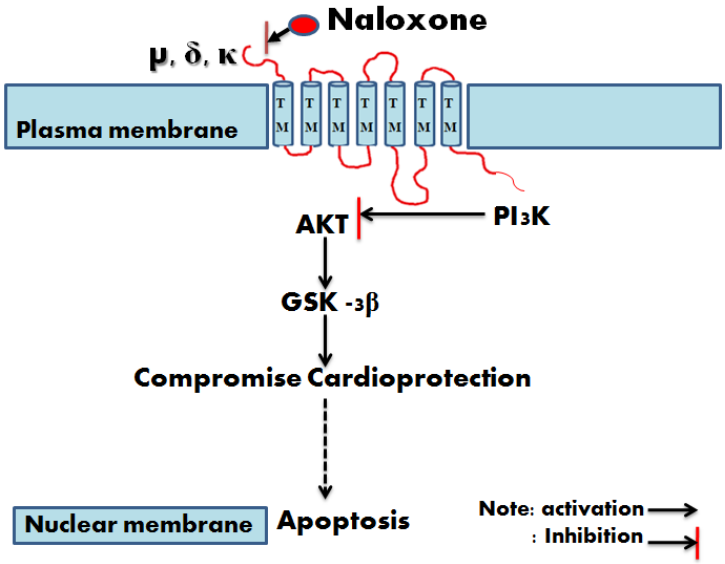

Figure: 53. Hypothesized mechanism of naloxone induced infarct size elevation: Naloxone deactivates PI3K-Akt at ser that lead to apoptosis and compromise cardioprotection of effects of endogenous opioid peptides in rat.

The p38 MAP kinases are stress-activated MAP kinases. It is activated in response to many cellular stresses and hematopoietic growth factors (Tamura et al., 2000). It regulates differentiation and/or survival of various cells types, including cardiomyocytes (Adams et al., 2000). The elevated p38 activity is associated to decreased myocardial contractility and onset of heart failure (Cross et al., 2009; Adams et al., 2000).

The significant elevated p-p38 immunoreactivity shown in immunoperoxidase stained heart tissue in naloxone and IR-induced diabetic rats imply inhibition of opioid receptors that increase the bioavailability of opioid in the blood due to opioid receptors reduction in diabetic rats. The ischemia-reperfusion-induced and inhibited opioid receptors activated p38 MAP kinases phosphorylation in diabetic rats` heart coincide with the result that shown the elevated apoptotic nuclei of cardiomyocytes in diabetic, and IR-induced rats. Histopathological evaluation of this study has shown wavy shaped fibers, necrosis of cells and a form of pink deposition as a result of release of necrotic cells content and higher phosphorylation levels of p38which implicate the damage of myocytes in IR-

induced diabetic rats. The changes in elevated p38 phosphorylation immunoreactivity and TUNEL positive apoptotic nuclei (DNA fragmentation) of myocytes in diabetic rats in the presence of naloxone corresponds to the observed appearance of massive infarct/lesions in IR-induced rat heart slices, higher percentage of infarct size, and morphological abnormalities of naloxone injected IR-induced diabetic rats.

The significant downregulation of DOR-1 and KOR-1 immunoreactivity, and mRNA encoding Oprd1 and Oprk1 in diabetic heart might be due to apoptotic nuclei of myocytes, infarction, and histopathological changes observed in diabetic rat heart tissue and the vulnerability of diabetic rats in neuropathy. These receptors could be regulated by ERK1/2 and AKT that are downregulated in the presence of naloxone.

The infarct and apoptotic cells death could be the reduction of opioid receptors observed in diabetic rats. This decreases the binding of opioids available in the blood to the receptors result in the reduction the known cardioprotection effects of opioid receptors. The bioavailable opioids effectiveness could be compromised.

According to the previous studies done by Marvin et al., 1980, parasympathetic innervations of the heart develops before birth, while sympathetic innervations develops during postnatal 7 to 10 days (Robinson, 1996; Mouse et al., 2011). Except the gradual disappearance of MOR; DOR and KOR are increased in number in adulthood (Zimilichman et al., 1996) in the heart with the increased number of MOR, DOR and KOR within CNS (Spain et al., 1985).

It is again reported that DOR co-localization with VAChT principal neurons from the first day of birth and with small intensely fluorescent catecholaminergic cells, and CGRP with in intracardiac ganglia and atrial myocardium. Moreover, the co-expression DOR with neuronal markers increasing with age (neonatal to adulthood) (Mousa et al., 2011) and these developmental expressions of opioid receptors and sympathetic and parasympathetic and sensory innervations of the heart imply the regulation of opioid receptors by cardiac autonomic innervations.

5.5. Conclusion

This study shows down-regulation of δ and κ ORs at proteins and mRNA levels in diabetic rat heart. It is known that opioid receptors (δ- & κ) play beneficiary role in protecting the heart against IRI. However; the down regulation of opioid receptors may compromise the effectiveness of pharmacological activities of opioids in diabetic rats that could also reduce the potential role of opioid receptors in the regulation of cardiac tissue of diabetic conditions in rat. The downregulation might be due to neuropathic and diabetic conditions observed in rats` heart.

The extent of lower pro-survival kinases (ERK1/2 and AKT) phosphorylation, higher p38 phosphorylation, elevated apoptotic nuclei and percentage of infarct size, and histopathological abnormalities in naloxone treated and IR-induced diabetic rats suggest a possible mechanism of increased susceptibility of diabetic rat heart to IRI through mediating action of ERK1/2 and AKT pathways in opioid activities.

CHAPTER SIX

6. A comparative study on expression of k- and δ- opioid receptors in pulmonary artery and aorta in rats

6.1. Background

Opioid receptors possess potential cardiovascular protective properties and play roles on vasodilation (Pei et al., 2003) and its agonists exert direct actions on vascular smooth muscle (el-Sharkawy et al., 1991; Zhou et al., 2015). Partially relaxation of the aorta in rat due to KOR stimulation via K (ATP) channel has also reported (Pei et al., 2003). Endothelium is the major regulator of vascular homeostasis and plays a key role in physiology and pathology of the vascular system. Stimulation KOR improves endothelial function in hypoxic pulmonary hypertension (Wu et al., 2013). This study was aimed to compare the expression of kappa and delta opioid receptors on aorta and pulmonary artery in rats.

6.2. Materials and methods

Aorta and pulmonary artery were taken from rats weighing 350 – 400g and processed in FFPE for immunohistochemical study as described in the fourth chapter. Processed tissues were observed under confocal inversted microscope for analysis.

6.3. Results

6.3.1. Double immunofluorescence stained KOR-1 and DOR-1 immunoreactive containing signals in pulmonary artery in rat

In this study, our qualitative immunofluorescence data showed immunofluorescence labeled immunoreactivity signals of KOR-1 in both endothelial and smooth muscle cells of pulmonary artery. Kappa was also expressed in endothelial cells of aorta. The kappa-OR was shown dominant in pulmonary artery; however, kappa was poorly detected in smooth muscle cells of the aortic tissue sections as compared to pulmonary artery. Moreover, delta opioid receptor was also detected in pulmonary artery smooth muscle cells (Fig. 54).

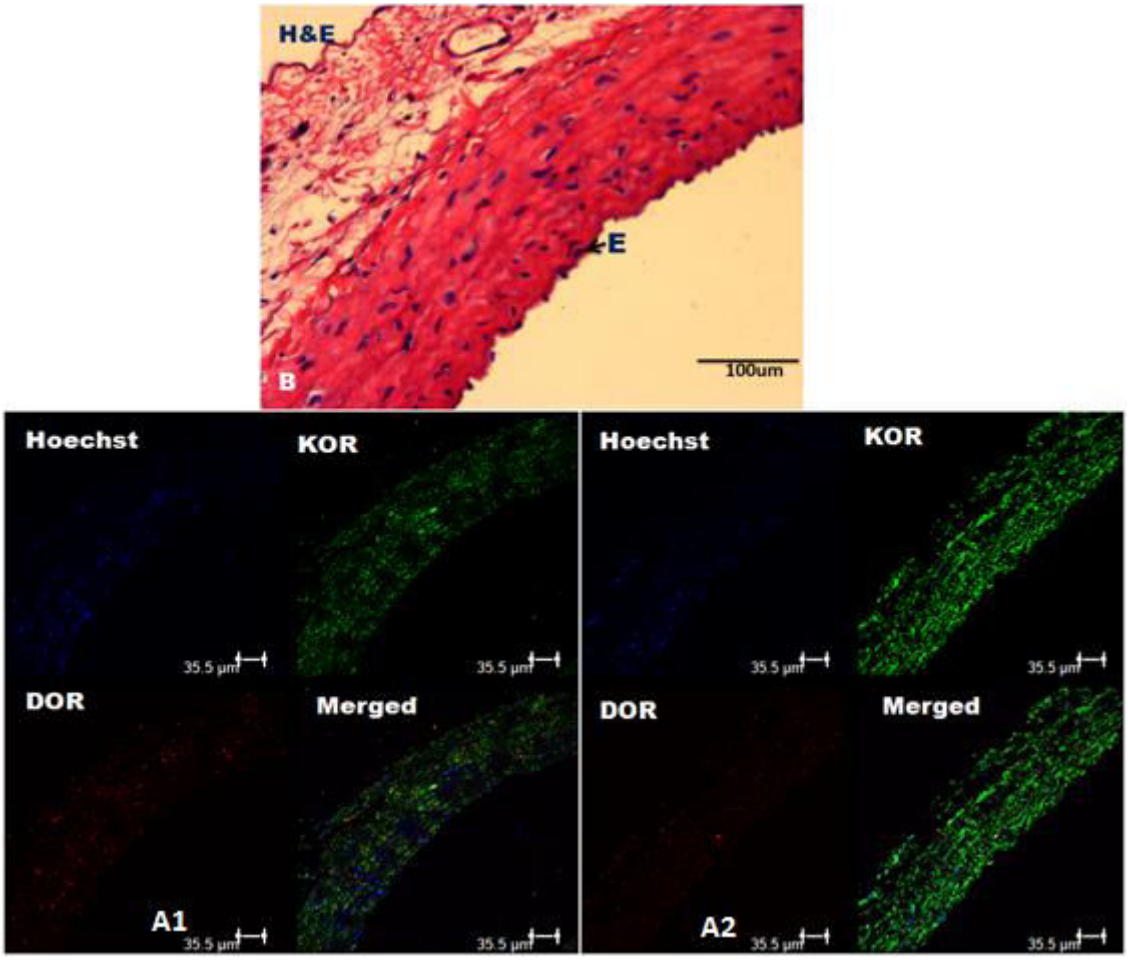

Figure: 54. Crossection view of confocal double immunofluorescence microscopy of KOR-1 and DOR immunoreactive signals in pulmonary artery and aortic tissue section in rat: KOR-1, Kappa opioid receptor; DOR-1, Delta opioid receptors; E, endothelium. Scale bar = 35.5um.

6.3.2. Immunoperoxidase and double immunofluorescence KOR-1 labeled immunoreactive signals on aortic tissue sections in rat

Both immunoperoxidase and immunofluorescence data showed detection of KOR-1 immunoreactive in endothelial cells of aorta (Fig. 55). However, its immunoreactivity in smooth muscle of aorta was poorly expressed.

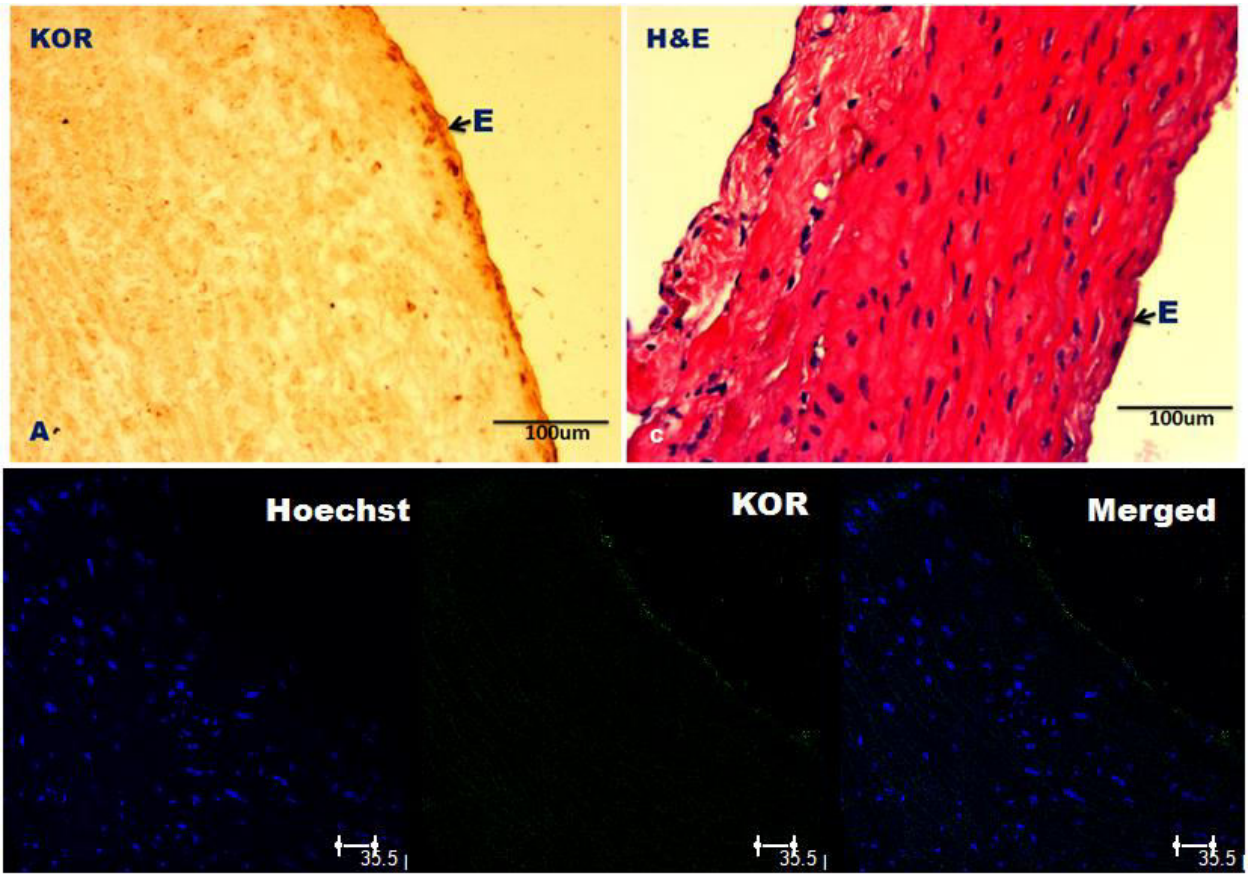

Figure: 55. Microscopy of KOR immunoreactive smooth muscle and endothelial cells of aorta and pulmonary artery: A: Microscopic observation of KOR-1 immunoreactive endothelial cells. B: Confocal microscopy of KOR immunofluorescence reactive endothelial cells in aortic tissue section of rat. KOR-1, Kappa opioid receptor; E, Endothelium. Scale bar = 35.5um for fluorescence image, 100microns for immunoperoxidase image.

7. General discussion, conclusion, and recommendation

Down-regulation of opioid receptors (δ & κ) in denervated and neuropathic diabetic rat heart

The findings of this study reveal the presence in myocardium of mRNA encoding delta and kappa ORs, MOR-1 immunoreactive myocytes in the orthotopically transplanted heart in the human, δ- and κ-ORs mRNA and proteins in heterotopic transplanted heart. Moreover, kappa and delta were also identified in STZ-induced diabetic rat heart. These findings are in agreement with previous studies showing the presence of mu, delta and kappa opioid receptors on cardiomyocytes of humans (Sobanski, 2014) and (δ & κ) animals' heart (Theisen et al., 2014; Cao, 2003; Patel et al., 2006; Weil et al., 1998; Howells et al., 1986).

Interestingly, this study found out down-regulation of Oprk1 and Oprd1 mRNA in both orthotopically transplanted (in human) and heterotopic transplanted heart (in rats). This implies a great contribution and influence of innervation to the functioning of opioid receptors in the heart. The concur findings obtained from rat and human transplants models have shown that heterotopic transplanted heart in rats is important in basic and translational studies concerningcardiac transplantation.

Qualitative and quantitative analysis of our data revealed that although kappa and delta are identified in STZ-induced diabetic rat heart, they are poorly expressed in diabetic heart. It is known that patients with diabetes are at high risk of preoperative myocardial infarction (Lei et al., 2015) with an undefined mechanism. In this study reduction of mRNA encoding kappa and delta opioid receptors in STZ-induced diabetic rat heart could be linked to a serious complication in diabetic patients undergoing surgery, indeed patients with diabetes have less resistance to myocardial ischemia and reperfusion injury (Lei et al., 2015). Thus, diabetic conditions could compromise the proven opioid conditioning against ischemia and reperfusion injury.

Down-regulation of neuronal marker (CGRP-1) in denervated and neuropathic diabetic rat heart

In our study of Calcitonin gene-related peptide (CGRP-1) in transplanted and diabetic heart to see how it is expressed in denervated and neuropathic heart, this neuronal marker was detected as a sparse individual fiber of myocytes in transplanted heart (human and rat) and diabetic heart. However, analysis of the optical density reveals that this marker is poorly expressed in transplanted and diabetic heart.

CGRP-1 is a neuropeptide found in both sensory and motor neurons (Rosenfeld et al., 1983; Kashihara et al., 1989), playing role in cardiovascular homeostasis, and contributing to regeneration following nerve injury in mice (Chen et al., 2010). The reduction of CGRP-1 in transplanted heart might imply a lower level of denervation in the heart. It is known that the presence of an innervated heart is important for normal cardiovascular physiology. This could give insights to understand the transplant cardiovascular physiology related to opioid administration.

KOR and DOR mRNA in myocardial tissue

In this study mRNA encoding, Oprd1 and Oprk1 in rat heart were detected with down-regulation in transplanted and diabetic heart. However, Oprm1 was not amplified even at 50 cycles in both control and diabetic rat heart. Since the description of ORs (Pert and Snyder, 1973) in CNS and endogenous opioids (Hughes et al., 1975), large amounts of endogenous peptides (preproenkephalin mRNA) have been detectecd in rats' cardiac ventricular tissue (Howells et al., 1986) in differents species (guinea pig, bovine and mouse hearts) This study also confirms their presence in heart tissue in both human and rats with downregulation in transplanted and diabetic heart.

Histopathology of transplanted, diabetic, ischemic, reperfused heart

In our evaluation of histopathology of transplanted heart, we observed severe cellular rejection in heterotopic transplanted heart tissue. Acute cellular rejection (ACR) is most common in the first 6 months after heart transplantation (HT) and is predominantly T-

cell-mediated. Approximately 20% to 40% of heart transplant recipients experienced at least 1 episode of ACR in the first postoperative year (Taylor, 2010).

Effects of naloxone on infarct size after ischemia and reperfusion

In this study, we have screened effects of naloxone infarct size after ischemia and reperfusion. The data from naloxone and control groups are showing a higher percentage of infarct size in the presence of non-selective antagonist of opioid receptors in heart slices. In various studies, naloxone is known for its capcity to decrease cardioprotective effects obtained through different conditioning, such as ischemic, pharmacological and exercise preconditioning. We have also shown in this study that naloxone has indirectly abolished effects of cardioprotection by elevating percentage of infarct size leading to a massive infarct/lesions in rats treated with the drug.

The changes in elevated p38 phosphorylation immunoreactivity and TUNEL positive apoptotic nuclei (DNA fragmentation) of myocytes in diabetic rats in the presence of naloxone is associated with the appearance of massive infarct/lesions in IR-induced rat heart slices, higher percentage of infarct size, and morphological abnormalities of diabetic rats.

Apoptotic nuclei of cardiomyocytes in denervated, neuropathic and diabetes heart, and effects of non-selective antagonist of opioid receptors on apoptotic nuclei after ischemia-reperfusion induced in diabetic heart

In this study, using fluorescent and histochemical TUNEL positive nuclei of myocytes, we have observedhigher number of apoptotic nuclei in cardiomyocytes as well as all tissue tested from the denervated and diabetic. Moreover, a higher number of apoptotic nuclei were also detected in the presence of antagonist (naloxone) after ischemia-reperfusion diabetic rats` heart. The indicated denervation and diabetic conditions may dephosphorylate the pro-survival kinases that are responsible for inhibitions of pro-apoptotic proteins.

Effect of the opioid receptors non-selective antagonist on pro-survival signaling pathways

Western blot analysis of pro-survival proteins (ERK1/2 and AKT) have shown that both pAKT and perk1/2 have declined their phosphorylation levels in diabetic IR-induced rats` heart in the presence of naloxone compared to IR-induced control heart.

It is known that Akt is a well established pro-survival mediator of cardioprotective against ischemia-reperfusion injury (Sun et al., 2013). It is phosphorylated and activated by PI3K and blocks the expression of many pro-apoptotic proteins (Caspases, Bax, Bad, p53) to promote cell survival (Yu et al., 2010; Cantley, 2002). The activated Akt influences cellular physiology (Hemmings and Restuccia, 2012) including regulation of apoptosis. The elevated apoptotic nuclei and lower phosphorylation of Akt observed in this study in the condition of naloxone IR-induced diabetic heart suggests the involvement of Akt in mediating opioid receptors activities against ischemia-reperfusion injury in rats.

Evidences from our study have also shown that the infarct effect of ORs antagonist (naloxone) is mediated by ERK1/2. This result is consistent with the results of Kim et al., (2011) mentioning a direct anti-infarct effect of KOR agonist via ERK1/2 which leads to the effective reduction of myocardial infarction by inhibition of ERK1/2 obtained from the anti-infarct effect of KOR agonist.

The p38 phosphorylation changes in the diabetic heart after ischemia and reperfusion

In this study, the ischemia-reperfusion-induced and inhibited-opioid receptors in the body have been associated with elevation in the levels of p38 phosphorylated immunoreactive cells in the myocardium. The activated p38 MAP kinases in diabetic rats` heart due to diabetic conditions, ischemia, and reperfusion injuries coincide with elevated apoptotic nuclei of cardiomyocytes in the diabetic and IR-induced heart.

It is known that the p38 MAP kinases are stress-activated MAP kinases and activated in response to many cellular stresses and hematopoietic growth factors (Tamura et al., 2000). It regulates differentiation and/or survival of various cells types, including cardiomyocytes (Adams et al., 2000). Previous reports have shown that elevated p38 activity can be associated with poor myocardial contractility and onset of heart failure (Cross et al., 2009; Adams et al., 2000).

Thus, the activation of p38 due to stress, ischemia, and reperfusion in heart could be potentiated in the presence of naloxone as shown by higher phosphorylation of the protein. This implies that dysfunctional opioid receptors could increase the bioavailability of opioid in the blood due to a reduction of opioid receptors activity as observed in diabetic and neuropathic heart, leading to an ipairement of cardioprotective roles of opioids.

Consistently we have observed that the ischemia-reperfusion-induced heart, inhibition of opioid receptors activation of p38 MAP kinases in diabetic rats` heart are associated to the elevated apoptotic nuclei of cardiomyocytes in diabetic rats, and with appearance of massive infarct/lesions in IR-induced rat heart slices, higher percentage of infarct size, and morphological abnormalities of naloxone injected IR-induced diabetic rat heart.

Effect of naloxone on phosphorylation of GSK-3β

Another finding of our study has also shown higher extent of GSK-3β phosphorylation in diabetic rat heart in the presence of naloxone. It is reported that GSK-3 can promote apoptosis through two ways either by activating p53 (Watcharasit et al., 2002) or by inactivating survival promoting factors (Grimes and Jope, 2001). According to a study done by Wang et al., (2009), inactivation of GSK-3β prevents diabetes-induced cardiac energy metabolism changes, fibrosis, and inflammation. Therefore, the higher phosphorylation of GSK-3β may implicate with the interference of glucose metabolism in effect of naloxone and influence the apoptosis which was seen in diabetic rats.

Expression of κ- and δ-ORs on aorta and pulmonary artery in normal rats

Our findings show the presence of kappa and delta opioid receptors on endothelial cells of both aorta and pulmonary artery; however, DOR is weaker in expression than KOR in aorta and pulmonary artery. The opioid receptors have potential cardiovascular protective properties and play roles on vasodilation (Pei et al., 2003). In our study, kappa opioid receptor has been expressed dominantly in endothelial cells of aorta. Pulmonary artery has dominant expression of kappa opioid receptors on smooth muscle cells compared to aorta. Kappa is more limited endothelial cells of aorta than smooth muscle cells of aorta. The dominant expression of kappa opioid receptor implicates its significance to regulate vascular system both in aorta and pulmonary artery in rats compared to delta opioid receptor in rats.

Implication of down-regulation of opioid receptors on ischemia-reperfusion injury

The downregulation of opioid receptors observed in our study in transplanted and diabetic heart may impair the cardioprotective effects against declining cardiac tolerance to arrhythmogenic effects of ischemia (Maslov et al., 2013), worsen ischemia (Tsai et al., 2015), arrhythmia as it is observed in canine (Estrada et al., 2016; Tsai et al., 2015), and cardiomyocyte cell death (Tsai et al., 2015).

Bofetiado and colleagues (1996) have shown elevation of survival time during lethal hypoxia by a mechanism of neuroprotection via decreasing body temperature using delta agonist (BW373U86), DPDPE ([D-Pen2, D-Pen5]-enkephalin). The contribution of opioid compounds in stability and systemic distribution could favor clinical application. However, poor availability of opioid receptors and their mRNA in denervated and neuropathic and diabetic heart might compromise the effectiveness of the drug.

In conclusion, overall our data suggest that opioid receptors have cardioprotective roles against ischemia-reperfusion injury and they may be mediated by pro-survival kinases (ERK1/2 and Akt). Phosphorylation of p38 can also involve in increasing the damaging rate using opioid receptors antagonist.

Given this important role of opioid receptors to ischemia and reperfusion injuries, they represent as such a potential therapeutic strategy that could be associated to surgery and/or transplantation to improve the patient health. Developing a drug that restores opioids-induced cardioprotection in diabetes can be a good way to minimize IRI in diabetic heart. The opioid receptors may also play a great role on endothelial and smooth muscle cells in vascular system dominantly KOR opioid receptor in rats.

8. References

Adams RH, Porras A, Alonso G, Jones M, Vintersten K, Panelli S, Valladares A, Perez L, Klein R, Nebreda AR. Essential role of p38alpha MAP kinase in placental but not embryonic cardiovascular development.Mol Cell. 2000; 6(1):109-16.

Al-Hasani R, Bruchas MR. Molecular mechanisms of opioid receptor-dependent signaling and behavior. Anesthesiology. 2011; 115(6):1363-1381. doi: 10.1097/ALN.0B013e318238bba6.

Alvarez L, Escudero C, Alzueta J, Silva L, Márquez-Montes J, Castillo-Olivares JL. Electrophysiology of heterotopic heart transplant: experimental study in dogs. Eur Heart J. 1990; 11(6):517-24.

American Heart Association. Heart transplantation. 2009; http://www.heart.org/idc/groups/heart.

American Medical Association. Heart transplant rejection tests (Heartsbreath and Allomap^{TM}, molecular expression test). Clinical Coverage Guideline. 2014; PN: HS-060.

Ardell JL. Intrathoracic neuronal regulation of cardiac function. In Basic and Clinical Neurocardiology. 2004; 118–152. Oxford University Press, New York.

Armour JA. Potential clinical relevance of the 'little brain' on the mammalian heart. Exp Physiol. 2008; 93(2):165-76. DOI: 10.1113/expphysiol.2007.041178.

Arrowood JA, Minisi AJ, Goudreau E, Davis AB, King AL. Absence of parasympathetic control of heart rate after human orthotopic cardiac transplantation. Cicrulation. 1997; 96:3492-3498. doi: 10.1161/01.CIR.96.10.3492.

Bansal V, Kalita J, Misra UK. Diabetic neuropathy. Review. Postgrad Med J. 2006; 82(964): 95–100. doi: 10.1136/pgmj.2005.036137.

Barnard CN. A human cardiac transplantation: An interim report of a successful operation performed at Groote Schuur Hospital, Cape Town. S Afr Med J. 1967; 41(48):1271-4.

Barron BA. Cardiac opioids. Proceedings of the Society for Experimental Biology and Medicine. 2000; 224:1-7. doi:10.1111/j.1525-1373.2000.22358. x.

Barry U, Zuo Z. Opioids: Old drugs for potential new applications. Curr Pharm Des. 2005; 11:1343–1350.

Benedict PE, Benedict MB, Su T, Bolling SF. Opiate drugs and delta-receptor mediated myocardial protection. American Heart Association, Circulation. 1999; 100: II-357-II-360.

Berg JM, Tymoczko JL, Stryer L. Biochemistry. Fifth edition. 2002; NewYork: W H Freeman. ISBN-10:0-7167-3051-0.

Bofetiado DM, Mayfield KP et al. Alkaloid delta agonist BW373U86 increases hypoxic tolerance. Anesthesia and Analgesia. Ovid Technologies, Inc. 1996; 82(6):1237-41.

Bokkelen G, Werner M. The application of regenerative medicine products abd technologies toward areas of significant medical need-improving clinical outcomes and reducing costs. Alliance for regenerative medicine. 2013.

Bolte C, Newman G, Schultz JE. Hypertensive state, independent of hypertrophy, exhibits an attenuated decrease in systolic function on cardiac k-opioid receptor stimulation. Am J Physiol Heart Circ Physiol. 2009; 296:H967-H975. doi: 10.1152/ajpheart.00909.2008.

Borges JP, Verdoorn KS, Daliry A, Scott K. Powers SK, Ortenzi VH, Fortunato RS, Eduardo Tibirica´ E, Lessa MA. Delta Opioid Receptors: The link between exercise and cardioprotection. PLoS ONE. 2014; 9(11): e113541. doi: 10.1371/journal.pone.0113541

Botta DM, Geibel J, Mancini MC. Heart transplantation technique: Approach Considerations, Transplantation of Heart, Complications. The Heart.Org. Medscape. 2016; p1-10.

Bott-Flügel L, Weig H, Ühlein H, Nabauer M, Laugwitz K, Seyfarth M. Quantitative analysis of apoptotic markers in human end-stage heart failure. European Journal of Heart Failure. 2008; 129–132. doi: 10.1016/j.ejheart.2007.12.013.

Bovet P, Paccaud F. Cardiovascular disease and the changing face of global public health: A focus on low and middle income countries. Public health reviews. 2012; 33(2):397-415.

Brack KE. The heart's 'little brain' controlling cardiac function in the Rabbit. Exp Physiol. 2015; pp 348–353. DOI: 10.1113/expphysiol.2014.080168.

Brink JG, Hassoulas. The first human heart transplant and further advances in cardiac transplantation at Groote Schuur Hospital and the University of Cape Town. Cardiovasc J Afr. 2009; 20(1): 31–35.

Brutsaert DL, Fransen P, Andries LJ, Keulenaer GW, Sys SU. Cardiac endothelium and myocardial function. Cardiovascular Research. 1998; 38:281-290.

Budde K, Matz M, Dürr M, Glander P. Biomarkers of over-immunosuppression. Translation, nature publishing group. 2011; 90(2):316-322. doi: 10.1038/clpt.2011.111.

Burch M, Aurora P. "Current status of paediatric heart, lung, and heart-lung transplantation". Archives of Disease in Childhood. 2004; 89 (4): 386-389. doi:10.1136/adc.2002.017186.

Burton RAB, , Plank G, Schneider JE, Grau V, Ahammer H, Keeling SL, Lee J, Smith NP, Gavaghan D, Trayanova N, Kohl P. Three-Dimensional Models of Individual Cardiac Histoanatomy: Tools and Challenges. Ann N Y Acad Sci. 2006; 1080: 301–319. doi: 10.1196/annals.1380.023.

Caffrey JL, Boluyt MO, Younes A, Barron BA, O`Neill L, Crow MT, Lakatta EG. Aging, cardiac proenkephalin m RNA and enkephalin peptides in the Fisher 344 rat. Journal of Molecular and Cellular Cardiology. 1994; 26(6):701-711. doi:10.1006/jmcc.1994.1085.

Calvo E, Bolós V, Grande E. Multiple roles and therapeutic implications of Akt signaling in cancer. Onco Targets Ther. 2009; 2: 135–150.

Cantley LC. The phosphoinositide 3-kinase pathway. Science. 2002; 296(5573): 1655–1657. doi: 10.1126/science.296.5573.1655.

Cao N, Huang Y, Zheng J, Spencer CI, Zhang Y, Fu JD, Nie B, Xie M, Zhang M, Wang H, Ma T, Xu T, Shi G, Srivastava D, Ding S. Conversion of human fibroblasts into functional cardiomyocytes by small molecules. Science. 2016; 352(6290):1216-20. doi: 10.1126/science.aaf1502. Epub 2016.

Cao Z, Liu L, Van Winkle DM. Activation of δ- and k-opioid receptors by opioid peptides protects cardiomyocytes via K_{ATP} channels. Am J Physiol Heart Circ Physiol. 2003; 285:H1032-H1039.

Carden DL, Granger DN. Pathophysiology of ischaemia-reperfusion injury. J Pathol. 2000; 190:255–266.

Caspi O, Huber I, Kehat I, Habib M, Arbel G, Gepstein A, Yankelson L, Aronson D, Beyar R, Gepstein L. Transplantation of human embryonic stem cell-derived cardiomyocytes improves myocardial performance in infarcted rat hearts. J Am Coll Cardiol. 2007; 50(19):1884-93. DOI:10.1016/j.jacc.2007.07.054.

Castedo E, Segovia J, Escudero C, Olmedilla B, Granado F, Blas C, Guardiola JM, Isabel Millán, f Pulpón LA, Ugarte J. Ischemia-Reperfusion Injury During Experimental Heart Transplantation. Evaluation of Trimetazidine's Cytoprotective Effect. Rev Esp Cardiol. 2005; 58(8):941-50.

Caves PK, Stinson EB, Billingham ME, Shumway NE. Serial transvenous biopsy of the transplanted human heart. Improved management of acute rejection episodes. 1974; 1(7862):821-6.

Chao D, Bazzy-Asaad A, Balboni G, Xia Y. δ-, but not μ-, opioid receptor stabilizes K+ homeostasis by reducing Ca2+ influx in the cortex during acute hypoxia. J Cell Physiol. 2007; 212(1):60–7.

Chao D, Xia Y. Ionic storm in hypoxic/ischemic stress: can opioid receptors subside it? Prog Neurobiol. 2010; 90(4):439–70.

Chen L, Zhang F, Li J, Song H, Zhou L, Yao B, Li F, Li W. Expression of calcitonin gene-related peptide in anterior and posterior horns of the spinal cord after brachial plexus injury. Journal of Clinical Neuroscience. 2010; 17:87–91. doi: 10.1016/j.jocn.2009.03.042.

Chung T, Prasad K, Lloyd TE . Peripheral Neuropathy – Clinical and Electrophysiological Considerations. Neuroimaging Clin N Am. 2014; 24(1): 49–65. doi: 10.1016/j.nic.2013.03.023.

Collard CD, Gelman S. Pathophysiology, Clinical Manifestations, and Prevention of Ischemia–Reperfusion Injury. Anesthesiology, Society of Anesthesiologists. 2001; 94:1133–8, Inc. Lippincott Williams & Wilkins, Inc.

Cook JA, Shah KB, Quader MA, Cooke RH, Kasirajan V, Rao KK, Smallfield MC, Tchoukina I, Tang DG. The total artificial heart. J Thorac Dis. 2015; 7 (12):2172-2180. doi: 10.3978/j.issn.2072-1439.2015.10.70.

Cooper DKC. A brief history of cross-species organ transplantation. Proc (Bayl Univ Med Cent). 2012; 25(1): 49–57.

Cooper GM. The cell: A molecular approach. 2nd edition, Sunderland (MA): Sinauer Associates. 2000; ISBN-10:0-87893-106-6.

Cotts WG, Oren RM. Function of transplanted heart: Unique physiology and therapeutic implications. American Journal of the Medical Sciences. 1997; 314(3):164-172.

Cox BM, Christie MJ, Devi L, Toll L, Traynor JR. Challenges for opioid receptor nomenclature: IUPHAR Review 9. British Journal of Pharmacology. 2015; 172:317-323.

Cristóbal C, Segovia J, Alonso-Pulpón LA, Castedo E, Vargas JA, Martínez JC. Apoptosis and Acute Cellular Rejection in Human Heart Transplants. Rev Esp Cardiol. 2010; 63:1061-9 - Vol. 63 Num.09 DOI: 10.1016/S1885-5857(10)70210-3

Cross HR, LiM, Petrich BG, Murphy E, Wang Y, Steenbergen C. Effect of p38 MAP kinases on contractility and ischemic injury in intact heart. Acta Physiol Hung. 2009; 96(3): 307–323. doi:10.1556/APhysiol.96.2009.3.5.

Davies RR, Russo MJ, Morgan JA, Sorabella RA, Naka Y, Chen JM. Standard versus bicaval techniques for orthotopic heart transplantation: an analysis of the United Network

for organ sharing database. J Thorac Cardiovasc Surg. 2010; 140(3):700-8, 708.doi: 10.1016/j.jtcvs.2010.04.029.

DiBardino DJ. The History and Development of cardiac Transplantation. History and Development of Cardiac Transplantation Tex Heart Inst J. 1999; 26:198-205.

DeBosch B, Treskov I, Lupu TS, Weinheimer C, Kovacs A, Courtois M, Muslin AJ. Akt1 is required for physiological cardiac growth. Circulation. 2006; 113:2097-2104. Doi: org/10.1161/Circulation AHA.105.595231.

Dietz JR. Mechanisms of atrial natriuretic peptide secretion from the atrium. Cardiovascular Research. 2005; 68:8 – 17. doi: 10.1016/j.cardiores.2005.06.008

Ding H, Czoty PW, Kiguchi N, Cami-Kobeci G, Sukhtankar DD, Nader MA, Husbands SM, Ko M. "A novel orvinol analog, BU08028, as a safe opioid analgesic without abuse liability in primates." Proc. Natl. Acad. Sci. USA. 2016; 0:1605295113v1-201605295 http://www.pnas.org/cgi/content/abstract/1605295113v1.

Dingová D. Study of the cholinergic system in the heart and its potential pharmacological targeting. Neuroscience. 2015; Université René Descartes - Paris V.

Eisen HJ. Heart Transplantation: Graft Rejection Basics* Proceedings, Adv Stud Med. 2008; 8(6):174-181.

Eisenstein TK. Opioids and the immune system: what is their mechanism of action? Br J Pharmacol. 2011; 164(7): 1826–1828. doi: 10.1111/j.1476-5381.2011.01513.x.

el-Sharkawy TY, al-Shireida MF, Pilcher CW. Vascular effects of some opioid receptor agonists. Can J Physiol Pharmacol. 1991; 69(6): 846–851.

Ela C, Barg J, Vogel Z, Hasin Y, Eilam Y. Distinct components of morphine effects in cardiac myocytes are mediated by the κ and δ opioid receptors. J Mol Cell Cardiol. 1997; 29:711-720.

Erbas O, Oltulu F, Yilmaz M, Yavasoglu A, Taskiran D. Neuroprotective effects of chronic administration of levetiracetam in a rat model of diabetic neuropathy. Diabetes Res Clin Pract. 2016; DIAB-6535, 30:30-30.

Estrada JA, Williams AG, Sun J, Gonzalez L, Downey HF, Caffrey JL, Mallet RT. δ-opioid receptor (DOR) signaling and reactive oxygen species (ROS) mediate intermittent hypoxia induced protection of canine myocardium. Basic Res Cardiol. 2016; 111:117. doi: 10.1007/s00395-016-0538-5.

Fassini A, Scopinho AA, Resstel LBM, Corrˆea FMA. κ-Opioid receptors in the infralimbic cortex modulate the cardiovascular responses to acute stress. Exp Physiol. 2015; 100.4 pp 377–387.

Feng Y, He X, Yang Y, Chao D, Lazarus LH, Xia Y. Current research on opioid receptor function. Current Drug Targets. 2012; 13(2):230-246.

Feric NT, Radisic M. Strategies and Challenges to Myocardial Replacement Therapy. Stem Cells Transl Med. 2016; (4):410-6. doi: 10.5966/sctm.2015-0288.

Feuerstein G. The opioid system and central cardiovascular control: Analysis of controversies. Peptides. 1985; 6 (2): 51-56.

Feuerstein G and Siren A. The opioid system in cardiac and vascular regulation of normal and hypertensive states. Circulation. 1987; 1-125.

Finley MJ, Happel CM, Kaminsky DE, Rogers TJ. Opioid and nociceptin receptors regulate cytokine and cytokine receptor expression. Cell Immunol. 2008; 252(1–2):146–54.

Fiorelli AI, Junior WM, Stolf NAG. Endomyocardial biopsy guided by echocardiography. Establishing Better Standards of Care in Doppler Echocardiography, Computed Tomography and Nuclear Cardiology. 2011; ISBN: 978-953-307-366-8, InTech.

Freye E. Opioids in medicine. A comprehensive review on the mode of action and the use of analgesics in different clinical pain states. Springer. Dordrecht, the Netherlands. 2008; pp 120-121.

Fu Y, Huang C, Xu X, Gu H, Ye Y, Jiang C, Qiu Z, Xie X. Direct reprogramming of mouse fibroblasts into cardiomyocytes with chemical cocktails. Cell Research. 2015; 25:1013–1024. doi:10.1038/cr.2015.99.

Gaziano TA, Bitton A, Anand S, Abrahams-Gessel S, Murphy A. Growing epidemic of coronary heart disease in low- and middle- income countries. Curr Probl Cardiol. 2010; 35(2):72-115. doi: 10.1016/j.cpcardiol.2009.10.002.

Gómez-Ríos MÁ. Anesthesia for non-cardiac surgery in a cardiac transplant recipient. Indian Journal of Anesthesia. 2012; 54(1): 88-89.

Grimes CA, Jope RS. CREB DNA binding activity is inhibited by glycogen synthase kinase-3 beta and facilitated by lithium. J Neurochem. 2001; 78 (6): 1219–32. doi:10.1046/j.1471-4159.2001. 00495.x.

Gross DR. Animals models in cardiovascular research. 3rd edn, Springer Dordrecht Heidelberg London NY. 2004; ISBN: 978-0-387-95961-0. doi: 10.1007/978-0-387-95962-7.

Gross GJ. Role of opioids in acute and delayed preconditioning. Journal of Molecular and Cellular Cardiology. 2003; 35:709-718.

Gullberg D, Ekblom P. Extracellular matrix and its receptors during development. Int. J. Dev. Bioi. 1995; 39: 845-854.

Guo HT, Zhang RH, Zhang Y, Zhang LJ, Li J, Shi QX, Wang YM, Fan R, Bi H, Yin W, Pei JM. Endogenous k-opioid peptide mediates the cardioprotection induced by ischemic postconditioning. J Cardiovasc Pharmacol^{TM}. 2011; 58:207-215.

Hammond EH, Yowell RL, Nunoda S, Menlove RL, Renlund DG, Bristow MR, Gay WA Jr, Jones KW, O'Connell JB. Vascular (humoral) rejection in heart transplantation: Pathologic Observations and Clinical Implications. 1989; 8(6): 430-443.

Hanlon KE, Herman DS, Agnes RS, Largent-Milnes TM, Kumarasinghe IR, Ma SW, Guo W, Lee Y, Ossipov MH, Hruby VJ, Lai J, Porreca F, Vanderah TW. Novel peptide ligands with dual acting pharmacophores designed for the pathophysiology of neuropathic pain. Brain Res. 2011; 1395: 1–11. doi: 10.1016/j.brainres.2011.04.024.

Hara H, Virmani R, Ladich E, Mackey-Bojack S, Titus J, Reisman M, Gray W, Nakamura M, Mooney M, Poulose A, Schwartz RS. J Am Coll Cardiol. 2005; 46:1768–76. doi: 10.1016/j.jacc.2005.08.038.

Hardwick JC, Baran CN, Southerland EM, Ardell JL. Remodeling of the guinea pig intrinsic cardiac plexus with chronic pressure overload. Am J Physiol Regul Integr Comp Physiol. 2009; 297: R859–R866. doi:10.1152/ajpregu.00245.2009.

Harris IS, Black BL. Development of the endocardium. Pediatr Cardiol. 2010; 31(3):391-9. doi: 10.1007/s00246-010-9642-8. Epub 2010.

Headrick JP, Hoe LE, Toit EF, Peart JN. Opioid receptors and cardioprotection `opioidergic conditioning` of the heart. British Journal of Pharmacology. 2015; 172:2026-2050. doi:10.1111/bph.13042.

Heiss A, Ammer H, Eisinger DA. δ-Opioid receptor-stimulated Akt signaling in neuroblastoma × glioma (NG108-15) hybrid cells involves receptor tyrosine kinase-mediated PI3K activation.Experimental Cell Research. 2009; 315 (12): 2115–2125.doi.org/10.1016/j.yexcr.2009.04.002

Helm PA, Younes L, Beg MF, Ennis DB, Leclercq C, Faris OP, McVeigh E, Kass D, Miller MI, Winslow RL. Evidence of structural remodeling in the dyssynchronous failing heart. Circ Res. 2006; 98(1):125-32.Epub 2005.

Hervàs I, Arnau MA, Almenar L, Péres-Pastor JL, Chirivella M, Osca J, Bello P, Osa A, Marti JF, Vera F, Mateo A. Ventricular natriuretic peptide (BNP) in heart transplantation: BNP correlation with endomyocardial biopsy, laboratory and hemodynamic measures. Laboratory Investigation, Technical Report. 2004; 84:1138-145.

Herzog E. Management of pericardial diseases. Springer International Publishing, Switzerland. 2014; pp5-6 ISBN 978-3319-06123-8. DOI:10.1007/978-3-319-06124-5.

Hirao A, Imai A, Sugie Y, Yamada Y, Hayashi S, Toide K. Pharmacological characterization of the newly synthesized nociceptin/orphanin FQ-receptor agonist 1—[1-(1-methylcyclooctyl)-4-piperidinyl]-2-[(3R)-3-piperidinyl]-1H-benzimidazole as an antiplytic agent. Journal of Pharmacological Sciences. 2008; 106(3): 361-6. Doi:10.1254/jphs. fp0071742. PMID 18319566.

Ho SY. Structure and anatomy of the aortic root. European Journal of Echocardiography. 2009; 10, i3–i10 doi:10.1093/ejechocard/jen243.

Ho SY, Nihoyannopoulos P. Anatomy, echocardiography, and normal right ventricular dimensions. Heart. 2006; 92(Suppl I): i2–i13. doi: 10.1136/hrt.2005.077875.

Hosenpud JD, Cobanoglu A, Norman DJ, Starr A. Cardiac transplantation: A manual for health care professionals. First edition, Springer-Verlag NY, Inc. 1991; doi: 10.1007/978-1-4612-3008-3.

Howells RD, Kilpatrick DL, Bailey LC, Noe M, Udenfriend S. Proenkephalin mRNA in rat heart. Neurobiology. 1986; 83:1960-1963.

Hughes J. Isolation of an Endogenous Compound from the Brain with Pharmacological Properties Similar to Morphine. Brain Research. 1975; 88(2): 295-308.

Iacobellis G, Willens HJ. MD. Echocardiographic Epicardial Fat: A Review of Research and Clinical Applications. J Am Soc Echocardiogr. 2009; 22:1311-9.

Ibrahim M, Navaratnarajah M, Kukadia P, Rao C, Siedlecka U, Cartledge JE, Soppa GK, Doorn CV, Yacoub MH, Terracciano CM. Heterotopic abdominal heart transplantation in rats for functional studies of ventricular unloading. j o u r n a l of surg i c a l r e s earch. 2 0 1 3; 179 e 3 1ee 3 9. doi: 10.1016/j.jss.2012.01.053

Ieda M, Tsuchihashi T, Ivey KN, Ross RS, Hong TT, Shaw RM, Srivastava D. Cardiac fibroblasts regulate myocardial proliferation through beta1 integrin signaling. Dev Cell. 2009; 16(2):233-44. doi: 10.1016/j.devcel.2008.12.007.

Imamura T, Kinugawa K, Nitta D, Fujino T, Inaba T, Maki H, Hatano M, Kinoshita O, Nawata K, Yao A, Kyo S, Ono M. Is the internal jugular vein or femoral vein a better approach site for endomyocardial biopsy in heart transplant recipients? Int Heart J. 2015; 56:000-000.

Janecka A, Fichna J, Janecki T. Opioid receptors and their ligands. Current Topics in Medicinal Chemistry. 2004; 4:1-17.

Jensen EC. Quantitative Analysis of Histological Staining and Fluorescence Using ImageJ. AR Insights, The anatomical record. 2013; 296:378–381.

Jensen EC. The Basics of Western Blotting. The anatomical record. 2012; 295:369-371. DOI 10.1002/ar.22424.

Karlsson LO, Bergh N, Li L, Bissessar E, Bobrova I, Gross GJ, Akyürek LM, Grip L. Dose-dependent cardioprotection of enkephalin analogue Eribis peptide 94 and cardiac expression of opioid receptors in a porcine model of ischaemia and reperfusion. European Journal of Pharmacology. 2012; 674(2-3): 378-383. doi: 10.1016/J.ejphar.2011.11.012.

Kashihara Y, Sakaguchi M, Kuno M. Axonal transport and distribution of endogenous calcitonin gene-related peptide in rat peripheral nerve. The Journal of Neuroscience. 1989; 9(1): 3796-3802.

Katz AM. Physiology of the heart. Fifth edition. 2010; pp576 Lippincott Williams and Wilkins. ISBN/ISSN 9781608311712.

Kawashima T. The autonomic nervous system of the human heart with special reference to its origin, course, and peripheral distribution. Anat Embryol. 2005; 209: 425–438. DOI 10.1007/s00429-005-0462-1.

Khachaturian AM, Lewis MA, Akil H, Watson SJ. Autoradiographic differentiation of Mu, Delta, and Kappa opioid receptors in the rat forebrain and midbrain. The journal of Neuroscience.1987; 7(8): 2445-2464.

Klabunde RE. Cardiovascular Physiology Concepts. 2nd edition, Lippincott Williams & Wilkins. 2012. Indianapolis, Indiana.

Kilo J, Laufer G, Antretter H. Endomyocardial biopsy-jugular/subclavian vein approach: 1-6, Multimedia manual of cardiothoracic surgery. European Association for Cardiothoracic Surgery. 2006; doi:10.1510/mmcts.2005.001149.

Kim JH, Jang YH, Chun KJ, Kim J, Park YH, Kim JS, Kim KM, Lee YM. Kappa-opioid receptor activation during reperfusion limits myocardial infarction via ERK1/2 activation in isolated rat hearts. Korean J Anesthesiol. 2011; 60(5):351-356. doi: 10.4097/kjae.2011.60.5.351.

Kobilka BK. G protein coupled receptor structure and activation. Biochimica et Biophysica Acta. 2007; 1768:794-807.

Koch A, Roth W, Steffek TM, Dengler TJ, Haass M, Karck M, Sack FU, Schirmacher P, Schnabel PA. Impact of apoptosis in acute rejection episodes after heart transplantation: immunohistochemical examination of right ventricular myocardial biopsies. Transplant Proc. 2008; 40(4):943-6. doi: 10.1016/j.transproceed.2008.03.034.

Koch T, Höllt V. Role of receptor internalization in opioid tolerance and dependence. Pharmacol Ther. 2008; 117(2):199–206.

Kohl P. Heterogeneous Cell Coupling in the Heart: An Electrophysiological Role for Fibroblasts. Circ Res. 2003; 93:381-383. DOI: 10.1161/01.RES.0000091364.90121.0C.

Kolk MVV, Meyberg D, Deuse T, Tang-Quan KR, Robbins RC, Reichenspurner H, Schrepfer S. LAD-Ligation: A Murine Model of Myocardial Infarction. Journal of Visualized Experiments. 2009; 32:1-3. doi: 10.3791/1438.

Koneru A, Satyanarayana S, Rizwan S. Endogenous opioids: Their physiological role and receptors. Global Journal of Pharmacology. 2009; 3(3):149-153.

Koolhaas JM. The laboratory rat. Biological Review. The UFAW Handbook on the Care and Management of Laboratory and Other Research Animals: Eight edition. 2010; ISBN: 978-1-405-17523-4. The Universities Federation for Animal Welfare.

Krieg T, Qin Q, McIntosh EC, Cohen MV, Downey JM. ACh and adenosine activate PI3-kinase in rabbit hearts through transactivation of receptor tyrosine kinases. Am J Physiol Heart Circ Physiol. 2002; 283(6):H2322-2330.

Krijnen PAJ, Nijmeijer R, Meijer CJLM, Visser CA, Hack CE, Niessen HWM. Apoptosis in myocardial ischaemia and infarction. Journal of Clinical Pathology. 2002; 55(11):801-811.

Krumins SA, Feden AI, Feuerstein G. Opiate binding in rat hearts: Modulation of binding after hemorrhagic shock. Biochem Biophys Res Commun. 1985; 127(1):120-8.

Kukanova B, Mravec B. Complex intracardiac nervous system. Bratisl Lek Listy. 2006; 107(3):45-51.

Kupinski MA. The Vascular system. 2nd edn. Diagnostic medical sonograpohy. Lippincott Williams and Wilkins. ISBN 1496380592. Pp. 1-480.

Lee SJ, Hong SG. Current status of heart transplantation and left ventricular assist device: Major changes in the last decade. Hanyang Med Rev. 2014; 34:185-196.

Lei S, Su W, Xue R, Liu H, Zhang L, Miao H, Liu Y, Li H, Irwin MG, Xia Z. Opioid-Induced Cardioprotection against Ischemia-Reperfusion Injury: The Challenge in Diabetes. Lei et al., J Diabetes Metab. 2015, 6:10. doi.org/10.4172/2155-6156.1000616.

Lendeckel U, Müller C, Röcken C, Laube B, Täger M, Huth C, Klein HU, Goette A. Expression of opioid receptors subtypes and their ligands in fibrillating human atria. PACE. 2005; 28: S275-S279.

Lesniak A, Lipkowski AW. Opioid peptides in peripheral pain control. Acta Neurobiol Exp. 2011; 71:129-138.

LeWinter MM, Kabbani S. Pericardial diseases. In: Zipes DP, Libby P, Bonow RO, Braunwald E, eds. Braunwald's Heart Disease. 7th ed. Philadelphia, Pa: Elsevier Saunders. 2005:1757–1780.

Li R, Wong GT, Wong TM, Zhang Y, Xia Z, Irmin MG. Intrathecal morphine preconditioning induces cardioprotection via activation of delta, kappa, and mu opioid receptors in rats. Anesthesia and Analgesia. 2009; 108(1):23-29.

Lin J, Wang H, Li J, Wang Q, Zhang S, Feng N, Fan R, Pei J. Kappa-opioid receptor stimulation modulates TLR4/NF-kappa B signaling in the rat heart subjected to ischemic-reperfusion. Journal of Cytokines. 2013; 61(3):842-848. doi: 10.1016/j.cyto.2013.01.002.

Little WC, Freeman GL. Pericardial Disease. Contemporary Reviews in Cardiovascular Medicine. Circulation. 2006; 113:1622-1632. DOI: 10.1161/CIRCULATIONAHA.105.561514.

Livak KJ, Schmittgen TD. Analysis of relative gene expression data using real-time quantitative PCR and the $2^{-\Delta\Delta CT}$method. Methods. 2001; 25:402-408. doi: 10.1006/meth.2001.1262.

Lodish H, Berk A, Zipursky SL, Matsudaira P, Baltimore D, Darnell J. Molecular cell biology. 4th edition, New York: W H Freeman. 2000; ISBN-10:0-7167-3136-3.

López-Bellido R, Barreto-Valer K, Sánchez-Simón FM, Rodríguez RE. Cocaine Modulates the Expression of Opioid Receptors and miR-let-7d in Zebrafish Embryos. PLOS. 2012; https://doi.org/10.1371/journal.pone.0050885.

Lopez-Gimenez J F, Milligan G. Opioid regulation of mu receptor internalization: relevance to the development of tolerance and dependence. CNS and Neurological Disorders: Drug Targets. 2010; 9(5):616-626.

Lord JA, Waterfield AA, Hughes J, Kosterlitz HW. Endogenous opioid peptides: Multiple agonists and receptors. Nature. 1977; 267(5611): 495-499.

Ma Y, Wang G. Comparison of 2 Heterotopic Heart Transplant Techniques in Rats: Cervical and Abdominal Heart. Experimental and Clinical Transplantation. 2011; 9(2): 128-133.

Malik SB, Kwan D, Shah AB, Hsu JY. The heart atrium: Gateway to the heart –anatomic and pathologic imaging findings. RadioGraphics. 2015; 35(1):14-31.

Mandal A. History of diabetes. 2012; Retrieved from https://www.news-medical.net/health/History-of-Diabetes.aspx.

Manglik A, Kruse AC, Kobilka TS, Thian FS, Mathiesen JM, Sunahara RK, Pardo L, Weis WI, Kobilka BK, Granier S. Crystal structure of the μ-opioid receptor bound to a morphian antagonist. Nature. 2012; 485 (7398):321-326.

Mansour A, Watson SJ. Anatomical distribution of opioid receptors in mammalians: An overview. Handbook of Experimental Pharmacology. 1993; 104(1): 79-105.

Marczak ED, Jinsmaa Y, Myers PH, Blankenship T, Wilson R, Balboni G, Salvadori S, Lazarus LH. Orally administered H-Dmt-Tic-Lys-NH-CH2-Ph (MZ-2), a potent mu/delta-opioid receptor antagonist, regulates obese-related factors in mice. Eur J Pharmacol. 2009; 616(1–3):115–21. doi: 10.1016/j.ejphar.2009.06.041.

Martin WR, Eades CG, Thompson JA, Huppler RE, Gilbert PE. The effects of morphine- and nalorphine-like drugs in the non-dependent and morphine-dependent chronic spinal dog. JPET. 1976; 197(3): 517-532.

Martins RT, Almeida DB, Monteiro FM, Kowacs PA, Ramina R. Opioid receptors to date. Rev Dor. São Paulo. 2012; 13(1):75-79.

Marvin WJ, Hermsmeyer JK, McDonald RI, Roskoski LM, Jr. RR Ontogenesis of cholingergic innervation in the rat heart. Circ. Res. 1980; 46;690-695.

Maslov LN, Hanus L, Pei J, Krylatov AV, Naryzhnaia NV, Barzakh EI, Lishmanov A. Signaling mechanism of cardioprotective effects of opioids. Eksp Klin Farmakol. 2013; 76(3):41-48.

Maslov LN, Headrick JP, Mechoulam R, Krylatoy AV, Lishmanov AY, Barzakh EI, Naryzhnaya NV, Zhang Y. The role of receptor transactivation in the cardioprotective effects of preconditioning and postconditioning. Neuroscience and Behavioral Physiology. 2013; 43(9):1015-1022.

Maslov LN, Naryzhnaya NV, Podoksenov YK, Mrochek AG, Gorbunov AS, Tsibul'nikov SY. Opioids as Triggers of the Adaptive Phenomenon of Ischemic Preconditioning of the Heart. Neuroscience and Behavioral Physiology. 2016; DOI 10.1007/s11055-016-0236-7.

Mason JW, Stinson EB, Harrison DC. Autonomic nervous system and arrhythmias: studies in the transplanted denervated human heart. Cardiology. 1976; 61(1):75-87.

Matesanz R. Newsletter transplant. International figures on donation and transplantation 2015. 2016; 21 EDQM.

Matthes HW, Maldonado R, Simonin F, Valverde O, Slowe S, Kitchen I, Befort K, Dierich A, Le Meur M, Dollé P, Tzavara E, Hanoune J, Roques BP, Kieffer BL. Loss of morphine-induced analgesia, reward effect and withdrawal symptoms in mice lacking the mu-opioid-receptor gene. Nature. 1996; 383 (6603):819-23. DOI:10.1038/383819a0.

Mauro MS. Nerves of the heart. A comprehensive review with a clinical point of view. Neuroanatomy. 2009; 8:26.31.

Mayfield KP, D`Alecy LG. Delta-1 opioid agonist acutely increases hypoxic tolerance. J Pharmacol Exp Ther. 1994; 268(2):683.8.

Metz RP, Patterson JL, Wilson E. Vascular smooth muscle cells: isolation, culture, and characterization. Methods Mol Biol. 2012; 843:169-76. Doi: 10.1007/978-1-61779-523-7_16.

Milgrom-Hoffman M, Harrelson Z, Ferrara N, Zelzer E, Evans SM, Tzahor E.The heart endocardium is derived from vascular endothelial progenitors. Development. 2011; 138: 4777-4787. Doi:10.1242/dev.061192.

Miller LE, McGinnis GR, Peters BA, Ballmann CG, Nanayakkara G, Amin R, Quindry JC. Involvement of the δ-opioid receptor in exercise-induced Cardioprotection. Exp Physiol. 2015; 100.4 pp 410–421

Miniati DN and Robbins RC. Heart transplantation: A thirty-year perspective. 2002; 53:189-205.

Molina PE. Experimental Biology Symposium on Autonomic and Cardiovascular Regulation: Focus on Nociceptin and Opioid Peptides: STRESS-SPECIFIC OPIOID MODULATION OF HAEMODYNAMIC COUNTER-REGULATION. Clinical and Experimental Pharmacology and Physiology. 2002; 29, 248–253.

Montgomery M, Zhang B, Radisic M. Cardiac Tissue Vascularization: From Angiogenesis to Microfluidic Blood Vessels. J Cardiovasc Pharmacol Ther. 2014; 9(4):382-393. Epub 2014.

Moorman A, Webb S, Brown NA, Lamers W, Anderson RH. Development of the heart: (1) formation of the cardiac chambers and arterial trunks. Heart. 2003; 89(7): 806–814.

Mousa SA, Shaqura M, Scha¨per J, Treskatsch S, Habazettl H, Scha¨fer M, Abdul-Khaliq H. Developmental expression of d-opioid receptors during maturation of the parasympathetic, sympathetic, and sensory innervations of the neonatal heart: Early Targets for Opioid Regulation of Autonomic Control. J. Comp. Neurol. 2011; 519:957–971.

Movahed A, Gnanasegaran G, Buscombe GR, Hall M. Integrating Cardiology for Nuclear Medicine Physicians: A Guide to Nuclear Medicine Physicians.2009; ISBN 978-3-540-78673-3 e-ISBN 978-3-540-78674-0. DOI 10.1007/978-3-540-78674-0.

Murphy JG, Lloyd MA. Myo Clinic Cardioilogy concise textbook. 4th edition, Mayo Clinic Scientific Press, Oxford University Press, Mayo Foundation for Medical Education and Research. 2013; pp 20.

Mutolo D, Bongianni F, Einum J, Dubuc R, Pantaleo T. Opioid-induced depression in the lamprey respiratory network. Neuroscience. 2007; 150(3):720–9.

Naidu PS, Lichtman AH, Archer CC, May EL, Harris LS, Aceto MD. NIH 11082 produces antidepressant-like activity in the mouse tail-suspension test through a delta-opioid receptor mechanism of action. Eur J Pharmacol. 2007; 566(1–3):132–6.

Nam J, Onitsuka I, Hatch J, Uchida Y, Ray S, Huang S, Li W, Zang H, Ruiz-Lozano P, Mukouyama Y. Coronary veins determine the pattern of sympathetic innervation in the developing heart. Development. 2013; 140(7): 1475–1485. doi: 10.1242/dev.087601

Nakano S, Muramatsu T, Nishimura S, Senbonmatsu T. Cardiomyocyte and Heart Failure. Current Basic and Pathological Approaches to the Function of Muscle Cells and Tissues – From Molecules to Humans. 2012; doi.org/10.5772/47772.

Narita M, Kuzumaki N, Miyatake M, Sato F, Wachi H, Seyama Y, Suzuki T. Role of delta-opioid receptor function in neurogenesis and neuroprotection. J Neurochem. 2006; 97(5):1494–505.

Okon UA, Davies KG,Olubobokun TH. Improvement in nutrient handling in STZ induced diabetic rats treated with Ocimum gratissimum Int J Appl Basic Med Res. 2015; 5(1): 49–53. doi: 10.4103/2229-516X.149242.

Olshansky B, Sabbah HN, Hauptman PJ, Colucci WS. Parasympathetic Nervous System and Heart Failure. Pathophysiology and Potential Implications for Therapy. Circulation. 2008; 118:863-871. DOI: 10.1161/CIRCULATIONAHA.107.760405.

Orton RJ, Sturm OE, Vyshemirsky V, Calder M, Gilbert DR, Kolch W. Computational modelling of the receptor-tyrosine-kinase-activated MAPK pathway.Biochem J. 2005; 392(Pt 2): 249–261. doi: 10.1042/BJ20050908.

Osaki M, Oshimura M, Ito H. PI3K-Akt pathway: its functions and alterations in human cancer. Apoptosis. 2004; 9:667–676.

Pan ZZ. Opioid research methods and protocols. Humana Press Inc. 2003; pp 37.

Paradis P, Dumont M, Belichard P, Rouleau JL, Lemaire S, Brakier-Ginqras L. Increased preproenkephalin A gene expression in the rat heart after induction of a myocardial infarction. Biochem Cell Biol. 1992; 70(7): 593-8.

Park J, Ann SH, Chung HC, Lee JS, Kim AJ, Garg S, Shin ES. Remote ischemic preconditioning in hemodialysis: A pilot study. Heart and Vessels. 2014; 29(1):58-64. doi: 10.1007/s00380-013-0463-6.

Parkar N, Addepalli V. Effect of Nobiletin on Diabetic Neuropathy in Experimental Rats. Austin J Pharmacol Ther. 2014; 2 (5): 1028.

Patel HH, Head BP, Petersen HN, Niesman IR, Huang D, Gross GJ, Insel PA, Roth DM. Protection of adult rat cardiac myocytes from ischemic cell death: Role of caveolar microdomains and δ-opioid receptors. Am J Physiol Heart Circ Physiol. 2006; 291: H344-H350.

Patel JK, Kobashigawa JA. Should we be doing routine biopsy after heart transplantation in a new era of anti-rejection? Curr Opin Cardiol. 2006; 21(2):127-131.

Pattinson KT. Opioids and the control of respiration. Br J Anaesth. 2008; 100:747–58.

Pauziene N, Pauza DH, Stropus R. Morphology of human intracardiac nerves: an electron microscope study. J. Anat. 2000; 197, pp. 437-459.

Peart JN, Gross ER, Gross GJ. Opioid induced preconditioning: Recent advances and future perspectives. Vascul Pharmacol. 2005; 42:211-8.

Peart JN, Gross GJ. Cardioprotective effects of acute and chronic opioid treatment are mediated via different signaling pathways. Am J Physiol Heart Circ Physiol. 2006; 291:H1746-H1753.

Peart JN, Gross GJ. Exogenous activation of δ- and κ- opioid receptors affords cardioprotection in isolated murine heart. Basic Res Cardiol. 2004; 99:27-37.

Pei JM, Chen M, Wang YM, Wen J, Zhu YL. Kappa-opioid receptor stimulation contributes to aortic artery dilation through activation of K (ATP) channel in the rats. Sheng Li Xue Bao. 2003; 55(1):91-5.

Perriard JC, Hirschy A, Ehler E. Dilated cardiomyopathy: a disease of the intercalated disc? Trends Cardiovasc Med. 2003; 13(1):30-8.

Pert CB, Snyder SH. Opiate receptor: Demonstration in nervous tissue. Science. 1973; 179:1011-1014.

Peters SR. A practical guide to frozen section technique. Neward, NJ. 2010; pp, 1-197. doi: 10.1007/978-1-4419- 1234 3.

Polakiewicz RD, Schieferl SM, Gingras A, Sonenberg N, and Comb MJ. m-Opioid Receptor Activates Signaling Pathways Implicated in Cell Survival and Translational Control. The Journal of Biological Chemistry. 1998; 273 (36): 23534–23541.

Pugsley MK. The diverse molecular mechanisms responsible for the actions of opioids on cardiovascular system. Pharmacology and Therapeutics. 2002; 93:51-75.

Purves D, Augustine GJ, Fitzpatrick D, Katz LC, LaMantia A, McNamara JO, Williams SM. Neuroscience. 2nd edition, Sunderland (MA): Sinauer Associates. 2001; ISBN-10:0-87893-742-0.

Rao VR, Prescott E, Shelke NB, Trivedi R, Thomas P, Struble C, Gadek T, O'Neill CA , Kompella UB. Delivery of SAR 1118 to the Retina via Ophthalmic Drops and its Effectiveness in a Rat Streptozotocin (STZ) Model of Diabetic Retinopathy (DR). Invest Ophthalmol Vis Sci. 2010; 51:5198–5204) DOI: 10.1167/iovs.09-5144.

Rasband WS. ImageJ, U.S. National Institutes of Health, Bethesda, Maryland, USA. 1997-2015; http://imagej.nih.gov/ij.

Redrobe JP, Calo` G, Regoli D, Quirion R. Nociceptin receptor antagonists display antidepressant-like properties in the mouse forced swimming test. Naunyn-Schmiedeberg`s Archives of Pharmacology. 2002; 365 (2): 164-7. Doi: 10.1007/s00210-001-0511-0. PMID 1189035.

Roberts PJ, Der CJ. Targeting the Raf-MEK-ERK mitogen-activated protein kinase cascade for the treatment of cancer. Oncogene. 2007; 26(22):3291-310.

Robinson TF, Cohen-Gould L, Factor SM, Eghbali M, Blumenfeld OO. Structure and function of connective tissue in cardiac muscle: collagen types I and III in endomysial struts and pericellular fibers. Scanning Microsc. 1988; 2(2):1005-15.

Rodrigues TR, Miranda RC, Lichter AP, Lobo NC, Figueroa CS, da Consolação Moreira M. Heart rate variability in myocardial infarction with and without malignant arrhythmias: comparison with heart transplant recipients and normal subjects. Pacing Clin Electrophysiol. 1996; 19(11 Pt 2):1857-62.

Rosenfeld MG, Mermod J, Amara SG, Swanson LW, Sawchenko PE, Rivier J, Vale WW, Evans RM. Production of a novel neuropeptide encoded by the calcitonin gene via tissue-specific RNA processing. Nature. 1983; 304:129-135. doi:10.1038/304129a0.

Rubart M, Field LJ. Cardiac regeneration: repopulating the heart. Annu Rev Physiol. 2006; 68:29-49.

Rüegg MA, Meinen S. Histopathology in hematoxylin and eosin stained muscle sections. 2014; MDC1A_M.1.2.004, pp 1-9.

Rungatscher A, Linardi D, Giacomazzi A, Tessari M, Menon T, Mazzucco A, Faggian G. Cardioprotective effect of δ- opioid receptor agonist vs mild therapeutic hypothermia in a rat model of cardiac arrest with extracorporeal life support. Resuscitation. 2013; 84:244-248.

Said G. Diabetic neuropathy—a review. Nature clinical practice. 2007; 3(6):331-340.
Saitoh A, Yoshikawa Y, Onodera K, Kamei J. Role of delta-opioid receptor subtypes in anxiety-related behaviors in the elevated plus-maze in rats. Psychopharmacology (Berl). 2005; 182(3):327-34. Epub 2005.

Salemi S, Aeschlimann A, Reisch N, Jüngel A, Gay RE, Heppner FL, Michel BA, Gay S, Sprott H. Detection of kappa and delta opioid receptors in skin-outside the nervous system. Biochemical and Biophysical Research Communications. 2005; 338:1012-1017.

Samsamshariat SA, Samsamshariat ZA, Movahed M. A novel method for safe and accurate left anterior descending coronaryartery ligation for research in rats. Cardiovascular Revascularization Medicine. 2005; 6:121– 123. doi: 10.1016/j.carrev.2005.07.001.

Saraste A, Pulkki K, Kallajoki M, Heikkilä P, Laine P, Mattila S, Nieminen MS, Parvinen M, Voipio-Pulkki LM. Cardiomyocyte apoptosis and progression of heart failure to transplantation.Eur J Clin Invest. 1999; 29(5):380-6.

Sarbassov DD, Guertin DA, Ali SM, Sabatini DM. Phosphorylation and regulation of Akt/PKB by the rictor-mTOR complex. Science. 2005; 307:1098–1101. 3.

Sartiani L, Elisabetta Cerbai E, Mugelli A. The funny current in cardiac non-pacemaker cells: Functional role and pharmacological modulation, modern pacemakers - Present and Future. 2011; ISBN: 978-953-307-214-2.

Schultz JE, Rose E, Yao Z, Gross GJ. Evidences for involvement of opioid receptors in ischemic preconditioning in rat hearts. American Journal of Physiology. 1995; 268(5): H2157-H2161.

Schultz JJ, Hsu AK, Gross GJ. Ischemic preconditioning and morphine-induced cardio protection involve the delta (δ)- opioid receptor in the intact rat heart. J Mole Cell Cardiol. 1997; 29:2187-2195.

Scoto GM, Arico` G, Ronsisvalle S, Parenti C. Blockade of the nociceptin/orphanin FQ/NOP receptor system in the rat ventrolateral periaqueductal gray potentiates DAMGO analgesia. Ppeptides. 2007; 28(7): 1441-6. Doi: 10.1016/j.peptides.2007.05.013. PMID 17628212.

Shaikh AS, Somani RS. Animal models and biomarkers of neuropathy in diabetic rodents. Indian J Pharmacol. 2010; 42:129-34.

Shapiro PA, Sloan RP, Bigger JT Jr, Bagiella E, Gorman JM. Cardiac denervation and cardiovascular reactivity to psychological stress. Am J Psychiatry. 1994; 151(8):1140-7.

Shen H, Aeschlimann A, Renate N, Gay RE, Simmen BR, Michel BA, Gay S, Sprott H. Kappa and DOR opioid receptors are ecpressed but down-regulated in fibroblast like synoviocytes of patients with rheumatoid arthritis and osteoarthritis. Arthritis and Rheumatism. 2005; 52(5):1402-1410. doi:10.1002/art.21141.

Snyder SH and Pasternak GW. Historical review: Opioid receptors. TRENDS in Pharmacological Sciences. 2003; 24(4):198-205. Doi:10.1016/S0165-6147(03)00066-X.

Sobanski P, Krajnik M, Shaqura M, Bloch-Boguslawska, Schafer M, Mousa SA. The presence of mu-, delta-, and kappa- opioid receptors in human heart tissue. Heart Vessels. 2014; Springer Japan. doi:10.1007/s00380-013-0456-5.

Song Y, Du Y, Prabhu SD, Epstein PN. Diabetic cardiomyopathy in OV E26 mice shows mitochondrial ROS production and divergence between in vivo and in vitro contractility. Rev Diabet Stud. 2007; 4:159-168. DOI 10.1900/RDS.2007.4.159.

Souders CA, Bowers SLK., Baudino TA. Cardiac Fibroblast: The Renaissance Cell. Circ Res. 2009; 105:1164-1176. DOI: 10.1161/CIRCRESAHA.109.209809.

Spain JW, Roth BL, Coscia CJ. Differential ontogeny of multiple opioid receptors (mu, delta, and kappa). J Neurosci. 1985; 5(3):584-8.

Steele PA, Aromataris EC, Riederer BM. Endogenous opioid peptides in parasympathetic, sympathetic and sensory nerves in the guinea-pig heart. Cell Tissue Res. 1996; 284(2):331-9.

Stewart S, Winters GL, Fishbein MC, Tazelaar HD, Kobashigawa J, Abrams J, Andersen CB, Angelini A, Berry GJ, Burke MM, Demetris AJ, Hammond E, Itescu S, Marboe CC, McManus B, Reed EF, Reinsmoen NL, Rodriguez ER, Rose AG, Rose M, Suciu-Focia N, Zeevi A, Billingham ME. Revision of the 1990 working formulation for the standardization of nomenclature in the diagnosis of heart rejection. The Journal of Heart and Lung Transplantation. 2005; 24(11):1710-1720. doi: 10.1016/j.healun.2005.03.019.

Strecker T, Rösch J, Weyand M, Agaimy A. Endomyocardial biopsy for monitoring heart transplant patients: 11-years-experience at a German Heart Center. Int J Clin Exp Pathol. 2013; 6(1): 55-65.

Sun Z, Tong G, Ma N, Li J, Li X, Li S, Zhou J, Xiong L, Cao F, Yao L, Wang H, Shen L. NDRG2: a newly identified mediator of insulin cardioprotection against myocardial ischemia-reperfusion injury.Basic Res Cardiol. 2013; 108(3):341. doi: 10.1007/s00395-013-0341-5.

Sundberg-Cohon J, Gnanasegaran G, Buscombe JR, Hall M. Integrating cardiology for nuclear medicine physicians: A guide to nuclear medicine physicians. 2009; ISBN 978-3-540-78674-0.

Swami AC, Kumar A, Rupal S, Lata S. Anesthesia for non-cardiac surgery in a cardiac transplant recipient. Indian Journal of Anesthesia. 2011; 55(4):405-407. doi: 10.4103/0019-5049-84849.

Takagawa J, Zhang Y, Wong ML, Sievers RE, Kapasi NK, Wang Y, Yeghiazarians Y, Lee RJ, Grossman W, Springer ML. Myocardial Infarct Size Measurement in the Mouse Chronic Infarction Model: Comparison of Area- and Length-Based Approaches. J Appl Physiol. 2007; 102(6): 2104–2111. doi:10.1152/japplphysiol.00033.2007.

Tamura K, Sudo T, Senftleben U, Dadak AM, Johnson R, Karin M. Requirement for p38a in erythropoietin expression: A role for stress kinases in erythropoiesis. Cell. 2000; 102:221-231.

Tanaka K, Kersten JR, Riess ML. Opioid-induced Cardioprotection. Curr Pharm Des. 2014; 20(36): 5696–5705.

Taylor AJ. Vaddadi G. Pfluger H. Butler M, Bergin P, Leet A, Richardson M, Cherayath J, Iles L, Kaye DM. Diagnostic performance of multisequential cardiac magnetic resonance imaging in acute cardiac allograft rejection.Eur J Heart Fail. 2010; 12(1): 45–51. doi: 10.1093/eurjhf/hfp174

Taylor D, Meiser B, Webber S, Baran DA, Carboni M, Dengler T, Feldman D, Frigerio M, Kfoury A, Kim D, Kobashigawa J, Shullo M, Stehlik J, Teuteberg J, Uber PA, West L, Tanaka K, Kersten JR, Riess ML. Opioid-induced Cardioprotection. Curr Pharm Des. 2014; 20(36): 5696–5705.

Thakur A, Scheinman RI, Rao VR, Kompella UB. Pazopanib, A Multitargeted Tyrosine Kinase Inhibitor, Reduces Diabetic Retinal Vascular Leukostasis and Leakage. Microvasc Res. 2011; 82(3): 346–350. doi: 10.1016/j.mvr.2011.09.001.

Thakur V, Gonzalez M, Pennington K, Nargis S, Chattopadhyay M. Effect of exercise on neurogenic inflammation in spinal cord of Type 1 diabetic rats. Brain Research. 2016; 1642: 87–94. http://dx.doi.org/10.1016/j.brainres.2016.03.012.

Theisen MM, Schlottmann S, August C, Herzog C, Theilmeier G, Maas M, Blumenstiel JM, Weber TP, Van Aken HK, Kaerlein KT. Detection and distribution of opioid peptide receptors in porcine myocardial tissue. Pharmacological Research. 2014; 84:45-49.

Thomas D. Cardiology: ECG interpretation CEUFast Nursing CE 2015; Retrieved April 30, 2016 from https://ceufast.com/course/ecg-interpretation.

Tirziu D, Giordano FJ, Simons M. Cell Communications in the Heart.Circulation. 2010; 122(9): 928–937. doi: 10.1161/CIRCULATIONAHA.108.847731.

Treskatsch S, Shaqura M, Dehe L, Feldheiser A, Roepke TK, Shakibaei M, Spies CD, Schäfer M, Mousa SA. Upregulation of the kappa opioidergic system in left ventricular rat myocardium in response to volume overload: Adaptive changes of the cardiac kappa opioid system in heart failure. Pharmacological Research. 2015; 102:33-41.

Triposkiadis F, Karayannis G, Giamouzis G, Skoularigis J, Louridas G, Butler J. The Sympathetic Nervous System in Heart Failure Physiology, Pathophysiology, and Clinical Implications. J Am Coll Cardiol. 2009; 54:1747–62. doi: 10.1016/j.jacc.2009.05.015

Tsai H-J, Huang S-S, Tsou M-T, Wang H-T, Chiu J-H. Role of Opioid Receptors Signaling in Remote Electrostimulation - Induced Protection against

Ischemia/Reperfusion Injury in Rat Hearts. PLoS ONE. 2015; 10(10): e0138108. doi: 10.1371/journal.pone.0138108.

Tsibulnikov SY, Maslov LN, Mukhomedzyanov AV, Krylatov AV, Tsibulnikova MR, Lishmanov YB. Prospects of using of k-opioid receptor agonist U-50,488 and ICI 199,441 for improving heart resistance to ischemia/reperfusion. Bulletin of experimental Biology and Medicine. 2015; 159(6):718-721. DOI: 10.1007/s10517-015-3057-8.

Valerio Jr R, Durra O, Gold ME. Anesthetic considerations for an adult heart transplant recipient undergoing noncardiac surgery: A case report. AANA Journal. 2014; 84(4): 293-299.

Valtchanova-Matchouganska A, Ojewole JA. Mechanisms of opioid delta (delta) and kappa (kappa) receptors` cardioprotection in ischaemic preconditioning in a rat model of myocardial infarction. Cardiovasc J S Afr. 2003; 14(2): 73-80.

Vascular Disease Foundation/VDF. Focus on Ischemia. 2012, 8206 Leesburg Pike, Suite 301, Vienna, VA 22182. 26vdf2012.

Vaseghi M, Shivkumar K. The Role of the Autonomic Nervous System in Sudden Cardiac Death. Prog Cardiovasc Dis. 2008; 50(6): 404–419. doi: 10.1016/j.pcad.2008.01.003.

Ventura C, Bastagli L, Bernardi P, Caldarera CM, Guarnieri C. Opioid receptors in rat cardiac sarcolemma: Effect of phenylephrine and isoproterenol. Biochimica et Biophysica Acta. 1989; 987(1):69-74.

Verma S, Fedak PWM, Weisel RD, Butany J, Rao V, Maitland A, Li R, Dhillon B, Yau TM. Fundamentals of reperfusion injury for the Clinical Cardiologist. Circulation. 2002; 105:2332-2336. doi: 10.1161/01.CIR.0000016602.96363.36.

Vicente-Carrillo A, Álvarez-Rodríguez M, Rodríguez-Martínez H. The mu (μ) and delta (δ) opioid receptors modulate boar sperm motility. Mol Reprod Dev. 2016; 83 (8):724–734. DOI: 10.1002/mrd.22675.

Vivanco I, Sawyers CL. The phosphatidylinositol 3-kinase Akt pathway in human cancer. Nat Rev Cancer. 2002; 2:489–501.

Vunjak-Novakovic G, Tandon N, Godier A, Maidhof R, Marsano A, Martens TP, Radisic M. Challenges in cardiac tissue engineering. Tissue Eng Part B Rev. 2010; 16(2):169-87. doi: 10.1089/ten.TEB.2009.0352.

Waldhoer M, Bartlett SE, Whistler JL. Opioid receptors. Annu Rev Biochem. 2004; 73:953-990.

Walsh K. Akt signaling and growth of the heart. Circulation. 2006; 113:2032-2034. doi.org/10.1161/CirculationAHA.106.615138.

Wang-Fisher Y. Manual of stroke models in rats. CRC Press, Science. 2008; pp233-235.

Wang Y, Feng W, Xue W, Tan Y, Hein DW, Li X, Cai L. Inactivation of GSK-3β by Metallothionein Prevents Diabetes-Related Changes in Cardiac Energy Metabolism, Inflammation, Nitrosative Damage, and Remodeling. Diabetes. 2009; 58:1391–1402.

Watcharasit P, Bijur GN, Zmijewski JW, Song L, Zmijewska A, Chen X, Johnson GV, Jope RS. Direct, activating interaction between glycogen synthase kinase-3beta and p53 after DNA damage. Proc Natl Acad Sci. 2002; 99 (12): 7951–5. doi*:*10.1073/pnas.122062299. PMC 123001.

Weil J, Eschenhagen T, Fleige G, Mittmann C, Orthey E, Scholz H. Localization of preproenkephalin mRNA in rat heart: Selective gene expression in left ventricle myocardium. Am J Physiol. 1998; H378-H384.

Welters ID. Is immunomodulation by opioid drugs of clinical relevance? Curr Opin Anaesthesiol. 2003; 16(5):509-13.

WHO. Global Report on Diabetes. WHO Library –in- Publication, ISBN 9789241565257 (NLM Classification: WK 810). 2016; 1-86.

WHO. Global status report on noncommunicable diseases: "the nine global noncommunicable disease targets; a shared responsibility". 2014; ISBN. 978-92-4-156485-4.

Wider J, Przyklenk K. Ischemic conditioning: the challenge of protecting the diabetic heart. Cardiovascular Diagnosis and Therapy. 2014; 4(5):383-396. doi: 10.3978/j.issn.2223-3652.2014.10.05.

Wild S, Roglic G, Green A, Sicree R, King H. Global prevalence of diabetes. Diabetic Care. 2004; 27(5):1047-1053.

Williams-Pritchard G, Headrick JP, Peart JN. Myocardial opioid receptors in conditioning and cytoprotection. Pharmaceuticals. 2011; 4:470-484.

Wittert G, Hope P, Pyle D. Tissue distribution of opioid receptor gene expression in the rat. Biochemical and Biophysical Research Communications. 1996; 218:877-881.

Wong GT, Ling Ling J, Irwin MG. Activation of central opioid receptors induces cardioprotection against ischemia-reperfusion injury. Anesth Analg. 2010; 111(1): 24-28. Doi: 10.1213/ANE.0b013e3181b8b77e.

Wong KK, Raffel DM, Koeppe RA, Frey KA, Bohnen NI, Gilman S. Pattern of cardiac sympathetic denervation in idiopathic Parkinson disease studied with 11C hydroxyephedrine PET. Radiology. 2012; 265(1):240-7.

Wong ND. Epidemiological studies of CHD and the evolution of preventive cardiology. Nat. Rev. Cardiol. 2014; 11:276-289.

Wood KJ and Goto R. Mechanisms of rejection: Current perspectives. Transplantation Lippincott Williams and Wilkins. 2012; 93:1-10. doi: 10.1097/TP.0b013e31823cab44.

Wu H, Wacker D, Mileni M, Katritch V, Han GW, Vardy E, Liu W, Thompson AA, Huang X, Carroll FI, Mascarella SW, Westkaemper RB, Mosier PD, Roth BL, Cherezov V, Stevens R. Structure of the human κ-opioid receptor in complex with JDTic. Nature. 2012; 485: 327-332. doi: 10.1038/nature10939.

Wu Q, Wang H., Li J., Zhou P, Wang Q, Zhao Lei, Fan R, Wang Y, Xu X, Yi D, Yu S, Pei J. k-Opioid Receptor Stimulation Improves Endothelial Function in Hypoxic Pulmonary Hypertension. PLoS ONE. 2013; 8(5): e60850. doi: 10.1371/journal.pone.0060850.

Wu S, Li HY, Wong TM. Cardioprotection of Preconditioning by metabolic inhibition in the rat ventricular myocyte. Involvement of kappa-opioid receptor. Circ Res. 1999; 84(12):1388–95.

Wu S, Wong MCY, Chen M, Cho CH, Wong TM. Role of opioid receptors in cardioprotection of cold-restraint stress and morphine. J Biomed Sci. 2004; 11:726-731. doi: 10.1159/000081818.

Wu S, Wong TM. Roles of kappa opioid receptors in cardioprotection against ischemia: The signaling mechanisms. Sheng Li Xue Bao. 2003; 55: 115-20.

Xin M, Olson EN, Bassel-Duby R. Mending broken hearts: cardiac development as a basis for adult heart regeneration and repair. Nat Rev Mol Cell Biol. 2013; 14(8): 529–541. doi:10.1038/nrm3619.

Young B, Lowe J, Steven A, Heath J. Wheater's Functional Histology: A Text and Color Atlas. 5th edn, Churchill Livingstone, Elsevier. 2006; pp. 288-327.

Yu LN, Yu J, Zhang FJ, Yang MJ, Ding TT, Wang JK, He W, Fang T, Chen G, Yan M. Sevoflurane postconditioning reduces myocardial reperfusion injury in rat isolated hearts via activation of PI3K/Akt signaling and modulation of bcl-2 family proteins. Biomed and Biotechnol. 2010; 11(9):661–672. doi: 10.1631/jzus. B1000155.

Yu M, Bozek J, Lamoy M, Kagan M, Benites P, Onthank D, Robinson SP. LMI1195 PET imaging in evaluation of regional cardiac sympathetic denervation and its potential role in antiarrhythmic drug treatment. Eur J Nucl Med Mol Imaging. 2012; 39(12):1910-9. doi: 10.1007/s00259-012-2204-y.

Zatta AJ, Kin H, Yoshishige D, Jiang R, Wang N, Reeves JG, Mykytenko J, Guyton RA, Zhao ZQ, Caffrey JL, Vinten-Johansen J. Evidence that cardioprotection by

postconditioning involves preservation of myocardial opioid content and selective opioid receptor activation. Am J Physiol Heart Circ Physiol. 2008; 294:H1444-51. doi: 10.1152/ajpheart.01279.2006.

Zhang J, Haddad GG, Xia Y. delta-, but not mu- and kappa-, opioid receptor activation protects neocortical neurons from glutamate-induced excitotoxic injury. Brain Res. 2000; 885(2):143-53.

Zhang MA, Shah M. ROS signalling between endothelial cells and cardiac cells Cardiovascular Research. 2014; 102 (2, 1)249–257. https://doi.org/10.1093/cvr/cvu050.

Zhang S, Wang N, Xu J, Gao Q, Lin G, Bruce J, Xia Q. k-opioid receptors mediate cardioprotection by remote preconditioning. Anesthesiology. 2006; 105:550-556.

Zhang XX, Shi WX. Dendritic glutamate-induced bursting in prefrontal pyramidal cells: role of NMDA and non-NMDA receptors. Zhongguo Yao Li Xue Bao. 1999; 20(12):1125-31.

Zhou X, Wang D, Zhang Y, Zhang J, Xiang D, Wang H. Activation of κ-opioid receptor by U50,488H improves vascular dysfunction in streptozotocin-induced diabetic rats. BMC Endocrine Disorders. 2015; 15:7. doi:10.1186/s12902-015-0004-7.

Zhu Y, Hsu M, Pintar JE. Developmental expression of the μ, δ, and κ opioid receptors mRNA in mouse. The Journal of Neuroscience. 1998; 18(7):2538-2549.

Zimlichman R, Gefel D, Eliahou H, Matas Z, Rosen B, Gass S, Ela C, Eilam Y, Vogel Z, Barg J. Expression of opioid receptors during heart ontogeny in normotensive and hypertensive rats. Circulation. 1996; 93:1020-1025. doi: 10.1161/01.CIR.93.5.1020.

Zimmermann M. Ethical guidelines for investigations of experimental pain in conscious animals. Pain. 1983; 16(2):109-110.

9. Appendices

9.1. Appendix I: Buffer preparation

a. Diluting solutions (converting g/L to M and vice versa)
   - Amount (in moles) = amount in g/molar mass in g.mol-1
   - Concentration (M) = amount in mol/volume in L

b. To determine volume in a certain concentration: $C_1 \times V_1 = C_2 \times V_2$ (match units)

c. SDS-Laemilli Buffer Solution preparation

Table: 8. Buffer preparation

SN	Buffer solutions	Working solutions	Remarks
1	**RIPA buffer**		
	1L ddH2O 50ml 1M Tris 7.4 37.5ml 4M NaCl 4ml 0.5M EDTA 10ml NP-40 10ml 10% SDS	70ul/20 sections	
2	**Running buffer (10X) for 1L**	**Running buffer (1X) for 1L**	
	700ml ddH_2O 10g Tris-base 144g Glycine 10g SDS Add to bring to 1L	900ml ddH2O 100ml Running buffer (10X)	
3	***Transfer Buffer (10X) for 1L***	***Transfer Buffer (1X) for 1L***	
	30g Tris-base 144g Glycine 25g SDS Add ddH_2O up to 1L	900ml ddH_2O 100ml Transfer buffer (10X)	
4	**5X SDS loading sample buffer (100ml)**		
	• 25ml of 250mM Tris-HCl (pH 6.8) (Stock 1M) • 10g of 10% SDS • 30ml of 30%Glycine • 5ml of 5% BME (Add only while using due to its diminished vapor pressure and unpleasant odor		

properties)
- 2ml of 0.02% Bromophenol blue (Stock 1%)

5x Sample buffer (8.1ml)

- 3.9 ml deionized water
- l 0.5M Tris, pH 6.8
- 0.8 ml Glycerol
- 1.6 ml 10% SDS
- 0.4 ml 2-mercaptoethanol
- 0.4 ml 1% bromophenol blue

5	**1M stock**	**50 mM stock**
	0.5ml 14.3 M 2-ME 6.6 ml dH20 Store at 4°C	5ml 1M 2-ME 95 ml H2O stir Store at 4°C Dilute to 50 µM (final) for use
6	**5% Beta-Mercaptanol**	
	5ml of 50mM (0.05%) 100ml of 5X SDS loading sample buffer (laemmli buffer)	
7	**10% SDS**	
	50g SDS Dilute in 450ml deionized H_2O Store at RT	
8	**40% Acrylamide for 1L**	***30% Acrylamide***
	380g of acrylamide 20g of N, N'-methylbisacrylamide 600ml of ddH_2O Heat to dissolve Adjust the volume to 1L with H_2O, pH ≤7 Filter by 0.45 µm filter paper Cover with aluminum foil (in dark bottle) and store at 4°C Acrylamide is a neurotoxin	30g Acrylamide 0.8g N`N`-bis-methylene acrylamide Dilute with deionized water Store (cover with aluminum foil) in the dark at 4°C
9	**Lower Tris-HCl buffer 4x**	***Tris-HCl buffer 4x/ stacking gel***
	18.17g Tris-base 4ml of 10% SDS Dilute in 100ml ddH_2O pH 8.0 Store at 4°C	6.06g Tris-base 4ml of 10% SDS Adjust pH 6.8
10	**APS (10%) Stock of 5ml**	

	↓ 500mg of Ammonium persulfate ↓ 5ml ddH2O ↓ Store at 4°C	
11	**10% ammonium persulfate (APS)**	
	↓ 0.1g ammonium persulfate /APS) (electrophoresis) ↓ 1ml deionized H_2O	
12	**TBS-(10X) for 1L** ↓ 80g NaCl ↓ 2g KCl ↓ 30g Tris-base ↓ 1L ddH_2O	**TBS-T (1X) for 1L** ↓ 900ml ddH_2O ↓ 100ml TBS-(10X) ↓ 500ul Tween (%)
13	**5% Blocking buffer (100ml)**	
	↓ 5g non-fat milk ↓ 100ml TBS-T (1x)	
14	Sodium Azide (NaN3) can be used to preserve antibody for later use, if stored at -20°c or -80°c depends on the antibody to a final concentration of:	
	0.02% (w/v), or 2:10,000 dilutions (can be used 0.02% to 0.05%	
16	**DAB substrate**	
	1 drop for 1ml of diluents	
17	**Counterstaining (for nuclei)**	
	DAPI, 1: 10,000 Hoechst 33342, 1: 10,000	

Note: TBS-T, Tris Buffered Saline with Tween; SDS, Sodium Dodecyl Sulfate (NaDodSO4; anionic detergent); APS, ammonium persulfate; TEMED/TMEDA, Tetramethylethylenediamine; Tris, Tris (Hydroxymethyl) aminomethane; or THAM, BME, Beta-mercapitanol; Solutions preparation of protocol was modified in Cardiovascular Research Laboratory, U. O. Heart Surgery, University of Verona, VR, IT.

9.2. Appendix II: Protein size based approximate acrylamide percentage of gel

Table: 9. Protein size estimation percentage of acrylamide gel

Protein size, kDa	**%**
25-200	8
15-100	10
10-70	12.5
12-45	15
4-40	20
Abcam, 2017, http:// www.docs.abcam.com, note: it is neurotoxic	